Journal of Double Star Observations

VOLUME 13 NUMBER 1 January 1, 2017

Inside this issue:

Magnitude Anomalies in the WDS

T. V. Bryant III
Little Tycho Observatory
703 McNeill Road, Silver Spring, Md 20910
rkk_529@hotmail.com

Abstract: Visual magnitude entries in the WDS often differ from those in other catalogs by a magnitude or more. Using the 2MASS, PPMXL, Tycho, UCAC4, and URAT1 catalogs, we provide listings of the WDS entries that have no corresponding entries in the other catalogs that are within a magnitude (visual band) of the WDS primary stars' magnitude and are also within 10" of the WDS primary.

Those stars with two digit fractional magnitudes must be within 0.5mv of the catalog stars. WDS stars that are marked by the WDS as dubious, infrared, Johnson red band, have no primary visual magnitude, have no precise coordinates, are marked as uncertain, or are brighter than 6.0mv or fainter than 17.0mv are not included in this study.

The Little Tycho Observatory currently specializes in visual double star observations, and uses the WDS as its main catalog for choosing which pairs to examine on a given night. Over the years, it has become apparent that a few pairs were non-existent, but that many more were significantly fainter than their listings indicated.

The WDS[2] currently contains 137,225 entries. The USNO[1], which maintains the WDS, generally takes their data from previously published papers on double stars and enters these data into the WDS. Some of the magnitude estimates vary considerably from the actual brightness of the pair. The discoveries of Robert Jonckheere, for instance, are notorious for their estimates of stellar brightness that are often too bright by a magnitude or more. Progress has been made in this matter as some of the lists (W. Struve's STF list, for example) have been updated with accurate magnitudes, usually taken from Tycho[5] or APASS[8] data. These updated magnitudes are listed with two decimal fractions in the WDS, and are subject to a more stringent tolerance (±0.5mv) that those stars without accurate magnitudes.

Five catalogs were used to check the WDS data. They were:

- 2MASS[3]
- PPMXL[4]
- Tycho[5]
- UCAC4[6]
- URAT1[7]

The catalogs were downloaded, and programs were written to convert each catalog to a standard format. A search was then made for each WDS star in all of the catalogs. A WDS entry was considered confirmed if an entry from any of the catalogs was within 10 arc seconds of the WDS position and that entry was within a magnitude (or half magnitude, in the case of two decimal entries) the primary magnitude listed in the WDS. The version of the WDS used for this study was dated 2016 June 23.

If the primary star of a pair failed the magnitude test, the combined magnitude of the pair was calculated and the test was again done. If the combined pair magnitude was within the the full or half magnitude range, the pair was considered confirmed.

Combined magnitudes are derived from the magnitude - luminosity relation [10]:

$$mc = -2.5\log\left[10^{-0.4m_1} + 10^{-0.4m_2}\right]$$

Magnitude Anomalies in the WDS

A star was also considered confirmed if the WDS notes about the pair had any of these caveats:

- The pair's identification is uncertain.
- K band infrared magnitude.
- Johnson red band magnitude.
- The pair is dubious.
- WDS primary stars that were fainter than 16.99mv.
- WDS primary stars that were brighter than 6.0mv.

There were 2604 WDS pairs found with no catalog star that was within 0.5 or 1 mv of the WDS primary star listing. Of these, 1019 pairs had a greater separation than 10", and 1585 were found that were closer than this. This separation is important, as close pairs can easily have magnitude errors in the survey catalogs used to verify the WDS pairs. This is because the catalogs themselves are generated by computer analysis of digital images that can easily be thrown off by the presence of a bright star within the "aperture" of the scanning software. 10" is the figure of merit where these effects become noticeable [9]. In other words, the closer the pair, the less certain the error.

These 2604 stars with anomalous magnitudes are listed on the author's web site: http://mainsequence.org/html/wds/magnitudeStudy/html/WdsMagnitudeAnomalies.html.

Table 1 lists the 48 WDS pairs that have no corresponding catalog star (as of December 2016). Table 2 lists the 169 WDS pairs that have no corresponding catalog star within 4mv of the WDS primary.

The column explanation for Table 2 is as follows:

- WDS ID: The WDS designation of the pair.
- Discover: The Discoverer's designation of the pair.
- RA: The WDS precise J2000 right ascension of the star.
- Dec: The WDS precise J2000 declination of the star.
- mva-mvb: The WDS visual magnitudes of the primary and secondary stars.
- Rho: The separation of the pair, at the most recent epoch, in arc seconds.
- Theta: The position angle of the pair, at the most recent epoch, in degrees.
- dmv: The smallest difference in visual magnitude between the WDS listing and a catalog listing.

The column explanation for Table 1 is the same as Table 2, but lacking the dmv column.

Please note that many of the WDS pairs in these two appendices are currently undergoing a detailed review by the USNO. Their listing might be changed in subsequent versions of the WDS.

Acknowledgments

The author wishes to acknowledge the edits and improvements from Tom Corbin, William Hartkopf, and Kathie Bryant in their review of this paper.

References

[1] U.S. Naval Observatory, 3450 Massachusetts Ave, NW, Washington, DC 20392

[2] The Washington Double Star Catalog, Brian D. Mason, Gary L. Wycoff, William I. Hartkopf, Geoffrey G. Douglass, and Charles E. Worley, 2001

[3] http://irsa.ipac.caltech.edu/Missions/2mass.htm

[4] http://irsa.ipac.caltech.edu/Missions/ppmxl.html

[5] http://www.astro.ku.dk/~erik/Tycho-2/

[6] http://www.usno.navy.mil/USNO/astrometry/optical-IR-prod/ucac

[7] http://www.usno.navy.mil/USNO/astrometry/optical-IR-prod/urat

[8] http://www.aavso.org/apass

[9] William Hartkopf, Astrometry Department, U.S. Naval Observatory, 3450 Massachusetts Ave, NW, Washington, DC 20392. Personal communication.

[10] https://en.wikipedia.org/wiki/Apparent_magnitude#Magnitude_addition

Magnitude Anomalies in the WDS

Table 1. 48 WDS Pairs That Have No Corresponding Catalog Star

WDS ID	Discover	RA	Dec	mva-mvb	Rho	Theta
00334+1418	LDS9094	0:33:22.04	14:18:5.6	14.3-18.5	11.000	0.00
01344-0412	LDS5336	1:34:29	-4:13:18	11.9-14.7	344.000	352.00
02419+2909	LDS3415	2:41:55	29:9:0	16.7-18.0	173.000	231.00
03533+2540	LDS5446	3:53:26	25:39:48	10.6-17.9	14.000	225.00
03590+2315	LDS6123	3:59:2	23:14:42	15.4-15.5	21.000	135.00
04128+1404	LDS5519	4:12:49	14:4:12	15.4-19.0	10.000	330.00
04275+1323	LDS5580	4:27:32	13:22:48	12.2-14.3	21.000	283.00
04371+1848	LDS3599	4:37:6	18:47:30	15.4-16.8	2.000	175.00
04483+5729	LDS3618	4:48:26	57:29:36	16.8-18.2	155.000	353.00
04569+2019	LDS5630	4:56:58	20:19:54	15.1-16.4	155.000	262.00
04594+2215	LDS6153	4:59:24	22:14:48	14.5-19.0	2.590	124.10
05250+3645	FYM 375	5:25:1	36:45:6.7	13.8-13.8	9.800	230.80
05406+2632	ITF 45	5:40:36.87	26:32:32.3	13.5-14.5	3.981	62.80
06105+2307	POU1101	6:10:29	23:6:54	12.8-12.8	10.600	207.70
06177+2348	POU1196	6:17:42	23:48:12	14.0-14.4	7.900	188.70
06214+2203	L 58	6:20:8.35	22:2:5.5	11.4-11.9	1.220	120.50
06220+2339	POU1261	6:22:2	23:39:0	12.2-12.6	5.300	66.10
07015+2317	POU2282	7:1:29	23:17:0	13.2-13.6	6.000	293.70
07430+2410	POU2877	7:42:59	24:10:24	12.5-13.4	11.320	327.20
09164+3014	LDS3868	9:16:23	30:14:6	14.7-17.4	35.000	230.00
09259-1530	LDS3891	9:25:52	-15:30:24	14.2-17.0	327.970	279.00
09332-7433	KOH 84	9:33:9.7	-74:33:10	15.4-.	0.222	231.40
09550+2738	FYM 230	9:54:57.01	27:38:6.59	11.4-12.9	36.000	280.00

Table 1 concludes on next page.

Magnitude Anomalies in the WDS

Table 1 (conclusion). 48 WDS Pairs That Have No Corresponding Catalog Star

WDS ID	Discover	RA	Dec	mva-mvb	Rho	Theta
10038+2246	POU3071	10:3:46	22:46:24	12.9-13.0	6.100	161.20
10386-7151	LDS6177	10:38:35	-71:51:18	14.1-14.6	4.000	340.00
11431+5546	LDS4137	11:42:59	55:45:6	13.5-17.5	6.000	244.00
13027+1521	LDS4309	13:2:36	15:20:54	15.2-17.5	163.000	237.00
13194-0939	LDS4344	13:19:17	-9:38:24	14.0-17.0	20.000	104.00
13289+2350	POU3141	13:28:49	23:49:48	12.6-13.6	13.700	90.00
13468-2759	LDS5793	13:46:54	-28:9:6	13.6-19.5	76.000	306.00
13484+5306	LDS5801	13:48:25	53:5:54	16.0-17.3	5.000	222.00
13485+0331	LDS3103	13:48:19	3:31:18	16.3-17.3	72.000	282.00
13507+0722	LDS3111	13:50:38	7:22:36	15.2-16.8	7.720	354.70
14086+2349	POU3157	14:8:36	23:48:48	11.2-13.0	8.200	16.70
15160+7111	LDS1815	15:16:2	71:11:6	13.3-15.8	10.000	49.00
15488-2842	LDS5846	15:48:50	-28:42:48	16.9-18.0	41.000	158.00
21117+2447	POU5236	21:11:43	24:46:12	12.2-13.5	6.000	91.10
21324+1054	LDS4894	21:32:28	10:52:48	16.2-18.7	6.950	7.00
22229-3341	LDS4961	22:22:58	-33:41:6	16.4-16.4	46.000	128.00
22300+0426	STF2912Ba,Bb	22:29:57	4:25:54	8.0-8.8	0.060	268.50
22391-2912	LDS5964	22:39:3	-29:12:18	13.0-16.0	120.000	260.00
22470+0325	FAR 21	22:46:57.3	3:24:42	16.46-19.82	2.400	58.00
22478-2510	LDS5977	22:47:36	-25:10:48	13.9-19.8	73.000	38.00
22575-2933	LDS5991	22:57:31	-29:33:48	15.0-16.8	28.000	315.00
23149-3047	LDS6017	23:15:2	-30:48:12	16.3-17.8	38.000	208.00
23194+2417	POU5798	23:19:26	24:16:24	11.8-11.8	19.100	90.20
23316-2549	LDS6036	23:31:36	-25:49:36	16.6-19.8	257.000	169.00

Magnitude Anomalies in the WDS

Table 2. 169 WDS Pairs that have no Corresponding Catalog Star Within 4mv of the WDS Primary

WDS ID	Discover	RA	Dec	mva-mvb	Rho	Theta	dmv
00200+3814	FYM 147DG	20:00.4	+38:13:38.6	15.4-15.4	3.2	279.7	7.6
00536+0510	OCC 917	53:33.0	+5:9:50	6.6-8.8	0.049	-1	4.85
01460+3254	J 3305	45:53.9	+32:54:18.09	11.3-13.0	3.659	158.7	18.9
02442+4914	STF 296BC	44:10.3	+49:13:54	10.-11.08	88.2	231.8	20.34
02557+3028	GII 2Ba,Bb	2:55:39	+30:28:3.19	13.4-13.8	0.454	155.1	4.08
02594+6034	MZA 14EF	59:22.1	+60:33:56.79	14.0-14.6	0.992	24.5	4.92
03423+3141	COU 691	42:15.9	+31:40:49.5	9.0-9.0	0.216	244.2	9.05
03447+3210	DCH 15	44:40.3	+32:9:32.59	12.8-13.7	0.13	186.6	17.59
03495-3504	LDS3537	49:32.1	-35:4:13.6	15.0-15.2	3	185	15.65
03541+3153	SLV 2BC	54:07.4	+31:52:49.8	9.16-11.24	32.23	309	7.89
03541+3153	SLV 2BD	54:07.4	+31:52:49.8	9.16-10.44	85.43	193	8.04
04290+1338	SIG 2	29:02.9	+13:37:58.7	13.2-13.7	0.294	131.6	17.33
04293-3124	SIG 4	29:18.4	-31:23:56.79	11.18-12.38	0.511	40.7	4.83
04352+5858	LDS3594	4:35:26	+58:57:6	14.1-14.6	2	80	16.43
05145-0812	BU 555BC	14:32.3	-8:12:5.89	7.5-7.6	0.124	29.8	6.49
05154+3241	STF 653BC	15:24.5	+32:41:25.29	10.9-7.33	22.65	209.9	2.28
05174+2424	POU 635	5:17:26	+24:23:54	12.9-13.5	16.3	227.4	17.59
05272+1758	STT 107BC	27:09.5	+17:57:49.89	10.1-11.8	7	57	20.1
05302-4705	RST 136BC	30:09.4	-47:4:38.4	11.7-12.7	0.778	84.6	5.8
05352-0522	GET 20FG	35:13.8	-5:22:6.89	14.40-.	2.2	-1	15.6
05352-0522	SMN 1Ha,Hb	35:13.9	-5:22:2.49	12.35-13.92	0.367	126	17.87
05352-0522	SMN 2Na,Nb	35:14.8	-5:22:29.29	12.40-12.40	0.301	145	18.35
05352-0523	GET 9DE	35:10.5	-5:22:45.69	14.76-.	1.8	-1	15.24
05352-0523	GET 25NO	35:14.7	-5:22:38.19	13.96-.	2.6	-1	16.04
05352-0524	PRS 11GH	35:12.2	-5:23:48.2	15.00-15.81	0.1	163	15.42
05352-0525	GET 16	35:13.1	-5:24:52.8	15.10-.	2.9	-1	14.9
05353-0522	GET 33HI	35:15.5	-5:22:48.49	16.06-.	2.3	-1	13.94
05353-0522	GET 44LM	35:16.9	-5:22:22.39	14.86-.	2	-1	15.14
05353-0522	GET 45NO	35:16.9	-5:22:35.49	14.60-.	2.6	-1	15.4
05353-0522	PRS 17Ua,Ub	35:17.6	-5:22:56.69	14.91-16.85	0.384	248.1	15.25
05353-0522	PRS 19Xa,Xb	35:18.6	-5:22:56.69	13.77-15.58	0.91	339	16.41
05353-0523	PTR 1Aa,Ab	35:15.8	-5:23:14.3	6.55-9.83	0.193	9.4	6.39
05353-0523	STF 748AB	35:15.8	-5:23:14.3	6.55-7.49	8.69	31.7	6.06
05353-0523	STF 748AC	35:15.8	-5:23:14.3	6.55-5.06	12.59	132.1	4.71
05353-0523	STF 748AD	35:15.8	-5:23:14.3	6.55-6.38	21.33	96.1	5.6
05353-0523	STF 748AE	35:15.8	-5:23:14.3	6.55-11.1	4.61	352.3	6.43
05353-0523	STF 748AH	35:15.8	-5:23:14.3	6.55-15.8	8.18	177.1	6.44
05353-0523	SMN 5Ba,Bb	35:16.1	-5:23:6.8	7.49-8.5	0.996	252.6	7.02
05353-0523	SMN 5Ba,Bc	35:16.1	-5:23:6.8	7.49-10.50	0.593	298.2	7.32
05353-0523	PTR 1Ba,Bd	35:16.1	-5:23:6.8	7.49-.	1.029	250.7	7.39
05353-0523	SMN 5Bb,Bc	35:16.1	-5:23:6.8	8.5-10.50	0.6	37	8.24

Table 2 continues on next page.

Magnitude Anomalies in the WDS

Table 2 (continued). 169 WDS Pairs that have no Corresponding Catalog Star Within 4mv of the WDS Primary

WDS ID	Discover	RA	Dec	mva-mvb	Rho	Theta	dmv
05353-0523	PTR 1Bb,Bd	35:16.1	-5:23:6.8	8.5-.	0.117	219.7	8.4
05353-0523	STF 748BC	35:16.1	-5:23:6.8	7.49-5.06	16.65	163.7	4.84
05353-0523	STF 748BD	35:16.1	-5:23:6.8	7.49-6.38	19.24	120.6	5.94
05353-0523	STF 748BE	35:16.1	-5:23:6.8	7.49-11.1	6.05	240.5	7.35
05353-0523	STF 748BF	35:16.1	-5:23:6.8	7.49-11.5	20.49	153.4	7.36
05353-0523	KSS 1Da,Db	35:17.2	-5:23:16.6	6.38-.	0.019	41	6.28
05353-0523	STF 748DE	35:17.2	-5:23:16.6	6.38-11.1	22.95	287	6.26
05353-0523	STF 748DF	35:17.2	-5:23:16.6	6.38-11.5	11.46	221.2	6.27
05353-0523	STF 748DG	35:17.2	-5:23:16.6	6.38-16.7	7.84	270.2	6.27
05353-0523	GET 37Ea,Eb	35:15.8	-5:23:9.8	11.1-.	2.2	-1	8.9
05353-0523	STF 748HI	35:15.8	-5:23:22.5	15.8-16.3	1.547	270.1	4.73
05353-0523	GET 30JK	35:15.2	-5:22:54.29	14.26-.	2.8	-1	15.74
05353-0523	GET 36LM	35:15.7	-5:23:22.5	14.5-.	1.6	-1	5.5
05353-0523	GET 39Na,Nb	35:16.1	-5:23:7.1	7.96-.	1	-1	7.86
05353-0523	PTR 2Qa,Qb	35:17.8	-5:23:15.5	9.69-13.0	0.303	178.3	9.53
05353-0523	GET 42RS	35:16.3	-5:23:16.5	11.4-.	2.6	-1	5.25
05353-0523	GET 43TU	35:16.6	-5:23:16.1	11.4-.	2	-1	5.25
05353-0524	PAD 2Da,Db	35:15.7	-5:23:47.8	14.-15.	0.49	-1	16.36
05353-0524	SMN 7Ea,Eb	35:15.9	-5:23:50.1	13.79-.	0.52	39.2	16.21
05353-0524	GET 38FG	5:35:16	-5:23:52.9	12.50-.	1	-1	17.5
05353-0524	PRS 24Ha,Hb	35:16.7	-5:24:4.5	13.77-15.58	0.13	339	16.41
05353-0524	SMN 6Ia,Ib	35:16.8	-5:23:26.7	12.97-13.44	0.396	34.6	6.28
05353-0524	GET 48JK	35:17.0	-5:23:37	14.9-12.9	3	155	17.25
05353-0524	SMN 8La,Lb	35:17.7	-5:23:41	12.6-.	0.88	98.5	17.39
05353-0524	PRS 22Ta,Tb	35:20.4	-5:23:30.2	15.73-19.09	0.68	278.7	14.31
05353-0525	PAD 3Aa,Ab	35:15.9	-5:24:54.69	15.9-16.	0.52	-1	14.8
05353-0526	PAD 4Ca,Cb	35:17.7	-5:25:32.3	16.1-16.	0.24	-1	14.7
05353-0526	PAD 5Ea,Eb	35:18.0	-5:25:33.3	14.9-16.	0.3	-1	15.43
05354-0524	PRS 34AB	35:21.2	-5:23:45.2	16.26-20.38	1.09	232	13.76
05354-0524	GET 56CD	35:21.8	-5:23:53.8	13.27-.	2.1	-1	16.73
05354-0524	PAD 8EF	35:22.1	-5:24:12.2	14.5-17.5	1.75	-1	15.56
05354-0524	GET 57GH	35:22.3	-5:24:14.3	13.82-.	1.9	-1	16.18
05355-0524	GET 60	35:28.4	-5:25:3.4	15.36-.	2.9	-1	14.64
05416-0153	BCK 3Ea,Eb	41:36.9	-1:52:33.29	11.6-12.2	0.42	200	5.54
05416-0154	BCK 1Ea,Eb	41:36.6	-1:53:54.49	10.6-11.1	0.18	40	19.93
05518-4434	BLR 1	51:46.0	-44:34:13	14.86-15.39	2.2	359.6	15.65
06221+2427	POU1262AB	6:22:06	+24:26:48	13.2-14.4	6.2	139.3	4.46
06221+2427	POU1263AC	6:22:06	+24:26:48	13.2-14.4	13.3	122.9	4.46
06234+2332	POU1285	6:23:21	+23:32:18	14.2-14.3	5.1	107.7	16.5
06323+5225	WOR 6	32:18.4	+52:24:50.2	10.4-10.5	0.77	159.8	8.6
06451-1643	AGC 1BC	45:08.9	-16:43:2	8.5-12.6	79.08	29.7	8.37
07178-2559	BRG 26Aa,Ab	7:17:47	-25:59:8.69	13.5-.	0.1	311.6	4.72

Table 2 continues on next page.

Magnitude Anomalies in the WDS

Table 2 (continued). 169 WDS Pairs that have no Corresponding Catalog Star Within 4mv of the WDS Primary

WDS ID	Discover	RA	Dec	mva-mvb	Rho	Theta	dmv
07179+2319	POU2648	7:17:59	+23:18:54	13.0-14.1	22.36	350.3	6.08
07274+0514	WDK 2	27:24.1	+5:14:5.19	10.03-.	0.17	327	6.02
07412+0219	BAL1806	41:09.9	+2:19:54.29	12.3-13.2	12	247.6	6.68
07467+2001	RED 9	46:42.6	+20:0:32.2	12.23-12.83	0.351	214.3	18.26
09047+3441	ALI 122	04:41.2	+34:40:51.7	12.79-12.86	5.66	32	17.92
09086-2550	TOK 357BC	08:36.6	-25:50:20.19	11.8-19.3	0.102	268.6	4.96
09252+1602	FAR 8	25:13.5	+16:1:44.2	16.26-17.30	4.51	287	14.09
10522+4423	DUP 2	52:13.5	+44:22:55.89	14.99-15.50	0.055	97.2	15.53
11112-4106	JAO 5	11:14.8	-41:5:31.2	13.2-17.3	4.28	62.2	5.64
12302+3211	LDS4221	12:30:07	+32:10:0	16.6-16.9	93	102	14.01
12538-6022	CRU9008CD	53:48.9	-60:22:44.2	10.0-10.4	7.73	87.4	3.47
13062+2902	BU 1083BC	06:10.0	+29:1:40.79	11.7-12.0	0.416	252.2	4.55
13172-1230	GWP1964	17:12.1	-12:30:26.1	10.3-15.6	10.21	64.4	8.14
13529-1943	GWP2116	52:54.5	-19:43:22	11.5-14.9	500.4	147.9	5.98
14048-3200	LPR 2	04:49.5	-31:59:33	14.9-16.1	0.134	275.3	15.41
14125+1636	WSI 117	12:27.9	+16:35:42.39	16.3-16.6	0.882	47.1	3.67
14325+4911	HU 57BC	32:30.9	+49:11:2.6	12.62-11.77	1.21	135	2.92
14503+2355	POT 1BC	50:15.9	+23:54:41.79	13.9-14.2	0.1	316.9	7.34
15096-6843	DAM 20DG	09:36.6	-68:43:16.8	11.39-11.39	5.8	82	3.79
15186+2356	COU 307	18:34.8	+23:56:42.8	9.5-9.6	0.35	3.4	21.2
15200-4423	BUG 12	20:02.2	-44:22:41.9	13.55-14.70	1.174	152.9	16.77
15500-0355	RST4553BC	49:57.3	-3:55:11	12.5-13.0	1.49	304.8	4.82
15503-4524	DON 764BC	50:16.3	-45:24:9.39	11.6-11.9	0.34	328.5	4.83
15582-3005	BRT3026	58:10.5	-30:4:17.2	11.2-.	3.61	107.9	4.12
16078-1750	LDS4632	16:07:45	-17:49:30	12.9-18.8	220	136	5.34
16264-2425	ALO 2CD	26:25.3	-24:24:45	13.2-16.9	7.76	273.1	16.83
16268-2428	BNY 1	26:48.5	-24:28:38.89	11.3-12.9	4.15	343.2	18.92
16268-2438	BNY 2	26:49.0	-24:38:25.1	10.0-11.7	3.57	291.1	8.24
16274-2430	ALO 8AB	27:22.0	-24:29:39.79	15.4-19.9	6	84	14.61
16274-2430	ALO 9CD	27:24.6	-24:29:35.4	14.7-15.0	8.47	313	15.91
17113-2725	CHN 26AC	11:17.3	-27:25:8.2	14.3-15.0	5.068	329.7	16.15
17296+2916	LDS4744	29:29.3	+29:16:9.29	16.9-18.0	15.93	162.2	13.43
17297-3143	PRO 165	29:42.4	-31:43:19	12.0-12.6	3.52	202.3	18.49
17408-3052	BSS 1	17:40:50	-30:52:4.29	10.0-15.9	0.41	206	20
17465+2743	AC 7BC	46:25.1	+27:43:1.39	10.2-10.7	0.75	289.2	20.33
17465+2743	ABT 14BC,D	46:25.1	+27:43:1.39	9.78-12.33	335.04	9.9	20.31
18138-2104	SLV 7BD	13:44.6	-21:3:35.4	10.48-9.96	40.92	331	20.56
18138-2104	SLV 7BE	13:44.6	-21:3:35.4	10.48-9.22	64.43	105.8	21.07
18146+0422	BAL2922	14:34.5	+4:21:56.39	11.6-12.1	53.81	84.3	6.73
18173+2832	LDS4782	17:18.2	+28:31:10.69	16.6-18.0	48.02	61.1	13.66
18178-1537	J 2205AB	17:49.1	-15:37:21.8	11.0-13.0	4.581	99.9	5.72
18178-1537	J 2205AC	17:49.1	-15:37:21.8	11.0-14.5	13.86	47.2	5.61

Table 2 concludes on next page.

Magnitude Anomalies in the WDS

Table 2 (conclusion). 169 WDS Pairs that have no Corresponding Catalog Star Within 4mv of the WDS Primary

WDS ID	Discover	RA	Dec	mva-mvb	Rho	Theta	dmv
18289+0515	LDS5237	18:28:52	+5:14:36	15.6-19.5	6	329	14.42
18342-3158	PRO 205	34:08.8	-31:57:15	11.91-12.2	3.57	178.8	18.7
18369+3846	STF3136BC	36:56.1	+38:45:44.8	9.5-11.0	83.7	310	20.74
18451-6358	BIL 1	45:07.1	-63:57:47.39	12.6-.	1.2	170.2	4.97
19025+2432	POU3663	19:02:36	+24:31:42	12.7-13.3	2.6	176	17.79
19064-1154	RST4028Ba,Bb	19:06:25	-11:53:50	12.9-13.0	0.252	78.2	3.61
19121+0254	AST 1	12:13.5	+2:53:15.59	11.29-13.11	0.125	296.9	5.29
19302+3842	ADP 5	30:13.3	+38:41:49.79	15.0-15.8	2.35	18.6	15.42
19390+1528	J 774	38:58.4	+15:28:11	9.5-10.0	3.68	220.4	8.16
19407+2343	FYM 103CD	40:39.6	+23:43:4.69	11.4-14.8	31	94	4.7
19484+2518	POU4090	19:48:23	+25:17:54	14.6-14.7	14.18	213.7	4.87
19492+2316	POU4103	19:49:07	+23:16:0	14.3-14.7	8.8	142.4	16.27
19495+3843	ES 84BC	49:27.8	+38:42:26	11.1-13.2	20.29	67.4	19.04
19563+3505	BU 980CE	56:18.4	+35:5:0.6	10.5-11.5	8.31	264	6.12
20090+3258	SEI 916	09:00.4	+32:57:29.4	10.5-11.0	5.442	29.4	8.19
20097+3240	SEI 933	09:46.6	+32:39:59.59	11.0-11.0	4.482	334.8	7.55
20098+3130	SEI 932	09:47.6	+31:30:5.59	10.0-10.0	5.394	291	8.05
20181-1233	AGC 12BC	18:03.3	-12:32:48	11.2-11.5	1.2	245.4	6.9
20286+5924	ADP 6	28:34.0	+59:24:17.6	15.0-16.5	4.43	158.9	15.24
20322+1759	GWP2966	32:10.6	+17:58:50.29	10.7-12.2	121.03	74.7	19.54
20357+3901	SEI1185	35:42.6	+39:1:8.7	10.5-11.0	3.467	298.4	20.03
20358+4123	NML 1	35:48.1	+41:22:42.4	16.2-16.4	0.149	15.8	4.42
20380+3806	SEI1197	37:55.5	+38:5:20.1	11.0-11.0	14.728	173.5	19.75
20400+2350	POU4832	20:40:00	+23:50:24	11.8-13.9	16.47	26.6	5.19
20476+4347	CHN 28	47:37.5	+43:47:24.79	15.4-.	5.01	56.9	4.09
20549+4451	LDS2466	54:52.0	+44:50:46.2	15.0-16.3	4.52	285.7	15.28
21009+4730	BU 1290CD	02:40.7	+45:53:5.2	14.0-15.0	2.9	90	5
21023+3931	WRD 4AG	02:30.0	+39:30:38.3	6.62-12.46	95	230	4.22
21179+3454	STT 433BC	17:54.3	+34:53:37.09	10.0-10.0	10.13	141.3	20.75
21203+4921	BU 839CB	20:17.5	+49:20:35.7	10.12-11.9	13.69	29.6	4.53
21214+3321	J 3136	21:01.8	+33:18:59.7	12.5-12.6	7.8	177.6	18.2
21231+6414	LDS4882	23:04.3	+64:14:25.3	15.9-21.0	11.38	162.4	14.1
21401+2426	POU5456	21:40:11	+24:26:18	12.2-12.3	3.7	263.5	18.5
21415+3817	SEI1532	41:28.7	+38:17:27.19	10.8-11.0	5.06	138.5	8.08
21491-6413	CVN 30	49:06.2	-64:12:55.9	15.5-.	0.074	122	14.5
22200+4304	LOS 10BC	20:02.4	+43:6:2.69	16.0-17.2	1.08	138.8	3.99
22225+2922	AZC 119	22:28.8	+29:22:12.49	16.2-17.2	36.11	13.6	5.14
22234+4531	LOS 11BC	23:22.4	+45:30:42	14.5-15.3	2.65	198.8	4.73
22464+2336	POU5747	22:46:24	+23:35:48	12.8-13.0	15.2	339.2	17.85
22468+4420	HER 5BC	46:49.5	+44:20:21.1	12.4-12.9	1.214	255	18.13
23177+4901	KUI 116BF	17:44.8	+49:0:47	13.0-16.	6.36	184.7	7.91
23205+0002	LDS5254	23:20:30	+0:2:12	13.1-20.7	6	323	4.65
23526+2417	POU5868	23:52:34	+24:17:54	13.6-13.8	8.9	74.7	5.99

Another Kind of Data Mining - Looking for Anomalies

Wilfried R.A. Knapp
Vienna, Austria
wilfried.knapp@gmail.com

Abstract: Comparing the data of different star catalogs with the WDS catalog data is a highly suitable method to find WDS entries that need to be further checked. This approach is similar to the WDS Neglected Doubles lists but it also adds the magnitude discrepancies between the WDS and the other catalogs.

Report

It should be noted that the WDS is a compilation of previously published lists, quite often with estimated visual magnitudes. Errors in these older lists are carried over into the WDS, if not meanwhile corrected by recent precise measurements. This explains why less often observed WDS entries are sometimes listed with magnitudes quite different from those given in other catalogs.

A data mining study by Tom Bryant (2017, previous article) using software written by himself for comparison of the data of different star catalogs with the content of the WDS catalog (see his website http://mainsequence.org/html/wds/magnitudeStudy/MagnitudeAnomalies.html) selected objects with an assumed magnitude discrepancy larger than 1 mag. That this approach delivered a list of several thousand entries with suspect data is not very surprising. The study also lists ~60 stars not found in other catalogs. This study alone does not help much to make the WDS catalog a better one - but it can be used for selecting objects in need of measurement similar to the WDS Neglected Doubles lists but with additional data about the magnitude discrepancies.

This report takes a randomly selected sample of objects from Bryant's list that were close to the meridian at the date of this research with separation and magnitudes suitable for resolution with remote telescopes iT18 and iT27 (see specifications in the acknowledgements).

The current (beginning of 2016) WDS catalog data for these objects is listed in Table 1.

The measurement results are given in Table 2. The Notes column provides additional information, especially the comparison of the measurement results with the current WDS catalog data. Abbreviations in the

(Continued on page 12)

Table 1: WDS catalog values per beginning of 2016 for the selected objects intended for measurement

WDS ID	Name		RA	Dec	Sep	Mv A	Mv B	PA	Con
10191+3620	ES 2566	AB	10:19:12.20	+36:19:49.9	4.1	11.00	11.10	218	LMi
10457+3209	MLB 845	AB	10:45:40.24	+32:09:46.6	3.4	10.50	11.00	359	LMi
10566+2714	SLE 887	AB	10:56:37.94	+27:13:42.7	15.2	11.20	12.40	342	LMi
10513-5431	BRT2055	AB	10:51:21.30	-54:29:24.7	3.3	10.63	10.60	153	Vel
10346-5607	BRT2564	AB	10:34:41.66	-56:05:54.7	3.5	11.70	12.30	236	Vel
10158-5225	CPO 286	AB	10:15:48.78	-52:24:48.2	7.3	10.50	12.00	318	Vel
10560-4445	DON1092	AB	10:56:02.09	-44:45:16.6	3.5	11.00	12.80	82	Vel
10570-5545	BRT2572	AB	10:57:02.44	-55:44:55.0	4.3	10.50	11.00	259	Vel
08416-4615	DON1074	AB	08:41:33.28	-46:15:47.8	3.3	11.00	13.00	332	Vel

Another Kind of Data Mining - Looking for Anomalies

Table 2: Photometry and astrometry results for the selected objects

		RA	Dec	dRA	dDec	Sep	Err Sep	PA	Err PA	Mag	Err Mag	SNR	dVmag	Date	N	Notes
ES 2566	A	10 19 12.182	36 19 49.49	0.16	0.12	4.006	0.200	219.304	2.858	13.151	0.083	15.95	0.05	2016.20	2	iT18 stack 2x3s. SNR A and B <20. Measurement confirms WDS Sep and PA but both listed WDS Mags are far too bright
	B	10 19 11.972	36 19 46.39							13.115	0.085	15.40				
MLB 845	A	10 45 40.193	32 09 44.85	0.17	0.24	3.522	0.294	358.14	4.774	13.332	0.135	13.28	0.11	2016.20	2	iT18 stack 2x3s. SNR A <20 and B <10. Measurement confirms WDS Sep and PA but both listed WDS Mags are far too bright
	B	10 45 40.184	32 09 48.37							14.578	0.231	4.86				
SLE 887	A	10 56 37.946	27 13 43.26	0.20	0.18	14.553	0.269	340.401	1.059	12.750	0.123	19.14	0.11	2016.20	2	iT18 stack 2x3s. SNR A <20 and B <10. Measurement confirms WDS Sep and PA but both listed WDS Mags are far too bright
	B	10 56 37.580	27 13 56.97							14.042	0.159	8.95				
BRT2055	A	10 51 21.297	-54 29 24.81	0.11	0.11	3.061	0.156	156.162	2.909	12.664	0.083	53.04	0.08	2016.26	2	iT27 stack 2x3s. WDS Sep and PA slightly different but within or at least near the calculated error range. Both WDS Mags far too bright
	B	10 51 21.439	-54 29 27.61							13.395	0.088	28.52				
BRT2564	A	10 34 41.629	-56 06 54.81	0.12	0.12	3.718	0.170	235.419	2.614	12.021	0.102	58.55	0.10	2016.26	2	iT27 stack 2x3s. WDS Sep and PA within the calculated error range. Both WDS Mags ~0.3 too bright
	B	10 34 41.263	-56 06 56.92							12.592	0.103	46.26				
CPO 286	A	10 15 48.752	-52 24 47.87	0.11	0.11	7.444	0.156	318.323	1.197	12.092	0.091	70.40	0.09	2016.26	2	iT27 stack 2x3s. WDS Sep and PA within the calculated error range. Both WDS Mags far too bright
	B	10 15 48.211	-52 24 42.31							13.073	0.093	42.63				
DON1092	A	10 56 02.083	-44 45 16.62	0.10	0.10	3.465	0.141	81.870	2.337	12.781	0.073	56.92	0.07	2016.26	2	iT27 stack 2x3s. WDS Sep and PA very close to the measurement results. Both WDS Mags far too bright
	B	10 56 02.405	-44 45 16.13							13.570	0.075	38.41				
BRT2572	A	10 57 02.446	-55 44 54.89	0.08	0.08	4.394	0.113	260.304	1.475	11.498	0.081	71.11	0.08	2016.26	2	iT27 stack 2x3s. WDS Sep and PA very close to the measurement results. Both WDS Mags far too bright
	B	10 57 01.933	-55 44 55.63							12.246	0.084	42.18				
DON1074	A	08 41 33.293	-46 15 47.69	0.09	0.10	3.656	0.135	331.727	2.107	11.708	0.081	73.07	0.08	2016.27	2	iT27 stack 2x3s. WDS Sep somewhat outside error range but PA very close to the measurement result. Both WDS Mags a bit too bright but delta is less than 1 mag
	B	08 41 33.126	-46 15 44.47							13.494	0.094	21.74				

table headings are as follows:

- **RA, Dec:** J2000 coordinates based on 4th-order fit plate solving with URAT1 (for LMi) and UCAC4 (for Vel) reference stars in the 10.5 to 14.5Vmag range
- **dRA, dDec:** Average RA and Dec plate solving errors provided by Astrometrica software
- **Sep:** Separation in arc seconds calculated from the RA/Dec coordinates using the formula provided by R. Buchheim (2008)
- **Err Sep:** Separation error range estimation in arc seconds calculated from the average plate solving errors as $\sqrt{dRA^2 + dDec^2}$.
- **PA:** Position angle in degrees calculated from the RA/Dec coordinates using the formula provided by R. Buchheim (2008)
- **Err PA:** PA error range estimation in degrees calculated as arctan(*Err_Sep*/*Sep*) assuming the worst case that *Err_Sep* points in the right angle to the direction of the separation means perpendicular to the separation vector
- **Mag:** Visual magnitudes, as photometry result provided by the Astrometrica software
- **SNR:** Signal to noise ratio for a given star
- **dVmag:** The average Vmag error over all used URAT1/UCAC4 reference stars
- **Err Mag:** Magnitude error range estimation calculated using
- **Date:** The Bessel epoch of the observations
- **N:** The number of observations

$$dmag = \sqrt{dVmag^2 + \left[2.5\log_{10}\left(1 + \frac{1}{SNR}\right)\right]^2}$$

Summary

The measurement results of the randomly selected objects confirm Bryant's study. While the measured Sep and PA values correspond in most cases with the current WDS catalog data rather well, the measured magnitudes were in most cases more than 1 magnitude fainter than WDS listed. A quick check of other catalogs like APASS and UCAC4 show that the methods used in this study are consistent. However, these catalogs do mostly not offer sufficient data usable for correcting the WDS catalog, only in case of SLE887 APASS offers Vmags for both components with values near the measurement results.

Acknowledgements

The following tools and resources have been used for this research:

- Washington Double Star Catalog as data source for the selected objects
- iTelescope: Images were taken with
- iT27: 700mm CDK with 4531mm focal length. CCD: FLI PL09000. Resolution 0.53 arcsec/pixel. V-filter. Located in Siding Spring, Australia. Elevation 1122m
- iT18: 318mm CDK with 2541mm focal length. CCD: SBIG-STXL-6303E. Resolution 0.73 arcsec/pixel. V-filter. Located in Nerpio, Spain. Elevation 1650m
- AAVSO VPhot for initial plate solving and stacking
- AAVSO APASS providing Vmags
- UCAC4 catalog (online via the University of Heidelberg website and Vizier and locally from USNO DVD) for counterchecks
- UCAC4 and URAT1 catalog for high precision plate solving
- MaxIm DL6.12 for countercheck plate solving with UCAC4
- Aladin Sky Atlas v8.0 for counterchecks
- SIMBAD, VizieR for counterchecks
- 2MASS All Sky Survey Images for counterchecks
- AstroPlanner v2.2 for object selection, session planning and for catalog based counterchecks
- Astrometrica v4.9.1.420 for plate solving with UCAC4 and URAT1 astrometry and photometry measurements

Special thanks to Paul Rodman (author of AstroPlanner) for providing me with the current APASS catalog for local use with AstroPlanner.

References

Buchheim, Robert, 2008, "CCD Double-Star Measurements at Altimira Observatory in 2007", *Journal of Double Star Observations*, **4**, 27-31.

Bryant, Tom, 2017, "Magnitude Anomalies in the WDS", *Journal of Double Star Observations*, **13**, 2-8.

Quasi-Speckle Measurements of Close Double Stars With a CCD Camera

Richard Harshaw
Brilliant Sky Observatory
Cave Creek, AZ
rharshaw51@cox.net

Abstract: CCD measurements of visual double stars have been an active area of amateur observing for several years now. However, most CCD measurements rely on "lucky imaging" (selecting a very small percentage of the best frames of a larger frame set so as to get the best "frozen" atmosphere for the image), a technique that has limitations with regards to how close the stars can be and still be cleanly resolved in the lucky image. In this paper, the author reports how using deconvolution stars in the analysis of close double stars can greatly enhance the quality of the autocorellogram, leading to a more precise solution using speckle reduction software rather than lucky imaging.

1. Introduction

For about a year now I have been measuring double stars with a CCD and a C-11 SCT telescope (Harshaw, 2016A, 2016B, 2016C). As a general rule, the CCD gives good results for wider and brighter pairs, but is not as efficient an instrument on close and fainter pairs.

For instance, the CCD can do speckle interferometry well (Harshaw, 2015; Anton, 2015). But speckle requires short integration times (usually 40 ms or less) and this means the Skyris 618C I have been using is limited to about 7.50 magnitude for the stars to register on the chip at such short integration times.

Speckle also requires both stars to be in the same isoplanatic patch, which means they must be normally 5 arc seconds or closer (perhaps up to 7" on nights of superb seeing).

Fainter pairs, of course, require longer integration times—up to 2 seconds for an 11.00 magnitude star. Such integration times are far too long for speckle interferometry, and, for that matter, lucky imaging.

However, I use David Rowe's "The Speckle Toolbox" for my data reductions and image measurements, even for those pairs too faint or wide for speckle.

The Speckle Toolbox (STB) contains many powerful tools for speckle analysis of a double star, but it can also render excellent solutions for CCD measurements. When making a speckle measurement, I normally capture 1000 frames (which are compiled into a FITS cube) of the target star, and then capture 1,000 frames of a nearby single star that is used to deconvolve the target star image. Deconvolution is a process that computes the Fourier Transform of a single star, which of course includes the telescope's optical behavior, and applies that solution for that single star to the image of a close double star. The result is a cleaner final image that is normally very easy to measure with STB.

As an example, consider the autocorellograms of a speckle pair, BU 560 (a 7.77, 8.24 magnitude pair, 1.702" rho) shown in Figure 1.

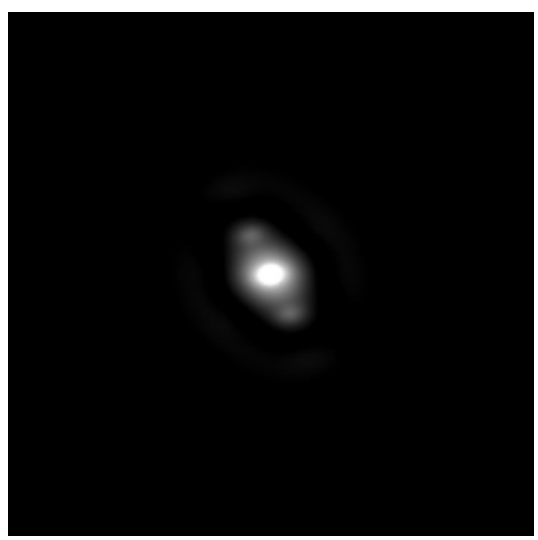

Figure 1: Bu 560 Autocorellogram without Deconvolution

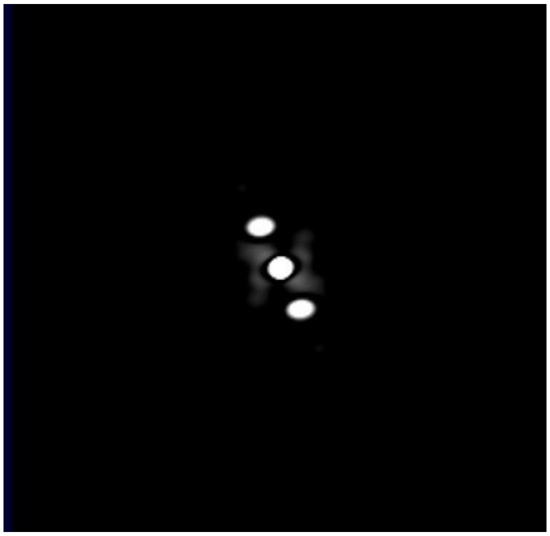

Figure 2: Bu 560 with Deconvolution

Figure 2 shows the same star with the deconvolution star processed in the autocorellogram.

Obviously, deconvolution can vastly improve an autocorellogram, letting one make precise measurements without ambiguity.

And after reading a paper in the 2013 issue of JDSO (Wiley, 2013), I began to wonder if the speckle analysis functions of STB, including using deconvolution stars, could be used to provide a better analysis of a pair than lucky imaging, even for pairs with integration times far longer than are acceptable for speckle.

For comparison purposes, Figure 3 is a lucky image rendered by Reduc, a powerful analytical program by Florent Losse.

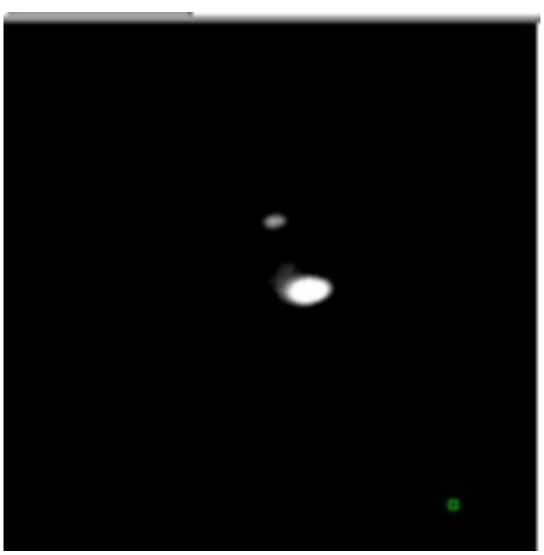

Figure 3: Lucky Image of Bu 560.

2. Equipment Used

The camera I used for these tests is a Skyris 618C color CCD camera sold by Celestron (but built by the German firm The Imaging Source). The Skyris was mounted downstream of a Televue 2.5x PowerMate mated to one arm of a flip mirror, the other arm directing starlight to the acquisition eyepiece. A picture of the setup is shown in Figure 4.

The camera was controlled with FireCapture 2.5 Beta, a very utilitarian program by Torsten Edeleman of WonderPlanets (www.wonderplanets.de). The telescope was controlled by a Lenovo computer running Windows 10 via TheSky 6.0 software. Images were saved to a 2 TB external hard disk drive that could be detached after the observing run and taken indoors for processing and analysis later.

3. Methodology

When doing speckle work, I take 1,000 frames (a “FITS cube”) of both the target pair and the deconvolution star (a star that is within 4 degrees of the target pair and nearly the same in magnitude). I usually take several 1,000 frame FITS cubes of each target, but only one set for the deconvolution star.

However, when I am doing CCD imaging (not speckle)— mainly for pairs that are wider than 5 arc seconds in rho or fainter than 7.5 magnitude— I make files of 200 frames each for the target pair and the deconvolution star. Whereas a typical integration time for speckle might be in the neighborhood of 30 ms, integration times for fainter pairs may run as high as 1.75 seconds or even longer.

Losse’s Reduc program is then used to select the best 25% of the Signal-to-Noise ratio frames. These frames are then bound into a small FITS cube of 50 frames. These mini-cubes are then pre-processed by

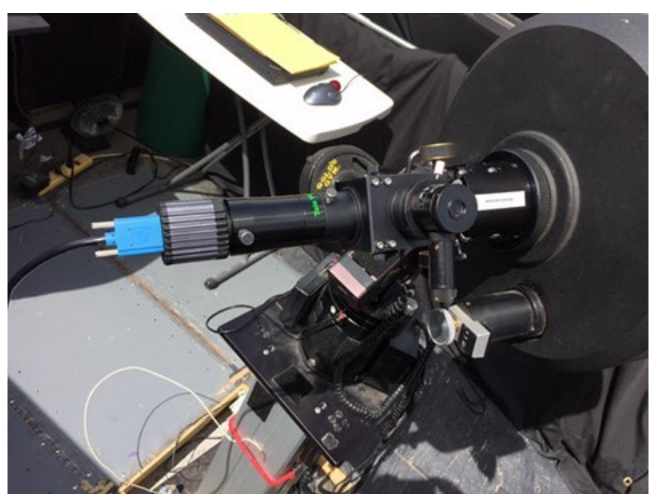

Figure 4: The Skyris 618C attached to the C-11 SCT.

Table 1: The Target Pairs and Their Deconvolution Stars

Pair	Discoverer Code	Deconvolution Star
1	STF 170	SAO 4541
2	STF 182	SAO 12065
3	STF1413	SAO 99004
4	STF1476	SAO 137795

STB and, after pre-processing, analyzed using STB's speckle analysis routine, in which the target pair file is chosen and the deconvolution star is also selected.

Once STB generates the autocorellogram, it is a simple matter to use STB's astrometry function to make the measurements for theta and rho. STB can render values to the nearest thousandth in both degrees and arc seconds, and it does so with a little higher accuracy than measuring a lucky image.

Four pairs were imaged and analyzed as shown in Table 1.

4. Results

In Figures 5 through 8, I present, side by side, the autocorellograms for each of the four pairs of Table 1. In all but one case (STF 182), the deconvolution star improved the autocorellogram, resulting in a better measurement.

Table 2 shows the resulting measuements with and without deconvolution.

5. Discussion

The data sample is too small to draw general conclusions, but it does suggest that significant differences are to be found between deconvolved autocorellograms and those made without deconvolution.

6. Conclusion

This brief experiment shows that deconvolution stars can help generate quality autocorellograms for double stars even when they are not being measured as speckle candidates (due to their faint magnitudes pushing the integration times beyond the 40 ms guideline considered the upper limit for speckle interferometry). In all four cases, STB was not able to lock onto the companion star to obtain a measurement in the autocorellograms made without deconvolution, but could lock onto the companion in every deconvolved autocorellogram (except STF 1413).

It is my plan going forward to obtain deconvolution star images for all close pairs that are too faint for speckle.

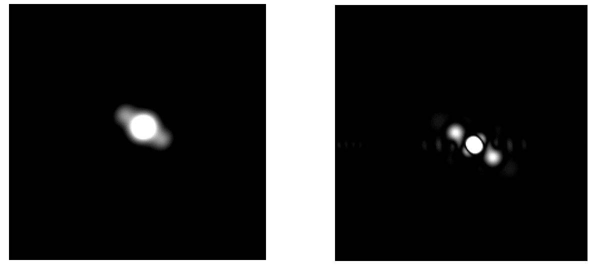

Figure 5. STF 170. Without deconvolution (left image), and with deconvolution.

Figure 6. STF 182, without deconvolution (left) and with deconvolution.

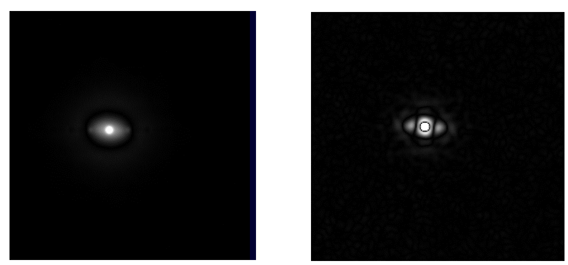

Figure 7. STF 1413, without deconvolution (left) and with deconvolution.

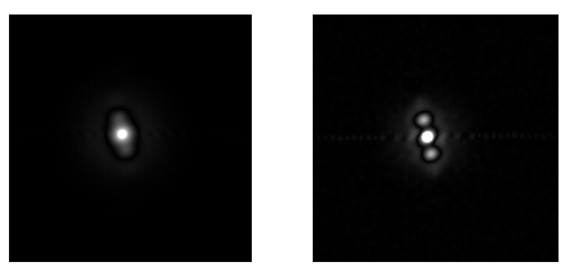

Figure 8. STF 1475, without deconvolution (left) and with deconvolution.

Quasi-Speckle Measurements of Close Double Stars With a CCD Camera

Table 2: Measured Theta and Rho With and Without Deconvolution

Star	Last Theta	Last Rho	Theta No	Theta Yes	Diff	Rho No	Rho Yes	Diff
STF 170	243	3.1	244.335	244.406	-0.071	3.0126	3.1400	-0.1274
STF 182	124	3.6	126.876	124.113	2.763	2.9440	3.7080	-0.764
STF1413	271	1.8	n/a	270.868	—	n/a	2.0120	—
STF1476	16	2.3	17.167	17.859	-0.692	2.4250	2.3700	0.055

7. Acknowledgements

This research has made use of the Washington Double Star Catalog maintained at the U.S. Naval Observatory.

8. References

Anton, Rainer, 2015, "Double Star Measurements at the Southern Sky with a 50 cm Reflector and a Fast CCD Camera in 2014", *JDSO*, **11**, 81-90.

Harshaw, Richard, 2015, "Measurements of 42 Wide CPM Pairs with a CCD", *JDSO*, **11**, 424-428.

Harshaw, Richard, 2016A, "CCD Measurements of 66 Rectilinear and Probable Rectilinear Pairs: The Autumn 2015 Observing Program at Brilliant Sky Observatory, Part 1", *JDSO*, **12**, 376-387.

Harshaw, Richard, 2016B, "CCD Measurements of 8 Double Stars With Binary Nature The Autumn 2015 Observing Program at Brilliant Sky Observatory, Part 2", *JDSO*, **12**, 388-393.

Harshaw, Richard, 2016C, "CCD Measurements of 141 Proper Motion Stars: The Autumn 2015 Observing Program at the Brilliant Sky Observatory, Part 3", *JDSO*, **12**, 394-399.

Wily, Ed, 2013, "A Pixel Correlation Technique for Smaller Telescopes to Measure Double Stars", *JDSO*, **9**, 142-151.

The Winter 2015 Observing Program at Brilliant Sky Observatory: Report on the Measurement of 112 Pairs

Richard Harshaw
Brilliant Sky Observatory
Cave Creek, AZ
rharshaw51@cox.net

Abstract: I report on the measurement of 111 double stars as a continuation of the seasonal observing program conducted at Brilliant Sky Observatory in Cave Creek, Arizona, using a C-11 and Skyris 618C color CCD camera.

1. Introduction

The Winter 2015 observing program at Brilliant Sky Observatory (located in Cave Creek, AZ at N 33.794742° and W 111.980638°) was truncated this year due to two months of the cycle being consumed with testing various CCD, EMCCD, and CMOS cameras for use in speckle interferometry with an 11-inch SCT. However, several weeks were available for observing double stars using a Skyris 618C color CCD camera (sold by Celestron and manufactured by The Imaging Source). A similar program was conducted in the autumn of 2015 and was reported in three articles in the JDSO (Harshaw 2015A, 2015B, and 2015C). These articles explain the equipment used and my methodology. Interested readers may wish to read those articles if they wish to know the details of how I obtain measurements with the Skyris.

2. Equipment Used

The equipment used in this program is as follows:

- Telescope: Celestron C-11 SCT mounted on a Celestron CGEM-DX mount affixed atop a PierTech elevating pier
- Camera control: FireCapture 2.5.2 Beta (by Torsten Edelman)
- Telescope control: TheSky 6.0
- 2TB external HDD for data storage
- Analysis software: REDUC (by Florent Losse), and the Speckle Toolbox 1.03 (“ST”, by David Rowe).

3. Methodology

After “awakening” the mount and accurate synching of the telescope to the sky, the telescope control software (TheSky 6.0) is then started and the telescope synched to TheSky. The star used for mount alignment is then imaged with the camera to adjust focus and integration times.

Once everything is ready, I then run 12 to 20 drift images of the alignment star if needed. On most nights, there is no need to do this unless the camera has been moved or the optical train modified (by the addition of a Barlow or filter set). If drifts are needed, they are analyzed using the Drift function in the Speckle Toolbox.

Stars to measure are then accessed via TheSky and centered on the camera chip using an illuminated reticle on the telescope’s flip mirror acquisition eyepiece arm. Once the star is centered on the crosshairs, the flip mirror is moved so the starlight falls on the camera chip.

A region of interest, measuring 256 pixels by 256 pixels (or, for much wider pairs, 512 x 512 pixels) is then centered around the star, and the image enlarged 200% to fine-tune the focus. Once all is set and ready, a file name is created for the star and the exposure begun.

For speckle cases, I shoot 1,000 frames (at integration times of 40 ms or less), each set of frames being shot in FITS format and later bound into a FITS cube for analysis by STB. Usually 3 or more such files are recorded. A deconvolution star (a single star of nearly the same magnitude or a little brighter and less than 4° away from the target star and within 4 minutes of shooting the target star) is then shot with 1,000 frames. [The deconvolution star is used to model the telescope’s optical quirks and atmospheric turbulence so these corrections can be applied to the double star image, resulting in a cleaner autocorellogram (Harshaw, 2016 D submitted).]

For CCD cases (too faint for speckle or wider than 5") I shoot 500 frames and use REDUC to select the best 10% for signal-to-noise ratio and bind the 50 chosen frames into a FITS mini-cube for analysis. For pairs closer than 4" I also shoot a single deconvolution star (even though I am not performing speckle analysis on this pair) as I discovered that using a deconvolution star for non-speckle cases can render better results using STB than doing lucky imaging.

4. Results

The results of the Winter 2015 observing program at Brilliant Sky Observatory are summarized in the following four tables:

- Table 1: 59 proper motion pairs
- Table 2: 3 short arc binaries
- Table 3: 3 linear cases
- Table 4: 1 speckle case

Column headers in the tables are defined as follows:

- WDS No: the WDS number of the pair
- Disc Code: the Discoverer's code and components
- Date: decimal date of the observation
- Obs: number of measurements made on the star
- Last Meas: year of the last measure listed in the WDS
- Last Theta: value of theta for the year of the last measure
- Last Rho: value of rho for the year of the last measure
- Meas Theta: value of theta as measured on the night of observation
- Meas Rho: value of rho as measured on the night of observation
- Residual Theta: difference between my measurement of theta and the last one recorded in the WDS
- Residual Rho: difference between my measurement of rho and the last one recorded in the WDS

In addition to these measurements, several of these stars have older measurements that appear to be quadrant reversals, quadrant flips, or outright errors. These include:

- WDS 02278+7247 (HJ 2132AB): HJ 1831.83.
- WDS 02425+4016 (STF 292): Mai 1863.8.
- WDS 02548+4332 (HJ 2162 AB): HJ 1831.98.
- WDS 03070+6744 (HJ 1131): HJ 1828.0 and Sin 1989.03.
- WDS 03111+5544 (SCA 9 AB): Sca 1985.61.
- WDS 03136+3909 (STF 364): Vat 1906.03.
- WDS 03207+8459 (STF 319): Shr 1910.87.
- WDS 10205+0626 (STF 1426 AB): Wz 1907.26.
- WDS 10376+0505 (HJ 2540): HJ 1830.29.

Also, deconvolution stars were used for WDS 01554+7613 (3.10"), WDS 10123+1621 (1.80"), and WDS 10493-0401 (2.30").

All of my measurements plotted at or near the center of the scatter pattern of the historical measurements.

Figure 1 is a data plot for WDS 09200+0500. It shows what appears to be an emerging segment of an arc, and the nearly identical proper motions suggest that this may be a true binary.

Figure 2 shows the data plot for WDS 10271+1804. The pair is showing a slightly curved track and the nearly identical proper motions again suggest a truly physical pair.

Figure 3 shows the data plot for WDS 10545+4730. The R^2 figure is the degree of fit of the data to the trend line drawn (1.00 being a perfect fit, 0.00 being no fit whatsoever). Clearly, this pair is starting to trace an arc and, given the identical proper motions, is probably physical.

Note, however, that Excel (the tool I used to gener-

(Continued on page 22)

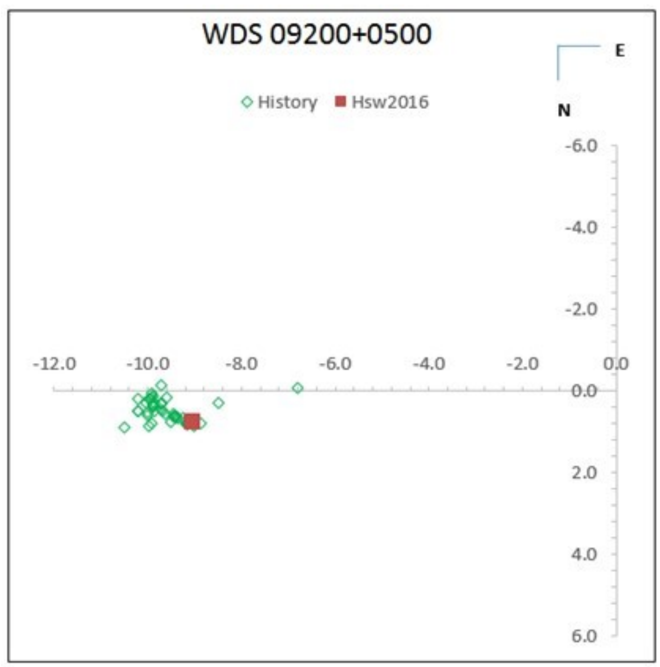

PM: -083-041 -074-037

Figure 1: Data plot for WDS 09200+0500

The Winter 2015 Observing Program at Brilliant Sky Observatory: Report on the Measurement of 112 Pairs

Table 1. 105 Proper Motion Pairs

							Means		Residuals	
WDS No	**Disc Code**	**Date**	**Obs**	**Last Meas**	**Last Theta**	**Last Rho**	**Meas Theta**	**Meas Rho**	**Theta**	**Rho**
00318+3658	STT 132AB	2015.8630	4	2011	131.00	6.90	96.621	22.489	34.379	-15.589
01554+7613	STF 170	2015.9945	4	2008	243.00	3.10	244.406	3.140	-1.406	-0.040
01564+6116	STF 182AB	2015.9945	4	2006	124.00	3.60	124.113	3.708	-0.113	-0.108
02124+5508	HJ 2115	2015.9920	4	2003	56.00	8.30	55.527	8.275	0.473	0.025
02186+4017	STF 245AB	2105.9863	10	2011	293.00	11.00	293.691	11.013	-0.691	-0.013
02234+4441	ES 1306	2015.9920	4	2007	275.00	9.40	275.000	9.396	0.000	0.004
02238+4920	STF 256AB	2105.9863	8	2013	197.00	21.30	197.560	21.144	-0.560	0.156
02238+4920	STF 256AC	2105.9863	6	2013	45.00	35.80	45.103	35.492	-0.103	0.308
02252+5223	ARG 53AB	2105.9863	8	2013	246.00	17.20	246.558	16.936	-0.558	0.264
02265+5417	STF 260	2105.9863	12	2003	347.00	6.40	346.300	6.626	0.700	-0.226
02278+7247	HJ 2132AB	2015.9589	4	2012	158.30	30.12	158.149	29.773	0.151	0.347
02292+7305	HJ 2133AB	2015.9589	4	2007	151.00	30.20	151.305	28.492	-0.305	1.708
02333+5619	FAB 4AC	2105.9863	8	2009	261.00	18.80	260.611	18.735	0.389	0.065
02340+4409	AG 303AB	2105.9863	6	2007	292.00	15.80	292.539	15.425	-0.539	0.375
02343+4017	AG 42	2105.9863	10	2007	144.00	6.40	144.108	6.340	-0.108	0.060
02420+4248	HJ 1123	2105.9863	8	2011	249.00	20.20	249.114	20.017	-0.114	0.183
02424+3837	AG 49AB	2105.9863	6	2012	342.00	14.10	343.752	14.369	-1.752	-0.269
02425+4016	STF 292	2105.9863	14	2011	212.00	22.70	212.035	22.922	-0.035	-0.222
02427+7649	HN 2146	2015.9589	6	2003	84.00	31.80	84.382	31.624	-0.382	0.176
02454+5634	STF 297AB	2105.9863	12	2013	278.00	15.40	278.532	15.799	-0.532	-0.399
02470+4705	AG 50AB	2105.9863	6	2003	4.00	11.90	4.747	11.406	-0.747	0.494
02476+5357	STF 301	2105.9863	12	2011	17.00	8.20	17.181	8.197	-0.181	0.003
02505+4118	ES 1613	2015.9920	4	2011	18.00	6.90	19.616	6.899	-1.616	0.001
02516+6033	BU 1374AB	2015.9589	8	2003	196.00	21.20	195.602	20.940	0.398	0.260
02521+3718	STF 316	2015.9920	4	2011	135.00	14.30	135.668	14.241	-0.668	0.059
02548+4332	HJ 2162AB	2015.9920	2	2008	40.00	12.80	41.298	12.633	-1.298	0.167
02558+3429	STF 325AB	2015.9920	4	2013	147.00	22.70	147.470	22.992	-0.470	-0.292
02563+5852	STF 321	2015.9920	4	2003	25.00	18.80	25.875	18.386	-0.875	0.414
02579+6400	STI 409AB	2015.9589	4	2011	208.00	8.90	207.528	8.625	0.472	0.275
03006+6548	MLR 122	2015.9589	4	2007	331.00	6.20	330.460	5.931	0.540	0.269
03009+5221	STF 331	2105.9863	11	2012	85.00	11.90	85.255	11.864	-0.255	0.036
03012+5902	STF 329	2105.9863	6	2003	274.00	16.30	274.090	16.005	-0.090	0.295
03015+3225	STF 336	2105.9863	10	2013	8.00	8.30	8.011	8.623	-0.011	-0.323
03023+4124	STF 337AB	2015.9920	4	2012	163.00	17.90	163.324	17.575	-0.324	0.325
03038+7039	HJ 2164	2015.9589	4	2011	320.00	5.70	321.650	5.294	-1.650	0.406
03063+5100	AG 305AB	2015.9920	4	2007	100.00	11.40	99.936	11.161	0.064	0.239
03070+6744	HJ 1131	2015.9589	6	2003	119.00	18.50	118.049	18.158	0.951	0.342
03108+6347	STF 349	2015.9589	8	2011	323.00	5.90	322.756	5.624	0.244	0.276
03111+5544	SCA 9AB	2015.9920	4	2012	137.00	27.70	137.564	27.599	-0.564	0.101
03126+3258	SEI 28	2015.9920	4	2010	232.00	10.30	232.002	10.251	-0.002	0.049
03136+3909	STF 364	2015.9920	4	2011	311.00	11.80	311.614	11.650	-0.614	0.150
03146+6702	HJ 1132	2015.9589	6	2011	24.00	7.30	23.205	7.056	0.795	0.244

Table 1 continues on the next page.

The Winter 2015 Observing Program at Brilliant Sky Observatory: Report on the Measurement of 112 Pairs

Table 1 (continued). 105 Proper Motion Pairs

							Means		Residuals	
WDS No	Disc Code	Date	Obs	Last Meas	Last Theta	Last Rho	Meas Theta	Meas Rho	Theta	Rho
03163+6002	STF 362AB	2015.9589	10	2005	142.00	7.20	142.685	7.044	-0.685	0.156
03166+3238	STF 370	2015.9920	4	2005	319.00	16.80	320.214	16.914	-1.214	-0.114
03168+7830	STF 345	2015.9945	4	2011	86.00	6.90	87.967	6.609	-1.967	0.291
03193+4559	STF 372AB	2015.9920	4	2008	292.00	7.70	292.684	7.923	-0.684	-0.223
03207+8459	STF 319	2015.9945	2	2011	302.00	17.80	302.451	17.786	-0.451	0.014
03213+4743	ES 464	2015.9920	4	2008	67.00	6.90	66.227	6.976	0.773	-0.076
03221+6244	STF 373AB	2015.9945	2	2010	118.00	20.30	119.709	20.013	-1.709	0.287
03242+6728	STF 374	2015.9945	2	2012	297.00	11.20	298.342	11.224	-1.342	-0.024
03247+4417	ARG 55AB	2015.9920	4	2008	199.00	26.20	199.869	25.971	-0.869	0.229
03298+5001	ES 2599AB	2015.9920	4	2011	299.00	19.40	298.850	19.247	0.150	0.153
08008-1621	ARA 50	2016.2550	3	1999	5.80	12.65	6.466	12.471	-0.666	0.175
08014-1722	ARA 206	2016.2550	1	1999	81.70	10.10	80.141	10.110	1.559	-0.011
08034-1312	STF1178	2016.2550	4	2010	329.60	5.19	329.207	5.264	0.393	-0.077
08121-1540	HJ 4050	2016.2795	2	2004	303.90	22.71	304.769	21.944	-0.869	0.766
08287-1732	ARG 20	2016.2795	3	2003	174.00	14.81	173.148	14.972	0.852	-0.162
08407-1156	STF1261	2016.2795	3	2008	302.90	19.63	302.562	29.470	0.338	-9.840
08407-1210	STF1260	2016.2795	5	2011	302.40	4.94	300.883	5.210	1.517	-0.270
08448-1044	HJ 795	2016.2795	3	2005	17.30	6.00	16.942	6.152	0.358	-0.152
09005+2244	STF1297AB	2016.2520	3	2011	158.00	5.40	159.330	5.012	-1.330	0.388
09019+2612	STF1301	2016.2520	3	2013	0.00	10.20	359.733	10.139	-359.733	0.061
09050-0359	STF1308	2016.2300	5	2010	85.00	10.30	84.727	10.537	0.273	-0.237
09066+0249	STF1309	2016.2490	3	2011	274.00	11.70	273.351	11.686	0.649	0.014
09092+1514	STF1317	2016.2520	3	2013	62.00	7.80	62.559	7.766	-0.559	0.034
09111+0835	STF1319	2016.2490	2	2013	51.00	13.50	50.008	13.467	0.992	0.033
09133+0540	WFC 81	2016.2490	2	2012	76.00	8.20	75.678	8.148	0.322	0.052
09137+1109	HJ 122	2016.2520	2	2007	91.00	9.90	92.595	9.875	-1.595	0.025
09140+2611	STF1324	2016.2520	2	2011	349.00	11.50	348.637	11.493	0.363	0.007
09150+1253	HJ 2490	2016.2520	2	2007	68.00	21.70	67.327	21.410	0.673	0.290
09153+0531	HJ 124AB	2016.2329	1	2013	72.00	15.80	71.875	15.826	0.125	-0.026
09153+0531	HJ 124AB	2016.2330	1	2013	72.30	15.83	71.875	15.826	0.425	0.004
09182-0036	HJ 126	2016.2330	3	2015	32.90	30.00	32.542	30.175	0.358	-0.175
09204+0409	BAL2834	2016.2490	1	2012	4.00	19.50	3.774	19.140	0.226	0.360
09207+0810	A 2976AB	2016.2490	2	2009	237.00	28.60	236.566	28.594	0.434	0.006
09233+0330	STF1347	2016.2330	4	2012	314.00	21.70	311.974	21.116	2.026	0.584
10019+7334	STF1393	2016.2250	1	2011	254.40	9.48	253.362	9.459	1.038	0.021
10029+0742	STF1403	2016.2490	3	2011	335.00	2.90	333.536	2.942	1.464	-0.042
10034+0203	HJ 1174	2016.2490	2	2012	134.00	13.40	133.663	13.371	0.337	0.029
10040-1806	SHJ 110AC	2016.2795	2	2014	273.80	21.17	273.094	21.186	0.706	-0.016
10069-0143	HDO 125	2016.2330	3	2012	189.50	2.85	191.020	2.685	-1.520	0.165
10072+0117	BAL1436	2016.2330	1	2014	228.30	10.72	228.021	10.598	0.279	0.122
10123+1621	STF1413	2016.2520	3	2013	271.00	1.80	270.868	2.012	0.132	-0.212
10160+7928	STF1409	2016.2250	1	2012	194.50	19.01	192.809	19.292	1.691	-0.282

Table 1 concludes on the next page.

Table 1 (conclusion). 105 Proper Motion Pairs

							Means		Residuals	
WDS No	Disc Code	Date	Obs	Last Meas	Last Theta	Last Rho	Meas Theta	Meas Rho	Theta	Rho
10167+5737	HJ 1176AB	2016.2250	1	2004	318.50	8.89	317.440	8.911	1.060	-0.021
10170+1007	STF1419	2016.2520	3	2013	224.00	4.40	223.715	4.442	0.285	-0.042
10205+0626	STF1426AB	2016.2330	4	2013	11.00	7.60	11.365	7.655	-0.365	-0.055
10258+0312	HJ 1177	2016.2520	1	2011	41.00	13.30	40.575	13.394	0.425	-0.094
10284+0310	CHE 148	2016.2330	2	2010	64.30	4.94	64.270	4.921	0.031	0.019
10285+1309	STF1438	2016.2520	1	2013	245.00	9.50	276.201	2.524	-31.201	6.976
10358+0233	STF1452A,BC	2016.2330	3	2010	325.00	9.30	328.032	10.392	-3.032	-1.092
10376+0505	HJ 2540	2016.2330	1	2002	305.60	28.11	305.674	27.871	-0.074	0.239
10383+0115	STF1456	2016.2490	3	2010	49.00	15.20	45.135	13.675	3.865	1.525
10416-0016	STF1464AB	2016.2300	3	2000	302.00	5.60	302.276	5.761	-0.276	-0.161
10429-0006	BAL1155	2016.2300	2	2000	203.00	17.70	202.828	17.631	0.172	0.069
10457-0130	FIL 26	2016.2300	3	2009	260.00	20.70	259.802	20.238	0.198	0.462
10493-0401	STF1476	2016.2300	5	2012	16.00	2.30	17.859	2.370	-1.859	-0.070
10522+0728	STF1482	2016.2300	4	2010	295.00	13.10	305.447	11.943	-10.447	1.157
11033-1726	ARA 64	2016.2795	2	1999	305.90	7.05	305.362	7.263	0.538	-0.213
11086-0442	J 1572	2016.2330	1	2011	21.80	8.25	20.661	8.246	1.139	0.004
11110-0620	STF3067	2016.2330	3	2012	236.00	21.00	235.862	21.078	0.138	-0.078
11114-0921	STF3068	2016.2330	3	2012	313.00	19.40	312.413	19.285	0.587	0.115
11194-0139	STF1529	2016.2330	5	2012	255.00	8.90	254.555	9.428	0.445	-0.528
11197-0654	STF1530	2016.2330	4	2013	313.00	7.70	313.621	7.600	-0.621	0.100
11353+7048	STF1551	2016.2250	1	2011	111.30	6.62	110.521	6.818	0.779	-0.198

Table 2: Three Short-Arc Binaries

							Means		Residuals	
WDS No	Disc Code	Date	Obs	Last Meas	Last Theta	Last Rho	Meas Theta	Meas Rho	Theta	Rho
09200+0500	STF1343	2016.2490	3	2012	275.00	9.10	274.729	9.064	0.271	0.036
10271+1804	STF1434	2016.2520	3	2012	282.00	6.20	281.013	6.455	0.987	-0.255
10545+4730	STF1483	2016.2250	3	2010	242.50	2.40	243.096	2.237	-0.596	0.163

Table 3: Three Linear Cases

							Means		Residuals	
WDS No	Disc Code	Date	Obs	Last Meas	Last Theta	Last Rho	Meas Theta	Meas Rho	Theta	Rho
02392+6343	KR 14	2015.9589	10	2011	290.00	8.36	289.774	8.022	0.226	0.338
09168+0814	HJ 808AB	2016.2490	2	2009	206.00	24.20	203.856	24.336	2.144	-0.136
10285+1309	STF1438	2016.2520	1	2013	245.00	9.50	276.201	2.524	-31.201	6.976

Table 4: One Speckle Interferometry Solution

							Means		Residuals	
WDS No	Disc Code	Date	Obs	Last Meas	Last Theta	Last Rho	Meas Theta	Meas Rho	Theta	Rho
09245+0621	STF 1348 AB	2016.2490	5	2009	314.00	1.90	314.037	1.962	-0.037	-0.062

The Winter 2015 Observing Program at Brilliant Sky Observatory: Report on the Measurement of 112 Pairs

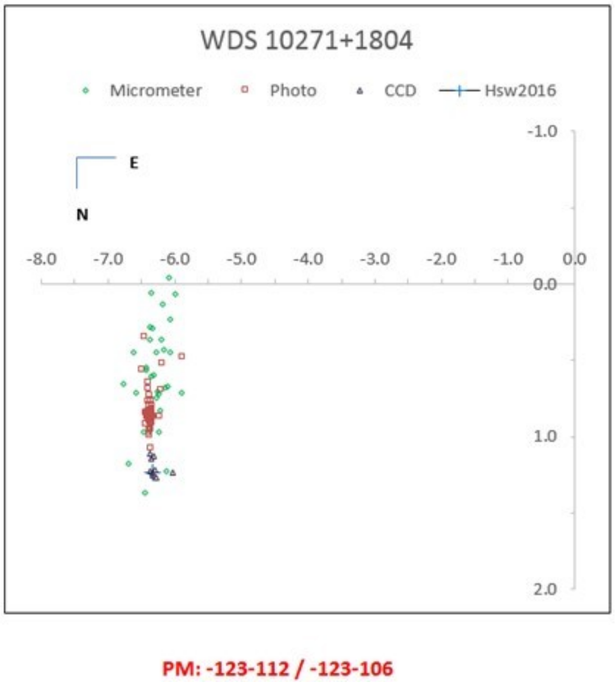

Figure 2: Data plot for WDS 10271+1804

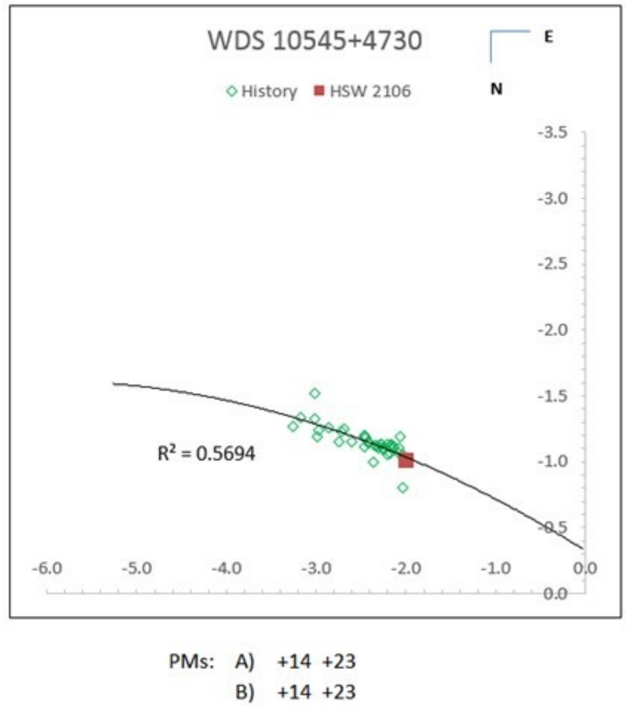

Figure 3: Plot for WDS 10545+4730

(Continued from page 18)

ate these plots) assigns equal weight to each data point, a practice not done when analyzing historical measurements for generating an orbital solution. Also note that in all my data plots, I have programmed Excel to adjust each measurement for precession.

Figure 4 shows the data plot for WDS 02392+6343. The R^2 value of 0.89 indicates an extremely good fit (using equal weights) of the data to the trend line, and this pair is probably ready for a linear solution.

Figure 5 shows the data plot for WDS 09168+0814. While the R^2 value is not that strong, the fact that the data points are trending along a line that is fairly long (almost 13 arc seconds since 1820) is strongly suggestive of a linear case.

Figure 6 shows the data for WDS 10285+1309. The very different proper motions combined with a linear trend with an R^2 value of 0.9715 is strongly suggestive of a linear case. The last measure on record was made by the U S Naval Observatory using speckle reduction of a CCD image and is indicated on the plot by a small arrow. While my data point lies almost exactly on the trend line, the gap of only 3 years in my measurement and the USNO's measurement, being some 6 arc-seconds in difference in sky position, suggests to me that my measurement may be in error and needs to be double-checked.

Figure 7 shows the data plot for WDS 09245+0621.

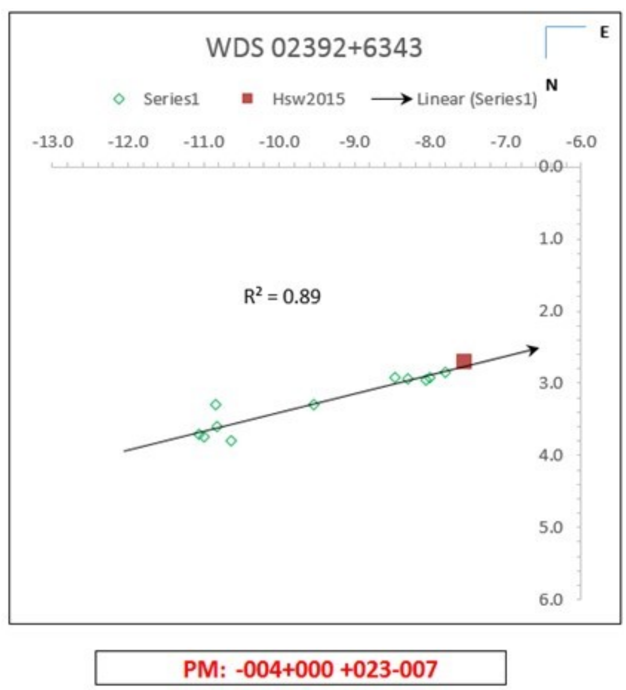

Figure 4: Data plot for WDS 02392+6343

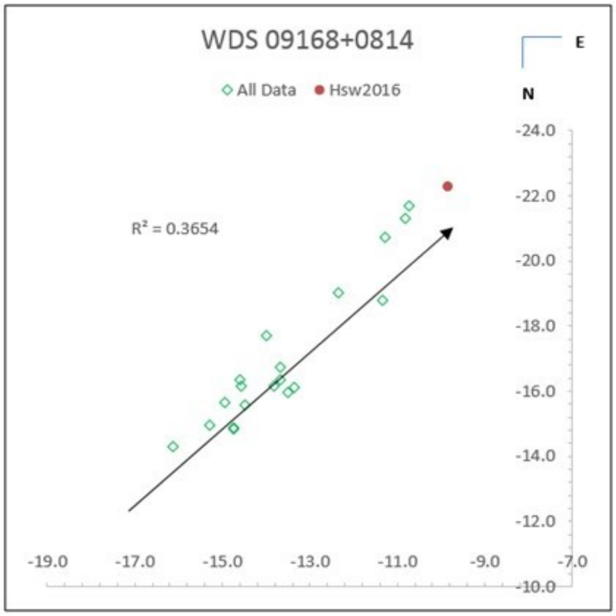

PM: -9 +1 / +32 -61

Figure 5: Data plot of WDS 09168+0814

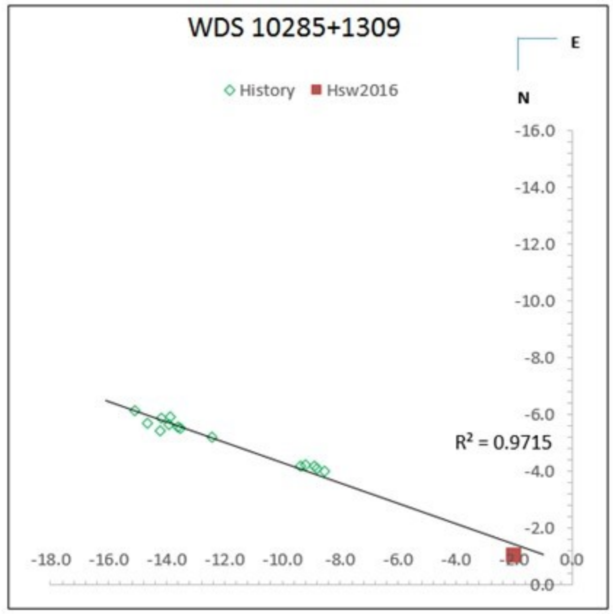

PM: -048-031 +006-017

Figure 6: Data plot for WDS 10285+1309

Despite the large proper motion and tight clustering of the data points over time, it is not yet possible to determine if it is truly physical or not.

5. Discussion

Clearly, speckle-like reduction of CCD images of double stars is a legitimate way to make accurate measurements of close visual double stars. In every pair presented in this paper, my data plot was in the middle of the grouping for common proper motion pairs, or on the end of the trend line for short arc binaries or linear pairs, the only questionable case being WDS 10285+1309, which will have to be re-visited next autumn.

Of particular difficulty in measuring close pairs are two physical constraints on my system: (1) the seeing in Arizona is usually poor to moderate at best, nights of truly pristine seeing being rare (although this is clearly not the case for the transparency of the skies), and (2) image distortion due to thermal currents inside the SCT's optical tube assembly (OTA). Use of a forced-air cooling system has the drawback of requiring the camera angle to be re-set for each observing run (as the camera and optical train have to be removed for the cooling fan to be inserted).

Tube currents in an SCT usually result in a star image that, out-of-focus at extremely high magnification (such as one uses in doing CCD imaging using a speckle train) does not resemble the classic "donut" with

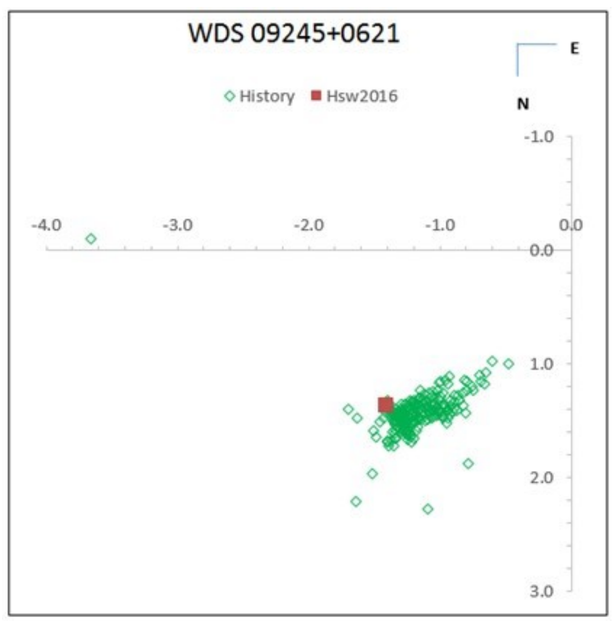

PM: -172-034 -172-034

Figure 7: Data plot for WDS 09245+0621

which most SCT users will be familiar, but rather resembles a diamond ring, with a thin halo of star light (the "normal" donut) and a bright pip on one side (the star). As one approaches ideal focus, this diamond ring morphs into a "gull wing" image, with the star flanked by two "wings" at about a 120° angle.

An interesting paper at the Astrogeeks site (http://www.astrogeeks.com/Bliss/OccultVideo/SCTCoolingFreestar8n.pdf) reports on measuring tube temperatures by a respected engineer and poses some interesting questions (and suggests possible remedies) for the SCT tube current problem. Another alternative, suggested by a very experienced telescope dealer and service engineer in Tucson, Arizona (Dean Koenig of Starizona, a telescope dealership), suggested using a small window air conditioner in the observatory and turning it on two or three hours before an observing run so the mirror can be at or below ambient at the start of the observing session. This is probably the less dangerous solution (as opposed to cutting holes in the SCT's OTA). I have noticed that as the night wears on and the air gets cooler, the images improve. But this improvement normally takes 3 to 4 hours to become evident.

I will be installing a portable air conditioning unit in the observatory the summer of 2016 to alleviate the thermal build-up during the day (it can reach 120°F in the observatory). This should greatly reduce tube current problems and enable me to start quality measurements much earlier in the night.

6. Conclusion

This project clearly shows that it is possible to achieve very high accuracy in measuring close double stars using speckle reduction techniques as compared to lucky imaging. It is particularly noteworthy that amateurs with modest equipment can do this work as well today as was possible 30 years ago with much larger telescopes and much more expensive cameras.

7. Acknowledgements

This research has made use of the Washington Double Star Catalog maintained at the U.S. Naval Observatory.

8. References

Harshaw, Richard, 2016A, "CCD Measurements of 66 Rectilinear and Probable Rectilinear Pairs: The Autumn 2015 Observing Program at Brilliant Sky Observatory, Part 1", *JDSO*, **12**, 376-387.

Harshaw, Richard, 2016B, "CCD Measurements of 8 Double Stars With Binary Nature: The Autumn 2015 Observing Program at Brilliant Sky Observatory, Part 2", *JDSO*, **12**, 388-393.

Harshaw, Richard, 2016C, "CCD Measurements of 141 Proper Motion Stars: The Autumn 2015 Observing Program at the Brilliant Sky Observatory, Part 3", *JDSO*, **12**, 394-399.

Harshaw, Richard, 2016D, "Quasi-Speckle Measurements of Close Double Stars With a CCD Camera", *JDSO*, **13**, 13-16.

Measurements of Faint and Wide Doubles in Boötes and Corona Borealis

Wilfried R.A. Knapp
Vienna, Austria
wilfried.knapp@gmail.com

Chris Thuemen
Double Star Imaging Project
Pembroke, Ontario, Canada
thuemen_cm@yahoo.ca

Abstract: Images of several double stars in Boötes and Corona Borealis published on the "Double Star Imaging Project" Yahoo Group page suggest magnitude issues compared with the corresponding WDS catalog data per Jan 2016. Taking additional images with V-filter enabled photometry and astrometry for these pairs as a counter-check.

1. Introduction

This paper identifies double star systems in both Boötes and Corona Borealis that appear to have visual magnitudes that are in conflict with the data as published in the Washington Double Star Catalog. During the course of a long term project to image double stars accessible to the backyard telescope, while employing a consistent imaging regime from one location, the sheer volume of images has allowed the authors to identify with a good degree of certainty double star systems having component magnitudes that are clearly in conflict with the published data. After visually identifying these suspect systems from the new images, the authors then consulted the University of Strasburg's website, VizieR, to access the online digital sky survey catalogs to confirm the visual observations.

The preliminary findings for the suspect Boötes systems are summarized below:

- SHJ 169 – WDS 13547+1824. Listed magnitudes are 2.72 & 9.99. The dim, very orange colored companion appears to be significantly dimmer, in the 10.5 to 11.0 range.
- STF 1791 – WDS 13568+1426. Listed magnitudes are 9.39 & 10.73. The image suggests that both components are dimmer than the records. An initial estimate suggests magnitudes of 10.0 and 11.3. The UCAC4 values do confirm slightly dimmer magnitudes than the WDS record but still a surprise given the new image. Vmag values are 9.616 and 10.516.
- ROE 74 – WDS 14156+2255. Listed magnitudes are 10.5 and 11.0. The image clearly shows that both components are dimmer than the data; an initial estimate being both, about a full magnitude dimmer. The UCAC4 provides a Vmag for A of 11.42 and an f-mag for B of 12.098.
- BU 1442 – WDS 14257+2338. This 5 component system has listed magnitudes in alphabetic order of 9.87, 10.21, 9.66, 13.06, and 9.90. The image (Figure 1) is very persuasive in that all components except D are within 0.3 mags of each other. This would suggest that the 10.21 listing for the magnitude of "B is incorrect. We estimate B to be mag. 9.8. The UCAC4 Vmag values for A through D are, 9.701, 9.921, 9.664, and 13.065. Figure 2 shows POSS I and POSS 2 images of this system.
- ALI 131 – WDS 14516+3453. Listed magnitudes are 9.69 and 12.3. With an exposure of 30 seconds and ISO of 800, my imaging setup has great difficulty resolving stars above magnitude 12.0. Bootes was high in the sky at the time ALI 131 was imaged, so the reduced atmosphere has provided some surprises. We estimate the secondary to be in the mag. 11.8 range. The UCAC4 data provides a Vmag for the primary of 9.657 with a formula gen-

Measurements of Faint and Wide Doubles in Boötes and Corona Borealis

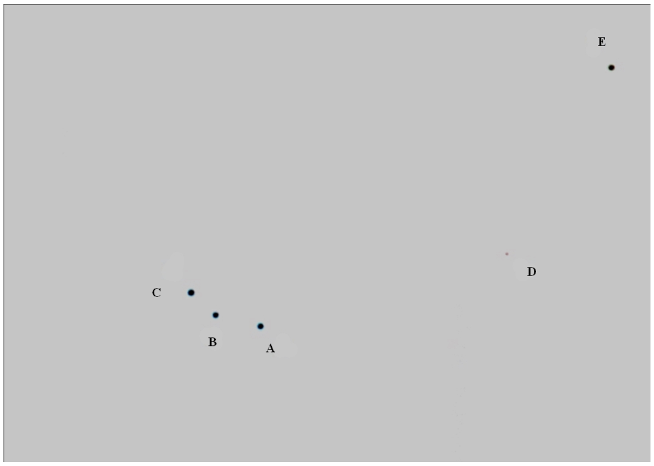

Figure 1. BU 1442 (2016)

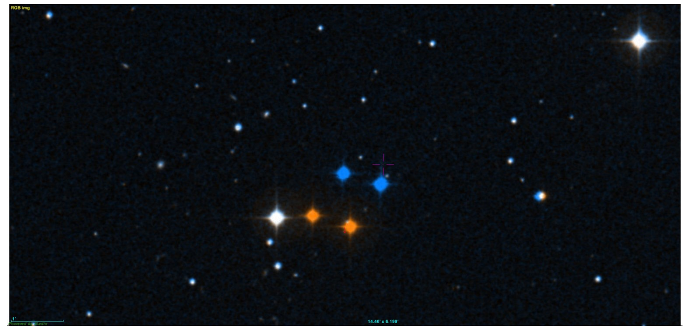

Figure 2. BU 1442 – POSS I (1950 in blue) to POSS II (1993 in orange). Only the components A and B move with common proper motion, while the other components show little to no motion.

erated Vmag for the secondary of 11.950.

- HLD 120 – WDS 14527+0746. Listed magnitudes are 8.05 & 10.84. The image readily supports the magnitude of the primary but the data for the secondary is suspect. Initial estimates place the magnitude for "B" in the 11.7 range. The UCAC4 confirms the estimate with a Vmag of 8.046 for "A" and a formula generated Vmag for "B" of 11.61.
- COU 101 – WDS 14537+2321. Listed magnitudes are 8.65 and 12. The data for the primary appears to be correct but the lack of any trace of the companion in the image suggests that the magnitude of "B" is in the order of mag. 13.0 or more. UCAC4 provides Vmags of 8.765 and 13.228.
- HJ 243 – WDS 14571+3529. Listed magnitudes are 7.41 & 13.0. Again, the primary reflects the magnitude listed in the WDS. Unlike COU 101 above, the image clearly resolves the companion, suggesting a magnitude in the 12.1 range. As noted earlier, the increased declination angle, in good sky conditions, improves the resolution of the imaging setup. The UCAC4 data provides a Vmag value for the primary of 8.831 which we find surprising. A formula generated Vmag for the secondary is 12.335.
- HJ 2766 – WDS 15086+2507. Listed magnitudes are 5.81 & 10.0. With no other bright stars in the field, the primary appears correct at mag. 5.81. With a magnitude listing of 10.0 and a comfortable separation of 56.4 arc-seconds, I was expecting a very obvious high contrast pair. One is hard pressed to pick up any sign of the companion in the image at a first glance, but careful study of the photograph does reveal the companion. First estimates for the companion would be mag. 12.2. Oddly, once again as with HJ 243, the UCAC4 Vmag value at 8.443 is significantly dimmer than the WDS data. Not surprisingly, the Vmag for the companion is 12.19.
- HJ 567 – WDS 15101+3741. Listed magnitudes are 8.87 & 13.28. The bench mark image settings of a 30 seconds exposure with ISO 800 is resolving clearly, albeit dimly, the companion. Therefore an initial estimate of mag. 12.3 appeared appropriate. The UCAC4, surprisingly, supports the WDS data with Vmags of 9.141 and 13.227.

The preliminary findings for the suspect Corona Borealis systems are summarized below:

- UC 3111 – WDS 16037+3709. Listed magnitudes are 10.2 & 12.8. Once again, the benchmark exposure reveals a tantalizing hint of the dim companion to suggest a magnitude in the 13.0 range. The UCAC4 Vmag for "A" is very close at 10.366 while the formula generated Vmag of 13.179 supports the estimate of a slightly dimmer "B" component.
- SHJ 223 – WDS 16315+0818. Listed magnitudes for this 5 star system listed alphabetically are, 5.87, 11.70, 10.44, 10.35, and 11.90. It is clear from the image (Figure 3) that the magnitude of component "B" has no resemblance to the mag. 11.70 listed in the WDS. A 30 seconds exposure at ISO 1600 generates only the slightest hint of the "B" companion. Initial estimates are therefore in the 13.0+ range. For all other system stars, the WDS data is generally supported by the image. UCAC4 Vmag values in order are 5.791, 13.903, 10.809, 10.249, and 12.167. Both B & E values were generated from the formula.
- KU 53 – WDS 16229+3815. Listed magnitudes are 10.1 & 10.5 suggesting a very equal pair visually. The image tells quite a different story with a very noticeable ΔM, likely in the 1.0 range. Estimates based on the image are 10.4 and 11.4. The UCAC4 paints a slightly brighter picture but supports the

Measurements of Faint and Wide Doubles in Boötes and Corona Borealis

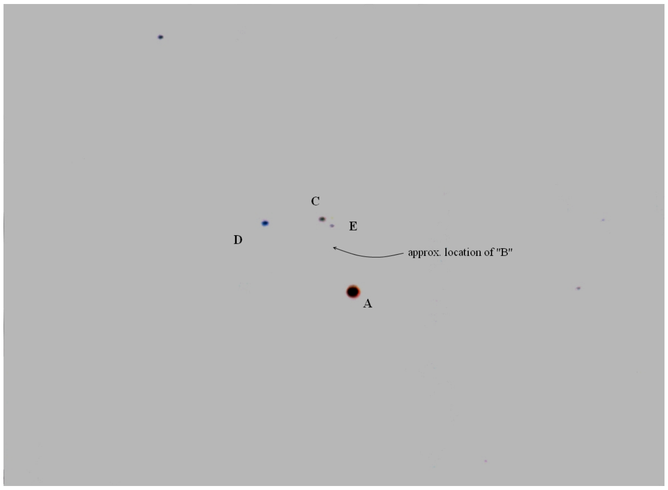

Figure 3. SHJ 223

estimated contrast in magnitudes. Values are 9.987 and 11.179 with the companion being formula generated.

Further Research

Images taken with iTelescope remote telescopes were in a first step plate solved and stacked with AAVSO VPhot. The stacked images were then plate solved with Astrometrica with URAT1 reference stars with Vmags in the range 10.5 to 14.5 mag. The RA/Dec coordinates resulting from plate solving with URAT1 reference stars in the 10.5 to 14.5 mag range were used to calculate Sep and PA using the formula provided by R. Buchheim (2008). *Err_Sep* is calculated as

$$Err\_Sep = \sqrt{dRA^2 + dDec^2}$$

with dRA and $dDec$ as average RA and Dec plate solving errors. *Err_PA* is the error estimation for PA calculated as

$$Err\_PA = \arctan\left(\frac{Err\_Sep}{Sep}\right)$$

in degrees assuming the worst case that *Err_Sep* points at a right angle to the direction of the separation means perpendicular to the separation vector. Mag is the photometry result based on UCAC4 reference stars with Vmags between 10.5 and 14.5mag. *Err_Mag* is calculated as

$$Err\_\mathrm{Mag} = \sqrt{dVmag^2 + \left[2.5\log_{10}\left(1 + 1/SNR\right)\right]^2}$$

with $dVmag$ as the average $Vmag$ error over all used reference stars and SNR is the signal to noise ratio for the given star. The results are shown in Tables 1 and 2.

3. Summary

In most cases the suspected magnitude issues were confirmed by the photometry results.

Tables 3 and 4 present all the WDS, UCAC4, and the occasional piece of Nomad data for the magnitudes of the listed objects compared with our photometry results.

Acknowledgements

The following tools and resources have been used for this research:

- Washington Double Star Catalog
- iTelescope
- iT18: 318mm CDK with 2541mm focal length. CCD: SBIG-STXL-6303E. Resolution 0.73 arcsec/pixel. V-filter. Located in Nerpio, Spain. Elevation 1650m
- iT24: 610mm CDK with 3962mm focal length. CCD: FLI-PL09000. Resolution 0.62 arcsec/pixel. V-filter. Located in Auberry, California. Elevation 1405m
- AAVSO VPhot
- AAVSO APASS
- UCAC4 catalog via the University of Heidelberg website
- Aladin Sky Atlas CDS, SIMBAD, VizieR, UCAC4, Nomad, URAT1, GAIA
- 2MASS All Sky Catalog
- AstroPlanner
- Astrometrica

References

Buchheim, Robert, 2008, "CCD Double-Star Measurements at Altimira Observatory in 2007", *Journal of Double Star Observations*, **4**, 27-31.

Measurements of Faint and Wide Doubles in Boötes and Corona Borealis

Table 1: Photometry and astrometry results for the selected Boo objects. Date is the Bessel epoch 2016 and N is the number of images used for the reported values. iT in the Notes column indicates the telescope used with number of images and exposure time given (Specifications of the used telescopes: See Acknowledgements).

Name		RA	Dec	dRA	dDec	Sep	Err Sep	PA	Err PA	Mag	Err Mag	SNR	dVmag	Date 2016	N	Notes
SHJ 169	A	13 54 41.000	18 23 45.76	0.10	0.09	114.033	0.135	85.070	0.068	5.677	0.075	38.15	0.07	.360	5	1) 2) 3)
	B	13 54 48.982	18 23 55.56							10.348	0.071	119.79				
STF1791	A	13 56 49.185	14 25 58.66	0.10	0.07	21.002	0.122	158.793	0.333	9.400	0.081	90.09	0.08	.356	5	4)
	B	13 56 49.708	14 25 39.08							10.609	0.083	51.50				
ROE 74	A	14 15 39.011	22 54 45.20	0.05	0.07	6.991	0.086	288.083	0.705	11.749	0.032	96.34	0.03	.360	5	5)
	B	14 15 38.530	22 54 47.37							12.223	0.034	70.64				
BU 1442	A	14 25 44.427	23 36 43.37	0.17	0.14	45.319	0.220	74.409	0.278	9.699	0.072	73.70	0.07	.356	4	6) 7)
	B	14 25 47.603	23 36 55.55							9.964	0.072	65.69				
BU 1442	A	14 25 44.427	23 36 43.37	0.17	0.14	75.370	0.220	62.450	0.167	9.699	0.072	73.70	0.07	.356	4	6) 8)
	C	14 25 49.289	23 37 18.23							9.440	0.071	84.19				
BU 1442	A	14 25 44.427	23 36 43.37	0.17	0.14	249.852	0.220	284.484	0.051	9.699	0.072	73.70	0.07	.356	4	6) 8) 9)
	D	14 25 26.826	23 37 45.86							12.960	0.109	12.59				
ALI 131	A	14 51 38.779	34 52 34.23	0.04	0.05	8.850	0.064	112.382	0.415	9.608	0.081	85.34	0.08	.356	4	6)
	B	14 51 39.444	34 52 30.86							11.867	0.088	28.65				
HLD 120	A	14 52 39.171	07 46 24.64	0.05	0.05	15.576	0.071	225.072	0.260	7.999	0.070	287.83	0.07	.360	5	5) 2) 8)
	B	14 52 38.429	07 46 13.64							11.606	0.071	116.74				
COU 101	A	14 53 40.590	23 20 42.93	0.17	0.08	63.317	0.188	71.939	0.170	8.647	0.080	132.40	0.08	.356	5	4) 2) 8) 9)
	B	14 53 44.961	23 21 02.56							13.194	0.108	14.52				
HJ 243	A	14 57 06.839	35 29 24.16	0.08	0.05	17.951	0.094	23.199	0.301	7.258	0.090	201.10	0.09	.356	5	4) 2)
	B	14 57 07.418	35 29 40.66							12.363	0.105	19.49				
HJ 2766	A	15 08 35.562	25 06 31.30	0.07	0.09	57.644	0.114	330.559	0.113	5.852	0.060	291.71	0.06	.360	5	5) 2)
	B	15 08 33.476	25 07 21.50							12.226	0.064	51.38				
HJ 567	A	15 10 07.627	37 41 26.20	0.14	0.12	33.818	0.184	14.971	0.312	8.794	0.090	119.43	0.09	.356	3	4) 2) 9)
	B	15 10 08.363	37 41 58.87							13.262	0.126	11.90				

Table 1 Notes:

1. iT24 stack 5x1s
2. A too bright for reliable photometry
3. Astrometry results influenced by significant proper motion of A and B in similar direction but with very different speed
4. iT18 stack 5x3s
5. iT24 stack 5x3s
6. iT18 stack 4x3s
7. Very solid CPM pair with ident pm vector direction and very similar pm vector length. PM/yr ~1,365 arcseconds
8. Astrometry results influenced by high proper motion speed of A
9. SNR B<20

Measurements of Faint and Wide Doubles in Boötes and Corona Borealis

Table 2. Photometry and astrometry results for the selected CrB objects. Date is the Bessel epoch 2016 and N is the number of images used for the reported values. iT in the Notes column indicates the telescope used with number of images and exposure time given (Specifications of the used telescopes: See Acknowledgements).

Name		RA	Dec	dRA	dDec	Sep	Err Sep	PA	Err PA	Mag	Err Mag	SNR	dVmag	Date 2016	N	Notes
KU 53	A	16 22 54.091	38 15 27.25	0.03	0.04	5.233	0.050	48.750	0.547	10.388	0.050	161.12	0.05	.412	5	1)
	B	16 22 54.425	38 15 30.70							11.106	0.051	114.45				
SHJ 223	A	16 16 44.819	29 09 00.50	0.02	0.02	53.797	0.028	23.082	0.030	6.668	0.030	272.99	0.03	.412	5	1) 2)
	B	16 16 46.429	29 09 49.99							13.911	0.039	42.17				
SHJ 223	C	16 16 47.225	29 10 22.11	0.02	0.02	63.020	0.028	92.246	0.026	10.776	0.031	176.27	0.03	.412	5	1)
	D	16 16 52.033	29 10 19.64							10.208	0.030	210.52				
SHJ 223	A	16 16 44.819	29 09 00.50	0.02	0.02	76.647	0.028	15.443	0.021	6.668	0.030	272.99	0.03	.412	5	1) 2)
	E	16 16 46.377	29 10 14.38							12.076	0.032	99.70				
SHJ 223	A	16 16 44.819	29 09 00.50	0.02	0.02	123.265	0.028	50.057	0.013	6.668	0.030	272.99	0.03	.412	5	1) 2)
	D	16 16 52.033	29 10 19.64							10.208	0.030	210.52				
SHJ 223	A	16 16 44.819	29 09 00.50	0.02	0.02	87.485	0.028	21.117	0.019	6.668	0.030	272.99	0.03	.412	5	1) 2)
	C	16 16 47.225	29 10 22.11							10.776	0.031	176.27				
SHJ 223	C	16 16 47.225	29 10 22.11	0.02	0.02	13.532	0.028	235.163	0.120	10.776	0.031	176.27	0.03	.412	5	1)
	E	16 16 46.377	29 10 14.38							12.076	0.032	99.70				
UC 311	A	16 03 42.627	37 08 57.56	0.02	0.02	9.582	0.028	15.117	0.169	10.380	0.021	210.53	0.02	.412		1)
	B	16 03 42.836	37 09 06.81							13.791	0.031	45.84				

Table 2 Notes:

1. iT24 stack 5x3s
2. A too bright for reliable photometry

Measurements of Faint and Wide Doubles in Boötes and Corona Borealis

Table 3. Comparison catalog Boötes Data with Photometry Results (in red for large delta)

Bootes - Suspect Systems							
WDS ID	Co-ordinates	Mag. A	Mag. B/C/D	Mag. A	Mag. B/C/D	Mag. A	Mag. B/C/D
		Currently Listed WDS Magnitudes		Vmag. Values from UCAC4 (f)=Vmag from formula , (N)=Nomad (N,f)=Vmag. from Nomad Values using formula		Photometry results (# = too bright for reliable result)	
SHJ 169	13547+1824	2.72	9.99	8.308	10.309	#	**10.348**
STF1791	13568+1426	9.39	10.73	9.616	10.516	9.400	10.609
ROE 74	14156+2255	10.5	11.0	11.42	12.098 (f)	**11.749**	**12.223**
BU 1442AB	14257+2338	9.87	10.21	9.701	9.921	9.699	**9.964**
BU 1442AC	14257+2338	9.87	9.66	9.701	9.664	9.699	9.440
BU 1442AD	14257+2338	9.87	13.06	9.701	13.056	9.699	12.960
ALI 131	14516+3453	9.69	12.3	9.657	11.950 (f)	9.608	**11.867**
HLD 120	14527+0746	8.05	10.84	8.046	11.61 (f)	7.999	**11.606**
COU 101	14537+2321	8.65	12	8.765	13.228	8.647	**13.194**
HJ 243	14571+3529	7.41	13.0	8.831	12.335 (f)	7.258	**12.363**
HJ 2766	15086+2507	5.81	10.0	8.443	12.19	5.852	**12.226**
HJ 567	15101+3741	8.87	13.28	9.141	13.227	8.794	13.262

Table 4. Comparison catalog Corona Borealis Data with Photometry Results (in red for large delta)

Corona Borealis - Suspect Systems							
WDS ID	Co-ordinates	Mag. A	Mag. B/C/D	Mag. A	Mag. B/C/D	Mag. A	Mag. B/C/D
		Currently Listed WDS Magnitudes		Vmag. Values from UCAC4 (f)=Vmag from formula , (N)=Nomad (N,f)=Vmag. from Nomad Values using formula		Photometry results (# = too bright for reliable result)	
UC 3111	16037+3709	10.2	10.366	13.179 (f)	12.8	10.380	**13.791**
SHJ 223AB	16315+0818	5.78	11.70	5.791	13.903(f)	#	**13.911**
SHJ 223AC		5.78	10.44	5.791	10.809	#	10.776
SHJ 223AD		5.78	10.35	5.791	10.249	#	10.208
SHJ 223AE		5.78	11.90	5.791	12.167(f)	#	**12.076**
KU 53	16229+3815	10.1	10.5	9.987 10.405(N)	11.179(f) 11.182(N,f)	10.388	**11.106**

A New Concept for Counter-Checking of Assumed CPM Pairs

It is always pleasant to have exact solutions in simple form at your disposal - Karl Schwarzschild, 1916

Wilfried R.A. Knapp
Vienna, Austria
wilfried.knapp@gmail.com

John Nanson
Star Splitters Double Star Blog
Manzanita, Oregon
jnanson@nehalemtel.net

Abstract: The inflation of "newly discovered" CPM pairs makes it necessary to develop an approach for a solid concept for counter-checking assumed CPM pairs with the target to identify false positives. Such a concept is presented in this report.

Introduction

Common proper motion pair means two stars moving through space in similar direction with similar speed. Such pairs are of interest because of their potential physical relationship in terms of common origin. Despite several attempts (especially from Halbwachs 1986) there exists no generally accepted set of criteria for identifying CPM pairs. Some often used criteria are:

- Minimum of pm/yr (most often 50mas following Halbwachs 1986)
- Maximum separation in terms of pm (separation/pm<1000 following Halbwachs 1986)
- 0.05 significance criterion ([μ1 - μ2]^2 < -2 [σ1^2 + σ2^2] ln [0.05] with μ1, μ2 as the two proper motion vectors and σ1, σ2 as the corresponding mean error following Halbwachs 1986 or modified by Caballero et al 2010 as (μ11 - μ21)2 < -2 σ12 ln (0.05) plus (μ12 - μ22)2 < -2 σ22 ln (0.05)
- Maximum delta in direction of the pm vectors (45° following Hartkopf 2013)
- Delta proper motion vector length less than given pm error.

All these criteria are pm number based with the usual problem that the pm data in the existing catalogs is often less than reliable as is easy to demonstrate by looking at pm numbers from different catalogs. So CPM pairs "discovered" using a single catalog violate a basic rule for astronomical data mining: never trust a single source. Yet even assuming the numbers are correct and the criteria for detecting CPM pairs are sufficient this is still not sufficient to assume a physical relationship in terms of a common origin – they might very well be fellow travelers by random. So some additional research seems necessary by checking as many sources as possible for hints of a physical relationship such as spectral type, color, radial velocity, distance, and so on. On the other hand stars with rather low proper motion might be candidates as physical pairs if color and magnitudes are similar as the probability that such a combination is given for close objects by random is rather very low.

The WDS catalog is by definition a compilation of trusted observations reports, which means usually published in peer reviewed journals. Thus many objects are included in the WDS catalog as CPM pairs based on such reports, which also means without applying a consistent set of criteria. As the number of CPM pair related reports is increasing rapidly we think there should be a simple but reliable concept for eliminating false CPM positives.

Description of the new concept

With the availability of new star catalogs with RA/Dec positions of high precision the obvious way for counter-checking assumed CPM pairs is the comparison of positions in such catalogs with some decades between the observation epochs. The procedure is straight forward:

- Calculating the distance and the position angle between the star positions in different epochs similar to calculating separation and position angle for double stars, including calculating corresponding error estimations
- Comparing the values for distance and position angle for the two components of an assumed CPM pair to check if the direction and the length of the proper motion vector is within the calculated error estimations
- To stay within a reasonable range of error estimations it is necessary to keep the relation of position error to the length of the proper motion vector rather small – else the resulting error estimation would allow results with absurdly high deviations to be considered as "similar"
- The same goes for the calculated proper motion vector length per year – the difference between the two values for the two components should be as small as possible to be reasonable
- As an historical reference we might also check if the pm vector is at least 50mas/yr according to Halbwachs 1986 – but in this context this seems not really important as we are not data mining but simply counter-checking.

In a first attempt the obvious catalog choice was for UCAC4 and URAT1 as the currently most precise catalogs used for plate solving. But here an unexpected issue arose – UCAC4 has different observations epochs for RA and Dec making it difficult to determine a reliable time frame between the UCAC4 and URAT1 observation epochs. To consolidate different RA/Dec epochs to a common mean epoch would be possible by applying the given pm data to the given coordinates – but this would mean using the existing pm data we wanted to avoid from the very beginning to keep our approach consistent. Simply averaging the RA/Dec epochs might have been a possibility for rather small differences of less than 1 year. But then the next issue arose: even in cases with very similar to identical UCAC4 RA/Dec epochs the counter-check results remained inconsistent as the resulting pm vector/yr values showed unexpectedly large deltas between the components of well-established CPM pairs. This led to the conclusion that there might be an observation epoch issue with UCAC4 we might not be able to resolve.

As an alternative for UCAC4 we looked at the Initial Gaia Source List created as starting point for the Gaia Initial Data Treatment. If IGSL is good enough to be used as starting point for the Gaia results then it should be good enough for our purpose. First checks showed promising results and for our purpose a very positive attribute of IGSL: a consistent observation epoch of 1983.89 giving a time frame of ~30 years when comparing positions with URAT1 – a time frame large enough to allow for significant proper motion results. One issue arose also with the use of IGSL positions as a starting point: the resulting proper motion vector lengths are consistently less than half of the given pm data values in IGSL or URAT1. A first idea was an error in our spreadsheet but using positions from POSS I 1954 and POSS II 1994 we got results similar to the current catalog values – this means our spreadsheet is working fine and that there must be some position issue either with the old plates or with the contemporary catalogs. We assumed the former but then additional issues arose with not very convincing results for several objects (for example STT30AC and SKF299CD). IGSL is a compilation catalog produced for the Gaia mission with combined data from the following catalogs: Tycho2, LQRF, UCAC4, SDSS-DR9, PPMXL, GSC23, GEPC, OGLE, Sky2000, 2MASS. According to the authors (Smart and Nicastro 2014) this catalog is reliable but includes unavoidable errors and the user should have in mind that it is to be used with care for individual objects – obviously we stumbled over this caveat.

We found then that such issues were easily resolved by using 2MASS as a reference catalog and that this setup also solved the issue with the pm/yr riddle given with UCAC4 and IGSL by providing reasonable pm values also per year. Using 2MASS instead of IGSL means in theory loss of about 15 years time distance between observation epochs but the results told us that this is an illusion as the IGSL mean epoch is obviously questionable. We then realized that URAT1 also uses 2MASS as reference for calculating pm values making our second reference catalog switch all the more understandable. However, the question of obvious observation epoch issues with UCAC4 and IGSL remains open and we can only hope that the evident shaky IGSL data quality will not have consequences for the future GAIA catalog data quality.

Finally another issue arose with the given quite small proper motion errors in URAT1 not matching very well with the pm error calculations we made based on the given 2MASS position errors. When investigating this further we found the cause is the use of a rather low estimated mean 2MASS position error for URAT1 with the consequence that any data mining based on URAT1 using the given e_pm value without any counter-checking is highly questionable.

Description of Details and Usage of the Check CPM spreadsheet

In the spreadsheet we developed for the CPM counter-check we use the following formulas and checks:

- Proper motion vector direction: Calculated from the RA Dec coordinates as arctan((RA2-RA1)*cos (Dec1))/(Dec2-Dec1)) in radians depending on quadrant (Buchheim 2008)
- Proper motion vector length: Calculated from the RA Dec coordinates as SQRT(((RA2-RA1)*cos (Dec1))^2+(Dec2-Dec1)^2) in radians (Buchheim 2008)
- Proper motion vector length error estimation e_PMVL: Calculated as SQRT(e_RA^2+e_Dec^2) with e_RA and e_Dec as given IGSL RA and Dec errors
- Proper motion vector direction error estimation e_PMVD: Calculated as arctan(e_PMVL/PMVL) in degrees assuming the worst case that e_PMVL points in the right angle to the direction of the proper motion vector means perpendicular
- Check for identical PMVD by comparison Δ PMVD with e_PMVD resulting in an "A" for being smaller, "B" for being larger but still smaller than 2*e_PMVD and "C" for being larger than that
- Check for identical PMVL by comparison Δ OMVL with e_PMVL resulting in an "A" for being smaller, "B" for being larger but still smaller than 2*e_PMVL and "C" for being larger than that
- Check relation of the position error to pm vector length: As both checks for identical PMVD and PMVL depend highly on the size of e_PMVL we check additionally the relationship between the size of e_PMVL to PMVL for both components resulting in an A if both e_PMVL are less than 5% of PMVL, in a "B" if at least one or both e_PMVL are less than 10% of PMVL and in a "C" if at least one e_PMVL is larger than 10% of PMVL. This check corresponds to some degree to the significance criterion according to Caballero et al 2010

The spreadsheet can be downloaded from http://www.sterngucker.eu/XLS/Check%20CPM%202MASS%20to%20URAT1.xlsx

Usage of the spreadsheet:

- Locate the object in Aladin V9
- Load the 2MASS catalog
- Load the URAT1 catalog
- Click on the primary to get the data for the "2 superimposed objects"
- Do the same for the secondary while pressing Upper Case to get the data for the additionally "2 superimposed objects"
- Right click on the data lines with "Copy all measurements (for Excel)"
- Copy into the spreadsheet with cell A7 marked
- Click the VizieR links in Aladin for 2MASS catalog entry details and enter 2MASS position errors and Julian observation date into the spreadsheet in lines 11 and 12 (usually identical except for very wide pairs)
- Enter the name of the object into cell D14
- Interpretation of the results

This procedure needs an additional step for Excel language versions using a decimal separator different from the decimal point – for example the decimal comma in the German version: in this case after copying the data into the spreadsheet you need to simply change all "." into "," for all fields marked after the copy command.

Interpretation of the result: The following is a kind of rating in form of A/B/C for the different criteria with a triple A for a perfect result.

- The first letter stands for the comparison of the pm vector direction: "A" means within the error range calculated from the given 2MASS position error but at least within 2.86°, "B" means within the double error range but at least within 5.72° and "C" means outside the double error range or outside 5.72°. An assumed CPM pair with a "B" would already need very good additional arguments like same spectral type of other physical attributes to be acceptable as assumed physical. And a "C" means clearly not CPM because moving in different directions. The requirement of less than 2.86° for an A is based on the assumption that two close stars within the same image should share a rather similar position error thus reducing the theoretical effect assumed in the error range calculation.
- The second letter stands for the comparison of the pm vector length: "A" means within the error range calculated from the given 2MASS position error and the vector length but at least within 5% of the pm vector length, "B" means within the double error range but at least within 10% of the pm vector

length and "C" means outside the double error range or outside 10%. An assumed CPM pair with a "B" would already need very good additional arguments like same spectral type of other physical attributes to be acceptable as assumed physical. And a "C" means clearly not CPM because of a too large delta in pm vector length. The requirement of less than 5% for an A is again based on the assumption that two close stars within the same image should share a rather similar position error so any delta should remain below this value.

- The third letter stands for the data quality in terms of the relation of the 2MASS position error to the length of the pm vector length: "A" stands for less than 5% allowing up to 2.86° delta in proper motion vector direction, "B" stands for less than 10% allowing up to 5.72° delta in proper motion vector direction and "C" stands for more than 5.72°. An assumed CPM pair with a "B" is thus already considered a bit shaky in terms of data quality and would already need very good additional arguments like same spectral type of other physical attributes to be acceptable as assumed physical. And a "C" means clearly not CPM because of a too large position error to pm vector length relation rendering such results as unreliable. This check is very important because it questions the results in the first two letters – in other words an "AA" followed by "B" or "C" indicates very similar pm direction and speed but with the possibility of a "lucky hit" within the given error range.
-

We then selected assumed CPM objects from the different sources listed in references and acknowledgements and applied the CPM Check Spreadsheet.

First Impressions

After finishing the draft of our table with the CPM check results we did an initial statistical analysis with in total 139 objects:

- 125 are WDS objects
- 92 of them have V-Codes and one has an O code (for orbit), which equals a total of 93 marked as CPM if we take O as close to CPM
- of these 93 objects only 14 got a solid AAA, 23 got an AAB and 7 an AAC, making a total of 44 objects with confirmed CPM results, which is less than 50% of the V-coded objects
- of these 93 objects 7 have an ABA to ABC rating so things get a bit shaky here
- Next we have 5 pairs with similar direction but different speed. Interestingly the O-coded object is in this group. It would be worth checking if this result is in agreement with the calculated orbit (see summary)
- Next we have 15 objects with BAB to BCC, meaning objects with rather different pm direction
- Finally we have 22 objects with CAB to CCC rendering the V-code as highly suspect, which is equal to about 25% of the total
- In the next group we have 32 WDS objects without V-code
- 15 of them with AAA to AAC rating means solid CPM
- 5 of them BAA to BBC means potential CPM
- 12 more with BCC to CCC
- Finally we have 14 objects not included in the WDS catalog
- 9 of them AAA to AAC means solid CPM pairs
- 2 with ABA and BAC means potential CPM
- 3 with CAC means pm in different directions thus probably not CPM

The mentioned 32 WDS objects without V-code were selected from different sources as declared or suspected CPM candidates – about 50% of them are confirmed as serious CPM objects.

Most interesting are the 14 objects mentioned above which are not included in the WDS catalog with about 75% of them serious CPM candidates – all were selected because of clear hints for being CPM objects and most of them from the LSPM catalog. It seems that the LSPM catalog is still a good source for finding so far not cataloged CPM pairs. Amazingly most close LSPM objects show very similar pm direction and speed and qualify as components of a CPM pair.

Next step was to counter-check the last group of 22 suspect WDS V-coded objects with POSS images to get an impression if our results were in line with images of these objects with a time distance of ~40 years.

This quickly resulted in a slightly confusing situation in which an object with a small PM is rather unspectacular when blinking POSS images or making Aladin mosaics of them – so we had to learn that no noticeable pm here is a confirmation of our non-CPM results. A side result was the detection of a few WDS errors in form of typos or mismatch of components.

Most interesting here is the fact that a good part of these objects showed significant changes in the proper motion data from the UCAC4 catalog to the URAT1 catalog, probably making the difference between whether CPM was assumed or not. This demonstrates once more that there are some risks in relying solely on the PM numbers in one single catalog and that it is necessary to check the CPM status for objects of interest from time to time, especially when new position

A New Concept for Counter-Checking of Assumed CPM Pairs

data is available.

Table 1 includes a selection of pairs that were evaluated as CCC by our Check CPM spreadsheet, in which we compare PM data from the UCAC4 and URAT1 catalogs. Those numbers which resulted in a noticeable change in relative motion between the components are highlighted in red in the table. In a few cases, such as GMC 13 DC and PNT 2, the change in data increased the possibility of shared proper motion. In addition, there were a few instances in which the data changes resulted in a change of direction of one of the components, such as PKO 5, SMR 67, and UC 306. However, in the majority of cases we looked at, the change from UCAC4 to URAT1 data resulted in an increased divergence of direction, making common proper motion less likely.

Some Examples

Table 2 shows the results of our CPM Check spreadsheet for CPM assumed objects from different sources indicated in the Notes column.

Summary

The approach presented here for checking assumed CPM pairs for validity is, as shown in the examples above, a useful tool to identify pairs with reliable data suggesting common proper motion in the sense of being within a reasonable error range for identical direction and speed. Such a check should in our opinion be applied on any object suggested to be a newly "discovered" CPM pair and over time also to all pairs currently in the WDS labeled with the V note code.

Known weaknesses of our approach and interesting side results of our study follow:

- URAT1 is available only for the northern skies – so our approach shares this limitation making it for example impossible to check AHD17 (Ahad 2013). Would have been of interest as the proper motion/yr of this pair is far below the Halbwachs 1986 criterion of 50mas.
- As already mentioned UCAC4 and IGSL seem to have serious data quality problems with the mean observation epoch as is shown by unrealistic low pm/yr values when dividing the calculated proper motion vector length by the time frame between the given observation dates.
- As already mentioned URAT1 provides rather optimistic pm error estimations by assuming a rather low average 2MASS position error of ~90mas resulting in modest ~6mas/yr with only minor variations due to the time difference in observation dates. As our research relies heavily on the effective given 2MASS position error we get rather often more than triple this value. This means that all CPM research relying exclusively on the URAT1 e_pm data (like for example Nicholson 2015) is rendered as highly suspect.
- While URAT1 was created with special considerations to include also brighter stars this can get complicated if proper motion is involved. Caveat in the "readme.urat1" file: "Stars with higher proper motions were not attempted to match for this release, neither were other catalogs used to improve the proper motions". An example for such a case is 61 Cyg mentioned by Aitken 1922 as special proper motion object or the WDS V-coded CPM pair OSV3. In the URAT1 catalog we have found objects corresponding with the 61 Cyg components are located far away from the corresponding star disks in images such as 2MASS due to the huge pm speed – it simply needs some time and patience to locate such objects.
- 61 Cyg shows also the limited value of our approach for very fast proper motion pairs. Based on our own measurement as a substitute for the URAT1 positions we were initially unable to find in the Aladin image of 61 Cyg, the result is a proper motion direction of ~52° with a delta of less than 0.5° and a proper motion vector length of amazing

(Continued on page 49)

Table 1: Examples for Proper Motion Data Change from UCAC4 to URAT1 Catalogs

Disc. Code	Catalog	PM in RA Primary	PM in DEC Secondary
GMC 13DC	UCAC4	+010.8 -003.8	-004.2 **-014.3**
	URAT1	+009.1 -002.7	-003.5 **-004.2**
PKO 5	UCAC4	**-001.3** +001.0	**-001.5** +000.2
	URAT1	**+003.7** +001.5	**+001.6** +001.3
PNT 2	UCAC4	+029.9 -079.7	+031.5 **-082.3**
	URAT1	+026.8 -073.3	+027.2 **-074.4**
SHY 378	UCAC4	-017.6 +018.6	**-017.8** +019.2
	URAT1	-014.4 +020.1	**-022.7** +020.1
SKF2325	UCAC4	-019.0 **+003.8**	-017.1 +004.7
	URAT1	-020.7 **+007.1**	**-024.1** +005.5
SMR 16AC	UCAC4	**+003.8** -007.0	+005.4 -007.4
	URAT1	**+014.8** -000.4	+006.4 -005.7
SMR 66	UCAC4	**+013.0 -015.5**	No data
	URAT1	**+006.1 -000.2**	-008.8 -004.0
SMR 67	UCAC4	-012.4 -023.1	**-014.9** -018.8
	URAT1	-009.8 -024.3	+001.0 -017.8
STI 117	UCAC4	**-020.0 -014.0**	-012.8 **-006.4**
	URAT1	**-006.5 -005.6**	-007.5 **-011.8**
UC 302	UCAC4	**+061.1 -000.2**	+056.2 **-003.9**
	URAT1	**+053.0 +015.0**	+051.2 **+013.2**
UC 306	UCAC4	+071.2 **-004.3**	**+051.8** -022.5
	URAT1	+075.8 **+005.2**	**+061.1** -016.3

A New Concept for Counter-Checking of Assumed CPM Pairs

Table 2. CPM Check results for the selected objects. Explanation of the content: Object = discoverer or catalog ID (in case of LSPM objects only for one of the components). PMVD A = proper motion vector direction in degrees for component A. PMVD B = proper motion vector direction in degrees for component B. e_PMVD = error estimation for the pm vector direction according to the given 2MASS position error. PMVL A mas = proper motion vector length of component A in mas. PMVL B mas = proper motion vector length of component B in mas. e_PMVL mas = error estimation for the pm vector length according to the given 2MASS position error. PMVD Δ = rating for the resulting proper motion vector direction delta between the components. PMVL Δ = rating for the resulting proper motion vector length delta between the components. e_PMVL = rating for the relation of the 2MASS position error to the proper motion vector length.

Object	PMVD A	PMVD B	e_PMVD	PMVL A mas	PMVL B mas	e_PMVL mas	PMVD Δ	PMVL Δ	e_PMVL	WDS Code	Notes
ADS1727	141.48	141.50	2.860	1,181.7	1,179.4	59.027	A	A	B	VD	Selected by random from Halbwachs 1986 (Table II). PM direction and speed very close, position error ~7% of pm vector length - solid AAB CPM rating.
ADS 191	104.26	101.94	2.860	1,260.1	1,239.2	62.481	A	A	B	VD	Selected by random from Halbwachs 1986. Relation position error to pm vector length ~8% so CPM confirmation not perfect.
ADS8108	66.79	68.44	2.860	2,534.3	2,415.6	123.748	A	A	B	VDZ	Selected by random from Halbwachs 1986. Relation position error to pm vector length ~6% so CPM confirmation just slightly not perfect.
ADS8168	170.72	173.55	2.860	1,276.0	1,292.7	64.216	A	A	B	VD	Selected by random from Halbwachs 1986. Relation position error to pm vector length ~7% so CPM confirmation not perfect.
AG 32AB	92.00	90.12	2.860	514.5	516.6	25.779	A	A	C	-	Picked at random from Harshaw, 2016. His results categorize AG 32 AB as CPM. Check CPM results good for vector direction and length, but position error in relation to PM vector length is slightly beyond the 10% cutoff for a B rating (16.5% for A, 16.4% for B). Simbad shows A as an F8 star, but doesn't provide a spectral class for B.
AG 193	282.19	283.24	2.860	1,648.2	1,608.3	81.414	A	A	B	VD	Cross reference object from Knapp 2016 (Measurements of some VizieR I/330 objects). e_PMVL larger than 5% of PVML for B, yet Check CPM result seems rather positive. Listed also in Vizier I/330 as MPN 4969 "newly discovered" from Nicholson 2015.
ARG 5	211.33	191.42	2.860	61.1	83.4	3.612	C	C	C	-	Picked at random from Harshaw, 2016. His results categorize ARG 5 as CPM. The vector direction and length are outside the 2x error range, while the position error in relation to the PM vector is well outside the 10% cutoff (138.9% for A, 101.8% for B). Simbad shows the primary with a spectral class of B9, none listed for the secondary.
ARN 55AD (HJL 1011)	127.37	132.97	2.860	889.0	739.4	40.709	B	C	C	-	Picked at random from Halbwachs, 1986. Check CPM results show the pair is in the 2x error range for vector direction and outside the 2x the error range for vector length; position error in relation to PM vector length is at the outside edge of the B range for the A component (9.5%) and just outside the B range for the secondary (11.5%). Both Halbwachs and Simbad show A with a spectral class of A3 and D as G5.
BEM 16	162.39	164.65	2.860	1,732.5	1,717.2	86.244	A	A	B	-	Cross reference object from Knapp 2016 (Measurements of some VizieR I/330 objects). B rating for only slightly above 5% position error ratio - looks like a good CPM confirmation. Listed in VizieR I/330 as "newly discovered pair" MPN 5359.
BGH 22	297.17	302.03	2.860	2,719.0	2,762.0	137.025	B	A	A	-	Picked at random from Benavides, et al, 2010. Check CPM results show the pair is in the 2x range for vector direction and within the error range for vector length; the position error in relation to the PM vector length is within the criteria for an A rating (4.3% for A, 4.2% for B).
BGH 35 (HJL 1064)	277.05	281.14	2.860	1,657.8	1,597.5	81.382	B	A	C	-	Picked at random from Halbwachs, 1986. Check CPM results show the pair is within the 2x error range for vector direction and within the error range for vector length; position error in relation to PM vector length is just inside the B range for the A component (9.2%) and outside the B range for the secondary (16.5%). Both Halbwachs and Simbad shows A with an F5 spectral class and B as G5.
BGH 1AB,C (HIP 190)	203.65	204.33	2.860	1,557.9	1,570.5	78.210	A	A	B	V	Selected from Shaya and Olling 2011. Solid AAB CPM rating, 2MASS position error ~6,5% of pm vector length.
BU 1442AB	144.34	144.36	0.683	16,395.2	16,477.9	196.469	A	A	A	VDP	Selected by random from the WDS catalog as V-coded object. Solid triple AAA CPM rating.

Table 2 continues on next page.

A New Concept for Counter-Checking of Assumed CPM Pairs

Table 2 (continued). CPM Check results for the selected objects. Explanation of the content: Object = discoverer or catalog ID (in case of LSPM objects only for one of the components). PMVD A = proper motion vector direction in degrees for component A. PMVD B = proper motion vector direction in degrees for component B. e_PMVD = error estimation for the pm vector direction according to the given 2MASS position error. PMVL A mas = proper motion vector length of component A in mas. PMVL B mas = proper motion vector length of component B in mas. e_PMVL mas = error estimation for the pm vector length according to the given 2MASS position error. PMVD Δ = rating for the resulting proper motion vector direction delta between the components. PMVL Δ = rating for the resulting proper motion vector length delta between the components. e_PMVL = rating for the relation of the 2MASS position error to the proper motion vector length.

Object	PMVD A	PMVD B	e_PMVD	PMVL A mas	PMVL B mas	e_PMVL mas	PMVD Δ	PMVL Δ	e_PMVL	WDS Code	Notes
BVD 14	147.25	156.24	2.860	204.2	273.4	11.938	C	C	C	-	Picked at random from Benavides, et al, 2010. Check CPM results show the pair is outside the 2x error range for both the vector direction and length; position error in relation to PM vector length is well outside the error range (61.4% for A, 45.6% for B). Simbad shows the primary with a spectral class of F6 and the secondary as K3.
BVD 18	118.37	125.76	2.860	1,285.1	1,290.6	64.392	C	A	B	-	Picked at random from Benavides, et al, 2010. Check CPM results show the vector direction is outside the 2x range, while the vector length is within the error range; the position error in relation to the PM vector length is just inside the criteria for a B rating (6.6% for both components). Simbad shows the primary with a spectral class of G8 and the secondary as G7.
CBL 105	44.91	45.56	2.860	832.0	889.1	43.028	A	B	C	V	Picked at random from Caballero, 2009. Check CPM results show the pair is within the error range for vector direction, vector length is in the 2x error range; and the position error in relation to PM vector length is just at the fringe of being outside the B range (10.2% for A and 9.5% for B). Simbad doesn't show spectral classes for either star.
CBL 119	165.57	165.64	2.860	1,236.8	1,236.7	61.837	A	A	B	V	Picked at random from Caballero, 2010. Check CPM results show the pair is within the error range for vector direction and length; position error in relation to PM vector length is in the middle of the B range (7.5% for both A and B). Simbad doesn't show spectral classes for either star.
CBL 148	238.13	236.48	2.860	951.8	925.8	46.940	A	A	C	V	Picked at random from Caballero, 2010. Check CPM results show the pair is within the error range for vector direction and length; position error in relation to PM vector length is decidedly outside the B range (18.8% for A and 19.3% for B). Simbad doesn't show spectral classes for either star.
CBL 167	171.83	171.20	2.860	604.8	784.3	34.728	A	C	C	V	Picked at random from Caballero, 2010. Check CPM results show the pair is within the error range for vector direction but outside the 2x error range for length; position error in relation to PM vector length is a bit outside the B range (14.0% for A and 10.8% for B). Simbad shows both stars with a G5 spectral class.
CBL 181	116.72	126.92	2.860	1,274.7	1,265.1	63.495	C	A	B	V	Picked at random from Caballero, 2010. Check CPM results show the pair is outside the error range for vector direction and within the error range for vector length; position error in relation to PM vector length is just inside the B range (6.7% for both A and B). Simbad shows both stars with a K0 spectral class (HD 358326 and HD 358327). Blinking suitable 2MASS and SERC (in lack of POSS) images suggest somewhat similar pm direction and speed. Comparisons of pm data show some changes from UCAC4 to URAT1 suggesting CPM rather with UCAC4 but no longer with URAT1.
CBL 193	95.00	95.16	2.860	2,113.3	2,085.8	104.976	A	A	A	V	Picked at random from Caballero, 2010. Meets all three Check CPM criteria for CPM. Simbad has no spectral class for A, but lists B as K4/5.
CBL 21	75.03	75.86	2.860	1,874.4	1,881.8	93.905	A	A	A	V	Picked at random from Caballero, 2009. Meets all three Check CPM criteria for CPM. No spectral class shown in Simbad for either star.
CBL 53	277.83	278.94	2.860	1,207.8	1,221.3	60.725	A	A	B	V	Picked at random from Caballero, 2009. Check CPM results show the pair is within the error range for vector direction and length; position error in relation to PM vector length is in the middle of the B range (7.6% for both A and B). Simbad doesn't show spectral classes for either star.
CBL 70	280.52	278.93	2.860	1,084.3	1,057.2	53.539	A	A	B	V	Picked at random from Caballero, 2009. Check CPM results show the pair is within the error range for vector direction and length; position error in relation to PM vector length a bit past the middle of the B range (8.5% for A and 8.7% for B). Simbad doesn't show spectral classes for either star.

Table 2 continues on next page.

A New Concept for Counter-Checking of Assumed CPM Pairs

Table 2 (continued). CPM Check results for the selected objects. Explanation of the content: Object = discoverer or catalog ID (in case of LSPM objects only for one of the components). PMVD A = proper motion vector direction in degrees for component A. PMVD B = proper motion vector direction in degrees for component B. e_PMVD = error estimation for the pm vector direction according to the given 2MASS position error. PMVL A mas = proper motion vector length of component A in mas. PMVL B mas = proper motion vector length of component B in mas. e_PMVL mas = error estimation for the pm vector length according to the given 2MASS position error. PMVD Δ = rating for the resulting proper motion vector direction delta between the components. PMVL Δ = rating for the resulting proper motion vector length delta between the components. e_PMVL = rating for the relation of the 2MASS position error to the proper motion vector length.

Object	PMVD A	PMVD B	e_PMVD	PMVL A mas	PMVL B mas	e_PMVL mas	PMVD Δ	PMVL Δ	e_PMVL	WDS Code	Notes
CBL 9	70.22	72.85	2.860	1,066.1	1,040.0	52.654	A	A	B	V	Picked at random from Caballero, 2009. Check CPM results show the pair is within the error range for vector direction and length; position error in relation to PM vector length is at the extreme edge of the B range (9.3% for A, 9.5% for B). Simbad doesn't show spectral classes for either star.
CBL 92	59.92	59.01	2.860	723.3	728.5	36.294	A	A	C	V	Picked at random from Caballero, 2009. Check CPM results show the pair is within the error range for vector direction and length; position error in relation to PM vector length is just beyond the B range (11.7% for A and 11.6% for B). Simbad doesn't show spectral classes for either star.
CLL 21AC	220.98	5.13	2.860	680.5	364.0	26.112	C	C	C	V	Obviously a WDS error regarding components should be BC and would then be ident with SKF 179 BC, which is shown below. Correspondence with Bill Hartkopf resulted in the V code being removed from CLL 21 AC after confirmation of error. That CLL 21 AC is not a CPM pair was confirmed also by counter-checking with blinking of POSS images.
CRB 8	86.06	85.62	2.695	2,770.1	2,754.8	130.384	A	A	A	V	Selected by random with own research in the LSPM catalog (Lepine and Shara 2005) for close objects. Solid triple AAA CPM rating.
CRB 9	115.05	114.95	2.860	2,278.6	2,344.9	115.589	A	A	B	V	Selected by random with own research in the LSPM catalog (Lepine and Shara 2005) for close objects. PM direction and speed very close, position error only for one component slightly above 5% of the pm vector length - very solid triple AAB CPM rating.
DAM 349	172.55	170.42	2.860	918.6	939.4	46.448	A	A	B	V	Selected by random from the WDS catalog as V-coded object. Relation position error to pm vector length slightly smaller than 10%, similar direction and speed thus considered a bit unreliable, otherwise CPM looks promising. Listed also in VizieR I/330 as MPN 5852 as "new discovery 2015."
DU 4 (HJL 325)	204.82	205.72	2.860	855.9	1,040.1	47.400	A	C	C	V	Picked at random from Halbwachs, 1986. Check CPM results show the pair is within the error range for vector direction and outside the 2x the error range for vector length; position error in relation to PM vector length is a bit outside the B range for the A component (11.6%) and within the B range for the secondary (9.5%). Both Halbwachs and Simbad shows each star with a spectral class of F8.
ES 149AB (HJL 320)	85.38	81.55	2.860	1,233.0	1,187.6	60.515	B	A	C	VD	Picked at random from Halbwachs, 1986. Check CPM results show the pair is within the 2x error range for vector direction and within the error range for vector length; position error in relation to PM vector length is a bit outside the B range for the A component (13.2%) and within the B range for the secondary (8.4%). Both Halbwachs and Simbad shows A with an F8 spectral class, but neither shows a class for B. The URAT1 PM numbers (+088.8 +007.2 and +083.6 +012.5) are very different from the PM numbers shown in the WDS (+057 +026 and +089 +005). The Simbad numbers also differ (+090.1 +008.6 and +088.9 +004.9).
GIC 168	46.84	47.63	2.696	2,513.6	2,548.4	120.000	A	A	A	V	Selected by random from the WDS catalog as V-coded object. Solid triple AAA CPM result.
GIC 24	91.64	91.71	2.014	3,981.1	3,905.7	140.000	A	A	A	V	Selected by random from the WDS catalog as V-coded object. Solid triple AAA CPM result.
GMC 13DE	106.77	219.17	2.860	131.0	75.7	5.168	C	C	C	V	Selected by random from the WDS catalog as V-coded object. Interesting idea that this should be a CPM pair. Difficult to detect any change in position in the primary when blinking POSSI (1954) and POSSII (1998) images; slight change toward the south is noticeable in the secondary. Rate of PM has lessened noticeably starting with NOMAD1 data and moving to UCAC4 and then to URAT1, which currently shows rates of +009.1 -002.7 for the primary and -003.5 and -004.2 for the secondary. Based on the URAT1 data, motion in the primary should be more obvious than in the secondary.

Table 2 continues on next page.

A New Concept for Counter-Checking of Assumed CPM Pairs

Table 2 (continued). CPM Check results for the selected objects. Explanation of the content: Object = discoverer or catalog ID (in case of LSPM objects only for one of the components). PMVD A = proper motion vector direction in degrees for component A. PMVD B = proper motion vector direction in degrees for component B. e_PMVD = error estimation for the pm vector direction according to the given 2MASS position error. PMVL A mas = proper motion vector length of component A in mas. PMVL B mas = proper motion vector length of component B in mas. e_PMVL mas = error estimation for the pm vector length according to the given 2MASS position error. PMVD Δ = rating for the resulting proper motion vector direction delta between the components. PMVL Δ = rating for the resulting proper motion vector length delta between the components. e_PMVL = rating for the relation of the 2MASS position error to the proper motion vector length.

Object	PMVD A	PMVD B	e_PMVD	PMVL A mas	PMVL B mas	e_PMVL mas	PMVD Δ	PMVL Δ	e_PMVL	WDS Code	Notes
GRV 840	244.30	244.38	2.860	1,509.1	1,509.4	75.463	A	A	B	-	Picked at random from Benavides, et al, 2010. Check CPM results show the pair is within the error range for vector direction and length; position error in relation to PM vector length is in the middle of the B range (7.0% for both components). Simbad shows A with a spectral class of G7 and B as K1.
GRV 589	212.67	209.26	2.860	1,524.2	1,600.2	78.112	B	A	B	V	Selected by random from the WDS catalog as V-coded object. PM direction slightly larger than 2.86° and position error slightly larger than 5% of the proper motion vector, potential CPM result, but far from perfect.
GRV 862	285.50	283.37	2.860	1,396.0	1,367.1	69.079	A	A	B	V	Selected by random from the WDS catalog as V-coded object. Position error near 10% of the proper motion vector, border case of plausible CPM result.
GWP 117	225.45	223.20	2.860	843.2	893.3	43.413	A	B	C	V	Selected by random from the WDS catalog as V-coded object. Position error in relation to proper motion vector length too large to be considered as confirmed CPM pair; also pm vector length delta a bit too large.
GWP 52	88.47	86.85	2.860	823.5	832.8	41.407	A	A	C	V	Selected by random from the WDS catalog as V-coded object. Position error in relation to proper motion vector length too large to be considered as reliable confirmed CPM pair.
GWP 964	180.95	181.85	2.860	1,808.9	1,740.8	88.742	A	A	A	V	Selected by random from the WDS catalog as V-coded object. Solid triple AAA CPM rating.
HAU 10	112.20	111.95	2.860	1,839.6	1,827.8	91.685	A	A	A	V	Selected by random from the WDS catalog as V-coded object. Solid triple AAA CPM confirmation.
HDS 2093	267.38	269.53	2.860	2,202.5	2,121.1	108.091	A	A	A	V	Cross reference object from Knapp 2016 (Measurements of some VizieR I/330 objects). PM direction and speed quite similar and position error below 5%. Solid triple AAA CPM confirmation. Listed also in VizieR I/330 as MPN 5211 as "new discovery 2015."
HJ 1267 (HJL 211)	252.23	259.13	2.860	935.5	882.1	45.439	C	B	C	V	Picked at random from Halbwachs, 1986. Check CPM results show the pair is outside the 2x error range for vector direction and within the 2x error range for vector length; position error in relation to PM vector length is just outside the B range for both components (11.4% for A and 12.1% for B). Halbwachs and Simbad show A with a spectral class of G5 but neither list a class for the B component. Mosaic and blinking of POSS images did not show anything conclusive - roughly similar direction and speed. The pm numbers in UCAC4 and URAT1 are rather different and do both not suggest CPM.
HJ 1930	229.38	234.90	2.860	80.2	87.0	4.180	B	B	C	-	Picked at random from Harshaw, 2016, where the results categorize HJ 1930 as CPM. Check CPM results show vector direction and length in the 2x range; the position error in relation to PM vector length is far outside the 10% cutoff for both stars. Simbad shows the two stars with spectral classes of B1.5 and B1.
HJ 547	209.99	213.39	2.860	1,322.2	1,293.5	65.392	B	A	B	-	Cross reference object from Knapp 2016 (Measurements of some VizieR I/330 objects). PM direction and speed not this close and position error far above 5%, looks like a not solid CPM confirmation. Listed also in VizieR I/330 as MPN 4983 as "new discovery 2015."
HJL 1	98.07	99.69	2.860	1,021.2	971.0	49.805	A	B	B	V	Picked at random from Halbwachs, 1986. Check CPM results show the pair is within the error range for vector direction and in the 2x error range for vector length; position error in relation to PM vector length is at the outer edge of the B range (9.0% for A and 9.5% for B). Simbad shows A with a spectral class of F6 and B as G1.

Table 2 continues on next page.

A New Concept for Counter-Checking of Assumed CPM Pairs

Table 2 (continued). CPM Check results for the selected objects. Explanation of the content: Object = discoverer or catalog ID (in case of LSPM objects only for one of the components). PMVD A = proper motion vector direction in degrees for component A. PMVD B = proper motion vector direction in degrees for component B. e_PMVD = error estimation for the pm vector direction according to the given 2MASS position error. PMVL A mas = proper motion vector length of component A in mas. PMVL B mas = proper motion vector length of component B in mas. e_PMVL mas = error estimation for the pm vector length according to the given 2MASS position error. PMVD Δ = rating for the resulting proper motion vector direction delta between the components. PMVL Δ = rating for the resulting proper motion vector length delta between the components. e_PMVL = rating for the relation of the 2MASS position error to the proper motion vector length.

Object	PMVD A	PMVD B	e_PMVD	PMVL A mas	PMVL B mas	e_PMVL mas	PMVD Δ	PMVL Δ	e_PMVL	WDS Code	Notes
HJL1019 AB	103.31	102.42	2.860	1,355.6	1,351.0	67.666	**A**	**A**	**B**	-	Picked at random from Halbwachs, 1986. Check CPM results show the pair is within the error range for vector direction and vector length; position error in relation to PM vector length is a bit inside the B range (6.8% for both A and B). Halbwachs shows A with a spectral class of A5m and B as F8.
HJL1020 (53 Ari)	314.82	158.79	2.860	133.3	307.8	11.027	**C**	**C**	**C**	-	Picked at random from Halbwachs, 1986. Check CPM results show the pair is well outside the 2x error range for both vector direction and vector length; position error in relation to PM vector length is well beyond the B range for both the A component (75.0%) and the B component (32.5%). Both Halbwachs and Simbad show A with a spectral class of B1.5 and B as G5. URAT1 PM's (-006.7 +006.7 and -008.1 -021.0) differ considerably from WDS PM's (-024 +008 and +001 -026). Simbad shows a PM for A of -024.3 +007.5 and for B of -001.1 -028.2.
HJL 54	314.03	315.68	2.860	943.2	921.8	46.624	**A**	**A**	**B**	**V**	Picked at random from Benavides, et al, 2010. Check CPM results good for vector direction and length; position error in relation to PM vector length is right at the edge of the cutoff for a B rating (9.0% for A, 9.2% for B). Simbad shows the primary with a spectral class of F6 and the secondary as F8.
HJL 234	202.39	200.45	2.860	788.8	814.5	40.084	**A**	**A**	**C**	**V**	Selected by random from the WDS catalog as V-coded object. Position error in relation to proper motion vector length too large to allow a fully reliable positive CPM result.
J0526 +6810N	159.84	160.82	2.860	2,407.5	2,355.9	119.085	**A**	**A**	**A**	**n.a.**	Selected by random with own research in the LSPM catalog (Lepine and Shara 2005) for close objects. No WDS catalog object. URAT1 791-095367 and 791-095369 objects with separation 14.070" and PA 28.257°. Solid triple AAA CPM rating. Also included in the VizieR I/330 catalog as MPN 1233 as "newly discovered 2015". Positive counter-checked by blinking POSS images.
J1047 +2117	256.58	257.22	2.860	2,665.6	2,591.5	131.427	**A**	**A**	**B**	**n.a.**	Selected by random with own research in the LSPM catalog (Lepine and Shara 2005) for close objects. No WDS catalog object. URAT1 557-171485 and 557-171484 objects with separation 21.457" and PA 359.171°. PM direction and speed very close, position error slightly outside 5% of the pm vector length - solid triple AAB CPM rating. Also included in the VizieR I/330 catalog as MPN 3088 as "newly discovered 2015". Positive counter-checked by blinking POSS images.
J 1369	138.28	138.73	2.860	2,566.5	2,592.5	128.975	**A**	**A**	**A**	**V**	Selected from the WDS catalog as J-object with code V - fully confirmed with triple AAA. Listed also in VizieR I/330 as MPN 3042 as "new discovery 2015."
J1522 +5942E	179.42	178.60	2.860	2,512.6	2,360.9	121.836	**A**	**B**	**A**	**n.a.**	Selected by random with own research in the LSPM catalog (Lepine and Shara 2005) for close objects. No WDS catalog object. Very faint ~15mag URAT1 749-239708 and 749-239711 objects with separation 14.454" and PA 113.978°. PM direction very similar, speed rather similar, position error less than 5% of the pm vector length - solid triple ABA CPM rating. Also included in the VizieR I/330 catalog as MPN 5479 as "newly discovered 2015."
J1523 +1613N	281.31	281.07	2.860	2,611.0	2,562.3	129.331	**A**	**A**	**A**	**n.a.**	Selected by random with own research in the LSPM catalog (Lepine and Shara 2005) for close objects. No WDS catalog object. URAT1 532-189347 and 532-189351 objects with separation 17.223" and PA 44.257°. Solid triple AAA CPM rating. Also included in the VizieR I/330 catalog as MPN 5480 as "newly discovered 2015". Positive counter-checked by blinking POSS images.
J1650 +2747N	313.04	312.81	2.860	2,436.5	2,335.1	119.291	**A**	**A**	**A**	**n.a.**	Selected by random with own research in the LSPM catalog (Lepine and Shara 2005) for close objects. No WDS catalog object. URAT1 589-215144 and 589-215148 objects with separation 20.999" and PA 44.450°. Solid triple AAA CPM rating. Also included in the VizieR I/330 catalog as MPN 6093 as "newly discovered 2015". Positive counter-checked by blinking POSS images.
J 1804	237.76	243.74	2.860	367.1	380.8	18.698	**C**	**A**	**C**	-	Selected as potential CPM pair with a Jonckheere designation well aware that the pm numbers are too small to be significant - position error in relation to the pm vector length far too large to allow any reliable positive conclusion. PM direction seems too different to suggest CPM.

Table 2 continues on next page.

A New Concept for Counter-Checking of Assumed CPM Pairs

Table 2 (continued). CPM Check results for the selected objects. Explanation of the content: Object = discoverer or catalog ID (in case of LSPM objects only for one of the components). PMVD A = proper motion vector direction in degrees for component A. PMVD B = proper motion vector direction in degrees for component B. e_PMVD = error estimation for the pm vector direction according to the given 2MASS position error. PMVL A mas = proper motion vector length of component A in mas. PMVL B mas = proper motion vector length of component B in mas. e_PMVL mas = error estimation for the pm vector length according to the given 2MASS position error. PMVD Δ = rating for the resulting proper motion vector direction delta between the components. PMVL Δ = rating for the resulting proper motion vector length delta between the components. e_PMVL = rating for the relation of the 2MASS position error to the proper motion vector length.

Object	PMVD A	PMVD B	e_PMVD	PMVL A mas	PMVL B mas	e_PMVL mas	PMVD Δ	PMVL Δ	e_PMVL	WDS Code	Notes
J1945 +3140E	356.50	355.79	2.855	2,406.4	2,365.5	119.297	A	A	A	n.a.	Selected by random with own research in the LSPM catalog (Lepine and Shara 2005) for close objects. No WDS catalog object. URAT1 609-386641 and 609-386725 objects with separation 19.850" and PA 122.948°. Solid triple AAA CPM rating. Surprisingly no entry in the VizieR I/330 catalog.
J1949 +1010E	53.02	51.80	2.860	2,217.4	2,228.9	111.156	A	A	A	n.a.	Selected by random with own research in the LSPM catalog (Lepine and Shara 2005) for close objects. No WDS catalog object. Very faint ~15mag URAT1 501-556660 and 501-556606 objects with separation 24.704" and PA 246.233°. Solid triple AAA CPM rating. Also included in the VizieR I/330 catalog as MPN 7870 as "newly discovered 2015."
J2026 +3156E	46.74	46.12	2.860	2,141.1	2,204.2	108.632	A	A	A	n.a.	Selected by random with own research in the LSPM catalog (Lepine and Shara 2005) for close objects. No WDS catalog object. URAT1 610-486991 and 610-487036 objects with separation 17.215" and PA 60,071°. Solid triple AAA CPM rating. Also included in the VizieR I/330 catalog as MPN 8144 as "newly discovered 2015." Positive counter-checked by blinking POSS images.
J2219 +6640	61.41	61.76	2.860	2,352.8	2,402.2	118.874	A	A	A	n.a.	Selected by random with own research in the LSPM catalog (Lepine and Shara 2005) for close objects. No WDS catalog object, may be ident with LDS 4958 but parameters besides PA do not match very well - and even for PA you have to switch the components for the fainter being A. Very faint ~16mag URAT1 784-195874 and 784-195879 objects with separation 20.668" and PA 13.815°. Solid triple AAA CPM rating. Also included in the VizieR I/330 catalog as MPN 8887 as "newly discovered 2015."
KU 53	173.25	175.37	2.860	1,509.5	1,628.6	78.452	A	B	B	V	V-coded object selected by random from the WDS catalog. PM direction very close and speed rather similar, position error in relation to the pm vector less than 10% - medium solid ABB CPM rating.
LDS2931	210.78	211.92	1.509	4,554.4	4,397.7	120.000	A	B	A	V	Selected by random with own research in the LSPM catalog (Lepine and Shara 2005) for close objects. PM direction very close, speed only slightly outside the error estimation allowed for an A, position error less than 5% of the pm vector length - solid triple ABA CPM rating.
LDS3127	82.49	82.93	2.860	2,387.3	2,387.0	119.356	A	A	A	-	Selected from Kirkpatrick et al 2016, Table 11, Sys. No. 7 as northern sky object with separation <30". Solid triple AAA CPM rating, yet not WDS V-coded.
LDS3131	96.19	96.39	2.860	2,284.5	2,321.5	115.152	A	A	C	V	Selected from Kirkpatrick et al 2016, Table 11, Sys. No. 9 as northern sky object with separation <30". Solid triple AAC CPM rating with a rather large 2MASS position error giving a C in the third position.
LDS4537	192.75	194.23	2.860	1,595.6	1,605.9	80.038	A	A	C	-	Cross reference object from Knapp 2016 (Measurements of some VizieR I/330 objects). PM direction and speed quite similar but large position error makes this a bit unreliable - yet CPM rather confirmed. Listed also in VizieR I/330 as MPN 5399 as "new discovery 2015."
LDS4803	212.99	204.87	2.860	218.0	279.7	12.444	C	C	C	-	Selected by random with own research in the LSPM catalog (Lepine and Shara 2005) for close objects. WDS object but without V-code and otherwise rather suspect parameters. URAT1 666-284685 and 666-284691 objects with separation 7.820" and PA 23.075°. This is certainly no CPM pair and the data suggests LDS 4803 being rather bogus or this is a mismatch.
LDS6302	126.37	125.84	2.860	4,090.1	4,129.5	205.490	A	A	A	I	Selected by random with own research in the LSPM catalog (Lepine and Shara 2005) for close objects. Solid triple AAA CPM rating.
LDS 883AC	128.46	122.45	1.604	5,369.5	5,115.3	150.333	C	B	A	V	Selected STF 326 from Wiley 2015 but URAT1 did not provide an object for the B component, so component C (WDS V-coded as LDS 883 AC) was taken as substitute. Similar pm direction and speed but not close enough to qualify for CPM. Comparison of POSS I and POSS II images confirmed similar pm for component B. Mosaic and blinking of POSS images suggests very similar pm in direction as well in speed. Comparison of UCAC4 and URAT1 pm data is not possible as URAT1 does not offer pm data for this object; however the position data from 2MASS and URAT1 suggests not CPM for this one. A reason for this might very well be a parabolic orbit suggested for STF 326 AB.

Table 2 continues on next page.

A New Concept for Counter-Checking of Assumed CPM Pairs

Table 2 (continued). CPM Check results for the selected objects. Explanation of the content: Object = discoverer or catalog ID (in case of LSPM objects only for one of the components). PMVD A = proper motion vector direction in degrees for component A. PMVD B = proper motion vector direction in degrees for component B. e_PMVD = error estimation for the pm vector direction according to the given 2MASS position error. PMVL A mas = proper motion vector length of component A in mas. PMVL B mas = proper motion vector length of component B in mas. e_PMVL mas = error estimation for the pm vector length according to the given 2MASS position error. PMVD Δ = rating for the resulting proper motion vector direction delta between the components. PMVL Δ = rating for the resulting proper motion vector length delta between the components. e_PMVL = rating for the relation of the 2MASS position error to the proper motion vector length.

Object	PMVD A	PMVD B	e_PMVD	PMVL A mas	PMVL B mas	e_PMVL mas	PMVD Δ	PMVL Δ	e_PMVL	WDS Code	Notes
LDS 969	244.89	244.76	2.860	2,393.8	2,403.2	119.925	A	A	B	-	Cross reference object from Knapp 2016 (Measurements of some VizieR I/330 objects). PM direction and speed quite similar and position error only slightly above 5%, looks like a solid CPM confirmation. Listed also in VizieR I/330 as MPN 5229 as "new discovery 2015."
LDS 972	314.45	315.20	6.141	1,397.2	1,393.3	150.333	A	A	B	-	Cross reference object from Knapp 2016 (Measurements of some VizieR I/330 objects). PM direction and speed quite similar but position error makes this result somewhat unreliable. Listed also in VizieR I/330 as MPN 5368 as "new discovery 2015."
LEP 1AD (STF 3060)	202.93	226.96	2.860	2,955.4	2,653.1	140.213	C	C	A	V	Selected by random with own research in the LSPM catalog (Lepine and Shara 2005) as substitute for AB because URAT1 missed an object for the B component. WDS notes regarding AD mention: "the visual binary at 573" is co-moving, same parallax. The D component is ~1.3m below the main sequence in the (K, V-K) color- magnitude diagram." Whatever this means, this is most certainly no CPM. Mosaic and blinking of POSS images did not show anything conclusive - roughly similar pm speed and slightly different pm direction. The pm numbers from UCAC4 to URAT1 for the B component are rather different and at least the latter do not suggest CPM.
LEP 2	93.59	94.83	2.860	2,393.0	2,420.0	120.326	A	A	A	V	Selected from Kirkpatrick et al 2016, Table 11, Sys. No. 11 as northern sky object with separation <30". Solid triple AAA CPM.
MLB 277	263.81	258.61	2.860	370.7	361.0	18.293	B	A	C	-	Picked at random from Harshaw, 2016. His results for MBL 277 were inconclusive (in the form of "???"). Check CPM results good for vector direction in the 2x range, while the vector length is within the error range. The position error in relation to PM vector length is outside the 10% cutoff for a B rating (22.9% for A, 23.5% for B). No spectral class for either star is shown in Simbad.
MLB 441AB	53.24	55.57	2.860	717.0	808.1	38.126	A	C	C	D	Picked at random from Harshaw, 2016. His results categorize MLB 441 as CPM. Check CPM results good for vector direction but vector length is outside the 2x range; the position error in relation to PM vector length is just beyond the 10% cutoff for a B rating (14.8% for A, 13.2% for B). Simbad shows A with a stellar class of G1, none listed for B.
MPN 115	182.34	174.51	2.860	931.7	966.0	47.443	C	A	C	n.a.	Selected by random from the VizieR I/330 catalog after applying the Halbwachs 1986 distinction criterion with negative result. Due to the in relation to the proper motion vector length far too large position error the "similar" direction and speed of proper motion is highly questionable - rather unlikely CPM.
MPN 4	77.86	82.68	2.860	1,261.7	1,302.5	64.105	B	A	C	n.a.	Selected by random from the VizieR I/330 catalog after applying the Halbwachs 1986 distinction criterion with negative result. Due to the in relation to the proper motion vector length far too large position error (~20%) the seemingly "similar" direction and speed of proper motion is a bit questionable. URAT1 gives here an e_pm of 6.5 and 6.6mas - far too optimistic with the given large 2MASS position error. Yet CPM not unreasonable.
MPN 49	77.94	87.55	2.860	975.2	1,003.5	49.466	C	A	C	n.a.	Selected by random from the VizieR I/330 catalog after applying the Halbwachs 1986 distinction criterion with negative result. Due to the in relation to the proper motion vector length far too large position error (~16%) the seemingly "similar" direction and speed of proper motion is highly questionable - rather unlikely CPM.
MPN 50	88.54	80.51	2.860	891.9	877.5	44.235	C	A	C	n.a.	Selected by random from the VizieR I/330 catalog after applying the Halbwachs 1986 distinction criterion with negative result. Due to the in relation to the proper motion vector length far too large position error the "similar" direction and speed of proper motion is highly questionable - rather unlikely CPM.

Table 2 continues on next page.

A New Concept for Counter-Checking of Assumed CPM Pairs

Table 2 (continued). CPM Check results for the selected objects. Explanation of the content: Object = discoverer or catalog ID (in case of LSPM objects only for one of the components). PMVD A = proper motion vector direction in degrees for component A. PMVD B = proper motion vector direction in degrees for component B. e_PMVD = error estimation for the pm vector direction according to the given 2MASS position error. PMVL A mas = proper motion vector length of component A in mas. PMVL B mas = proper motion vector length of component B in mas. e_PMVL mas = error estimation for the pm vector length according to the given 2MASS position error. PMVD Δ = rating for the resulting proper motion vector direction delta between the components. PMVL Δ = rating for the resulting proper motion vector length delta between the components. e_PMVL = rating for the relation of the 2MASS position error to the proper motion vector length.

Object	PMVD A	PMVD B	e_PMVD	PMVL A mas	PMVL B mas	e_PMVL mas	PMVD Δ	PMVL Δ	e_PMVL	WDS Code	Notes
PKO 5	67.83	52.51	2.860	53.4	26.6	2.001	C	C	C	V	Selected by random from the WDS catalog as V-coded object. There must be a special reason to list this object as physical - it cannot be proper motion as the position error is far larger than the proper motion vector length. Impossible to detect any significant change in position when blinking 1953 POSSI and 1995 POSSII images, which isn't surprising given the minimal rate of PM per URAT1 (+003.7 +001.5 and +001.6 +001.3).
PNT 2	159.97	159.93	2.860	1,042.2	1,060.1	52.558	A	A	B	V	V-coded object selected by random from the WDS catalog. At the time we first came across this pair, the PA and separation data had been reversed in the WDS listing, resulting in our identifying a companion with no shared CPM. Correspondence with Bill Hartkopf identified the problem. With the correct companion identified, the results show vector direction and length well within the error tolerance, while the position error in relation to the PM vector length is at the outer edge of the 10% cutoff (9.6% for the primary, 9.4% for the secondary). No spectral class for either of the correct components is shown in Simbad. Blinking of POSSI and POSSII images confirms direction of PM.
SEI 220	174.32	179.54	2.860	996.7	1,003.4	50.001	B	A	B	V	V-coded object selected by random from the WDS catalog. Rather similar pm direction, very similar pm speed and rather large position error in relation to the pm vector length - CPM possible but not very convincing.
SHJ 223AC	120.72	122.65	2.860	431.9	250.9	17.071	A	C	C	-	Selected by random from the WDS catalog for very similar pm direction. PM speed very different far outside any error estimation and position error in relation to the pm vector length far above 10%. Obviously not CPM.
SHY 227 (γ UMa)	71.16	89.87	2.860	1,503.1	1,420.7	73.095	C	B	C	V	Pair separated by 5.6 degrees. Selected from Wielen et al 1999 as example of one of the very wide pairs. Wielen argues this a binary pair, while the WDS catalog classifies the pair as physical based on proper motion per findings of Shaya and Olling, 2011. Proper motion direction is rather different as illustrated by the Check CPM results, which show vector direction is also well outside the 2x range; however this may be a side result of the very large 2MASS position error for the primary. The Check CPM results show the vector length is within 2x range; and finally the position error in relation to PM vector length is beyond the 10% cutoff for the primary (28.2%) and the secondary is just within the 10% cutoff (9.6%), so the CPM probability seems quite low. Simbad shows the primary (HIP 58001) with a spectral class of A0 and the secondary (HIP 61100)as K2. Very large and saturated star disks for both components - POSS images of no use for determining proper motion. Checking the pm data from UCAC4 and comparing with URAT1 provides a possible explanation for an earlier CPM assessment: UCAC4 suggests rather similar direction while URAT1 is identical with our calculation and shows completely different directions.
SHY 378 (HIP 201)	324.38	311.46	2.860	367.1	449.7	20.420	C	C	C	V	Selected from Shaya and Olling 2011. Slightly similar pm direction and speed, large position error - not a good CPM candidate. No obvious change in position seen when blinking POSSI (1954) and POSSII (1994) images. Slight change in PM data from UCAC4 (-017.6 +018.6 and -017.8 +019.2) to URAT1 (-014.4 +020.1 and -022.7 +020.1) indicates a greater disparity in RA motion with the URAT1 numbers.
SHY 569	236.70	240.72	2.860	1,062.9	940.1	50.075	B	C	C	V	Selected from the WDS catalog as one of the infamous 999.9" separation objects - this one is over 4° separated. The position error relation to the pm vector length renders this object as a rather questionable CPM object.
SKF1186	75.25	75.25	2.860	1,232.7	1,193.3	60.650	A	A	B	V	V-coded object selected by random from the WDS catalog. Very solid AAB CPM rating. Listed also in VizieR I/330 as MPN 9251 as "new discovery 2015."

Table 2 continues on next page.

A New Concept for Counter-Checking of Assumed CPM Pairs

Table 2 (continued). CPM Check results for the selected objects. Explanation of the content: Object = discoverer or catalog ID (in case of LSPM objects only for one of the components). PMVD A = proper motion vector direction in degrees for component A. PMVD B = proper motion vector direction in degrees for component B. e_PMVD = error estimation for the pm vector direction according to the given 2MASS position error. PMVL A mas = proper motion vector length of component A in mas. PMVL B mas = proper motion vector length of component B in mas. e_PMVL mas = error estimation for the pm vector length according to the given 2MASS position error. PMVD Δ = rating for the resulting proper motion vector direction delta between the components. PMVL Δ = rating for the resulting proper motion vector length delta between the components. e_PMVL = rating for the relation of the 2MASS position error to the proper motion vector length.

Object	PMVD A	PMVD B	e_PMVD	PMVL A mas	PMVL B mas	e_PMVL mas	PMVD Δ	PMVL Δ	e_PMVL	WDS Code	Notes
SKF 12	208.96	209.21	2.860	2,328.4	2,254.9	114.584	A	A	B	V	V-coded object selected by random from the WDS catalog. Very solid AAB CPM rating. Listed also in VizieR I/330 as MPN 5939 as "new discovery 2015."
SKF 179BC	1.66	5.13	2.860	350.1	364.0	17.851	B	A	C	V	Selected by random from the WDS catalog as V-coded object. Position error in relation to proper motion vector length too large to allow a reliable positive CPM result. PM direction also rather different. Component A of STI 1195 is obviously only optical.
SKF1840	219.99	223.56	2.860	256.1	208.6	11.618	B	C	C	V	Selected from Knapp 2016 (Measurement of some SKF objects) - proper motion vector far too short to allow a reasonable positive CPM result. 2MASS position error is average ~40% of the proper motion vector. PM direction indicates rather not CPM.
SKF 229CD	230.33	230.65	2.425	1,977.6	2,004.6	120.000	A	A	A	-	Object selected by random from Skiff 2016. Prime example for UCAC4 and IGSL errors and gaps. IGSL positon error for component C results in a CCC rating and UCAC4 does not allow any check as this object is simply missing. Check with 2MASS results in a plan triple AAA rating. Counter-check with POSS I and POSS II images shows also very clearly common proper motion. Notes from Skiff 2016: "I previously thought the proper motion of this pair was quite small, since the nearby fast-moving AB components are moving in the opposite direction. But in fact this pair has substantial motion itself, now shown correctly in the WDS."
SKF2325	288.80	282.75	2.860	316.2	357.3	16.837	C	C	C	V	Selected by random from the WDS catalog as V-coded object. Position error in relation to proper motion vector length far too large to allow a reliable positive CPM result. Delta in direction and speed too large to be considered CPM. Blinking of POSSI (1953) and POSSI (1998) images shows parallel motion to the northeast, which matches URAT1 PM data. URAT1 PM data (-020.7 +007.1 and -024.1 +005.5) shows and more disparity in RA motion in the primary than is shown in the UCAC4 PM data (-019 +003.8 and -017.1 +004.7).
SKF2460AB	279.85	283.01	2.860	191.5	199.9	9.786	B	A	C	V	Object selected by random from the WDS catalog. Check CPM result shows a rather small if similar proper motion speed combined with a too large PMVL error rendering "similar direction and similar speed" results a bit questionable - there have to be very good other arguments to consider this a CPM pair.
SKF2600	253.82	251.79	2.860	369.4	427.4	19.920	A	C	C	V	Selected by random from Skiff 2016. PM direction is quite similar but pm vector length seems rather different and the position error is about 30% of the pm vector length - not a good CPM candidate.
SKF 8	273.98	274.02	2.860	3,273.4	3,368.7	166.052	A	A	A	V	V-coded object selected by random from the WDS catalog. Very solid triple AAA CPM rating.
SMA 1	325.68	274.10	2.860	93.3	15.1	2.710	C	C	C	-	Picked at random from Harshaw, 2016. His results categorize SMA 1 as CPM. Check CPM results show vector length and direction well outside the 2x error range; position error in relation to PM vector length is far outside the error ranges for both components. Simbad shows the primary with a spectral class of A5, none listed for the secondary.
SMR 16 AC	91.82	131.87	2.860	238.3	136.5	9.368	C	C	C	V	Selected from WDS as SMR object with code V. Solid triple CCC rating, it remains unclear, why this object should be considered CPM. Blinking of POSSI (1953) and POSSII (1996) images shows no detectable motion. There's a significant change in PM data from UCAC4 (+003.8 -007 and +005.4 -007.4) to URAT1 (+014.8 -000.4 and +006.4 -005.7), which argues against there being shared proper motion between the A and C components.
SMR 48	267.10	316.88	2.860	21.4	38.5	1.496	C	C	C	-	Selected from Schlimmer 2013. Classic triple CCC - definitely not CPM. Schlimmer applied only the sep/pm<1000 Halbwachs1986 criterion for his CPM check, so this result was to be expected as the relationship of the position error to proper motion vector length makes given pm data completely unreliable.

Table 2 continues on next page.

A New Concept for Counter-Checking of Assumed CPM Pairs

Table 2 (continued). CPM Check results for the selected objects. Explanation of the content: Object = discoverer or catalog ID (in case of LSPM objects only for one of the components). PMVD A = proper motion vector direction in degrees for component A. PMVD B = proper motion vector direction in degrees for component B. e_PMVD = error estimation for the pm vector direction according to the given 2MASS position error. PMVL A mas = proper motion vector length of component A in mas. PMVL B mas = proper motion vector length of component B in mas. e_PMVL mas = error estimation for the pm vector length according to the given 2MASS position error. PMVD Δ = rating for the resulting proper motion vector direction delta between the components. PMVL Δ = rating for the resulting proper motion vector length delta between the components. e_PMVL = rating for the relation of the 2MASS position error to the proper motion vector length.

Object	PMVD A	PMVD B	e_PMVD	PMVL A mas	PMVL B mas	e_PMVL mas	PMVD Δ	PMVL Δ	e_PMVL	WDS Code	Notes
SMR 56	187.16	158.90	2.860	143.7	134.3	6.949	C	B	C	-	Selected from Schlimmer 2013. Classic triple CCC - very probably not CPM. Schlimmer applied only the sep/pm<1000 Halbwachs1986 criterion for his CPM check, so this result was to be expected as the relationship of the position error to proper motion vector length makes given pm data completely unreliable.
SMR 65	336.65	248.72	2.860	192.9	196.4	9.734	C	A	C	V	Selected from Schlimmer 2015. PM direction delta renders CPM negative. Schlimmer applied only the sep/pm<1000 Halbwachs1986 criterion for his CPM check, so this result was to be expected as the relationship of the position error to proper motion vector length makes given pm data completely unreliable. No suitable 1.1" POSS I image for blinking available; blinking with second choice POSS I 1.7" image suggests some noticeable pm of nearby UCAC4-503-061608 but not so for SMR65. UCAC4 offers pm data only for one component but URAT1 has data for both with quite different pm direction - so this object cannot be considered CPM.
SMR 66	92.04	245.36	2.860	80.7	133.0	5.342	C	C	C	V	Selected from Schlimmer 2015. Classic triple CCC - definitely not CPM. Schlimmer applied only the sep/pm<1000 Halbwachs1986 criterion for his CPM check, so this result was to be expected as the relationship of the position error to proper motion vector length makes given pm data completely unreliable. Blinking of POSSI and POSSII images inconclusive. No UCAC4 PM data exist for the secondary, but the primary shows data of +013 -015.5; URAT1 PM data (+006.1 -000.2 and -008.8 -004) shows significantly less motion for the primary.
SMR 67	201.90	176.97	2.860	350.0	237.2	14.680	C	C	C	V	Selected from Schlimmer 2015. Classic triple CCC - definitely not CPM. Schlimmer applied only the sep/pm<1000 Halbwachs1986 criterion for his CPM check, so this result was to be expected as the relationship of the position error to proper motion vector length makes given pm data completely unreliable. Blinking of POSSI (1954) and POSSII (1990) images shows slight southwesterly motion for the primary and due south motion for the secondary. Comparison of UCAC4 PM data (-012.4 -23.1 and -014.9 -018.8) with URAT1 PM data (-009.8 -024.3 and +001 -017.8) shows a significant change in speed and direction for the secondary which argues against shared proper motion.
SOZ 17 (HD 155060)	255.25	252.08	2.424	2,621.4	2,834.4	120.000	B	B	A	VK	Selected from Scholz 2016. Similar pm direction, rather high speed with a delta less than 10% - looks like a potential CPM candidate.
SO 8 (HD 18404)	96.70	94.23	2.511	3,487.8	3,291.4	152.971	A	B	A	VK	Selected from Scholz 2016. Very similar pm direction, rather high speed with only slightly larger delta than 5% - looks like a very good CPM candidate.
SRT 1	167.06	166.85	2.819	2,437.2	2,409.6	120.000	A	A	A	-	Picked at random from Benavides, et al, 2010. Meets all three Check CPM criteria for CPM. Simbad shows the primary with a spectral class of G5 and the secondary as G7.
STF1309 (HJL 104)	315.15	311.78	2.860	913.6	937.9	46.287	B	A	C	VDZ	Picked at random from Halbwachs, 1986. Check CPM results show the pair is within the 2x error range for vector direction and within the error range for vector length; position error in relation to PM vector length is just outside the B range for the A component (10.1%) and at the outer edge of the B range for the secondary (9.8%). Both Halbwachs and Simbad show the two components with an F5 spectral class.
STF1719	222.16	217.29	2.860	1,955.1	2,236.3	104.785	B	C	B	VD	The AB pair to TOK 155 AC being thought to form a CPM triple by Tokovinin - does not look good for either AB or for AC.
STF1927	301.88	302.60	2.826	2,641.1	2,593.9	130.384	A	A	A	VDZ	Selected by random from the WDS catalog as code V object. Solid CPM triple AAA rating.

Table 2 continues on next page.

A New Concept for Counter-Checking of Assumed CPM Pairs

Table 2 (continued). CPM Check results for the selected objects. Explanation of the content: Object = discoverer or catalog ID (in case of LSPM objects only for one of the components). PMVD A = proper motion vector direction in degrees for component A. PMVD B = proper motion vector direction in degrees for component B. e_PMVD = error estimation for the pm vector direction according to the given 2MASS position error. PMVL A mas = proper motion vector length of component A in mas. PMVL B mas = proper motion vector length of component B in mas. e_PMVL mas = error estimation for the pm vector length according to the given 2MASS position error. PMVD Δ = rating for the resulting proper motion vector direction delta between the components. PMVL Δ = rating for the resulting proper motion vector length delta between the components. e_PMVL = rating for the relation of the 2MASS position error to the proper motion vector length.

Object	PMVD A	PMVD B	e_PMVD	PMVL A mas	PMVL B mas	e_PMVL mas	PMVD Δ	PMVL Δ	e_PMVL	WDS Code	Notes
STF 289 (HJL 41)	103.34	112.03	2.860	1,169.0	1,075.1	56.102	C	B	B	VD	Picked at random from Halbwachs, 1986. Check CPM results show the pair is outside the 2x error range for vector direction and within the 2x error range for vector length; position error in relation to PM vector length is at the outer edge of the B range for the A component (9.1%) and in the middle of the B range for the secondary (7.9%). Halbwachs shows A with an A3 spectral class and B as A2. The POSS I images are overexposed for the A component so blinking and mosaic image show nothing of interest. The pm numbers from UCAC4 to URAT1 have changed and at least the latter do not suggest CPM .
STF 77	19.26	16.40	2.860	382.5	476.2	21.468	A	C	C	D	Picked at random from Harshaw, 2016, where the results categorize STF 77 as CPM. Check CPM results good for vector direction, while vector length is well outside the 2x range; position error in relation to PM vector length is beyond the 10% cutoff for a B rating (29.8% for A, 23.9% for B). Simbad shows both stars with a G0 spectral class.
STI 117	229.06	212.56	2.860	118.7	190.9	7.740	C	C	C	V	Selected by random from the WDS catalog as V-coded object. Besides significant pm direction and speed deltas, the position error in relation to proper motion vector length far too large to be considered as CPM pair. Blurring of the primary and secondary make it impossible to detect individual motion in the POSSI and POSSI images. Considerable change exists in PM data from UCAC4 (-020 -014 -012.8 -006.4) and URAT1 (-006.5 -005.6 and -007.5 -011.8).
STI1248	60.36	55.01	2.860	257.0	347.8	15.120	B	C	C	-	Picked at random from Harshaw, 2016, where the results categorize STI 1248 as CPM. Check CPM results show vector direction in the 2x range and vector length outside the 2x range; the position error in relation to PM vector length is well outside the 10% cutoff for a B rating (44.4% for A, 32.8% for B). Simbad shows both stars with a spectral class of K.
STI1560	192.94	244.93	2.860	5.9	49.3	1.380	C	C	C	-	Picked at random from Harshaw, 2016, where the results categorize STI 1560 as CPM. Check CPM results show vector direction and length well outside the 2x error range; the position error in relation to PM vector is far beyond the 10% cutoff. Simbad shows the primary with a spectral class of B1, none listed for the secondary.
STT 276AB-C	122.91	122.13	2.860	406.8	414.2	20.526	A	A	C	-	Picked at random from a list of STT pairs in Bootes. Check CPM results good for vector direction and length; position error in relation to PM vector length is slightly outside the 10% cutoff for a B rating (20.9% for AB, 20.5% for C). Simbad shows A with a G4 spectral class but has no classification for C.
STT 30AC	110.83	108.50	2.531	2,681.0	2,715.0	120.000	A	A	A	VDZ	Just another prime example for the bad data quality of the IGSL catalog at least for some objects - due to the given unreasonable small position error for B the Check CPM rating would be ACA. With 2MASS as reference catalog STT 30 AC gets a clear triple AAA rating confirmed by blinking of POSS images.
STT 547AB	99.38	99.73	0.674	13,601.2	12,955.3	160.000	A	C	A	ODZ	Found by random as very large proper motion pair during another research project. Nearly identical pm direction and rather similar pm vector length but clearly outside position error, the latter less than 1% of the pm vector length. This seems to be a pattern for very fast pairs: speed difference outside the position error range.
STT 547AF	99.38	99.08	0.596	13,601.2	13,164.1	141.421	A	C	A	VO	Similar to even better values for STT547AF - so this is obviously a common motion triple.
STTA 61AB (HJL 1040)	90.58	84.40	2.860	1,059.7	1,121.0	54.519	C	B	B	V	Picked at random from Halbwachs, 1986. Check CPM results show the pair is just outside the 2x error range for vector direction and within the 2x error range for vector length; position error in relation to PM vector length is in the middle of the B range for the A component (8.0%) and the B component (8.2%). Both Halbwachs and Simbad show A with a spectral class of F8 and B as G0. Blinking POSS images shows roughly similar pm direction and speed. PM values have changed from UCAC4 to URAT1 and at least the latter do not suggest CPM.

Table 2 continues on next page.

A New Concept for Counter-Checking of Assumed CPM Pairs

Table 2 (continued). CPM Check results for the selected objects. Explanation of the content: Object = discoverer or catalog ID (in case of LSPM objects only for one of the components). PMVD A = proper motion vector direction in degrees for component A. PMVD B = proper motion vector direction in degrees for component B. e_PMVD = error estimation for the pm vector direction according to the given 2MASS position error. PMVL A mas = proper motion vector length of component A in mas. PMVL B mas = proper motion vector length of component B in mas. e_PMVL mas = error estimation for the pm vector length according to the given 2MASS position error. PMVD Δ = rating for the resulting proper motion vector direction delta between the components. PMVL Δ = rating for the resulting proper motion vector length delta between the components. e_PMVL = rating for the relation of the 2MASS position error to the proper motion vector length.

Object	PMVD A	PMVD B	e_PMVD	PMVL A mas	PMVL B mas	e_PMVL mas	PMVD Δ	PMVL Δ	e_PMVL	WDS Code	Notes
TOK 155AC	222.16	217.01	2.860	1,955.1	1,797.8	93.823	B	B	B	V	Selected from the WDS catalog as one of the infamous 999.9" separation objects - obviously does not fulfill the numeric requirements for a CPM pair. Attention: URAT1 shows two objects for TOK 155 A, one of them with wrong pm data.
UC 193	202.90	201.90	2.860	1,058.3	1,068.1	53.161	A	A	B	V	Cross reference object from Knapp 2016 (Measurements of some VizieR I/330 objects). PM direction and speed very similar - position error in relation to the pm vector length a bit too large for a fully reliable result. Listed also in VizieR I/330 as MPN 4986 as "new discovery 2015."
UC 203	228.11	228.47	2.860	1,447.1	1,469.3	72.911	A	A	B	V	Cross reference object from Knapp 2016 (Measurements of some VizieR I/330 objects). PM direction and speed very similar - position error in relation to the pm vector length a bit large - yet good CPM candidate. Listed also in VizieR I/330 as MPN 5447 as "new discovery 2015."
UC 2692	296.48	295.61	2.860	2,135.5	2,126.0	106.536	A	A	B	V	Cross reference object from Knapp 2016 (Measurements of some VizieR I/330 objects). PM direction and speed very similar - position error in relation to the pm vector length a bit too large for a triple AAA, else solid. Listed also in VizieR I/330 as MPN 4868 as "new discovery 2015."
UC 2840	192.20	192.56	2.860	2,385.2	2,362.7	118.698	A	A	B	V	Selected by random with own research in the LSPM catalog (Lepine and Shara 2005) for close objects. PM direction and speed very close, position error slightly outside 5% of the pm vector length - solid triple AAB CPM rating. Also included in the VizieR I/330 catalog as MPN 5196 as "newly discovered 2015."
UC 2988	308.87	308.19	2.860	1,331.5	1,332.1	66.591	A	A	B	V	Cross reference object from Knapp 2016 (Measurements of some VizieR I/330 objects). PM direction and speed very similar - position error in relation to the pm vector length a bit large - yet good CPM rating. Listed also in VizieR I/330 as MPN 5467 as "new discovery 2015."
UC 302	74.30	86.55	2.860	729.1	633.6	34.068	C	C	C	V	Taken from Table 4 in Hartkopf, et al, 2013. Check CPM results show the pair is well outside the 2x error range for both vector direction and vector length; position error in relation to PM vector length is outside the B range for both the A component (23.3%) and the B component (14.6%). A is a class K2 star, no spectral class listed in Simbad for B. This is most probably no CPM pair. There's a significant change in PM data from UCAC4 (+061.1 -000.2 and +-056.2 -003.9) to URAT1 (+053 +015 and -051.2 +003.2) which shows an increase in northward motion of the primary. Surprisingly, blinking of POSSI (1955) and POSSII (12-1991) images shows a distinct eastward parallel motion for both primary and secondary.
UC 303	81.29	79.36	2.860	943.6	932.3	46.898	A	A	B	V	Taken from Table 4 in Hartkopf, et al, 2013. Check CPM results show the pair is within the error range for both vector direction and vector length; position error in relation to PM vector length is at the outer edge of the B range for both the A component (9.0%) and the B component (9.1%). No spectral class is shown for either star in Simbad.
UC 304	245.16	240.11	2.860	792.7	788.8	39.536	B	A	C	V	Taken from Table 4 in Hartkopf, et al, 2013. Check CPM results show the pairs is in the 2x error range for vector direction and within the range for vector length; position error in relation to PM vector length is just outside the B range for both the A component (10.7%) and the B component (10.8%). No spectral class is shown for either star in Simbad.

Table 2 concludes on next page.

A New Concept for Counter-Checking of Assumed CPM Pairs

Table 2 (conclusion). CPM Check results for the selected objects. Explanation of the content: Object = discoverer or catalog ID (in case of LSPM objects only for one of the components). PMVD A = proper motion vector direction in degrees for component A. PMVD B = proper motion vector direction in degrees for component B. e_PMVD = error estimation for the pm vector direction according to the given 2MASS position error. PMVL A mas = proper motion vector length of component A in mas. PMVL B mas = proper motion vector length of component B in mas. e_PMVL mas = error estimation for the pm vector length according to the given 2MASS position error. PMVD Δ = rating for the resulting proper motion vector direction delta between the components. PMVL Δ = rating for the resulting proper motion vector length delta between the components. e_PMVL = rating for the relation of the 2MASS position error to the proper motion vector length.

Object	PMVD A	PMVD B	e_PMVD	PMVL A mas	PMVL B mas	e_PMVL mas	PMVD Δ	PMVL Δ	e_PMVL	WDS Code	Notes
UC 306	86.11	105.00	2.860	1,038.8	863.7	47.562	C	C	C	VU	Taken from Table 4 in Hartkopf, et al, 2013. Check CPM results show the pair is well outside the 2x error range for both vector direction and vector length; position error in relation to PM vector length is outside the B range for both the A component (12.1%) and the B component (14.5%). Simbad shows no spectral class for either of the two stars. Blinking of POSSI (1954) and POSSII (1995) images shows distinct eastward motion of primary and distinct eastward motion with a slight southern component for the secondary. There's a significant change in PM data from UCAC4 (+071.2 -004.3 and +051.8 -022.5) to URAT1 (+075.8 +005.2 and +061.1 -016.3) which shows motion in declination of the primary changing from south to north, which wasn't detectable in the POSS images.
UC 309	156.40	114.89	2.860	739.0	766.4	37.634	C	A	C	VU	Taken from Table 4 in Hartkopf, et al, 2013. Check CPM results show the pairs is well outside the 2x error range for vector direction and within the range for vector length; position error in relation to PM vector length is outside the B range for both the A component (14.4%) and the B component (12.0%). No spectral class is shown for either star in Simbad. Mosaic and blinking of POSS images suggest roughly similar pm speed but slightly different direction. Comparison of pm data from UCAC4 to URAT1 shows significant changes, especially in direction; the URAT1 data does not suggest CPM at all.
UC 310	80.55	94.12	2.860	1,000.1	938.0	48.454	C	B	B	VU	Taken from Table 4 in Hartkopf, et al, 2013. Check CPM results show the pairs is outside the 2x error range for vector direction and within the range for vector length; position error in relation to PM vector length is in the B range for both the A component (8.5%) and the B component (9.1%). No spectral class is shown for either star in Simbad. Notable difference in PM numbers between URAT1 (+067.4 +011.3 and +063.9 -004.6) and WDS (+066 +020 and +071 +006). Mosaic and blinking of POSS images did not show anything conclusive - roughly similar speed and slightly different direction. The pm numbers from UCAC4 to URAT1 are rather different and at least the latter do not suggest CPM at all.
UC 3111	144.14	144.34	2.860	863.5	878.1	43.542	A	A	C	V	V-coded object selected by random from the WDS catalog. PM direction and speed very close, position error in relation to the pm vector length a bit large - yet rather solid AAC CPM rating.
UC 319	54.27	51.57	2.860	929.6	946.4	46.900	A	A	C	V	Selected by random from Hartkopf et al 2013. Very similar pm direction and speed but large position error in relation to pm vector length, yet very solid CPM rating.
UC 4962	126.77	122.61	2.860	882.3	917.1	44.984	B	A	C	V	Selected by random from Hartkopf et al 2013. Similar pm direction and very similar pm speed but large position error in relation to pm vector length.
UC 696	150.82	153.04	2.860	961.9	951.6	47.838	A	A	B	V	Selected by random from Hartkopf et al 2013. Very similar pm direction and speed and moderate large position error in relation to pm vector length gives a very solid CPM rating.
UC 715	233.35	237.83	2.860	770.7	791.7	39.059	B	A	C	V	Selected by random from Hartkopf et al 2013. Similar pm direction and very similar pm speed but large position error in relation to pm vector length gives in total a mediocre CPM rating.
UC 84	179.84	179.61	2.860	739.1	782.3	38.035	A	B	C	V	V-coded object selected by random from the WDS catalog. Similar pm direction, not this similar pm speed and rather large position error in relation to the pm vector length.
UCAC4-754-014689	133.36	135.03	2.860	443.6	437.1	22.017	A	A	C	n.a.	Found by chance by checking UCAC4 proper motion vectors in Aladin for another object. Very solid CPM AAC rating with only the position error a bit large in relation to the pm vector length but pm direction and speed very close. No WDS object so far - UCAC4 objects 754-014689 and 754-014693 with separation 12.557" and PA 126.64°.
UR 2	167.03	170.65	2.860	1,118.2	1,061.0	54.480	B	B	C	V	Selected by random from Skiff 2016. PM direction is nearly similar, pm vector length seems also nearly similar and the position error is about 12% of the pm vector length - not a perfect but possible CPM candidate.

A New Concept for Counter-Checking of Assumed CPM Pairs

(Continued from page 35)

~93,800mas in 17.9 years with a delta of less than 2%. This would very well deserve a triple AAA rating but due to the huge vector length the "allowed" deltas are far smaller so the rating is only a BCA. This means that our spreadsheet imposes for high speed objects a precision requirement hard to meet with the current available data.

- A similar lack of URAT1 objects is usually also given for Δμ Binaries (M dwarfs and white dwarf pairs) as for example reported by Khovritchev and Kulikova 2016.
- High proper motion pairs with an assumed orbit might get a C rating for different proper motion vector length as was for example the case for STT 547 AB (see table 2). The 6th Orbit catalog shows here 2 calculated orbits. The orbit calculation with Kiy2001 allows for ~0.65" difference in pm vector length between 1998 and 2013 - a good explanation for the measured pm vector length difference between 1998 and 2013. With Pop1996b we get ~0.5" - not such a good match but still large enough to be also a good explanation for the measured difference in pm vector length. When comparing the orbit calculations for 2016 with our current astrometry measurements then both orbits differ somewhat with Kiy2001 the better match with 6" and 188,53° compared to measured 6.085" and 188.22.
- According to the preliminary character of URAT1 some objects are listed with obvious errors as for example for the WDS V-coded CPM pair HZG7 – usually such errors are instantly recognizable due to inconsistent data.
- In many cases (of mostly rather close CPM pairs) like for example STF4 and STF326 (both highly interesting objects according to Wiley 2015) but also SOZ4AB,D, SMR44, MLB247, GIC17, FMR208, SKF269 or FMR192, URAT1 provides no object for at least one component with the consequence that no position comparison with 2MASS is possible.
- In a few cases like for example MLB203 the URAT1 data is simply off – usually easily to recognize by significant differences of the pm data in comparison with UCAC4. Such cases make clear why URAT1 is considered preliminary.
- 2MASS provides a time frame of about 15 years up to URAT1 and is obviously based on reliable observation epoch data of good use for proper motion calculations.
- This means that while a false positive CPM confirmation with our Check CPM spreadsheet might be highly unlikely an unexpected negative result needs an additional countercheck (for example by comparing 2MASS data with UCAC4 or visual comparison of POSS I and POSS II images) to make sure that this is not a case of faulty 2MASS data .
- Even a triple AAA result with our Check CPM spreadsheet is still no "proof" that this is actually a physical pair but can be considered as additional confirmation that the numbers suggest common proper motion. Yet it might still very well be a random fellow traveller pair – a check for being a physical pair was not our intention from the very beginning and would need checking of additional data.
- In the current version this check has to be done object by object and is not available as algorithm to be applied on a set of objects – but it should be possible to make software to do exactly this.
- A solid ACA result combined with a rather large pm value might not necessarily mean a falsification of a CPM assumption due to different pm speed but be a serious hint for an orbit as is shown by the example of STT 547 AB.
- Odd results for WDS V-coded objects suggest the need for further investigation – the WDS catalog has its fair share of errors starting with simple typos like for PNT 2 up to misidentification of components like for CLL 21 AC.

Acknowledgements

The following tools and resources have been used for this research:

- Washington Double Star catalog
- 2MASS All Sky catalog
- AAVSO APASS
- UCAC4 catalog
- URAT1 catalog
- IGSL catalog
- LSPM catalog
- Vizier I/330 catalog
- Aladin Sky Atlas v9.0
- SIMBAD, VizieR
- AstroPlanner V2.2

Special thanks to Brian Skiff, Bill Hartkopf and Norbert Zacharias for their useful advice during developing this concept.

References

Aitken R.G. – 1911, The Definition of the Term Double Star, Astronomische Nachrichten, Vol 188 Pages 283-294

A New Concept for Counter-Checking of Assumed CPM Pairs

Benavides, R. et al – 2010, New Wide Common Proper Motion Binaries, Journal of Double Star Observations, Vol. 6 No. 1 Pages 30-85

Buchheim, R. – 2008, CCD Double-Star Measurements at Altimira Observatory in 2007, Journal of Double Star Observations, Vol. 4 No. 1 Page 28: Formulas for calculating Separation and Position Angle from the RA Dec coordinates

Caballero, R. – 2009, Finding New Common Proper-Motion Binaries by Data Mining, Journal of Double Star Observations, Vol. 5 No. 3 Pages 156-167

Caballero, R. et al – 2010, New Common Proper-Motion Pairs from the PPMX Catalog, Journal of Double Star Observations, Vol. 6 No. 3 Pages 206-216

Halbwachs, J.L. – 1986, Common proper motion stars in the AGK3, Astronomy and Astrophysics Supplement Series (ISSN 0365-0138), Vol. 66 No. 2 Pages 131-148

Harshaw R.W. – 2016, CCD Measurements of 141 Proper Motion Stars: The Autumn 2015 Observing Program at the Brilliant Sky Observatory, Part 3, Journal of Double Star Observations Vol 12 No 4 Pages 394-399

Hartkopf, W.I. et al – 2013, DOUBLE STARS IN THE USNO CCD ASTROGRAPHIC CATALOG, The Astronomical Journal, 146:76 (8pp)

Khovritchev M.Y. and Kulikova A.M. – 2016, Δμ Binaries among Stars with Large Proper Motions, Astronomy Letters, Volume 41, Issue 12, Pages 833-847

Kirkpatrick J.D. – 2016, THE ALLWISE MOTION SURVEY PART 2, submitted to the Astrophysical Journal March 25th 2016

Knapp W. – 2016, Measurements of some SKF objects, Journal of Double Star Observations, Vol. x No. y Pages nn-mm

Knapp W. – 2016, Measurements of some VizieR I/330 objects, Journal of Double Star Observations, Vol. x No. y Pages nn-mm

Lepine S, and Shara M.M. – 2005, A CATALOG OF NORTHERN STARS WITH ANNUAL PROPER MOTIONS LARGER THAN 0B15 (LSPM-NORTH CATALOG), The Astronomical Journal 129 Pages 1483–1522

Nicholson, Martin P. – 2015, Binary star discoveries in the URAT1 catalog - separation under 60 arc sec, Amazon.com, Vizier I/330

Parker, R.J. et al – 2009, Do binaries in clusters form in the same way as in the field? Monthly Notices of the Royal Astronomical Society 397, 1577–1586

Probst R.G. – 1983, An Infrared search for Very Low Mass Stars: JHK Photometry and Results for Composite Systems, The Astrophysical Journal Supplement Series 53, Pages 335-349

Reipurth, B. and Mikkola, S. – 2012, Formation of the Widest Binaries from Dynamical Unfolding of Triple Systems, Nature 492, 221–224

Rica, F.M. – 2011, Determining the Nature of a Double Star: The Law of Conservation of Energy and the Orbital Velocity, Journal of Double Star Observations, Vol. 7 No. 4 Pages 254-259

Schlimmer, J.S. – 2013, Study of 17 New Stellar Pairs in the Constellation Aurigae with Three Possible New Common Proper Motion Pairs, Journal of Double Star Observations, Vol. 9 No. 4 Pages 262-266

Schlimmer, J.S. – 2015, Discovery of 4 New Double Stars in Constellation Serpens, Journal of Double Star Observations, Vol. 11 No. 1 Pages 9-11

Scholz, R.-D. – 2016, Overlooked wide companions of nearby F stars, Astronomy & Astrophysics, accepted 7 January 2016

Shaya, E.J. and Olling, R.P. – 2011, Very Wide Binaries and other Comoving Stellar Companions: A Bayesian Analysis of the Hipparcos Catalogue, Astrophys. J. Suppl. 192 2

Skiff B. – 2016, Common-proper motion pairs and other doubles found in spectral surveys - 10. Survey work for 2015, The Webb Deep-Sky Society, Double Star Section Circular No 24, Pages 43-87

Smart, R.L. and Nicastro, L. – 2014, The initial Gaia source list, Astronomy & Astrophysics 570, A87

Wielen R. et al – 1999, Indications on the binary nature of individual stars derived from a comparison of their HIPPARCOS proper motions with ground-based data, Astronomy and Astrophysics 346(2) Pages 675-685

Wiley, E.O. – 2015, Dynamic Studies of Struve Double Stars: STF4 and STF 236AB Appear Gravitationally Bound, Journal of Double Star Observations, Vol. 11 No. 1 Pages 2-8

A New Concept for Counter-Checking of Assumed CPM Pairs

Zacharias N. – 2015, Bright Star Astrometry with URAT, Instrumentation and Methods for Astrophysics, arXiv:1506.05853

Zacharias, N. et al – 2015, The First U.S. Naval Observatory Robotic Astrometric Telescope Catalog (URAT1), American Astronomical Society, AAS Meeting #225

The Speckle Toolbox: A Powerful Data Reduction Tool for CCD Astrometry

Richard Harshaw
Brilliant Sky Observatory
Cave Creek, AZ
rharshaw51@cox.net

David Rowe
PlaneWave Instruments
Rancho Dominguez, CA

Russell Genet
California Polytechnic State University
San Luis Obispo, CA

Abstract: Recent advances in high-speed low-noise CCD and CMOS cameras, coupled with breakthroughs in data reduction software that runs on desktop PCs, has opened the domain of speckle interferometry and high-accuracy CCD measurements of double stars to amateurs, allowing them to do useful science of high quality. This paper describes how to use a speckle interferometry reduction program, the Speckle Tool Box (STB), to achieve this level of result.

For over a year the author (Harshaw) has been using STB (and its predecessor, Plate Solve 3) to obtain measurements of double stars based on CCD camera technology for pairs that are either too wide (the stars not sharing the same isoplanatic patch, roughly 5 arc-seconds in diameter) or too faint to image in the coherence time required for speckle (usually under 40ms). This same approach - using speckle reduction software to measure CCD pairs with greater accuracy than possible with lucky imaging - has been used, it turns out, for several years by the U. S. Naval Observatory.

1. Introduction

The new generation of low-cost and high-performance CCD and CMOS cameras has revolutionized amateur astro imaging, especially in the area of visual double star astrometry. As far back as the early 1990's, amateurs were using web cams to make measurements of bright double stars with surprising accuracy using the X, Y coordinates of the star image centroids (often chosen manually) and simple Cartesian mathematics.

But the advent and availability of low-cost CCD cameras (and later CMOS cameras) allowed for a complete sea change for this aspect of amateur double-star astronomy, as it was now possible to image truly faint and challenging pairs. When merged with the new data reduction software coming into the market, amateurs had at their disposal powerful tools for the collection of double star data and its accurate reduction to meaningful measurements.

Most recently, advances in software that enable data reduction via Fourier Transforms that run on desktop computers have pushed the limits of where amateurs can do useful research even further out in terms of magnitude and resolution. Prior to this development, measurements of double stars using CCD images (and later CMOS images) had to be done with a process known as "lucky imaging." Lucky imaging is a method that begins with a very large number of frames shot at an integration time (shutter speed) that is as short as possible to help "freeze" the star image during moments of superb seeing. This file of images is then processed by selecting a small percentage of the best frames based on different criteria - best signal-to-noise ratio (where frame selection is based on the ratio of the signal-to-noise versus star density and is best used on noisy frames), or best maximum (where frame selection is based on the strength of the central concentration of light in the star's image, best used with low-noise frames and files with small star images). There may be other options available, depending on the software package used to select the frames used for a lucky image.

Once the frames have been selected, they can be "aligned and stacked", meaning the software will recenter each frame based on the centroid of the primary star. All selected frames are then blended into one final image, which often shows very clean stars that are easy to measure.

However, lucky imaging suffers from the fact that it is very difficult to use with accuracy on very close pairs (closer than about 5 arc seconds) or where one (or both) of the stars is bright, resulting in large star images that may overlap or in which it may be difficult to determine the centroids. Yet this is the domain where most of the interest lies in visual double star astrometry. It also requires fairly bright stars in order to get shutter speeds fast enough to freeze the star images.

This is where speckle data reduction software can be of immense help. Over the last 16 months, I have been gathering data on hundreds of double stars (with these observations being reported in this Journal) using two cameras—a Skyris 618C color CCD, and most recently, the ZWO ASI290 monochrome CMOS camera. I have been reducing my data and making measurements using a speckle reduction program written by David Rowe, chief technical officer at PlainWave Instruments. The original program provided to me by Rowe was called Plate Solve 3, and was a robust multipurpose program that did many things besides speckle reduction. About six months ago, Rowe released a special sub-set of Plate Solve, called Speckle Tool Box (STB for short in this paper). I will describe in this paper how to use STB to do accurate astrometry on close double stars, whether with speckle interferometry or CCD imaging, and explain how to obtain a free copy for use in your own observing program.

If you have ever requested data from the Washington Double Star Catalog for a particular pair of stars, the reply you got included a text file titled "datarequest_key". If you read that file, you will find a translation key for the methods used to report measurements. Two of those codes are Cu and Su, which are described in the datarequest_key file as "USNO CCD imaging (speckle-style reduction)." (The C and S refer to two different cameras used for the data collection.) Wanting to be sure if this method was like the one I have been using, I wrote Brian Mason at the USNO and asked him about this method. It is, indeed, the method I have been using, in which a CCD image of a double star is analyzed using speckle reduction software in order to obtain more precise measurements than possible with lucky imaging.

Mason (2007) writes, "Most of the systems observed with this camera (the "Cu" camera at the U. S. Naval Observatory in Washington, D. C.) have separations well beyond the regime in which there is any expectation of isoplanicity, so we classify the observing technique for all of these measures as just "CCD astrometry," rather than speckle interferometry. Despite this classification, there is an expectation that the resulting measurements have smaller errors than classical CCD astrometry. Each measurement is the result of many hundreds of correlations per frame, and up to several thousand frames per observation."

2. How Speckle Reduction Software Works

The Speckle Tool Box does speckle reduction by working on a FITS cube. A FITS cube is a set of FITS images bound into a single file. Normally, one should use several hundred to several thousand FITS images and bind them into a FITS cube. Since most camera control software simply captures FITS images and does not bind them into cubes, STB does that for you (I will explain the menu of processes later).

Once the FITS cubes have been compiled, it is best to pre-process the cubes. This is not a requirement in STB, but it does make for much faster solutions when it is time to do the speckle reduction. Pre-processing consists of STB reading each frame in the FITS cube and then computing its power spectrum using a Fourier transform and then taking the squared modulus of each complex pixel value. The frames are then averaged and saved as a file with a special suffix (_PSD) added to the file name.

During speckle reduction, a processed file is loaded into STB and the power spectrum is then graphically displayed on screen as an *autocorellogram*. See Figure 1.

Note that the autocorellogram displays radial symmetry. It is *not* an actual image of the double star, but rather a graphical portrayal of the two-dimensional autocorellation of the averaged power spectrum. The symmetric nature of the display results from the fact that autocorellation of any real function is inherently sym-

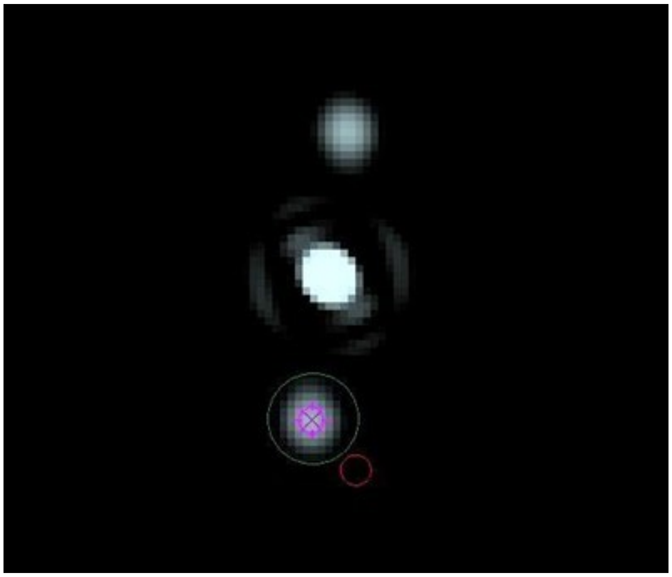

Figure 1. An autocorellogram generated by STB.

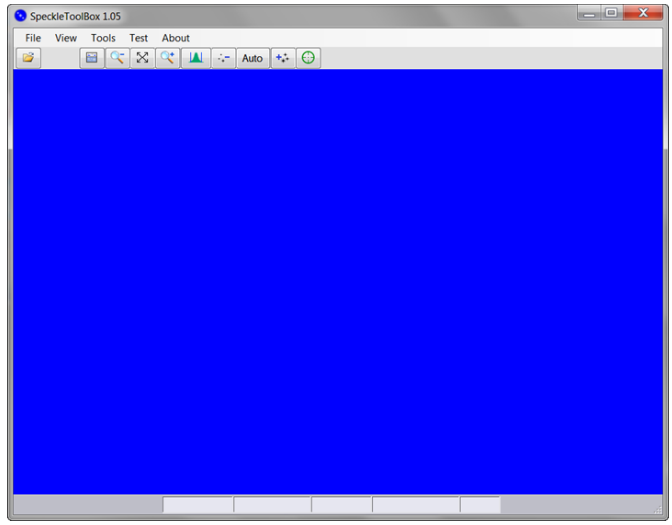

Figure 2: The home screen of The Speckle Toolbox

metrical. Rowe is working on a new feature for STB that can generate a recovered, high-resolution image by a method called Bispectrum analysis, which is extremely demanding on the computer's processor, normally requiring a special co-processor to be installed to allow the program to generate a solution in a reasonable amount of time. (Currently, bispectrum analysis is done mostly on high-speed mainframes, where it is still a time consuming process.)

So how does one use STB to generate autocorellograms that can then be measured with higher precision that lucky imaging?

3. Using The Speckle Tool Box to Make FITS Cubes

The Speckle Tool Box home screen is shown in Figure 2.

At the top of the screen is a list of commands and below that, a palette of tool icons. I will explain each part of STB in detail and show how each part contributes to an astrometric solution.

To make FITS cubes, click on TOOLS, then from the drop-down menu, select "Make FITS cube(s)…" A dialog box will appear, as shown in Figure 3.

The instructions in the "Operation" window detail how to select files for binding into Cubes. STB allows you to specify whether the original files are monochrome or color and even allow the user to crop the files to a uniform size. Since STB works best on images that have dimensions that are a power of two (256 x 256 and 512 x 512 being the norms), this is an important feature.

4. Doing a Drift Calibration with STB

A drift calibration is done by clicking on TOOLS and selecting "Drift Calibration Analysis…" This opens a powerful feature of STB: a simple way to determine the camera's angle with reference to true north as well as the pixel scale for the camera (how many arc seconds each pixel spans).

To obtain drift files for analysis, you must select a bright star near the meridian and at a medium declina-

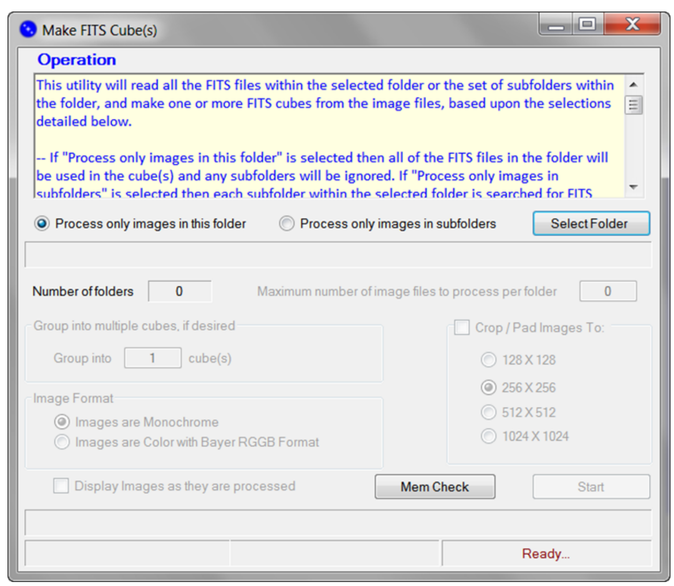

Figure 3: Dialog box to make FITS cubes

tion (between 30° and 60° works best, but any declination will work). Jot down the declination of the star for use later.

Use the telescope's slow motion controls to nudge the star just off the east edge of the camera chip (you may have to temporarily cut power to the polar axis drive motor to see which way the star drifts). Then (1) start recording the file and (2) kill power to the drive motor. When the star drifts off the west end of the chip, (3) stop the recording and (4) re-power the drive motor.

Use the slow motion controls to return the star to just off the east edge of the chip and repeat the process. I suggest you do at least 12 drifts, and more is even better. (I normally use 20 drifts when calibrating my system.)

Figure 4 shows the dialog box that starts the drift analysis process.

This window is very important and requires considerable user input, so I will cover it step by step and illustrate with an actual drift analysis.

The area tagged "1" in the red circle (Callout 1) is where you enter the maximum number of frames to use for the analysis. The default is 1,000 but you may specify any number you wish. For instance, if you have a camera chip whose long axis is east-to-west and you are shooting at very short integration times (which I recommend), you may well have over 1,000 frames in the drift file, so feel free to set the maximum at whatever level you think is best. STB will use only as many frames as the file contains, so if you set the value high, no harm is done.

Step 2 is indicated by Callout 2 and it and is where you select the drift file you wish to analyze. In my practice, I use an external USB hard disk drive on my observatory's computer and save my drift files to it. Once my observing session is finished, I power the computer down and take the USB drive into the house for analysis the next morning.

Callout 3 allows you to tell STB to not start analyzing the frames until some length of time into the file. I usually enter 0.2 seconds in this window in case my camera control software has a stutter when it starts capturing frames.

At Callout 4, you enter the declination of the drift star, leaving spaces between the degrees, minutes and seconds (dd mm ss).

We suggest you check the box by Callout 5, Reject Outliers, and set the rejection at 2 sigmas. This makes for a very tight band of acceptance of data points and improves the accuracy. (With a value of 2, all centroid positions more than 2 standard deviations from the RMS line of the drift are ignored in the calculation.)

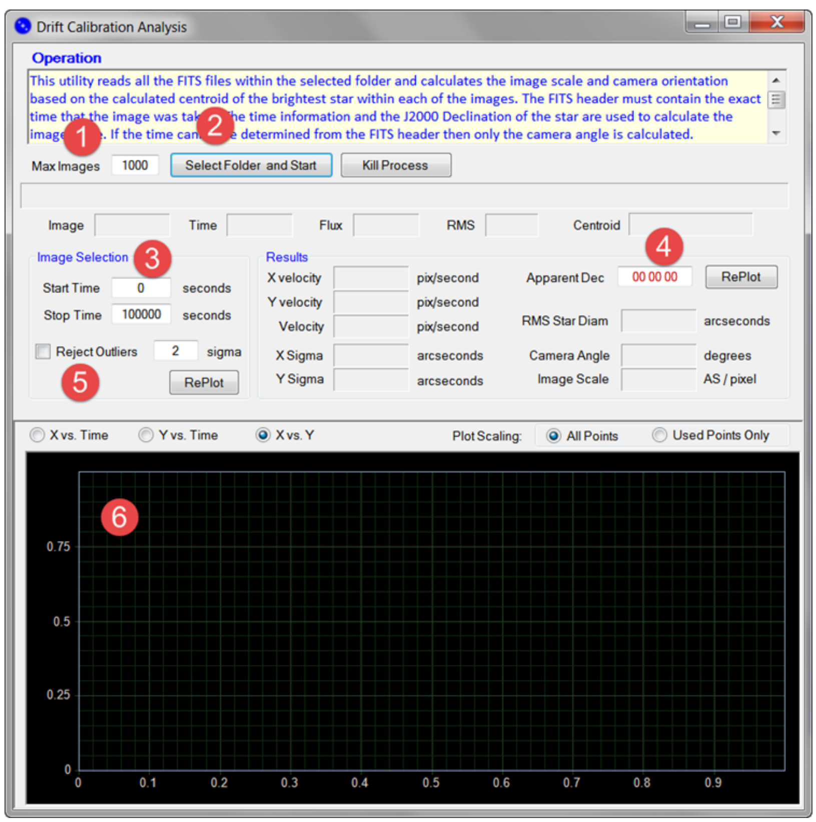

Figure 4: The Drift Analysis dialog window

Callout 6 is where STB displays its results and the final drift line.

Figure 5 shows the Drift Analysis window active with a drift file we captured of the star Regulus:

The numbered callouts in the window show (1) the maximum number of frames I used, (2) the start time of 0.2 seconds into the file, (3) the declination of Regulus, (4) rejection of outliers more than 2 sigmas from the mean, (5) the RMS diameter of Regulus in arc seconds, (6) the camera angle (with respect to true north), and (7), the pixel scale in arc seconds per pixel.

Since we did this drift with Regulus just west of the meridian (and the OTA on the east side of the mount), the camera angle shows -176.73°. Its actual orientation must be set by adding 180° to this to obtain 3.27°. With the OTA on the west side of the mount, the camera angle given by STB is the camera angle to use for measurements. But note that if you cross the meridian with your OTA (doing the notorious meridian flip), you'll need to add (or subtract) 180° to the camera angle for stars measured on the opposite side of the mount as the side on which you captured the drifts.

An Excel spreadsheet lets us input the results of each drift analysis to compute the mean, standard deviation, and standard error. (We find that beyond 25 drifts, the mean, standard deviation and standard error change very little, which is why we normally do 20 or so drift files for calibration purposes.)

The RMS diameter of the star (Callout 5) is a rough indication of the quality of the seeing for the drift observation, as the poorer the seeing, the larger the star's image. However, this value is also very dependent on the star's magnitude and the camera integration time. It is therefore a relative indicator of seeing, and experience will let you determine what sort of seeing you will have for the night based on the RMS diameter of the star.

This method is fast and accurate, normally only taking the first 20 or 25 minutes of an observing session (unless the camera was not moved from the last session, in which case you do not bother doing a drift).

5. Processing FITS Cubes

From the TOOLS menu, select "Process FITS Cubes…" to pre-process the data. This results in smaller file size and faster processing during speckle reduction of the images. The Process FITS Cubes dialog window is shown in Figure 6.

Begin by clicking the button by Callout 1. Clicking this button opens the computer's file directory from

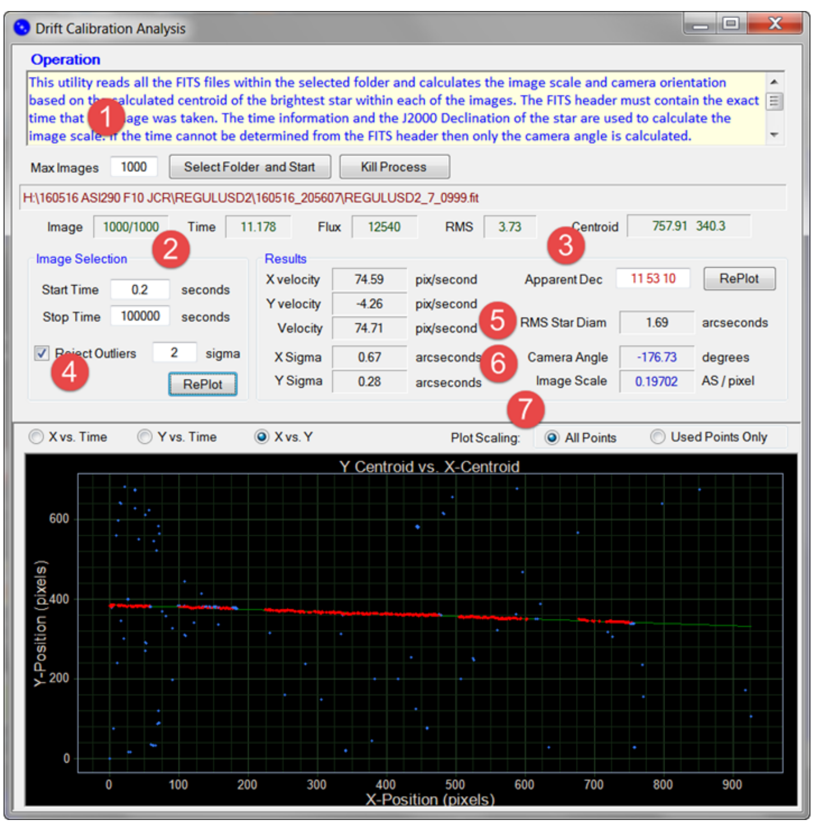

Figure 5: Drift Analysis using Regulus at f/10

which you may navigate to where you have stored the FITS cubes you wish to analyze. You may process one cube at a time or do a batch process on as many cubes as you wish.

If you want the processed cubes to be saved in a separate folder (which I always do, as I found that it makes it easier to locate them later), click the box next to Callout 2 and then use the browse button (Callout 3) to locate the folder you want the processed files to be stored in. If needed, create the folder.

You are then ready to begin processing. Click the Process button (Callout 4) to begin. STB will then display its progress as it opens, reads, and processes each FITS cube you have selected. Depending on the size of your files and your computer's processor speed, this normally takes between five and 10 minutes per 1000-frame cube.

When finished, you may close the Processing dialogue window. If you wish to check that your processed files went to the correct folder, use the Windows Explorer to find the folder you specified and be certain that your processed files are there.

6. Speckle Reduction with STB

Now that you have determined the camera's angle and pixel scale, and have built your FITS cubes and processed them, you are ready to start doing speckle reduction. To do so, use the TOOLS menu and select "Speckle Reduction…". The dialog window shown in Figure 7 will open.

This dialog window is the heart of STB. I will explain its use by first explaining how to generate an autocorrelogram (Callouts 1 and 2). Later, I will explain how to tweak the autocorrelogram using the options under Callout 3.

Figure 8 is the autocorrelogram generated for ARG 24 with no Reference-Star FITS Cube or PSD File selected. (We' ll explain that more in a moment.)

We need to work on this autocorrelogram before we do the measurement. First, it will help to enlarge the image. This can be done using the mouse wheel or by clicking the Enlarge button. The result is shown in Figure 9.

Next, we want to clean up some of the background noise and make the star images a little smaller. This is done by using two different buttons — levels and dimmer.

By clicking on the levels button, the dialog window shown in Figure 10 appears.

Note the slider near Callout 1. We must click the slider and drag it to the right about to the point where the intensity graph flattens out (Callout 2). Figure 11 is how the autocorrelogram looks after doing this.

Notice how the background is now much darker and "cleaner." But we still need to make the star images a bit smaller, so we click on the Dimmer button and end up with an autocorrelogram that looks like that shown in Figure 12.

We are now ready to perform the astrometry functions. We click the astrometry button which brings up the dialog window shown in Figure 13.

We have not actually measured anything yet, but I

(Continued on page 59)

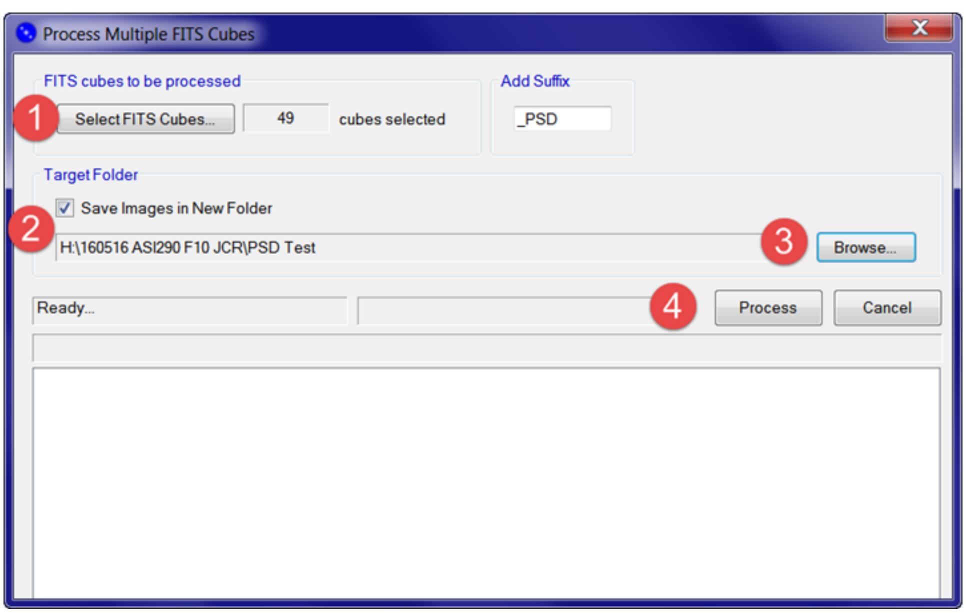

Figure 6: The Process FITS Cubes dialog window.

The Speckle Toolbox: A Powerful Data Reduction Tool for CCD Astrometry

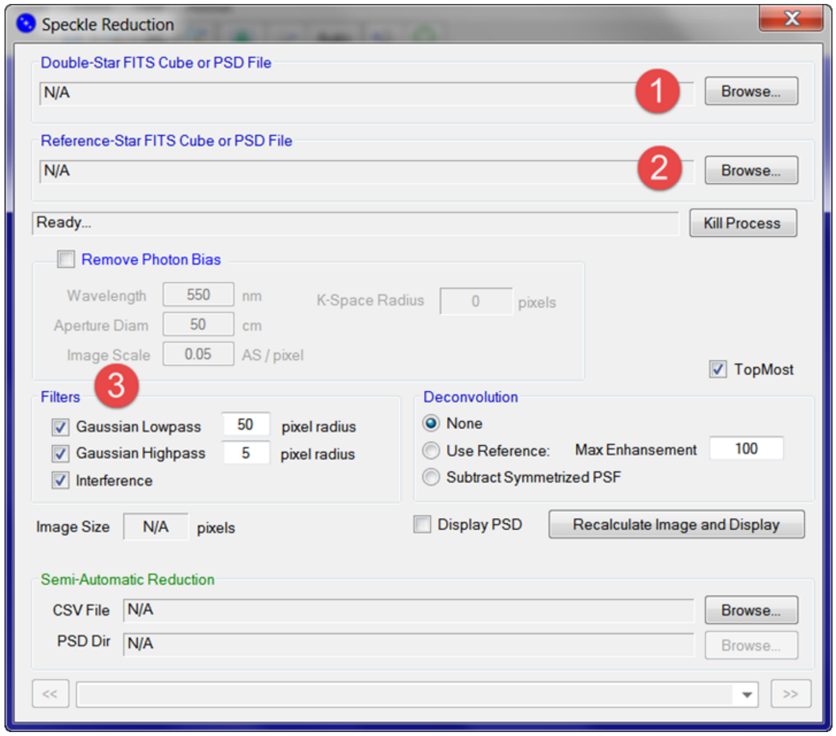

Figure 7: The Speckle Reduction dialog window.

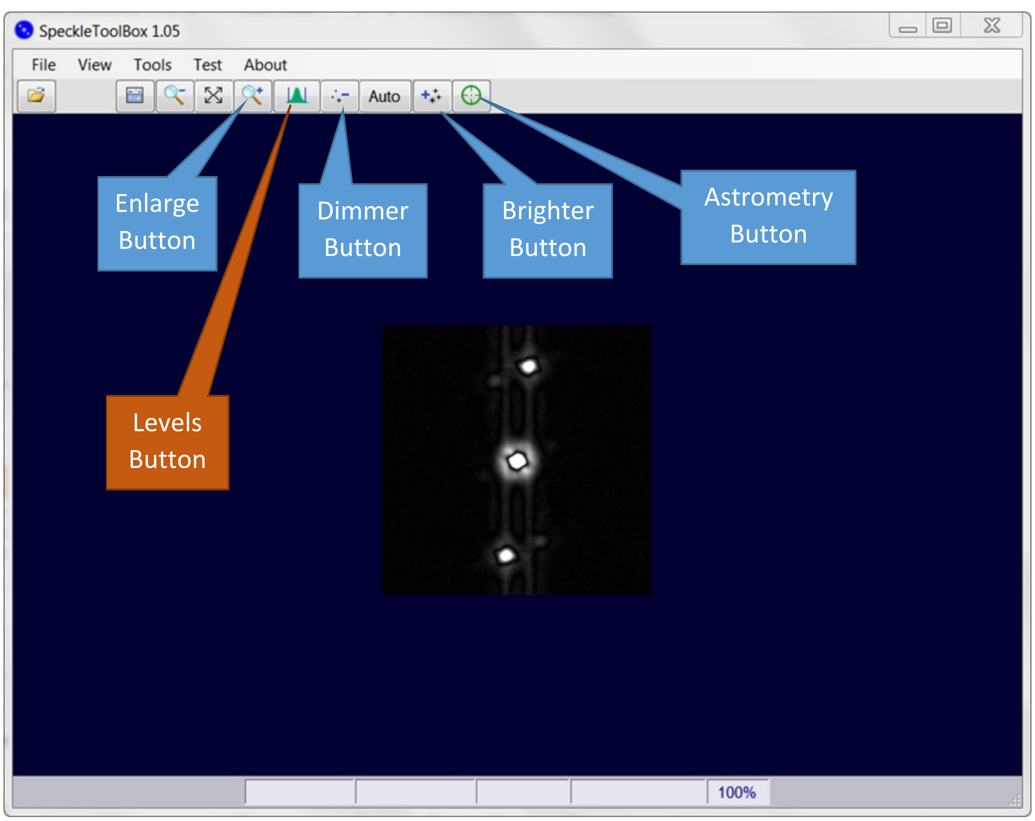

Figure 8: Autocorrelogram for ARG 24, unprocessed.

The Speckle Toolbox: A Powerful Data Reduction Tool for CCD Astrometry

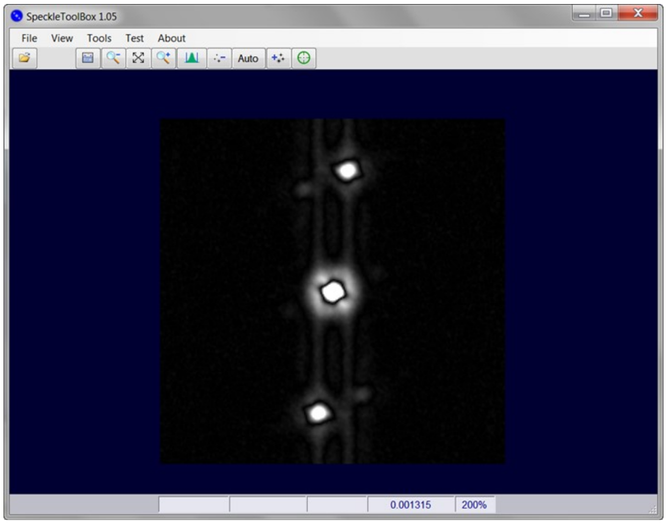

Figure 9: ARG 24 zoomed in.

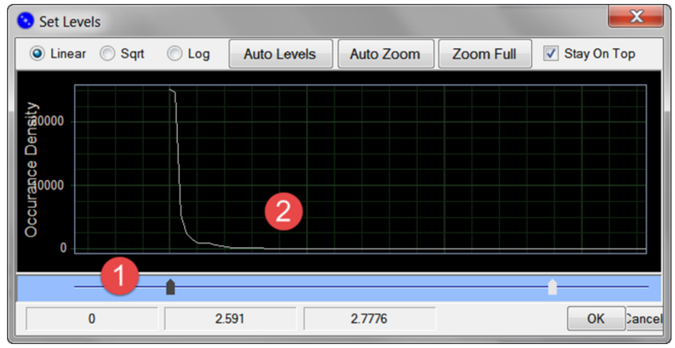

Figure 10: The Levels Button dialog window.

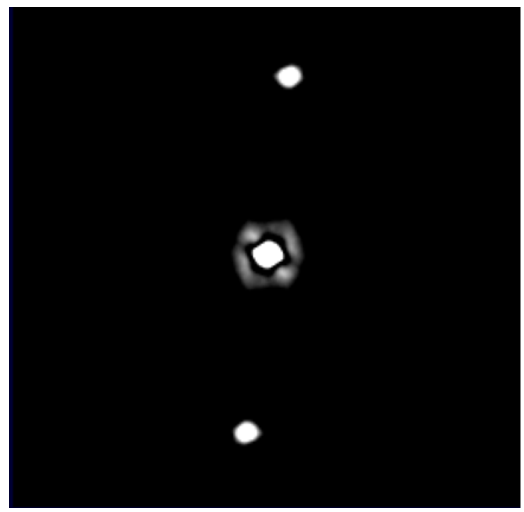

Figure 11: The "improved" autocorrelogram.

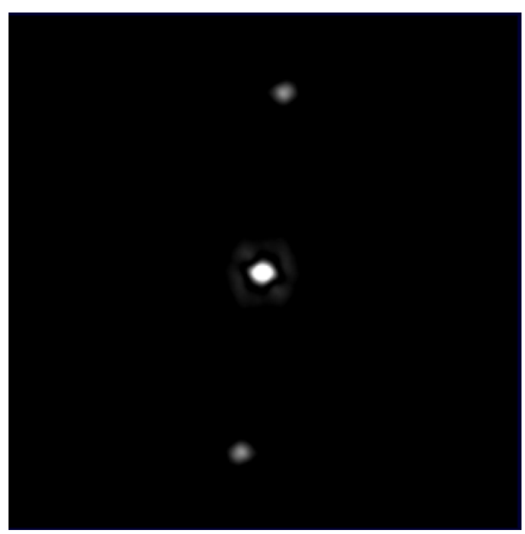

Figure 12: The autocorrelogram after dimming the stars 3x

(Continued from page 57)

did enter the camera angle and pixel scale from the night that I imaged ARG 24 (Callouts 1 and 2) . (We'll explain all of the features on this window but for now let us just focus on making the measurement.)

To obtain the measurement, click the button labeled "Auto Detect". When you do, the autocorellogram will change and look as shown in Figure 14.

It might be hard to see, but there is a small pink colored "ship's wheel" around the star at the top of the frame. Checking the bottom of the astrometry dialog window, we see the measurement made by STB as shown in Figure 15.

Notice that STB found the companion star to lie at a position of Theta = 170.07° and Rho = 17.7113". If we check the Washington Double Star Catalog we will find that the last measure (as of this date) was made in 2012 and had Theta = 350.2° and Rho = 17.57". STB appears to be about 180° off for Theta. This is easy to correct.

At the bottom of the astrometry dialog window is a button labeled "Remove Target". Clicking that removes the pink icon around the companion star. We must now manually indicate the companion star with the mouse. As we move the mouse cursor over the autocorello-gram, we notice that it appears as a small green circle.

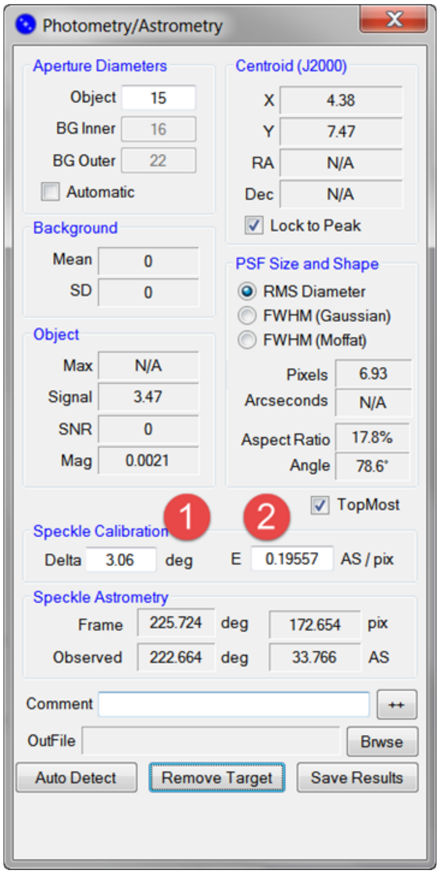

Figure 13: The Astrometry dialog window

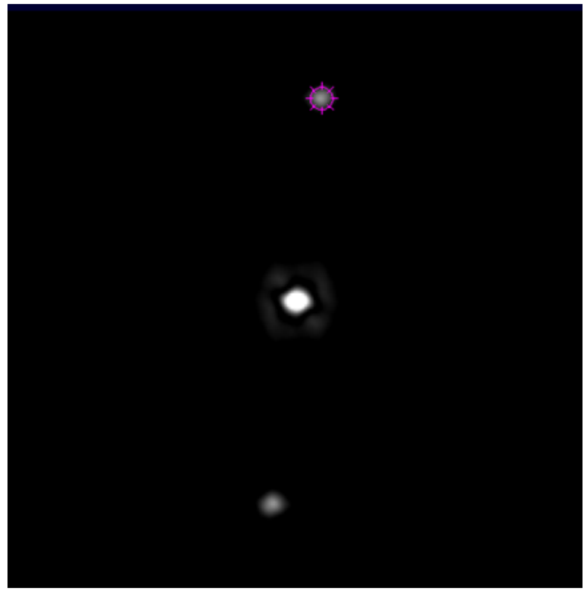

Figure 14: Results of the Auto Detect option.

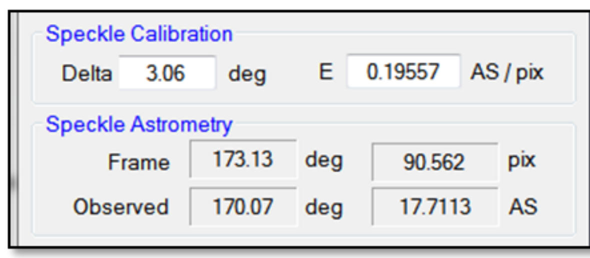

Figure 15: Astrometry results.

When we place the circle over the companion star at the bottom of the frame, the screen will look as shown in Figure 16.

By right clicking at this point a menu will fly out to the right of the mouse with several options as shown in Figure 17.

We want to select the last option on the menu, “Set Target Location.” When we do, the astrometry window will update to the new numbers as shown in Figure 18. These numbers are in close agreement to the 2012 measure and show that over four years, ARG 24 has moved about 0.14° clockwise in Theta and reduced Rho by about 0.1405".

Any time the companion star is at a value of Theta of 180° or less, STB will correctly identify it when the Auto Detect button is clicked. If the companion has a value of greater than 180° for Theta, the companion star will have to be manually selected.

Manual selection can be a tricky process. Figure 19 shows the settings for the Object Aperture used for the solution just derived. The setting for the Object Aper-

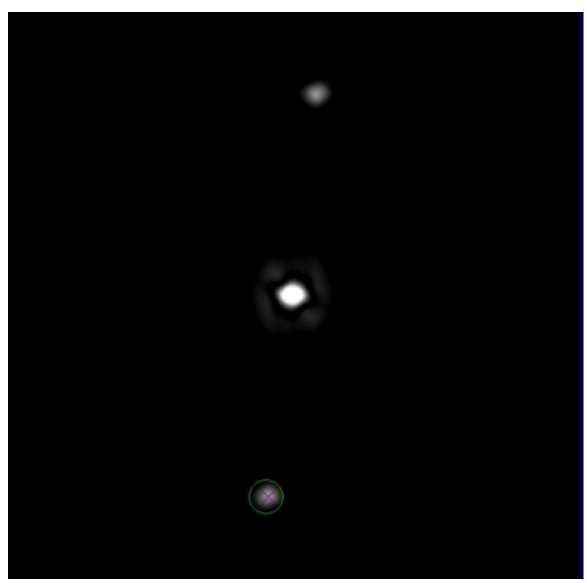

Figure 16: A manually-selected companion star.

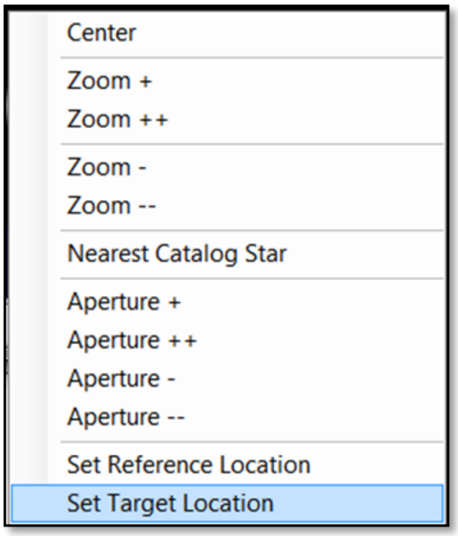

Figure 17: The manual selection fly-out menu.

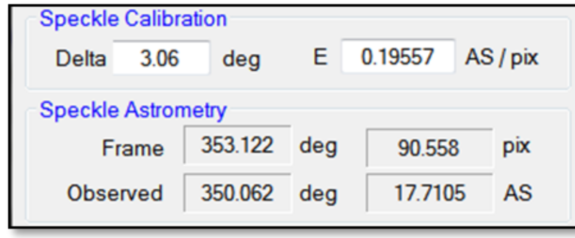

Figure 18: The updated astrometry window.

ture is critical for a good manual solution as well as having as clean an autocorrelogram as possible with star images that are smaller than the Object Aperture.

Note how the setting of 15 creates a selection circle that is larger than the companion star (Callout 2). Figure 20 shows the effect of making the Object Aperture larger while Figure 21 shows the effect of making it smaller.

Note how large the green circle is in Figure 20 — far larger than the companion star image — while in Figure 21 it is much smaller than the companion star. When the Object Aperture diameter is too large, STB may pick up background noise from the autocorrelogram and lead to a faulty solution. Conversely, when the Object Aperture is too small, important information about the precise location of the companion star may be truncated by the selection radius.

Also note that the checkbox "Lock To Peak" is checked. When this is the case, if the Object Aperture is large enough, centering the location circle over the companion star will place an X on its centroid, leading

Figure 19: Effect of Object Aperture on a manual solution (part 1)

The Speckle Toolbox: A Powerful Data Reduction Tool for CCD Astrometry

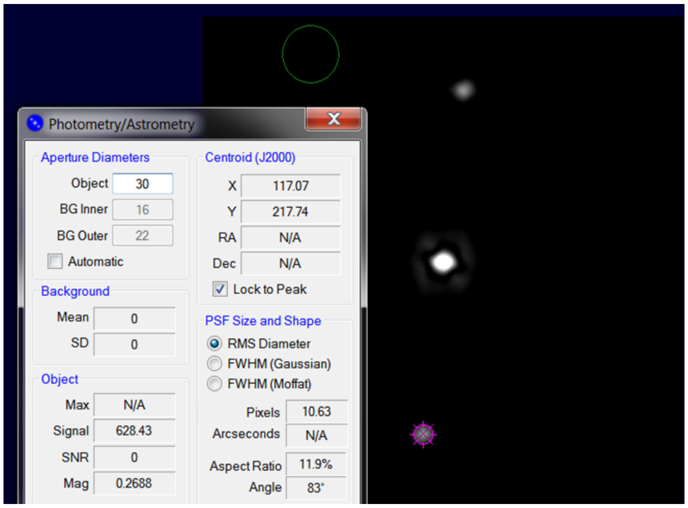

Figure 20: The Object Aperture is too large.

Figure 21: The Object Aperture is too small.

to a more accurate solution.

Sometimes it is not possible to get the background of the autocorellogram totally dark and noise free. (This will be particularly the case for close stars of unequal magnitude.) When that is the case, even with a properly sized Object Aperture, the Lock to Peak function will not work as designed. The noise around the companion star will pull the centroid selection off-center. When that happens, your only option is to clear the Lock to Peak box and manually center the X over the companion star. You will get a solution, but with a trade-off in some accuracy.

Figure 22 shows a pair of stars (STF 233) where the area around the companion is not free of noise.

In a case like this, STB would not be able to lock onto the companion (the star to the left of the primary) because there is too much competing noise. You would have to manually place the selection aperture over the companion with Lock to Peak unchecked, then right-click and select Set Target Location.

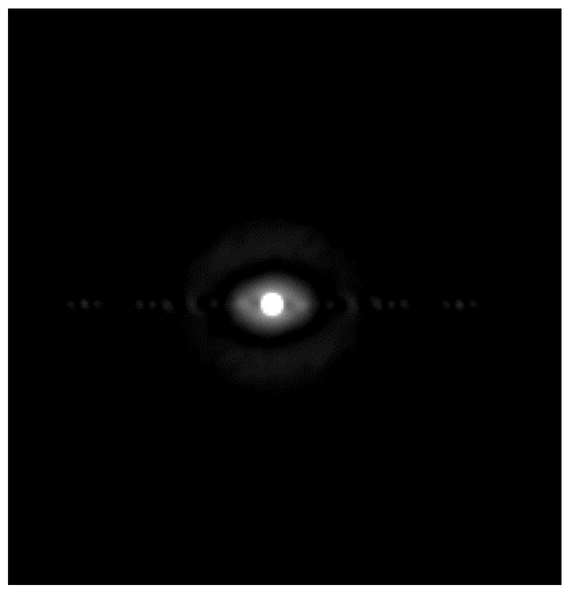

Figure 22: Autocorrelogram for STF 233 with the companion embedded in noise.

7. The Gaussian Filters

If we return to the Speckle dialog window, we notice that the bottom half has several options (shown in Figure 23).

Callout 1 is where we can adjust STB's filter settings. Callout 2 is where we set up the deconvolution star parameters. And Callout 3 is a checkbox that allows us to display the power spectral density as an image. We will now cover each of these functions in detail using material generously supplied by STB's author, David Rowe and his collaborator, Russ Genet.

Gaussian Lowpass Filter (Callout 1)

For a run on a specific telescope, the Filters can often be set once (perhaps after some experimentation) and then left alone for the reduction of an entire run. Proper setting of the two Gaussian filters should optimize the detection and measurement of the double.

A telescope's optical system is a spatial low pass filter where the low pass cutoff frequency (in pixels) is a function of the wavelength, the f/ratio of the telescope, and the size of the pixels. Recall that the Airy disk radius, R, is given by

$$R = 1.22\lambda\left(\frac{F}{D}\right)$$

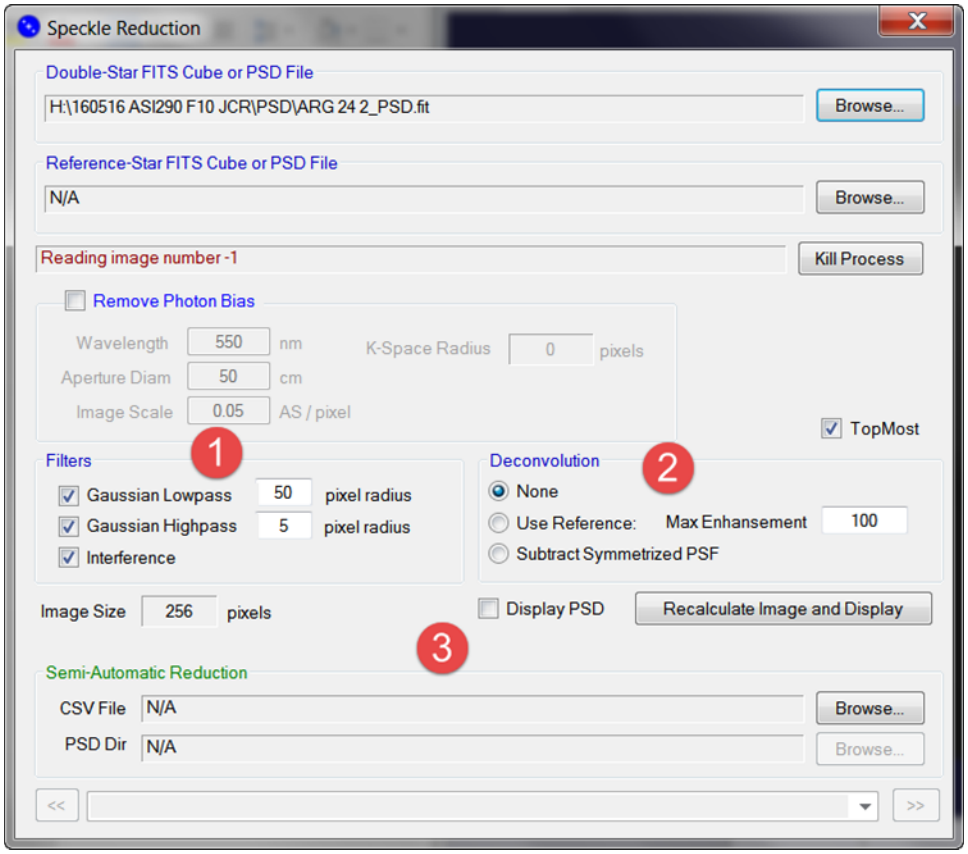

Figure 23: The Filters section of the Speckle dialog window.

where λ is the wavelength and *F/D* is the focal ratio of optical system. In pixels, this is given by

$$R(\text{pixels}) = 1.22\lambda\left(\frac{F}{D}\right)h$$

where *h* is the pixel dimension.

As an example, take the pixel dimension to be 10 microns, the wavelength to be 0.8 microns, and the focal ratio to be 50. The Airy disk radius will be approximately 5 pixels. The Fourier transform of the Airy disk will have most of its energy within a spatial frequency, fc, given by

$$f_c = \frac{N}{2R}$$

where *N* is the size of the image and *R* is the radius of the Airy disk, all values being in pixels.

In the spatial frequency domain, there is very little signal higher than this frequency. However, beyond this frequency there is considerable noise from the electronics, from the sky background, and from photon shot noise from the object. Therefore, to improve the signal-to-noise ratio and to reduce unwanted interference from the electronics, it is wise to apply a low pass filter with a cutoff proportional to this spatial frequency. Thus, the cutoff frequency, *fc* (pixel radius), should be approximately:

$$fc = \frac{hN}{2.44\lambda\,\mathrm{F/D}}$$

Taking an example from a speckle interferometry run at Pinto Valley Observatory, λ = 0.8 microns, *h* = 10 microns, *F/D* = 50, *N* = 256, yields *fc* = 26 pixels. For my C-11 and ASI290 camera (2.9 micron pixels at *F/D* of 11 and 15), the value of *fc* is 35 for the f11 optical train, and 25 for the f15 train. In practice, it is a good idea to make the low pass filter somewhat wider than this so that most of the signal information is allowed through the filter. For that reason, I usually set the low pass filter at about 40 for my setup. You will obviously need to calculate the settings for your particular optical setup when using STB.

This only provides a good starting point. In fact, the auto-correlation has noise and signal statistics that are more complicated than the above simplified argument would suggest. For PVO II, experimentation suggested that an *fc* of about 50 pixel radius worked best, although the solutions were not overly sensitive to this setting. I often find that running the low pass filter up to 50 or 60 improves the autocorellogram noticeably over my “standard” setting of 40.

Clicking Display PSD (Callout 3) will toggle from the normal autocorrelogram solution image to the PSD (Power Spectral Density) fringe pattern display. If, as shown in Figure 24, the Gaussian Lowpass is set too wide, noise beyond the telescope cutoff will be seen, suggesting that the setting should be reduced to a smaller pixel radius. On the other hand, if there is no signal at all beyond the telescope cutoff, then the filter is set too narrow and should be widened.

Gaussian Highpass Filter (Callout 1)

The Power spectral density (PSD) is the Fourier transform of the image. The purpose of the Gaussian Highpass Filter is to remove, as much as possible with a simple filter, the broad tail of the point spread function (PSF) that is due to seeing and optics. This filter removes the lowest-frequency information in the image and is typically set between a 2 to 5 pixel radius. It is set empirically to give the best auto-correlation.

A useful way to set the filter is to look at the PSD, which can be done by toggling Display PSD to bring up the fringe pattern. As shown in Figure 25, set the pixel radius to remove the bright spot in the zero-order PSD fringe pattern without hurting the rest of the fringe pattern. The Gaussian high pass is usually not needed when single star reference deconvolution is used.

Interference Filter (Callout 2)

In certain situations we have encountered significant interference, possibly due to the interaction of the camera with the main 120V AC power source at remote locations. Much of the unwanted interference was found to lie along the lines fx = 0 and fy = 0 in the spatial frequency domain. If the Interference filter is checked, the values along the fx = 0 and fy = 0 axes in Fourier space are replaced by the average values of their neighboring pixels. This filter is quite specific to the type of interference produced by the camera.

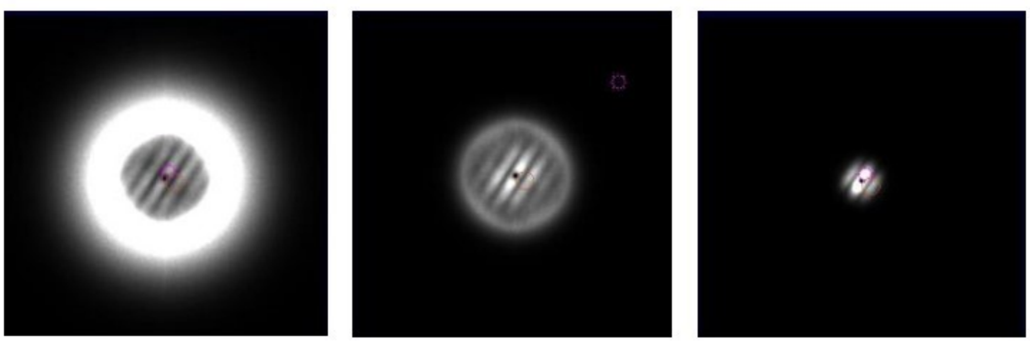

Figure 24: On the left, the Gaussian Lowpass filter was set too wide (70 pixels), allowing high frequency noise to be included. On the right, it was set too narrow, cutting off useful information. In the middle it was set just slightly larger than the spatial cutoff frequency imposed by the telescope’s aperture.

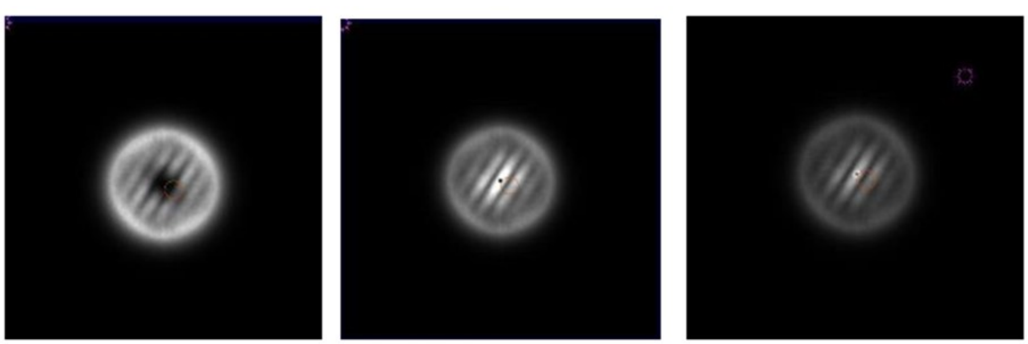

Figure 25: On the left, the Gaussian Highpass filter was set to wide, not only cutting out the bright central peak, but also much of the fringe pattern. On the right the filter was set too narrow, allowing the bright central peak to shine through. The center is set correctly.

Deconvolution (Callout 2)

There are three Deconvolution options: None, Use Reference PSD, and Subtract Symmetrized PSF. Each is discussed below.

None Although not recommended, speckle interferometry reduction can be accomplished without the use of single reference stars for deconvolution. For this option, simply select None under Deconvolution. It can be quite helpful to apply a Gaussian high pass filter when not using deconvolution. This is especially the case when using STB to analyze pairs too wide or faint for speckle but for which you want the accuracy of an STB solution compared to lucky imaging.

Use Reference PSD The use of deconvolution reference stars is highly recommended. Not only will it sharpen the double star image, it will also remove much of the telescope's optical aberrations, including the effect of the central obstruction. In addition, if the reference star was taken close in time and located near the double star, deconvolution will remove much of the atmospheric dispersion and broad tail due to the effects of seeing. Deconvolution will help in almost all instances. If the reference star is a poor match for the double star, there are cases where a false detection can occur for doubles with dim, close companions.

Deconvolution is based on the following mathematical properties: (1) the recorded image of a very short exposure is the convolution of the "perfect" image of the object with the PSF of the telescope plus the instantaneous atmosphere, and (2) the convolution operation can be implemented by taking the inverse Fourier transform of the product of the Fourier transforms of the "perfect" image and the point spread function (PSF) of the telescope plus instantaneous atmosphere. Symbolically:

$$F(I) = F(O) * F(T)$$

where $F(\,)$ denotes the Fourier transform, I is the actual image recorded, O is the "perfect" image of the object, and T is the PSF of the telescope plus instantaneous atmosphere. Speckle interferometry is based on averaging a large number of very short exposures which "freeze" the atmospheric seeing, allowing us to take the average of the above equation in transform space. If we let $<I>$, $<O>$, and $<T>$ denote the averages of the Fourier transforms of I, O, and T, as defined above, then we can calculate an approximation for the Fourier transform of the object's power spectral density (PSD) as:

$$\langle O \rangle = \frac{\langle I \rangle}{\langle T \rangle}$$

Taking the inverse Fourier transform of $<O>$ yields an approximation to the object's autocorrelation, with the telescope and atmosphere removed. This process is called deconvolution.

To perform this operation, we need an estimate of $<T>$, the autocorrelation of the telescope plus atmosphere. A convenient way to find this estimate is to obtain a speckle cube of a nearby single star. The most effective deconvolution will be based on single star speckle observations that are very near the object from the point of view of the atmospheric conditions and telescope pointing. We feel that it is good practice to observe a single reference star that is as near as possible to the double star in both time and space. The reference star must, of course, be bright enough to show excellent SNR after speckle preprocessing.

To use a reference star for deconvolution, check Use Reference PSD and set it to 100 percent. The percentage option was included so one can experiment with the strength of the deconvolution when using non-ideal reference PSDs.

Subtract Symmetrized PSF This option was developed for close, dim double stars without good reference stars. A symmetrized PSF is made from the image and is subtracted from it, yielding only the non-symmetrical part. This can highlight an otherwise difficult-to-detect companion. This technique should be used with caution, since non-rotationally symmetric telescope aberrations can mimic a close, dim double.

Display PSD (Callout 3)

Toggling Display PSD will move back and forth between the autocorrelogram solution and the power spectral density fringe pattern.

Kill Process (Callout 3)

Kill Process simply stops the FITS cube speckle preprocessing.

8. Creating an OutFile Using the Astrometry Dialog Window

Near the bottom of the astrometry dialog window are prompts for creating an OutFile. See Callouts 1, 2, and 3 in Figure 26.

After a star has been measured, STB allows you to generate a CSV file which can be read by Excel (or most other spreadsheet programs) so you may collect data and mathematically analyze it later, computing means, standard deviations, and standard errors. To do so, you need to specify a name and location for your OutFile. Click the "Brwse" button to the right of the OutFile name window and navigate to a folder (or create one) where you want STB to save the results. After the folder is selected, type a name for the file in the OutFile window.

The Speckle Toolbox: A Powerful Data Reduction Tool for CCD Astrometry

If you wish to add any comments to the measurement, type them in the window indicated by Callout 2.

When you are ready to save the measurement, click the button titled “Save Results”.

Once the OutFile has been created and the first record saved, all subsequent measurements you make during that run of STB will be appended to the OutFile as new records.

When you have completed your measurements, you may exit STB and open the OutFile CSV in your spreadsheet program. If you are using Excel, I suggest that you save the file immediately as an Excel file rather than the CSV file that STB generates.

9. Structure of the OutFile

As shown in Figure 27, the OutFile is comma delimited, one row per output record. The top row provides column content abbreviations. These abbreviations are provided below, followed by a short description.

Num This is the object sequence number from the input CSV file directory, when used. If an input CSV file is not used, this entry will be blank.

Target This is the target (double star) identification. Usually it is the Washington Double Star (WDS) catalog name, such as 09345+0723, but it can be some other identifier, such as GJ3579.

ThetaC This is the last catalog or predicted (input) double star position angle (PA, θ, and Theta are all abbreviations for position angles). This calculated (prediction) may be the last reported position angle, but could be an interpolated value from an orbit ephemeris, or even a maximum likelihood prediction. *ThetaC* is used by PS3 to place a small red circle on the autocorrelogram, where the secondary is expected.

ThetaO The observed position angle. This only has meaning when the user provides the camera angle, *Delta,* from some calibration external to the reduction. If not available, the user can enter any number and ignore the results, or enter a camera angle of “0” and the output would be the “uncorrected” camera angle.

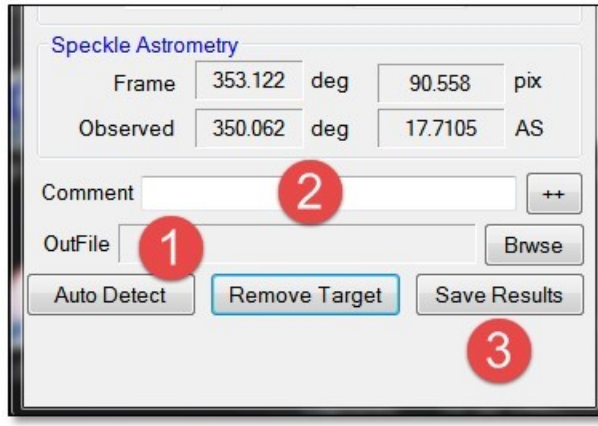

Figure 26: The OutFile options

ThetaO-C PS3 simply calculates this as *ThetaO* minus *ThetaC*. This is the difference between the observed position and the calculated (i.e. predicted or expected) position angle; the classic O-C.

RhoC This is the last catalog or predicted (input) double star separation (Sep, ρ, and Rho are all abbreviations for separation). This calculated (predicted) separation may be the last reported separation, but could be an interpolated value from an orbit ephemeris, or even a maximum likelihood prediction. *RhoC* is also used by PS3 to place the

Num	Target	ThetaO	ThetaC	ThetaO-C	RhoO	RhoC	RhoO-C	ThetaF	RhoF	ApD	RelInt	DMag	Comm
24	00283+6344	111.831	91	20.831	0.3857	0.4	-0.0143	100.531	33.251	12	0.2216		
76	01036+6341	4.098	19	-14.902	0.2226	0.3	-0.0774	352.798	19.192	12	0.2312		
1	00022+2705	228.354	273	-44.646	0.166	0.8	-0.634	217.054	14.312	12	0.0571		Close one!
2	00024+1047	69.213	73	-3.787	0.2468	0.2	0.0468	57.913	21.273	12	0.0535		Prediction close.
3	00029+4715	294.729	295	-0.271	1.5947	1.6	-0.0053	283.429	137.47	12	0.155		Wide and easy. Prediction right on.
4	00046+4206	105.922	95	10.922	0.1304	0.1	0.0304	94.622	11.244	5	0.0486		Very close but good solution.
5	00055+3406	307.239	304	3.239	0.15	0.2	-0.05	295.939	12.933	5	0.0675		Also close. Prediction off a bit.
6	00073+0742	321.309	323	-1.691	0.3515	0.4	-0.0485	310.009	30.3	11	0.2919		Easy. 2nd & 3rd order images.
7	00085+3456	52.817	79	-26.183	0.1383	0.1	0.0383	41.517	11.922	5	0.1508		Close. Solution not stable.
13	00118+2825	67.367	69	-1.633	0.4474	0.5	-0.0526	56.067	38.571	11	0.1454		Easy. Prediction close.
14	00121+5337	317.605	313	4.605	0.3344	0.3	0.0344	306.305	28.827	11	0.1709		Very easy.
18	00174+0853	305.499	307	-1.501	0.1556	0.2	-0.0444	294.199	13.417	5	0.0411		Difficult. Not quite stable.
19	00174+0853	303.657	307	-3.343	0.1553	0.2	-0.0447	292.357	13.386	11	0.1254		Easy and stable.
20	00205+4531	96.724	102	-5.276	0.656	0.7	-0.044	85.424	56.553	11	0.0896		Verey easy. Clean!
21	00209+1059	118.746	117	1.746	0.7557	0.7	0.0557	107.446	65.145	11	0.1286		Very easy. Clean.
23	00251+4803	273.507	242	31.507	0.3186	0.3	0.0186	262.207	27.464	11	0.0335		Prediction off, but not too far.

Figure 27: The OutFile structure.

small red circle on the autocorrelogram where the secondary is expected.

RhoO The observed separation angle. This only has meaning when the user provides the plate scale (arc seconds per pixel), *E,* from some calibration external to the reduction. If not available, the user can enter any number and ignore the results, or enter a plate scale of "1" and the output will be the "uncorrected" frame pixel separation.

RhoO-C PS3 simply calculates this as *RhoO* minus *RhoC.* This is the difference between the observed position and the calculated (i.e. predicted or expected) separation; the classic O-C.

ThetaF Position Angle in the Frame. *ThetaF* is calculated by PS3, using simple trigonometry, from the centroid pixel locations.

RhoF Separation in the Frame. *RhoF* is calculated, using simple trigonometry, by PS3 from the centroid pixel locations.

ApD Aperture Diameter (radius in pixels).

RelInt This is the total (integrated) intensity of the companion divided by the integrated intensity of the primary. This will eventually be used to form an estimate of the differential magnitude of the double star.

DMag This will be calculated in a future version of the program. At this time the entry is blank.

Comm User comment added during reduction.

DSFN Double star (FITS cube) file name.

RSFN Reference star (FITS) cube file name.

AR Elongation Aspect Ratio (degrees).

AA Elongation Angle (degrees). The angle that corresponds to the elongation aspect ratio.

Delta Camera Angle (degrees). Camera orientation angle with respect to the sky.

E Plate scale (arc seconds/pixel).

GLP Lowpass Radius (pixels). Settings for Gaussian lowpass filter.

GLPen Lowpass used (True/False).

GHP Highpass Radius (pixels). Setting for Gaussian highpass filter.

GHPen Highpass used (True/False).

IFen Interference Filter used (True/False).

DCon *Deconvolution* Type: *None*=0, *Use Reference PSD*=1, *Subtract Symmetrized PSF=2*.

DConP *Deconvolution percent,* usually set at 100%.

LTPen *Lock to Peak* (True/False).

JPEGFN Filename of the solution image.

DaT Date and time output created.

10. Computer Requirements for STB and Obtaining a Free Copy

STB has been designed to run on a Windows only platform (Windows 7 or later) and requires a 64-bit processor. Since the processing of fits cubes can be a very intensive operation, obviously the faster your computer's chip, the better.

If you would like a free copy of STB, please send an email to the author and indicate in your message that you would like a copy of the program. I will reply to your email and attach a zip folder to my reply. The zip folder it will be named STB.ZZZ, the ZZZ file extension being a fictitious one that lets an attachment slip past email servers that automatically block ZIP files. Once you receive the file, save it to a folder on your computer (a name like STB would work well). Navigate to the new folder and rename the file from STB.ZZZ to STB.ZIP and then extract it. Be sure to let the extraction process extract all files to the same folder.

Once the extraction is complete, find the file named SpeckleToolBox.exe and send it to your desktop as a shortcut.

11. Conclusion

The Speckle Tool Box has proved to be a very powerful and easy to use analytical tool for doing speckle interferometry and highly precise measurement of the CCD images. Those who are currently engaged in CCD measurements of double stars may very well wish to investigate this program.

12. Acknowledgements

The authors wish to thank Brian Mason for his help in reviewing the manuscript for this paper and offering explanations and advice.

13. References

Mason, Brian D., Hartkopf, William I., Wycoff, Gary L., "Speckle Interferometry at the U. S. Naval Observatory, XIV", *AJ*, **136**, 2223-2226.

Rowe, David and Genet, Russ, "User's Guide to PS3 Speckle Interferometry Reduction Program", *JDSO*, **11**, 266-276, 2015.

Micrometer Measures of Double Stars

Niels Wieth-Knudsen[1]

Abstract: Micrometer measures of double stars made with his own 10 cm and 30 cm reflectors are presented.

Introduction

In late 2001, Inger Wieth-Knudsen made available to Charles Worley the original measurement cards of Dr. Nils Wieth-Knudsen containing the observations made towards the end of his career at his personal observatory (Figure 1). The original cards are cataloged in the James Melville Gillis Library of the U.S. Naval Observatory. The 471 measures recorded on these cards are grouped into 211 means of 59 systems, and include 33 measures of differential magnitude. Made with his 10 cm and 30 cm telescopes, they are now part of the inventory of the Wieth-Knudsen Observatory[2]. The observation dates range from 1961.32 to 1989.34 and the measured separations range from 0.6" to 28.97".

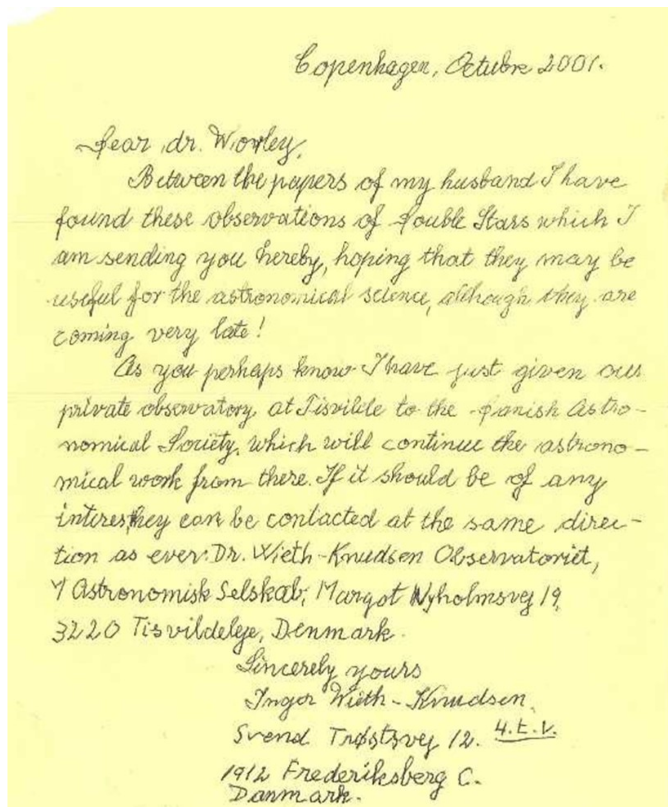

Copenhagen, Octubre 2001.

Dear dr. Worley,

Between the papers of my husband I have found these observations of Double Stars which I am sending you hereby, hoping that they may be useful for the astronomical science, although they are coming very late!

As you perhaps know I have just given our private observatory at Tisvilde to the Danish Astronomical Society, which will continue the astronomical work from there. If it should be of any interest they can be contacted at the same direction as ever: Dr. Wieth-Knudsen Observatoriet, Astronomisk Selskab, Margot Nyholmsvej 19, 3220 Tisvildeleje, Denmark.

Sincerely yours
Inger Wieth-Knudsen
Svend Trøstsvej 12. 4.t.v.
1912 Frederiksberg C.
Danmark.

Figure 1. Letter of Inger Wieth-Knudsen to Charles Worley.

Measures

Table 1 summarizes the measures of Niels Wieth-Knudsen from his prior publications and Table 2. The median separation and magnitude difference is provided as well as the aperture of the telescope and the years the measures were made for these data. Also, a brief description of the method of data collection is noted.

Table 2 presents these data. Included are the WDS and Discoverer Designations listing the systems observed in Columns 1 and 2. Columns 3 through 6 give the actual measures, epoch of observation, position angle (measured from north through east), separation (in seconds of arc), and V band magnitude difference (when provided). Column 7 gives the telescope aperture (in meters) while Column 8 gives the number of nights in the mean position. Column 9 gives any notes of the cataloger.

Compilation of the measurements and brief descrip-

(Continued on page 74)

[1]*Deceased: 14 April 1993*

[2]*WKO; see http://astronomisk.dk/wieth-knudsen-observatoriet/.*

Micrometer Measures of Double Stars

Table 1. Statistics of Samples

Dataset	Means	Measures	Separation Median (ρ)	Magnitude Difference Median (Δm)	Method	Aperture (m)	Years
1953	13	13	15.85"		1	0.2	1968-1975
1956a	51	51	1.47"	1.40	1	0.6	1973-1975
1956b	119	443	2.42"		2	0.3	1973-1975
1957	360	673		0.78	1	0.6	1951
Table 2	211	471	2.59"	1.20	3	0.1 & 0.3	1984-1990

Table Notes
1. photographic, with medium or long-focus technique
2. micrometer with refractor
3. micrometer with reflector

Table 2. Measurements of Double Stars

WDS Desig. α, δ (2000)	Discoverer Designation	Epoch 1900.+	θ (◦)	ρ ('')	Δm (V)	Tel. Aper. (m)	n	Note
00499+2743	STF 61	66.66	119.1	4.44		0.3	1	Q
01535+1918	STF 180 AB	66.99	1.3	7.68		0.3	1	
01535+1918	STF 180 AB	68.60	1.0	7.91		0.3	1	
01535+1918	STF 180 AB	69.70	1.8	7.66		0.3	1	
01535+1918	STF 180 AB	77.79	0.5	8.05		0.8	2	
02020+0246	STF 202 AB	68.76	288.0	2.14		0.3	1	
02020+0246	STF 202 AB	77.70	296.3	1.87		0.8	1	
02291+6724	STF 262 AB	79.90	238.3	1.95	1.67	0.8	1	
02592+2120	STF 333 AB	77.79	206.8	1.49		0.8	1	
07346+3153	STF 1110 AB	63.29	157.2	2.11		0.3	3	
07346+3153	STF 1110 AB	67.29	139.8	1.81		0.3	2	
07346+3153	STF 1110 AB	68.38	136.7	1.72		0.3	3	
07346+3153	STF 1110 AB	69.25	133.0	1.87		0.3	5	
07346+3153	STF 1110 AB	70.16	129.1	1.86		0.3	1	
07346+3153	STF 1110 AB	72.35	122.9	1.99		0.8	1	
07346+3153	STF 1110 AB	73.01	121.0	1.97		0.8	1	
07346+3153	STF 1110 AB	74.25	116.3	1.88		0.8	2	
07346+3153	STF 1110 AB	76.00	113.7	2.06	1.41	0.8	3	
07346+3153	STF 1110 AB	77.23	107.7	2.11	0.85	0.8	4	
07346+3153	STF 1110 AB	78.13	104.0	2.26	1.25	0.8	2	
07346+3153	STF 1110 AB	79.26	96.5	2.29	0.81	0.8	3	
07346+3153	STF 1110 AB	80.27	92.7	2.28	1.12	0.8	2	
07346+3153	STF 1110 AB	81.03	96.1	2.35		0.8	1	
07346+3153	STF 1110 AB	82.14	95.4	2.20		0.8	1	
07346+3153	STF 1110 AB	83.28	89.7	2.42		0.8	3	
07346+3153	STF 1110 AB	84.32	86.5	2.72		0.8	4	
08122+1739	STF 1196 AB	69.22	294.2	1.15		0.3	1	X
08508+3504	STF 1282	67.25	277.4	3.98		0.3	2	
09184+3522	STF 1333	67.25	46.3	2.01		0.3	1	
10200+1950	STF 1424 AB	67.35	120.8	4.51		0.3	2	
10200+1950	STF 1424 AB	69.26	121.0	4.43		0.3	2	
10200+1950	STF 1424 AB	74.22	120.7	4.50		0.8	1	
10200+1950	STF 1424 AB	77.29	121.8	4.03	1.09	0.8	1	
10200+1950	STF 1424 AB	89.34	123.4	4.52	1.15	0.8	2	
11182+3132	STF 1523 AB	74.27	116.4	3.29		0.8	1	
11182+3132	STF 1523 AB	84.32	90.7	2.46		0.8	4	
12043+2128	STF 1596	76.31	238.3	3.56	1.12	0.8	1	
12043+2128	STF 1596	89.33	245.3	3.34		0.8	1	
12417-0127	STF 1670 AB	63.34	307.6	4.76		0.3	2	

Table 2 continues on next page.

Micrometer Measures of Double Stars

Table 2 (continued). Measurements of Double Stars

WDS Desig. α, δ (2000)	Discoverer Designa-tion	Epoch 1900.+	θ (°)	ρ ('')	Δm (V)	Tel. Aper. (m)	n	Note
12417-0127	STF1670 AB	80.35	299.1	3.27		0.8	4	
12417-0127	STF1670 AB	85.39	292.2	3.08		0.8	4	
12492+8325	STF1694 AB	67.66	327.0	21.30		0.3	2	
13120+3205	STT261	74.37	341.8	2.40		0.8	5	
13120+3205	STT261	77.39	342.6	2.34		0.8	3	
13120+3205	STT261	80.36	343.6	2.43		0.8	1	
13120+3205	STT261	84.31	337.3	2.55		0.8	1	
13375+3618	STF1768 AB	73.40	105.8	1.83		0.8	1	
13375+3618	STF1768 AB	77.38	107.5	1.91	1.63	0.8	1	
14407+1625	STF1864 AB	62.44	107.8	5.86		0.3	4	
14407+1625	STF1864 AB	63.31	108.1	5.95		0.3	3	
14407+1625	STF1864 AB	73.41	107.2	7.32		0.8	1	X
14411+1344	STF1865 AB	73.41	303.4	1.34		0.8	2	
14411+1344	STF1865 AB	74.38	306.7	1.10		0.8	1	
14411+1344	STF1865 AB	77.37	309.0	1.11		0.8	4	
14411+1344	STF1865 AB	78.43	307.4	1.12		0.8	2	
14411+1344	STF1865 AB	80.40	309.3	1.13		0.8	2	
14450+2704	STF1877 AB	77.39	344.9	2.76	2.35	0.8	2	
14450+2704	STF1877 AB	78.41	344.6	2.68	2.50	0.8	4	
14450+2704	STF1877 AB	79.46	345.0	2.55	2.45	0.8	1	
14514+1906	STF1888 AB	76.39	335.1	7.67	2.23	0.8	1	
15038+4739	STF1909	73.40	355.2	0.53		0.8	1	
15038+4739	STF1909	75.43	11.8	0.73		0.8	4	
15038+4739	STF1909	76.48	18.3	0.85		0.8	4	
15038+4739	STF1909	77.39	20.1	0.87		0.8	2	
15038+4739	STF1909	78.42	26.7	0.99		0.8	4	
15038+4739	STF1909	82.42	31.4	1.40		0.8	3	
15038+4739	STF1909	85.39	38.3	1.43		0.8	2	
15038+4739	STF1909	88.45	46.0	1.61		0.8	1	
15075+0914	STF1910	77.41	211.8	4.15		0.8	1	
15232+3017	STF1937 AB	67.58	180.6	0.73		0.3	1	X
15232+3017	STF1937 AB	77.46	247.5	0.46		0.8	5	
15245+3723	STF1938 Ba,Bb	78.43	14.3	2.19		0.8	1	
15245+3723	STF1938 Ba,Bb	82.55	17.1	2.17		0.8	4	
15348+1032	STF1954 AB	67.40	177.9	4.01		0.3	2	
15348+1032	STF1954 AB	77.39	175.2	3.93	1.16	0.8	2	
15394+3638	STF1965	62.48	303.3	5.94		0.3	3	
15394+3638	STF1965	63.41	303.1	6.15		0.3	2	
15394+3638	STF1965	67.62	306.0	6.27		0.3	2	

Table 2 continues on next page.

Micrometer Measures of Double Stars

Table 2 (continued). Measurements of Double Stars

WDS Desig. α, δ (2000)	Discoverer Designation	Epoch 1900.+	θ (°)	ρ ('')	Δm (V)	Tel. Aper. (m)	n	Note
15394+3638	STF 1965	77.48	309.2	6.51	0.86	0.8	1	
16009+1316	STT 303 AB	77.48	163.4	1.34		0.8	1	
16009+1316	STT 303 AB	85.39	176.7	1.54		0.8	1	
16133+1332	STF 2021 AB	62.49	346.4	4.18		0.3	2	
16133+1332	STF 2021 AB	67.52	347.2	4.12		0.3	2	
16133+1332	STF 2021 AB	69.44	352.0	4.20		0.3	1	
16133+1332	STF 2021 AB	76.50	350.4	4.08		0.8	4	
16133+1332	STF 2021 AB	77.39	350.6	3.98		0.8	4	
16133+1332	STF 2021 AB	82.52	353.6	4.56		0.8	4	
16133+1332	STF 2021 AB	85.51	356.2	4.10		0.8	3	
16133+1332	STF 2021 AB	88.45	354.3	3.98		0.8	1	
16147+3352	STF 2032 AB	67.65	231.7	6.53		0.3	2	
16147+3352	STF 2032 AB	68.51	232.5	6.40		0.3	3	
16147+3352	STF 2032 AB	69.42	232.8	6.38		0.3	7	
16147+3352	STF 2032 AB	76.48	232.3	6.15	0.98	0.8	1	
16362+5255	STF 2078 AB	68.39	112.5	3.41		0.8	2	
16362+5255	STF 2078 AB	77.45	108.5	3.26		0.8	4	
16362+5255	STF 2078 AB	78.54	106.4	3.39	0.96	0.8	3	
17053+5428	STF 2130 AB	63.40	70.3	2.18		0.3	2	
17053+5428	STF 2130 AB	67.59	65.6	2.16		0.3	2	
17053+5428	STF 2130 AB	75.48	50.9	1.93		0.8	4	
17053+5428	STF 2130 AB	77.46	47.0	2.05		0.8	4	
17053+5428	STF 2130 AB	78.42	49.2	1.85		0.8	1	
17053+5428	STF 2130 AB	79.46	47.5	2.25		0.8	1	
17053+5428	STF 2130 AB	81.51	44.9	2.08		0.8	1	
17053+5428	STF 2130 AB	82.43	32.2	2.02		0.8	1	
17053+5428	STF 2130 AB	83.53	40.2	2.14		0.8	2	
17053+5428	STF 2130 AB	84.52	38.0	2.34		0.8	1	
17146+1423	STF 2140 AB	68.51	105.4	4.58		0.3	2	
17146+1423	STF 2140 AB	69.50	105.7	4.61		0.3	5	
17146+1423	STF 2140 AB	70.52	106.5	4.79		0.3	1	
17146+1423	STF 2140 AB	76.50	110.3	4.68	2.25	0.8	3	
17146+1423	STF 2140 AB	77.53	107.8	4.77	1.93	0.8	1	
17237+3709	STF 2161 AB	63.46	315.6	4.61		0.3	6	
17237+3709	STF 2161 AB	67.59	318.6	3.92		0.3	2	
17237+3709	STF 2161 AB	79.52	323.2	4.07	0.92	0.8	4	
17237+3709	STF 2161 AB	80.58	319.0	4.01	0.98	0.8	5	
17237+3709	STF 2161 AB	81.59	319.8	3.68		0.8	1	
17290+5052	STF 2180	77.53	262.4	3.13		0.8	4	

Table 2 continues on next page.

Micrometer Measures of Double Stars

Table 2 (continued). Measurements of Double Stars

WDS Desig. α, δ (2000)	Discoverer Designa-tion	Epoch 1900.+	θ (◦)	ρ ('')	Δm (V)	Tel. Aper. (m)	n	Note
17564+1820	STF2245 AB	82.57	294.7	2.62		0.8	4	
18002+8000	STF2308 AB	67.61	232.8	19.37		0.3	5	
18002+8000	STF2308 AB	68.35	232.4	19.17		0.3	5	
18015+2136	STF2264	68.60	259.1	6.46		0.3	2	
18031-0811	STF2262 AB	76.49	282.2	2.15		0.8	4	
18031-0811	STF2262 AB	79.57	278.2	1.91	0.44	0.8	1	
18031-0811	STF2262 AB	82.59	283.8	2.07		0.8	4	
18055+0230	STF2272 AB	63.48	86.3	3.89		0.3	2	
18239+5848	STF2323 AB	68.63	354.5	3.77		0.3	2	
18239+5848	STF2323 AB	75.51	0.8	3.79	2.50	0.8	1	
18239+5848	STF2323 AB	81.53	354.0	3.62	2.77	0.8	5	
18359+1659	STT358 AB	76.55	166.9	1.85		0.3	5	
18428+5938	STF2398 AB	61.32	162.6	12.92		0.3	1	
18428+5938	STF2398 AB	63.43	159.9	14.99		0.3	4	
18428+5938	STF2398 AB	66.91	162.5	15.41		0.3	2	
18428+5938	STF2398 AB	67.64	163.2	15.04		0.3	2	
18428+5938	STF2398 AB	68.45	165.0	14.20		0.3	1	
18428+5938	STF2398 AB	71.64	165.1	13.94		0.8	2	
18428+5938	STF2398 AB	74.48	167.0	14.35		0.8	2	
18428+5938	STF2398 AB	75.51	167.0	13.82		0.8	2	
18428+5938	STF2398 AB	76.50	168.1	13.87		0.8	1	
18428+5938	STF2398 AB	77.50	167.5	13.74		0.8	1	
18443+3940	STF2382 AB	66.66	1.4	2.78		0.3	1	
18443+3940	STF2382 AB	67.57	356.2	2.68		0.3	1	
18443+3940	STF2382 AB	68.59	2.2	2.81		0.3	2	
18443+3940	STF2382 AB	69.49	357.8	2.66		0.3	3	
18443+3940	STF2382 AB	73.58	357.8	2.49		0.8	1	
18443+3940	STF2382 AB	76.60	357.9	2.82	0.83	0.8	2	
18443+3940	STF2382 AB	77.56	359.0	2.87		0.8	2	
18443+3940	STF2382 AB	79.60	0.7	2.76	0.73	0.8	1	
18443+3940	STF2382 AB	80.60	356.3	2.62		0.8	5	
18443+3940	STF2382 AB	81.61	357.0	2.66		0.8	1	
18443+3940	STF2382 AB	82.58	357.7	2.72		0.8	3	
18443+3940	STF2382 AB	83.61	356.9	2.78		0.8	3	
18443+3940	STF2382 AB	84.52	359.4	2.67		0.8	1	
18443+3940	STF2383 CD	66.66	98.2	2.35		0.3	1	
18443+3940	STF2383 CD	67.57	100.2	2.42		0.3	1	
18443+3940	STF2383 CD	68.59	99.5	2.38		0.3	2	
18443+3940	STF2383 CD	69.49	97.9	2.34		0.3	3	

Table 2 concludes on next page.

Micrometer Measures of Double Stars

Table 2 (conclusion). Measurements of Double Stars

WDS Desig. α, δ (2000)	Discoverer Designa-tion	Epoch 1900.+	θ (◦)	ρ ('')	Δm (V)	Tel. Aper. (m)	n	Note
18443+3940	STF 2383 CD	76.60	97.2	2.12		0.8	2	
18443+3940	STF 2383 CD	77.56	92.8	2.07		0.8	2	
18443+3940	STF 2383 CD	80.60	91.5	2.21		0.8	7	
18443+3940	STF 2383 CD	81.60	90.1	2.19		0.8	2	
18443+3940	STF 2383 CD	82.58	90.6	2.27		0.8	3	
18443+3940	STF 2383 CD	83.61	90.0	2.24		0.8	3	
18443+3940	STF 2383 CD	84.52	90.3	2.09		0.8	1	
18455+0530	STF 2375 AB	68.45	119.4	2.44		0.3	1	
19450+4508	STF 2579 AB	72.62	244.0	2.86		0.8	5	X
19450+4508	STF 2579 AB	73.58	239.2	2.39		0.8	1	
19450+4508	STF 2579 AB	74.52	244.5	2.43	3.23	0.8	3	
19450+4508	STF 2579 AB	75.48	248.1	2.66	3.01	0.8	2	
19450+4508	STF 2579 AB	78.63	241.7	2.15	3.39	0.8	2	
19450+4508	STF 2579 AB	79.64	234.4	2.15	3.27	0.8	4	
19487+1149	STF 2583 AB	63.53	111.8	1.72		0.3	1	
19487+1149	STF 2583 AB	67.56	109.1	1.40		0.3	2	
19487+1149	STF 2583 AB	80.63	112.8	1.57		0.8	2	
19487+1149	STF 2583 AB	81.52	109.9	1.55		0.8	1	
19487+1149	STF 2583 AB	82.55	112.3	1.49		0.8	1	
20014+1045	STF 2613 AB	75.52	353.4	3.90		0.8	1	
20035+3601	STF 2624 AB	75.53	177.5	1.90		0.8	2	
20035+3601	STF 2624 AB	83.60	174.3	2.03		0.8	1	
20035+3601	STF 2624 AB	84.61	172.0	1.90		0.8	3	
20396+4035	STT 410 AB	82.73	9.5	0.98		0.8	1	
20467+1607	STF 2727	62.55	266.8	9.81		0.3	1	
20467+1607	STF 2727	63.55	268.5	9.69		0.3	2	
20467+1607	STF 2727	66.66	270.1	9.76		0.3	3	
20467+1607	STF 2727	67.56	268.6	9.83		0.3	2	
20467+1607	STF 2727	68.65	269.5	9.77		0.3	1	
20585+5028	STF 2741 AB	68.57	26.1	1.65		0.3	2	
20585+5028	STF 2741 AB	80.69	29.3	2.25		0.8	1	
20585+5028	STF 2741 AB	81.66	25.2	1.94		0.8	1	
20585+5028	STF 2741 AB	82.60	27.4	2.04		0.8	5	
20591+0418	STF 2737 AB,C	67.66	69.4	10.90		0.3	2	
21069+3845	STF 2758 AB	63.55	140.8	27.48		0.3	1	
21069+3845	STF 2758 AB	67.63	144.4	28.43		0.3	2	
21069+3845	STF 2758 AB	68.65	144.4	28.02		0.3	5	
21069+3845	STF 2758 AB	69.47	144.8	28.97		0.3	2	
21208+3227	STT 437 AB	75.61	24.6	2.14		0.8	1	

Micrometer Measures of Double Stars

(Continued from page 68)

tion prepared by Brian Mason. Additional information supplied by Michael Quaade (WKO).

References

Wieth-Knudsen, N. 1953a, *J. Obs*., **36**, 107.

Wieth-Knudsen, N. 1956a, *J. Obs.,* **39**, 193.

Wieth-Knudsen, N. 1956b, *J. Obs*., **39**, 201.

Wieth-Knudsen, N. 1957, *J. Obs*., **40**, 93.

STT Doubles with Large ΔM – Part VII: And Pisces Auriga

Wilfried R.A. Knapp
Vienna, Austria
wilfried.knapp@gmail.com

John Nanson
Star Splitters Double Star Blog
Manzanita, Oregon
jnanson@nehalemtel.net

Abstract: The results of visual double star observing sessions suggested a pattern for STT doubles with large ΔM of being harder to resolve than would be expected based on the WDS catalog data. It was felt this might be a problem with expectations on one hand, and on the other might be an indication of a need for new precise measurements, so we decided to take a closer look at a selected sample of STT doubles and do some research. Similar to the other objects covered so far several of the components show parameters quite different from the current WDS data.

1. Introduction

As follow up to our STT reports so far we continue in the constellations Andromeda, Pisces, and Auriga (see Table1.1). All values based on WDS data as of beginning of 2016.

With STT103 we have here again an object with a very bright primary making measurements difficult due to ADU values near CCD saturation.

2. Further Research

Following the procedure for the earlier parts of our report we concluded again that the best approach would be to check historical data on all objects, observe them visually with the target comparing with the existing data, and obtain as many images as possible suitable for photometry.

2.1 Historical Research and Catalog Comparisons

Several of the stars in this survey have notable aspects worth further investigation. Three main research sources were used for this section of this paper, the first of which was W.J. Hussey's *Micrometrical Observations of the Double Stars Discovered at Pulkowa*, published in 1901, which provided preliminary historical information on each of the stars. Hussey's book in-

Table 1. WDS Catalog Data at Beginning of 2016 for the Selected STT Objects

WDS ID	Name		RA	Dec	Sep	M1	M2	PA	Δ_M	Con
00439+3734	STT 19	AB	00:43:52.14	+37:33:38.0	9.7	8.54	11.40	115	2.86	And
01189+3958	STT 29	AB	01:18:53.15	+39:57:48.0	20.1	7.50	11.70	266	4.20	And
23486+3616	STT 506	AC	23:48:35.39	+36:16:28.4	21.1	7.37	10.80	80	3.43	And
00057+4549	STT 547	BP	00:05:41.00	+45:48:37.4	15.6	9.15	13.40	8	4.25	And
01256+3133	STT 30	AB	01:25:34.17	+31:33:01.9	4.6	8.09	11.80	245	3.71	Psc
01256+3133	STT 30	AD	01:25:34.17	+31:33:01.9	20.6	8.09	14.00	193	5.91	Psc
05074+5018	STT 94	AB	05:07:22.26	+50:18:20.2	17.9	7.44	11.10	305	3.66	Aur
05074+5018	STT 94	AC	05:07:22.26	+50:18:20.2	24.9	7.44	11.00	66	3.56	Aur
05091+4907	STT 96	AB	05:09:04.40	+49:07:18.8	20.6	6.67	11.10	105	4.43	Aur
05182+3322	STT 103	AB	05:18:10.56	+33:22:17.8	4.1	4.80	10.60	55	5.80	Aur
05232+4701	STT 104	AB	05:23:12.61	+47:01:17.9	7.1	4.80	11.10	190	4.00	Aur

STT Doubles with Large ΔM – Part VII: And Pisces Auriga

cludes his observations and measures of all the stars originally listed in Otto Wilhelm Struve's 1845 Pulkovo Catalog, as well as data beginning with the date of first measure and continuing through the following years up to 1900. That data, plus inclusion of the background for the Pulkovo Catalog, makes Hussey's book a valuable source of reference. Also consulted was S.W. Burnham's *A General Catalogue of Double Stars Within 121° of the North Pole, Part II*, for information on each of the three stars. In addition, Bill Hartkopf of the USNO graciously provided the text files for STT 30, STT 104, and STT 547.

Several of the stars in this survey were dropped from the second edition of Otto Struve's Pulkovo Catalogue (published in 1850) because the separations exceeded 16", which was the maximum catalog separation established for stars with companions fainter than ninth magnitude (Hussey, 1901, p. 16). The stars in this paper which were rejected are STT 29, STT 94, STT 96, and STT 506 AC. Fortunately, Hussey included all of the rejected stars in his 1901 book.

STT 30 (Psc). Hussey shows the first measures of the AB pair of STT 30 was made in 1843 by Otto Struve, although that measure is not listed in the WDS text file. Struve made two measures at that time (position angles of 227.8° and 234.6°, and separations of 4.39" and 4.53"), which are somewhat anomalous with the measures that have followed since. In general, the position angle of the AB pair has migrated from 238° (1869) to the most recent WDS reading of 244.8° (2004), and the separation has slowly increased from 4.3" to 4.6" over the same period.

Hussey (1901, p. 42) shows the AC pair was first measured by O. Struve in 1862 (105.0° and 56.98"), but the WDS text file shows Mädler preceded that with an 1843 measure (105.2° and 54"). The AC pair is remarkable for its lack of change since its discovery. There are a total of thirty-eight measures in the WDS for the pair, and there's very little difference between any of them. The most recent WDS (2011) measures are 105.7° and 56.78".

S.W. Burnham included a note on what is now the AD pair in his 1906 catalog entry on STT 30, although he didn't mention the year the observation was made (Burnham, 1906, Part II, p. 405). However the WDS text file shows he measured the pair in 1907 at 161.6° and 26.11", slightly different from his catalog estimate of 159° and 27". There's been a steady northward progression of the position angle and a narrowing of the separation since that time. The most recent WDS data goes back to 1998, which is 195.4° and 21.38". Those numbers are consistent with the change shown in the four measures in the years between 1907 and 1998, and

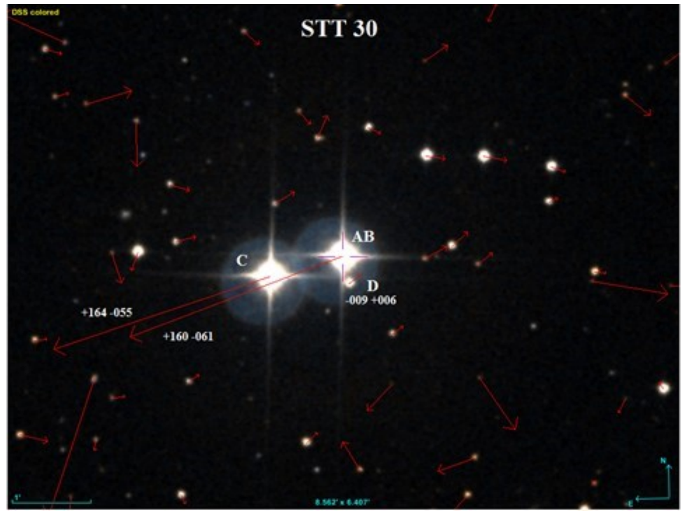

Figure 1. PM of STT 30 based on URAT1 data (Aladin image).

are caused by a high rate of proper motion for the AB pair (as well as C) in contrast to very little motion for D (Figure 1).

STT 94 (Aur). Hussey (1901, p. 65) shows Mädler was first with measures of both the AB and AC pairs. His 1843 measures for AB were 304.0° and 15.60"; for AC his measures were 63.3° and an estimated separation of 20". The most recent WDS measures (2011) are 305° and 17.9" for AB and 66° and 24.90" for AC. The AD pair was added in 1890 by S.W. Burnham (Figure 2). His measures were 340.9° and 26.1", and again little change is seen when compared with the most recent WDS measures (2002) of 344° and 26.3".

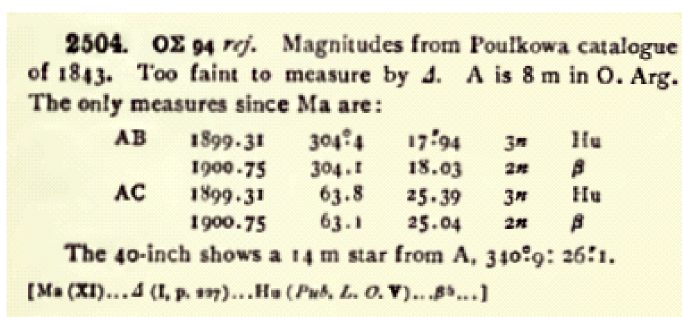

2504. OΣ 94 *rej.* Magnitudes from Poulkowa catalogue of 1843. Too faint to measure by Δ. A is 8 m in O. Arg. The only measures since Ma are:

AB	1899.31	304°.4	17".94	3n	Hu
	1900.75	304.1	18.03	2n	β
AC	1899.31	63.8	25.39	3n	Hu
	1900.75	63.1	25.04	2n	β

The 40-inch shows a 14 m star from A, 340°.9: 26".1.

[Ma (XI)... Δ (I, p. 197)...Hu (*Pub. L. O.* V)...β5...]

Figure 2. From Part II, p. 405, of Burnham's 1906 catalog.

STT 96 (Aur) Discovered in 1843 by Otto Struve, this is a difficult pair with a large ΔM between the primary and the secondary. The WDS shows magnitudes of 6.67 and 11.0 with a separation of 21.0" (PA 105°), which may explain why Otto Struve never provided a measure for it (Burnham, 1906, and Figure 3.).

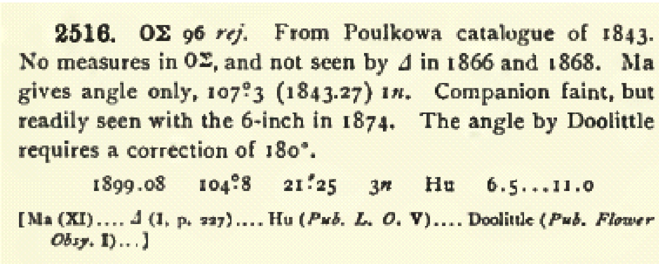

2516. OΣ 96 *rej.* From Poulkowa catalogue of 1843. No measures in OΣ, and not seen by Δ in 1866 and 1868. Ma gives angle only, 107°.3 (1843.27) 1*n*. Companion faint, but readily seen with the 6-inch in 1874. The angle by Doolittle requires a correction of 180°.

1899.08 104°.8 21″.25 3*n* Hu 6.5...11.0

[Ma (XI).... Δ (I, p. 227).... Hu (*Pub. L. O.* V).... Doolittle (*Pub. Flower Obsy.* I)...]

Figure 3. From p. 406 of Burnham's 1906 catalog, Part II.

Date	PA	Sep	Date	PA	Sep
1843.27	187.7		1911.55	190	18.42
1847.02	191.1	15.74	1911.895	190	18.12
1851.27	191.4	16.25	1958.18	189.8	19.62
1852.27	190.5		1996.918	189.1	20.74
1866.81	191.7	16.64	1999.78	189.4	20.73
1895.25	190.5	17.38	2002.846	189.9	20.579
1896.3	189.2	17.53	2007.655	190.15	21.092
1898.75	189.8	17.91	2011.29	189.2	20.87
1901.103	190.1	18.17	2012.938	189.8	21.18
1907.93	189	17.89	2014.85	190	21.4

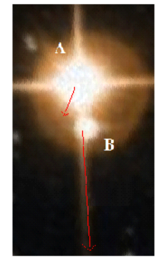

Figure 4. WDS text file data for STT 104 with Aladin image showing URAT1 proper motion arrows.

Burnham also mentions that Dembowski failed to see the secondary in 1866 and 1868. Both Burnham and Hussey (Hussey 1901, p. 65) include an 1843 observation by Mädler which lists a position angle (107.3°) but no separation. Hussey's three observations in 1898-1899 with the 36 inch Lick refractor average out to the numbers listed in Figure 2.2.3, 104.8° and 21.25". Our experience with this pair confirmed their visual difficulty.

STT 104 (Aur). This is another perplexing pair because it shows a surprising change in separation given the information available for it. As the data from the WDS text file in Figure 4 shows, the position angle has been remarkably consistent, while the separation has increased steadily. The most recent proper motion data from URAT1 for the pair shows the primary with a proper motion of +005.2 -013.5 and the secondary with proper motion of -003.6 -056, which give the secondary considerably more southerly motion than the primary. Simbad shows a distance for STT 104 A of 1929 light years, but no parallax for the secondary. Given the southerly motion in declination of the secondary relative to the primary, it's likely the fainter star is quite a bit closer to us than the primary, which would make this an optical pair

STT 547 (And). In his 1901 survey of Otto Struve's double stars, W.J. Hussey's first paragraph focused on a notable aspect of the AB pair of this multiple star: "Since discovery the angle has been increasing about three-fourths of a degree per year without appreciable change in distance. The angular motion is rapid for a binary of its distance and magnitudes" (Hussey, 1901, p. 215). With 398 observations of STT 547 AB in the WDS, that change has been documented in detail. A comparison of the first and last measurements clearly illustrates the dynamic nature of the pair, as well as confirming Hussey's description: 113.5° and 4.47" in 1876, and 189.30° and 6.030" in 2015. Our interest in STT 547 was primarily with the BP pair due to P's faint magnitude, but we quickly noticed the position angle of the pair in the Aladin photo didn't match the 2012 WDS position angle of 340° (Figure 2.2.5, top right). BP was added to the system in 1989, with an initial measure of 54.0° and 18.8", while the WDS 2012 data shows measures of 340° and 18.05". We were unable to find a date for the Aladin image, but it appears to have been made about 1989 since the positon angle in the photo is very close to 54°. As Figure 5 shows, P is virtually stationary (Simbad shows a proper motion of +000.1 +003.9 for P), while the AB pair is racing along at breakneck speed. Simbad's data shows identical proper motions for AB of +879 -154. Also shown in

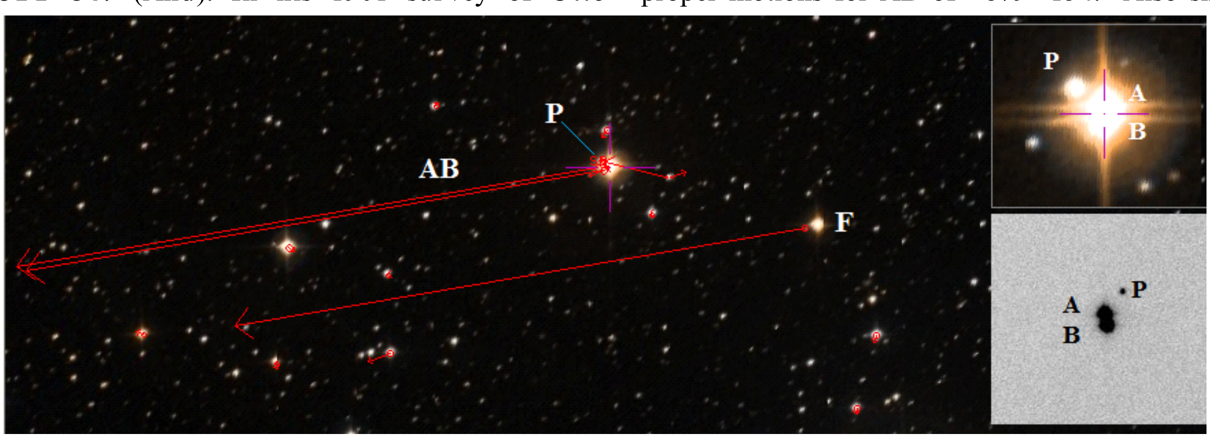

Figure 5. Aladin image with Simbad proper motion data shown for AB, F, and P. Inset at the right shows the change in the position angle of BP from about 1989 to our image taken late in 2015.

the image with a rapid pm is F, which Simbad lists at +870 -150.

2.2 Visual Observations

Both Nanson and Knapp made visual observations of the stars included in this report. John used a 152mm f/10 refractor, while Knapp utilized 140mm and 185mm refractors as well as a masking device to evaluate what could be seen at lesser apertures.

STT 19 (And): Knapp looked at STT 19 with a 140mm refractor and detected the secondary as a faint spot of light at 280x. It was still detectable with the aperture reduced to 110mm, suggesting the WDS magnitude of 11.40 is about right. John's observation with a six inch refractor at 152x found the secondary surprisingly difficult given the magnitude differential and separation. B appeared similar in brightness to a comparison star with a UCAC4 Vmag of 12.3, suggesting a fainter magnitude for B than the WDS value.

STT 29 (And): Nanson found several comparison stars for the secondary, all of which led to the conclusion the WDS magnitude of 11.7 is correct. Wilfried saw B as a faint spot of light in the 140mm refractor at 280x, which was still visible with the aperture reduced to 90mm, leading to the possibility the secondary is a bit brighter than the WDS magnitude.

STT 506 (And): Knapp's observation of STT 506 took place when it was low in altitude. At 280x in the 140mm refractor, C was faintly visible. With the aperture reduced to 60mm, it could still be seen, hinting it may be a bit brighter than the WDS magnitude of 10.80. At 84x in the six inch refractor, Nanson found C was similar in brightness to a comparison star with a UCAC4 Vmag of 11.9, suggesting a full magnitude of difference fainter than the WDS value.

STT 547 (And): The target for this complex multiple star was the BP pair, with WDS magnitudes of 9.15 and 13.40, separated by 18.10" per the WDS 2012 observation. In the six inch refractor at 152x, Nanson could see P with averted vision, indicating it may be as much as a full magnitude brighter than the WDS value, especially when the ninth magnitude glare of the AB pair is taken into consideration. Knapp was unable to resolve P in the 140mm refractor regardless of the magnification used, suggesting it's fainter than 13.0.

STT 94 (Aur): Knapp observed STT 94 with the 185mm refractor at 250x and was able to resolve B clearly and C only faintly. Using the masking device, the limit aperture for B was 140mm and for C 170mm, indicating the two components are fainter than the WDS magnitudes (11.10 for B, 11.0 for C), and also that C is fainter than B. John found both B and C were easily resolved in the six inch refractor at 152x, with B appearing a bit brighter than C. B appeared similar in magnitude to a comparison star with a UCAC4 Vmag of 11.9, suggesting that both B and C are fainter than the WDS values.

STT 96 (Aur): Using the six inch refractor, Nanson detected B at 152x, 190x, and 253x in the glare of the 6.7 magnitude primary. Given the 20.6" separation and the 11.1 magnitude for B currently listed in the WDS, it appears the WDS value for B is about right. On the first attempt, Knapp was unable to resolve B with the 185mm refractor under poor seeing conditions, which nevertheless hinted at a fainter magnitude for B than the WDS value. A second attempt resulted in faint resolution at 180x in the 185mm refractor. B could still be seen with the aperture reduced to 120mm at 250x, leading to the conclusion B is much fainter the WDS's 11.1 magnitude.

STT 103 (Aur): Knapp resolved B at 100x in the 185mm refractor, and could still see it with the aperture reduced to 140mm, suggesting the WDS magnitude of 10.6 is correct. Nanson needed magnifications of 487x and 607x in the six inch refractor in order to glimpse B, which led to the conclusion the WDS value for B is about right given the 4.1" separation and 5.8 magnitudes of difference between the primary and secondary.

STT 104 (Aur): Nanson resolved B at 152x in the six inch refractor and found it was similar in magnitude to a comparison star with a UCAC4 Vmag of 11.9, leading to the conclusion the WDS value of 11.1 is too bright. Knapp resolved B in the 185mm refractor at 100x and found it was still visible at 250x when the aperture was reduced to 90mm, suggesting the WDS value of 11.1 is correct.

STT 30 (Psc): Using the 140mm refractor at 280x, Knapp could detect a faint spot of light at the location of B for brief periods, suggesting it could be no brighter than the WDS value of 11.80. D, with a WDS magnitude of 14.0, was not seen. Nanson was able to detect B at 365x and 380x in the six inch refractor on two separate occasions, leading to the conclusion the WDS value for B is a likely a bit too bright. There was no hint of D, confirming Knapp's conclusion it's certainly fainter 13^{th} magnitude. Not part of the survey, but nevertheless still an interesting observation, was Nanson's conclusion that C (WDS magnitude of 8.06) was distinctly brighter than A (WDS magnitude of 8.09), which was confirmed during the course of observations on two separate nights at several magnifications.

2.3 Photometry and Astrometry Results

Several hundred images taken with iTelescope remote telescopes were in a first step plate solved and stacked with AAVSO VPhot. The stacked images were then plate solved with Astrometrica with URAT1 refer-

ence stars with Vmags in the range 10.5 to 14.5mag. The RA/Dec coordinates resulting from plate solving with URAT1 reference stars in the 10.5 to 14.5mag range were used to calculate Sep and PA using the formula provided by R. Buchheim (2008). *Err_Sep* is calculated as
with *dRA* and *dDec* as average RA and Dec plate solv-

$$Err\_Sep = \sqrt{dRA^2 + dDec^2}$$

ing errors. *Err_PA* is the error estimation for PA calculated as
in degrees assuming the worst case that *Err_Sep* points

$$Err\_PA = \arctan\left(\frac{Err\_Sep}{Sep}\right)$$

in the right angle to the direction of the separation means perpendicular to the separation vector. Mag is the photometry result based on UCAC4 reference stars with Vmags between 10.5 and 14.5mag. *Err_Mag* is calculated as
with *dVmag* as the average Vmag error over all used

$$Err\_Mag = \sqrt{dVmag^2 + \left[2.5\log_{10}\left(1 + 1/SNR\right)\right]^2}$$

reference stars and *SNR* is the signal to noise ratio for the given star. The results are shown in Table 2.

3. Summary

Tables 3 and 4 compare the final results of our research with the WDS data that was current at the time we began working on our current group of stars.

In Table 3 the results of our photometry have been averaged for each star. Because we're aware that both the NOMAD-1 and the UCAC4 catalogs are frequently consulted when making WDS evaluations of magnitudes changes, the data from those catalogs has also been included for each of the stars.

Red type has been used in Tables 3 and 4 to call attention to significant differences from the WDS data. With regard to Table 3, those magnitudes that differ by two tenths of a magnitude or more from the WDS values have been highlighted. In Table 4 differences in separation in excess of two-tenths of an arc second are highlighted, as are all position angles which differ by more than a degree.

Subsequent to our measures, as a quality check for our astrometry results we turned to the URAT1 catalog for the most recent precise professional measurements available. We used its coordinates to calculate the Sep and PA for all objects in this report for which URAT1 data was available and compared these values with our results, which are shown in Table 5.

Acknowledgements:

The following tools and resources have been used for this research:

- Washington Double Star Catalog as data source for the selected objects
- iTelescope: Images were taken with
    - iT24: 610mm CDK with 3962mm focal length. CCD: FLI-PL09000. Resolution 0.62 arcsec/pixel. V-filter. Located in Auberry, California. Elevation 1405m
    - iT11: 510mm CDK with 2280mm focal length. CCD: FLI ProLine PL11002M. Resolution 0.81 arcsec/pixel. B- and V-Filter. Located in Mayhill, New Mexico. Elevation 2225m
    - iT18: 318mm CDK with 2541mm focal length. CCD: SBIG-STXL-6303E. Resolution 0.73 arcsec/pixel. V-filter. Located in Nerpio, Spain. Elevation 1650m
    - iT21: 431mm CDK with 1940mm focal length. CCD: FLI-PL6303E. Resolution 0.96 arcsec/pixel. V-filter. Located in Mayhill, New Mexico. Elevation 2225m
- AAVSO VPhot for initial plate solving
- AAVSO APASS providing Vmags for faint reference stars (indirect via UCAC4)
- UCAC4 catalog (online via the University of Heidelberg website and Vizier and locally from USNO DVD) for counterchecks
- URAT1 catalog for high precision plate solving
- Aladin Sky Atlas v8.0 for counterchecks
- SIMBAD, VizieR for counterchecks
- 2MASS All Sky Catalog for counterchecks
- URAT1 Survey (preliminary) for counterchecks
- AstroPlanner v2.2 for object selection, session planning and for catalog based counterchecks
- MaxIm DL6 v6.08 for plate solving on base of the UCAC4 catalog
- Astrometrica v4.9.1.420 for astrometry and photometry measurements

(Continued on page 86)

STT Doubles with Large ΔM – Part VII: And Pisces Auriga

Table 2: Photometry and astrometry results for the selected STT objects. Date is the Bessel epoch and N is the number of images used for the reported values. iT in the Notes column indicates the telescope used with number of images and exposure time given (Specifications of the used telescopes: See Acknowledgements). The average results over all used images are given in the line below the individual stacks in bold. The error estimation over all used images is calculated as root mean square over the individual Err values. The N column in the summary line gives the total number of images used and Date the average Bessel epoch.

STT 19	RA	Dec	dRA	dDec	Sep	ErrSep	PA	Err PA	Mag	Err Mag	SNR	dVmag	Date	N	Notes
A	00 43 52.145	37 33 37.89	0.07	0.07	9.763	0.099	115.025	0.581	8.452	0.090	209.35	0.09	2015.785	5	1
B	00 43 52.889	37 33 33.76							11.437	0.092	54.01				
A	00 43 52.133	37 33 37.92	0.06	0.09	9.791	0.108	114.884	0.633	8.408	0.060	141.45	0.06	2015.807	5	1
B	00 43 52.880	37 33 33.80							11.438	0.065	41.93				
A	00 43 52.150	37 33 37.91	0.06	0.05	9.754	0.078	114.404	0.459	8.483	0.070	188.59	0.07	2015.774	5	2
B	00 43 52.897	37 33 33.88							11.500	0.071	80.33				
A	00 43 52.148	37 33 37.99	0.09	0.12	9.771	0.150	113.780	0.879	8.469	0.080	148.35	0.08	2015.779	5	2
B	00 43 52.900	37 33 34.05							11.504	0.083	46.69				
A	00 43 52.146	37 33 37.90	0.03	0.03	9.746	0.042	115.138	0.249	8.418	0.050	297.29	0.05	2015.782	5	2
B	00 43 52.888	37 33 33.76							11.410	0.051	98.11				
A	00 43 52.144	37 33 37.92	0.065	0.078	9.765	0.102	114.646	0.598	8.446	0.072			2015.785	25	3
B	00 43 52.891	37 33 33.85							11.458	0.074					
STT29	**RA**	**Dec**			**Sep**	**ErrSep**	**PA**	**ErrPA**	**Mag**	**ErrMag**	**SNR**	**DVmag**	**Date**	**N**	**Notes**
A	01 18 53.152	39 57 47.31	0.09	0.09	20.175	0.127	265.337	0.361	7.452	0.041	137.86	0.04	2015.779	5	1
B	01 18 51.403	39 57 45.67							11.838	0.051	34.46				
A	01 18 53.139	39 57 47.23	0.09	0.08	20.164	0.120	266.190	0.342	7.452	0.090	217.79	0.09	2015.785	5	1
B	01 18 51.389	39 57 45.89							11.808	0.093	42.51				
A	01 18 53.142	39 57 47.28	0.04	0.04	20.121	0.057	266.067	0.161	7.390	0.030	360.02	0.03	2015.774	5	2
B	01 18 51.396	39 57 45.90							11.762	0.033	82.82				
A	01 18 53.138	39 57 47.29	0.03	0.04	20.122	0.050	266.010	0.142	7.406	0.040	467.70	0.04	2015.782	5	2
B	01 18 51.392	39 57 45.89							11.768	0.042	87.00				
A	01 18 53.143	39 57 47.28	0.068	0.067	20.145	0.095	265.901	0.271	7.425	0.055			2015.780	20	3
B	01 18 51.395	39 57 45.84							11.794	0.059					
STT506	**RA**	**Dec**			**Sep**	**ErrSep**	**PA**	**ErrPA**	**Mag**	**ErrMag**	**SNR**	**DVmag**	**Date**	**N**	**Notes**
A	23 48 35.378	36 16 28.17	0.08	0.06	20.910	0.100	81.474	0.274	6.953	0.080	220.94	0.08	2015.785	5	1
C	23 48 37.088	36 16 31.27							11.002	0.082	60.81				
A	23 48 35.374	36 16 28.05	0.09	0.07	20.911	0.114	81.447	0.312	6.925	0.070	177.05	0.07	2015.807	5	1
C	23 48 37.084	36 16 31.16							10.986	0.073	56.161				
A	23 48 35.385	36 16 28.13	0.10	0.12	20.910	0.156	81.474	0.428	6.899	0.060	177.092	0.06	2015.779	5	1
C	23 48 37.095	36 16 31.23							10.962	0.063	54.572				
A	23 48 35.381	36 16 28.14	0.04	0.04	20.898	0.057	81.247	0.155	6.926	0.040	419.783	0.04	2015.774	5	2
C	23 48 37.089	36 16 31.32							10.994	0.041	113.77				
A	23 48 35.383	36 16 28.20	0.04	0.03	20.899	0.050	81.442	0.137	6.933	0.040	435.15	0.04	2015.782	5	2
C	23 48 37.092	36 16 31.31							10.973	0.041	120.27				
A	**23 48 35.380**	**36 16 28.14**	**0.074**	**0.071**	**20.906**	**0.103**	**81.417**	**0.282**	**6.927**	**0.060**			**2015.785**	**25**	**3**
C	23 48 37.090	36 16 31.26							10.983	0.062					

Table 2 continues on next page.

STT Doubles with Large ΔM – Part VII: And Pisces Auriga

Table 2 (continued). Photometry and astrometry results for the selected STT objects. Date is the Bessel epoch and N is the number of images used for the reported values. iT in the Notes column indicates the telescope used with number of images and exposure time given (Specifications of the used telescopes: See Acknowledgements). The average results over all used images are given in the line below the individual stacks in bold. The error estimation over all used images is calculated as root mean square over the individual Err values. The N column in the summary line gives the total number of images used and Date the average Bessel epoch.

STT 547	RA	Dec	dRA	dDec	Sep	ErrSep	PA	ErrPA	Mag	ErrMag	SNR	dVmag	Date	N	
A	00 05 42.367	45 48 41.00	0.06	0.07	5.944	0.092	188.395	0.889	8.959	0.090	142.65	0.09	2015.785	5	4
B	00 05 42.284	45 48 35.12							9.070	0.090	127.32				
A	00 05 42.378	45 48 41.26	0.11	0.11	6.200	0.156	189.219	1.437	8.958	0.072	57.76	0.07	2015.807	5	4
B	00 05 42.283	45 48 35.14							9.037	0.073	54.26				
A	00 05 42.362	45 48 41.02	0.03	0.03	6.043	0.042	188.257	0.402	8.947	0.040	227.49	0.04	2015.774	5	5
B	00 05 42.279	45 48 35.04							9.031	0.040	214.25				
A	00 05 42.356	45 48 41.11	0.08	0.09	6.126	0.120	187.058	1.126	8.959	0.071	121.68	0.07	2015.779	5	5
B	00 05 42.284	45 48 35.03							9.040	0.071	112.05				
A	00 05 42.363	45 48 41.11	0.06	0.06	6.112	0.085	188.163	0.795	8.931	0.050	201.98	0.05	2015.782	5	5
B	00 05 42.280	45 48 35.06							9.017	0.051	149.06				
A	00 05 42.365	45 48 41.10	0.073	0.077	6.085	0.106	188.220	0.998	8.951	0.067			2015.785	25	6
B	00 05 42.282	45 48 35.08							9.039	0.067					

STT 547	RA	Dec	dRA	dDec	Sep	ErrSep	PA	ErrPA	Mag	ErrMag	SNR	dVmag	Date	N	
B	00 05 42.284	45 48 35.12	0.06	0.07	19.704	0.092	332.643	0.268	9.070	0.090	127.32	0.09	2015.785	5	7
P	00 05 41.418	45 48 52.62							13.116	0.100	24.40				
B	00 05 42.283	45 48 35.14	0.11	0.11	19.951	0.156	333.212	0.447	9.037	0.073	54.26	0.07	2015.807	5	8
P	00 05 41.423	45 48 52.95							13.163	0.097	15.649				
B	00 05 42.279	45 48 35.04	0.03	0.03	19.681	0.042	333.156	0.124	9.031	0.040	214.259	0.04	2015.774	5	9
P	00 05 41.429	45 48 52.60							13.030	0.046	47.2910				
B	00 05 42.284	45 48 35.03	0.08	0.09	19.758	0.120	332.588	0.349	9.040	0.071	112.05	0.07	2015.779	5	9
P	00 05 41.414	45 48 52.57							13.087	0.086	21.17				
B	00 05 42.280	45 48 35.06	0.06	0.06	19.672	0.085	333.142	0.247	9.017	0.051	149.06	0.05	2015.782	5	9
P	00 05 41.430	45 48 52.61							13.036	0.056	43.71				
B	00 05 42.282	45 48 35.08	0.073	0.077	19.753	0.106	332.949	0.308	9.039	0.067			2015.785	25	10
P	00 05 41.423	45 48 52.67							13.086	0.080					

STT 30	RA	Dec	dRA	dDec	Sep	ErrSep	PA	ErrPA	Mag	ErrMag	SNR	dVmag	Date	N	
A	01 25 34.468	31 33 00.73	0.06	0.05	4.267	0.078	245.196	1.049	8.036	0.050	336.30	0.05	2015.782	1	11
B	01 25 34.165	31 32 58.94	0.06	0.05	4.267	0.078	245.196	1.049	11.540	0.053	57.36	0.05	2015.782	1	11
A	01 25 34.463	31 33 00.84	0.10	0.07	4.412	0.122	245.067	1.585	8.042	0.080	181.15	0.08	2015.785	5	12
B	01 25 34.150	31 32 58.98	0.10	0.07	4.412	0.122	245.067	1.585	11.567	0.111	13.72	0.08	2015.785	5	12
A	01 25 34.466	31 33 00.73	0.02	0.04	4.521	0.045	245.567	0.567	8.023	0.040	357.32	0.04	2015.774	5	13
B	01 25 34.144	31 32 58.86	0.02	0.04	4.521	0.045	245.567	0.567	11.599	0.051	34.32	0.04	2015.774	5	13
A	01 25 34.471	31 33 00.68	0.07	0.11	4.245	0.130	244.611	1.759	8.015	0.070	193.11	0.07	2015.779	5	13
B	01 25 34.171	31 32 58.86	0.07	0.11	4.245	0.130	244.611	1.759	11.341	0.076	34.71	0.07	2015.779	5	13
A	01 25 34.467	31 33 00.75	0.069	0.073	4.361	0.100	245.117	1.314	8.029	0.062			2015.780	16	14
B	01 25 34.157	31 32 58.91	0.069	0.073	4.361	0.100	245.117	1.314	11.512	0.077			2015.780	16	14

Table 2 continues on next page.

STT Doubles with Large ΔM – Part VII: And Pisces Auriga

Table 2 (continued). Photometry and astrometry results for the selected STT objects. Date is the Bessel epoch and N is the number of images used for the reported values. iT in the Notes column indicates the telescope used with number of images and exposure time given (Specifications of the used telescopes: See Acknowledgements). The average results over all used images are given in the line below the individual stacks in bold. The error estimation over all used images is calculated as root mean square over the individual Err values. The N column in the summary line gives the total number of images used and Date the average Bessel epoch.

STT 30	RA	Dec	dRA	dDec	Sep	ErrSep	PA	ErrPA	Mag	ErrMag	SNR	dVmag	Date	N	Notes
A	01 25 34.468	31 33 00.73	0.06	0.05	56.689	0.078	105.668	0.079	8.036	0.050	336.30	0.05	2015.782	1	15
C	01 25 38.738	31 32 45.42							8.010	0.050	373.63				
A	01 25 34.463	31 33 00.84	0.10	0.07	56.518	0.122	105.675	0.124	8.042	0.080	181.15	0.08	2015.785	5	16
C	01 25 38.720	31 32 45.57							8.004	0.080	179.40				
A	01 25 34.466	31 33 00.73	0.02	0.04	56.707	0.045	105.684	0.045	8.023	0.040	357.32	0.04	2015.774	5	17
C	01 25 38.737	31 32 45.40							7.998	0.040	393.43				
A	01 25 34.471	31 33 00.68	0.07	0.11	56.681	0.130	105.639	0.132	8.015	0.070	193.11	0.07	2015.779	5	17
C	01 25 38.741	31 32 45.40							7.993	0.070	212.13				
A	01 25 34.467	31 33 00.75	0.069	0.073	56.648	0.100	105.667	0.101	8.029	0.062			2015.780	16	18
C	01 25 38.734	31 32 45.45							8.001	0.062					
STT 30	**RA**	**Dec**	**dRA**	**dDec**	**Sep**	**ErrSep**	**PA**	**ErrPA**	**Mag**	**ErrMag**	**SNR**	**dVmag**	**Date**	**N**	**Notes**
A	01 25 34.468	31 33 00.73	0.06	0.05	21.421	0.078	203.865	0.209	8.036	0.050	336.30	0.05	2015.782	1	19
D	01 25 33.790	31 32 41.14							14.207	0.076	18.37				
A	01 25 34.463	31 33 00.84	0.10	0.07	21.535	0.122	202.400	0.325	8.042	0.080	181.15	0.08	2015.785	5	20
D	01 25 33.821	31 32 40.93							14.567	0.162	7.20				
A	01 25 34.466	31 33 00.73	0.02	0.04	21.241	0.045	203.967	0.121	8.023	0.040	357.32	0.04	2015.774	5	21
D	01 25 33.791	31 32 41.32							14.360	0.059	24.28				
A	01 25 34.471	31 33 00.68	0.07	0.11	21.279	0.130	203.997	0.351	8.015	0.070	193.11	0.07	2015.779	5	22
D	01 25 33.794	31 32 41.24							14.247	0.134	8.97				
A	01 25 34.467	31 33 00.75	0.069	0.073	21.368	0.100	203.554	0.268	8.029	0.062			2015.780	16	23
D	01 25 33.799	31 32 41.16							14.345	0.116					
STT 94	**RA**	**Dec**	**dRA**	**dDec**	**Sep**	**ErrSep**	**PA**	**ErrPA**	**Mag**	**ErrMag**	**SNR**	**dVmag**	**Date**	**N**	**Notes**
A	05 07 22.261	50 18 20.27	0.09	0.07	17.889	0.114	305.192	0.365	7.359	0.070	153.76	0.07	2016.093	5	24
B	05 07 20.735	50 18 30.58							11.640	0.089	19.52				
A	05 07 22.267	50 18 20.25	0.05	0.07	17.887	0.086	305.394	0.276	7.375	0.090	197.24	0.09	2016.107	5	25
B	05 07 20.745	50 18 30.61							11.636	0.101	23.37				
A	05 07 22.287	50 18 19.44	0.12	0.10	18.006	0.156	304.815	0.497	7.373	0.123	40.17	0.12	2016.108	5	26
B	05 07 20.744	50 18 29.72							11.552	0.125	30.85				
A	05 07 22.269	50 18 19.88	0.10	0.12	17.988	0.156	304.894	0.498	7.255	0.110	190.96	0.11	2016.119	5	26
B	05 07 20.729	50 18 30.17							11.434	0.111	63.99				
A	05 07 22.271	50 18 19.96	0.094	0.092	17.942	0.132	305.073	0.420	7.341	0.100			2016.107	20	3
B	05 07 20.738	50 18 30.27							11.566	0.107					
STT 94	**RA**	**Dec**	**dRA**	**dDec**	**Sep**	**ErrSep**	**PA**	**ErrPA**	**Mag**	**ErrMag**	**SNR**	**dVmag**	**Date**	**N**	**Notes**
A	05 07 22.261	50 18 20.27	0.09	0.07	25.403	0.114	65.931	0.257	7.359	0.070	153.76	0.07	2016.093	5	27
C	05 07 24.682	50 18 30.63							12.121	0.099	14.95				
A	05 07 22.267	50 18 20.25	0.05	0.07	25.354	0.086	65.858	0.194	7.375	0.090	197.24	0.09	2016.107	5	27
C	05 07 24.682	50 18 30.62							12.288	0.122	12.61				
A	05 07 22.287	50 18 19.44	0.12	0.10	25.396	0.156	65.081	0.352	7.373	0.123	40.17	0.12	2016.108	5	28
C	05 07 24.691	50 18 30.14							12.012	0.127	24.71				
A	05 07 22.269	50 18 19.88	0.10	0.12	25.291	0.156	66.017	0.354	7.255	0.110	190.96	0.11	2016.119	5	28
C	05 07 24.681	50 18 30.16							12.035	0.113	44.52				
A	05 07 22.271	50 18 19.96	0.094	0.092	25.360	0.132	65.722	0.297	7.341	0.100			2016.107	20	3
C	05 07 24.684	50 18 30.39							12.114	0.116					

Table 2 concludes on next page.

STT Doubles with Large ΔM – Part VII: And Pisces Auriga

Table 2 (conclusion). Photometry and astrometry results for the selected STT objects. Date is the Bessel epoch and N is the number of images used for the reported values. iT in the Notes column indicates the telescope used with number of images and exposure time given (Specifications of the used telescopes: See Acknowledgements). The average results over all used images are given in the line below the individual stacks in bold. The error estimation over all used images is calculated as root mean square over the individual Err values. The N column in the summary line gives the total number of images used and Date the average Bessel epoch.

STT 96	RA	Dec	dRA	dDec	Sep	ErrSep	PA	ErrPA	Mag	ErrMag	SNR	dVmag	Date	N	Notes
A	05 09 04.370	49 07 19.02	0.07	0.08	20.727	0.106	105.044	0.294	6.572	0.110	229.24	0.11	2016.093	4	29
B	05 09 06.409	49 07 13.64							12.043	0.128	15.96				
A	05 09 04.363	49 07 18.95	0.08	0.06	20.688	0.100	104.959	0.277	6.593	0.100	261.81	0.10	2016.107	5	30
B	05 09 06.399	49 07 13.61							12.142	0.131	12.29				
A	05 09 04.405	49 07 18.15	0.12	0.12	20.385	0.170	104.431	0.477	6.640	0.121	60.25	0.12	2016.108	5	31
B	05 09 06.416	49 07 13.07							12.143	0.127	25.26				
A	05 09 04.383	49 07 18.73	0.10	0.12	20.542	0.156	104.490	0.436	6.538	0.070	186.00	0.07	2016.119	5	31
B	05 09 06.409	49 07 13.59							12.209	0.073	48.83				
A	05 09 04.380	49 07 18.71	0.094	0.098	20.585	0.136	104.733	0.380	6.586	0.102			2016.107	19	3
B	05 09 06.408	49 07 13.48							12.134	0.118					
STT 103	**RA**	**Dec**	**dRA**	**dDec**	**Sep**	**ErrSep**	**PA**	**ErrPA**	**Mag**	**ErrMag**	**SNR**	**dVmag**	**Date**	**N**	**Notes**
A	05 18 10.599	33 22 15.11	0.10	0.12	3.929	0.156	56.994	2.277	4.573	0.100	416.07	0.10	2016.107	5	32
B	05 18 10.862	33 22 17.25							9.831	0.118	16.88				
A	05 18 10.599	33 22 14.94	0.11	0.12	3.603	0.163	53.762	2.587	4.552	0.120	340.72	0.12	2016.093	1	33
B	05 18 10.831	33 22 17.07							9.497	0.142	13.73				
A	05 18 10.599	33 22 15.02	0.105	0.120	3.764	0.160	55.448	2.427	4.563	0.110			2016.100	6	34
B	05 18 10.847	33 22 17.16							9.664	0.131					
STT 104	**RA**	**Dec**	**dRA**	**dDec**	**Sep**	**ErrSep**	**PA**	**ErrPA**	**Mag**	**ErrMag**	**SNR**	**dVmag**	**Date**	**N**	
A	05 23 12.642	47 01 17.59	0.11	0.09	21.371	0.142	189.307	0.381	6.849	0.110	204.77	0.11	2016.093	3	35
B	05 23 12.304	47 00 56.50							11.730	0.123	19.15				
A	05 23 12.644	47 01 17.55	0.07	0.06	21.427	0.092	189.227	0.247	6.837	0.090	227.72	0.09	2016.107	5	36
B	05 23 12.308	47 00 56.40							11.723	0.105	19.64				
A	05 23 12.666	47 01 17.29	0.12	0.08	21.325	0.144	189.857	0.387	6.644	0.071	80.81	0.07	2016.108	5	37
B	05 23 12.309	47 00 56.28							11.637	0.075	38.85				
A	05 23 12.647	47 01 17.44	0.10	0.11	21.195	0.149	189.077	0.402	6.721	0.070	210.90	0.07	2016.119	5	37
B	05 23 12.320	47 00 56.51							11.720	0.072	62.61				
A	05 23 12.650	47 01 17.47	0.102	0.087	21.329	0.134	189.367	0.359	6.763	0.087			2016.107	18	3
B	05 23 12.310	47 00 56.42							11.703	0.096					

Notes to Table 2

1. iT24 stack 5x1s. A too bright for reliable photometry
2. iT24 stack 5x3s. A too bright for reliable photometry
3. A too bright for reliable photometry
4. iT24 stack 5x1s. A and B too bright for reliable photometry
5. iT24 stack 5x3s. A and B too bright for reliable photometry
6. A and B too bright for reliable photometry
7. iT24 stack 5x1s. B too bright for reliable photometry
8. iT24 stack 5x1s. B too bright for reliable photometry. SNR P <20
9. iT24 stack 5x3s. B too bright for reliable photometry
10. B too bright for reliable photometry
11. iT24 1x3s. A too bright for reliable photometry. Touching star disks
12. iT24 stack 5x1s. A too bright for reliable photometry. Overlapping star disks. SNR B <20
13. iT24 stack 5x3s. A too bright for reliable photometry. Overlapping star disks
14. A too bright for reliable photometry
15. iT24 1x3s. A and B too bright for reliable photometry
16. iT24 stack 5x1s. A and C too bright for reliable photometry
17. iT24 stack 5x3s. A and C too bright for reliable photometry
18. A and C too bright for reliable photometry
19. iT24 1x3s. A too bright for reliable photometry. SNR D<20
20. iT24 stack 5x1s. A too bright for reliable photometry. SNR D<10
21. iT24 stack 5x3s. A too bright for reliable photometry
22. iT24 stack 5x3s. A too bright for reliable photometry. SNR D<10
23. A too bright for reliable photometry. SNR D<20
24. iT18 stack 5x3s. A too bright for reliable photometry. SNR B<20
25. iT18 stack 5x3s. A too bright for reliable photometry
26. iT24 stack 5x3s. Image quality rather low. A too bright for reliable photometry
27. iT18 stack 5x3s. A too bright for reliable photometry. SNR C<20
28. iT24 stack 5x3s. Image quality rather low. A too bright for reliable photometry
29. iT18 stack 4x3s. A too bright for reliable photometry. SNR B<20
30. iT18 stack 5x3s. A too bright for reliable photometry. SNR B<20
31. iT24 stack 5x3s. Image quality rather low. A too bright for reliable photometry
32. iT18 stack 5x1s. Heavily overlapping star disks. SNR B<20
33. iT18 1x1s. Heavily overlapping star disks. SNR B<20
34. A and B too bright for reliable photometry. A too bright for reliable astrometry
35. iT18 stack 3x3s. A too bright for reliable photometry. SNR B<20
36. iT18 stack 5x3s. A too bright for reliable photometry. SNR B<20
37. iT24 stack 5x3s. A too bright for reliable photometry
38. iT24 stack 5x3s. A too bright for reliable photometry

STT Doubles with Large ΔM – Part VII: And Pisces Auriga

Table 3. Photometry and Visual Results Compared to WDS

	WDS Mag	NOMAD-1 VMag	UCAC4 VMa	UCAC4 f. mag	Average of Photometry Measures	Results of Visual Observations
STT 19 B	11.40	-	-	11.247	11.458	One observation that WDS magnitude is about right and one suggesting as faint as 12.3
STT 29 B	11.70	11.570	-	11.746	11.794	One observation suggesting WDS magnitude is correct and one suggesting a bit brighter
STT 506 C	10.80	10.830	-	10.969	10.983	One observation suggesting C to be a bit brighter than WDS value, one suggesting a magnitude of about 11.9
STT 547 B	9.15	-	9.096	-	9.039	No estimations made of magnitude
STT 547 P	13.40	-	-	13.134	13.086	One observation that P is brighter than WDS value, one that B is fainter than 13.0
STT 30 B	11.80	12.864	-	-	11.512	One observation suggesting B could be no brighter than the WDS value,one observation suggesting the WDS value is a bit too bright.
STT 30 C	8.06	7.986	8.923	8.715	8.001	Two observations that C is brigher than A (WDS magnitude of 8.09)
STT 30 D	14.00	15.730	-	14.376	14.345	Not seen by either of the two observers
STT 94 B	11.10	-	-	11.367	11.566	Two observations that B is fainter than the WDS value
STT 94 C	11.00	12.310	-	11.702	12.114	Two observations that C is fainter than B
STT 96 B	11.10	-	-	11.978	12.134	One observation that the WDS value for B is about right based on visual difficulty, one that B is much fainter than the WDS value
STT 103 B	10.60	-	-	-	9.664	Two observations that the WDS value for B is about right 1)
STT 104 B	11.10	9.070	-	11.879	11.703	One observation suggesting a magnitude of about 11.9 for B, one observation that the WDS value is about right

Table 4. Astrometry Results Compared to WDS

	WDS Coordinates	WDS Sep	WDS PA	Astrometry Coordinates	Astrometry Sep	Astrometry PA
STT 19 AB	00:43:52.14 +37:33:38.0	9.70	115	00 43 52.144 +37 33 37.92	9.765	114.646
STT 29 AB	01:18:53.15 +39:57:48.0	20.10	266	01 18 53.143 +39 57 47.28	20.145	265.901
STT 506 AC	23:48:35.39 +36:16:28.4	21.10	80	23 48 35.380 +36 16 28.14	20.906	81.417
STT 547 AB	00:05:41.00 +45:48:37.4	6.0	187	00 05 42.365 +45 48 41.10	6.085	188.220
STT 547 BP	00:05:41.00 +45:48:37.4	18.10	340	00 05 42.365 +45 48 41.10	19.753	332.949
STT 30 AB	01:25:34.17 +31:33:01.9	4.60	245	01 25 34.467 +31 33 00.75	4.361	245.117
STT 30 AC	01:25:34.17 +31:33:01.9	57.20	106	01 25 34.467 +31 33 00.75	56.648	105.667
STT 30 AD	01:25:34.17 +31:33:01.9	21.40	195	01 25 34.467 +31 33 00.75	21.368	203.554
STT 94 AB	05:07:22.26 +50:18:20.2	17.90	305	05 07 22.271 +50 18 19.96	17.942	305.073
STT 94 AC	05:07:22.26 +50:18:20.2	24.90	66	05 07 22.271 +50 18 19.96	25.360	65.722
STT 96 AB	05:09:04.40 +49:07:18.8	20.60	105	05 09 04.380 +49 07 18.71	20.585	104.733
STT 103 AB *1)*	05:18:10.56 +33:22:17.8	4.10	55	05 18 10.599 +33 22 15.02	3.764	55.448
STT 104 AB	05:23:12.61 +47:01:17.9	21.40	190	05 23 12.650 +47 01 17.47	21.329	189.367

1) These results have to be taken with caution due to photometry and astrometry issues with the too bright primary (CCD saturation and overlapping star disks.

STT Doubles with Large ΔM – Part VII: And Pisces Auriga

Table 3.3: Astrometry Results Compared with URAT1 Coordinates

Object	URAT1 Sep	iTelescope Sep	Err Sep	Within Error Range?	URAT1 PA	iTelescope PA	Err PA	Within Error Range?
STT 19 AB	9.771	9.765	0.102	Yes	115.116	114.646	0.598	Yes
STT 29 AB	20.134	20.145	0.095	Yes	266.040	265.901	0.271	Yes
STT 506 AC	20.794	20.906	0.103	No	81.410	81.417	0.282	Yes
STT 547 AB	6.046	6.085	0.106	Yes	187.231	188.220	0.998	Yes
STT 547 BP 1)	18.752	19.753	0.106	No	337.258	332.949	0.308	No
STT 30 AC 2)	56.754	56.648	0.100	No	105.642	105.667	0.101	Yes
STT 30 AD 2)	21.261	21.368	0.100	No	203.050	203.554	0.268	No
STT 94 AB	17.883	17.942	0.132	Yes	305.126	305.073	0.420	Yes
STT 94 AC	25.357	25.360	0.132	Yes	65.729	65.722	0.297	Yes
STT 96 AB	20.757	20.580	0.136	No	104.970	104.733	0.380	Yes
STT 104 AB	21.328	21.329	0.134	Yes	189.508	189.367	0.359	Yes

1) “Negative” quality control result due to the high proper motion of STT 547 B; the given values for separation and PA of STT 547 BP should be quite correct for the given observation date.

2) “Negative” quality control result probably also due to the high proper motion of most but not all components of STT 30

(Continued from page 79)

References

Buchheim, Robert, 2008, "CCD Double-Star Measurements at Altimira Observatory in 2007", *Journal of Double Star Observations*, **4**, 27-31. Formulas for calculating Separation and Position Angle from the RA Dec coordinates given as

$$sep = \sqrt{\left[\left(RA_2 - RA_1\right)\cos\left(Dec_1\right)\right]^2 + \left(Dec_2 - Dec_1\right)^2}$$

in radians and .

$$PA = \arctan\left(\frac{RA_2 - RA_1 \cos(Dec_1)}{Dec_2 - Dec_1}\right)$$

in radians depending on quadrant

Burnham, S.W., 1874, "A Fifth Catalogue of 71 New Double Stars", *Monthly Notices of the Royal Astronomical Society*, **35**, 31-48. (ADS bibliographic codes 1874MNRAS..35...31B and 1874MNRAS..35...40).

Burnham, S.W. 1906, *A General Catalogue of Double Stars Within 120° of the North Pole, Part II*, University of Chicago Press, Chicago.

Greaney, Michael, 2012, "Some Useful Formulae" in R.W. Argyle, *Observing and Measuring Visual Double Stars, 2nd Edition*, p 359, Springer Press, New York.

Hussey, W.J., 1901, *Micrometrical Observations of the Double Stars Discovered at Pulkowa Made with the Thirty-Six-Inch and Twelve-Inch Refractors of Lick Observatory*, pp. 14 - 16, A.J. Johnston, Sacramento.

Knapp, Wilfried; Nanson, John; Smith, Steven, 2015, "STT Doubles with Large Δ M – Part I: Gem", *Journal of Double Star Observations*, **11**, 390-401.

Knapp, Wilfried; Nanson, John; Smith, Steven, 2016, "STT Doubles with Large Δ M – Part II: Leo and Uma", *Journal of Double Star Observations*, **12**, 110-126.

Knapp, Wilfried; Nanson, John, 2016, "STT Doubles with Large Δ M - Part III: Vir, Ser, CrB, Com and Boo", *Journal of Double Star Observations*, **12**, 127 -141.

Knapp, Wilfried; Nanson, John, 2016, "STT Doubles with Large ΔM – Part IV: Oph and Her", *Journal of Double Star Observations*, **12**, 361-373.

Knapp, Wilfried; Nanson, John, 2016, "STT Doubles with Large Δ M – Part V: Aql, Del, Cyg and Aqr", *Journal of Double Star Observations*, **12**, 474 - 484.

Knapp, Wilfried; Nanson, John, 2016, "STT Doubles with Large Δ M – Part VI: Cyg Multiples", *Journal*

Counter-Checking Tycho Double Stars with the SDSS DR9 Catalog

Wilfried R.A. Knapp
Vienna, Austria
wilfried.knapp@gmail.com

Abstract: As already reported (Knapp and Gould 2016), most Tycho Double Star objects in the WDS catalog are unconfirmed. Small separation and faint components make these objects hard to resolve either by visual observation or by imaging in the V-band and only few public domain star catalogs offer resolution for stars with less than 2-3 arcseconds. One exception is the SDSS DR9 catalog based on images with a resolution of 0.396 arcseconds per pixel. This report shows that SDSS DR9 is of good use for counter-checking double stars down to a separation of 1.5 arcseconds or even less.

Introduction

Looking for star catalogs reliable enough to deliver star coordinates suitable for proper motion calculations, I found in many cases SDSS DR9 of good use besides 2MASS and URAT1, especially for smaller separations. The SDSS DR9 catalog should, from the technical parameters, be suitable for resolving faint double stars with separations less than 2 arcseconds - keeping in mind that the SDSS covers only a part of the sky. To check this possibility, I selected Tycho Double Stars in Boötes (Boo) and Canes Venatici (CVn) (both constellations are covered by SDSS) with separation larger than 1.5 arcseconds, confirmed and unconfirmed ones, to check both situations to see how reliable this setup might be.

Further Research

First I selected the objects in CVn and checked SDSS images and SDSS DR9 catalog data for these objects. The results are shown in Table 1. Next I selected the following objects in Boo and checked SDSS images and SDSS DR9 catalog data for these objects. The results are shown in Table 2.

Summary

These results show the reliability of SDSS DR9 data to counter-check Tycho Double Stars down to separation of 1.5 arcseconds provided that SDSS covers the sky region in question. A quick check for TDS9213 in Boo (WDS confirmed with 1.4" separation) indicated that SDSS DR9 is probably also reliable for separations somewhat smaller than 1.5".

Potential Further Research

Boo and CVn are only a small portion of the sky covered by SDSS DR9. This offers the opportunity to counter-check hundreds of more Tycho Double Stars so far unconfirmed.

Acknowledgements

The following tools and resources have been used for this research:

Washington Double Star Catalog as data source for the selected objects

Aladin Sky Atlas v9.0

SIMBAD, VizieR

SDSS Photometric Catalog, Release 9

2MASS All Sky Catalog

URAT1 Survey (preliminary)

AstroPlanner v2.2 for object selection

Counter-Checking Tycho Double Stars with the SDSS DR9 Catalog

References

R. Buchheim, 2008, "CCD Double-Star Measurements at Altimira Observatory in 2007", *Journal of Double Star Observations*, **4**, 27-31.

Knapp, Wilfried; Gould, Ross, 2016, "Visual Observation and Measurements of some Tycho Double Stars", *Journal of Double Star Observations*, **12**, 427-436.

Table 1: All TDS objects in CVn with separation 1.5 arcseconds or larger so far not confirmed are according to the SDSS DR9 catalog to be considered as bogus. Only one object was already confirmed in the WDS catalog and was clearly also confirmed by SDSS DR9. Separation and PA calculated with the formulae provided by Buchheim 2008

CVn TDS objects not confirmed in the WDS catalog per beginning of 2016								
WDS ID	**Name**	**RA**	**Dec**	**Sep**	**M1**	**M2**	**PA**	**Counter-Check Result**
12152+5118	TDS8286	12:15:11.151	+51:18:07.8	2.1	12.17	13.27	180	SDSS9 obviously single, bogus assumed
13516+3851	TDS9002	13:51:35.151	+38:50:54.4	2.0	11.26	13.24	246	SDSS9 multiple spikes suggest multiple star - but all spikes suggest same centroid. Bogus assumed
13017+4617	TDS8649	13:01:42.029	+46:16:52.4	2.3	10.45	12.82	79	SDSS9 multiple spikes suggest multiple star - but all spikes suggest same centroid. Bogus assumed
12332+4802	TDS8432	12:33:13.081	+48:01:49.9	2.6	11.73	12.85	187	SDSS9 multiple spikes suggest multiple star - but all spikes suggest same centroid. Bogus assumed
13141+3712	TDS8741	13:14:06.311	+37:12:13.5	2.6	11.37	12.79	236	SDSS9 multiple spikes suggest multiple star - but all spikes suggest similar centroid. Bogus assumed
CVn TDS object already confirmed in WDS per begin of 2016								
13411+3719	TDS718	13:41:04.851	+37:18:41.6	1.7	11.82	11.8	221	SDSS objects for A (J134104.87+371841.7) and B (J134104.77+371840.5). Separation 1.673" and PA 222.799°. Observation epoch 2004.075

Counter-Checking Tycho Double Stars with the SDSS DR9 Catalog

Table 2. Five out of seven TDS objects in Boo with separation 1.5 arcseconds or larger so far not confirmed are according to the SDSS DR9 catalog to be considered as bogus but two could be confirmed. Seven objects were already confirmed in the WDS catalog and with one exception also clearly confirmed by SDSS DR9. Separation and PA calculated with the formulae

Boo TDS objects not confirmed in the WDS catalog per begin of 2016:								
WDS ID	**Name**	**RA**	**Dec**	**Sep**	**M1**	**M2**	**PA**	**Counter-Check Result**
14503+4520	TDS9320	14:50:19.682	+45:19:34.5	2.2	12.15	12.18	22	SDSS9 obviously single star. Bogus assumed
14040+1154	TDS9082	14:03:59.890	+11:54:23.4	2.6	11.36	12.73	88	SDSS9 multiple spikes suggest multiple star - but all spikes suggest same centroid. Bogus assumed
15335+4126	TDS9547	15:33:29.719	+41:26:13.4	2.6	12.32	12.53	214	SDSS9 objects for A (J153329.70+412613.4) and B (J153329.58+412611.1). Separation 2.645" and PA 210.953°. Observation epoch 2003.406
13542+0802	TDS9025	13:54:12.478	+08:02:22.7	1.5	11.25	11.81	185	SDSS9 objects for A (J135412.48+080222.3) and B (J135412.47+080220.7). Separation 1.595" and PA 184.100°. Observation epoch 2002.221
14374+3924	TDS9249	14:37:23.350	+39:24:18.9	1.5	11.13	12.88	348	SDSS9 obviously single star. Bogus assumed
14523+4437	TDS9330	14:52:19.769	+44:37:20.1	2.3	10.69	12.29	30	SDSS9 obviously single star. Bogus assumed
14187+5232	TDS9160	14:18:44.801	+52:32:08.3	2.1	11.21	12.32	123	SDSS9 obviously single star. Bogus assumed
Boo TDS objects already confirmed in WDS per begin of 2016:								
WDS ID	**Name**	**RA**	**Dec**	**Sep**	**M1**	**M2**	**PA**	**Counter-Check Result**
14560+3807	TDS9348	14:55:59.592	+38:07:19.2	1.6	11.21	11.47	81	SDSS9 multiple spikes suggest multiple star but no SDSS DR9 objects. Estimations from centroids using spikes as crosshairs: Separation 1.58" and PA 55.265°. Observation epoch 2003.226
15271+5127	TDS9521	15:27:07.439	+51:26:53.9	3.3	11.87	12.40	136	SDSS9 objects for A (J152707.41+512654.2) and B (J152707.67+512651.8). Separation 3.321" and PA 135.148°. Observation epoch 2002.437
14198+3016	TDS9165	14:19:48.281	+30:15:37.3	3.0	11.75	12.00	173	SDSS9 objects for A (J141948.28+301537.2) and B (J141948.31+301534.1). Separation 3.114" and PA 173.809°. Observation epoch 2004.283
13585+1409	TDS9050	13:58:30.959	+14:08:36.4	9.9	12.03	12.19	264	SDSS9 objects for A (J135830.95+140836.3) and B (J135830.27+140835.2). Separation 9.940" and PA 264.034°. Observation epoch 2003.409. Comparing the positions between 2MASS epoch 2000.157 and URAT1 epoch 213.751 suggests common proper motion because of ident proper motion vector direction of 332° and very similar proper motion vector length of ~600mas
14312+3426	TDS9227	14:31:09.931	+34:25:32.7	1.9	10.02	11.74	172	SDSS9 multiple spikes suggest multiple star - but all spikes suggest same centroid. Only one SDSS DR9 object. Also no hint of elongation in 2MASS J-band image. Bogus assumed despite confirmation recorded in WDS catalog
13433+1235	TDS8944	13:43:18.150	+12:35:24.7	3.0	10.98	11.12	25	SDSS9 objects for A (J134318.21+123523.4) and B (J134318.25+123527.6). Separation 4.337" and PA 7.963°. Observation epoch 2003.223
14415+4953	TDS9271	14:41:28.239	+49:53:10.5	2.2	11.06	11.86	20	SDSS9 objects for A (J144128.24+495310.4) and B (J144128.32+495312.2). Separation 1.976" and PA 21.123°. Observation epoch 2002.350

Crystal Lake Observatory Double Star Measurements: Report #1

Craig Young

2331 State Highway 31
Te Awamutu, New Zealand
craig.young.m8@gmail.com

Abstract: This paper reports updated astrometric measurements for 10 visual double stars located between 0 and -20 degrees declination and with magnitude between 10 and 12. Measurements were obtained using a 20 cm Ritchey–Chrétien telescope and CCD camera with photometric V filter and data reduction using Pixinsight™ software.

Instrumentation and Software

The telescope used is a GSO 20cm Ritchey–Chrétien design with a carbon fibre tube and 1624 mm focal length. The telescope is permanently mounted on an iOptron™ CEM60-EC mount and remotely operated over a CAT 6 network between the observatory and the data processing office.

The CCD camera is an SBIG STF-8300M. Combined with the telescope, the field of view is 38 x 29 arc-min and the plate scale is 0.685 arc-sec/pixel. The camera cooling system is set to operate at -5C. An Astrodon™ 50mm photometric V filter is fixed between the focuser and the camera.

SkyX™ software is used to remotely control the telescope, camera, focuser, and mount. The raw images are saved on a PC located at the observatory and later a copy transferred to a project computer in the lab.

Pixinsight software is used for the calibration, plate solving, astrometric, and photometric measurements. Custom software, written by Crystal Lake Observatory, is used to automate the process and format the results.

Methodology

For this dataset, each star was imaged twenty times over a period of twenty five minutes on an observing night. Due to clouds or instrument errors, the number of images measured may be less than this. These data are then combined with those taken on subsequent observing nights and the mean and standard deviation of the separation and position angle calculated. The exposure time for each image is sixty seconds and all images recorded using a Johnson-Cousins V photometric filter.

The first step in the data reduction process is calibration of the raw images. The Pixinsight process 'ImageCalibration' was used to perform the standard image calibration functions including dark frame subtraction and flat frame correction. Noise evaluation is included in the process and used to remove unwanted images.

Next, the Pixinsight script, AperturePhotometry (AP), written by Andres del Pozo and Vicent Peris is used to determine the center of each star. First, a plate solve of the image is performed using the PPMX star catalogue. This defines the J2000 equatorial center of the image and a distortion model.

Following the plate solve, a Point Spread Function (PSF) model of the star profile is used to determine the precise center of the star. The PSF function can be configured to use a specific type of model (e.g., Moffat) or several types of models and select the best fit. A Mean Average Deviation (MAD), which measures the differences between the model and the actual star profile, is used to select the best model. For this dataset the Gaussian model was used because it provided the best solution (lowest MAD value) across all of the stars.

Crystal Lake Observatory Double Star Measurements: Report #1

319	223			
Bounds	121.289596	-16.058374	121.950322	-15.582232
Aperture	16	1	1	
Background ring window	20	40		
DATE_OBS	NAME	FILTER	CATRA	CATDEC
2457474.8	3UCAC149-096628	Johnson V	121.316771	-15.619054

IMGRA	IMGDEC	IMGX	IMGY	f.mag	BKGROUND	BGSTDDEV	BGRJCT
121.316804	-15.618982	141.107	2326.478	8.436	142.7808	21.13574	0.1614

PSF_A	PSF_SIGMAX	PSF_SIGMAY	PSF_THETA	PSF_MAD	FLUX16	SNR16	FLAG
0.7510268	5.10854291	4.61938076	177.80477	1.16E-02	1037774.2	977.2975	0

Figure 1. Example of the output file from Pixinsight. See text.

An example of the output file from Pixinsight is shown in Figure 1.

The CATRA and CATDEC values are the equatorial J2000 coordinates of the star taken from the UCAC3 catalog. IMGX and IMGY are the center (in pixels) of the star as determined from the PSF model. The IMGRA and IMGDEC values are the equatorial J2000 coordinates calculated using the plate solution and image distortion model from the plate solve process and the pixels coordinates from the PSF process.

Pixinsight also annotates a copy of the image to show the detected stars (Figure 2).

The primary star is the brighter one, the bottom star in Figure 2. Given the orientation of the camera, the position angle is measured counter clockwise with 0 at the bottom. In this case, the position angle is slightly past 180 degrees (the measured value is 187 degrees).

Determination of separation (ρ) and position angle (θ)

The final step uses a custom software program written by Crystal Lake Observatory to calculate the separation and position angle of the double star. There are two commonly used methods for calculating the separation and position angle using a CCD camera, (a) rectangular method using the pixel coordinates of the star centers, and (b) equatorial method using the calculated equatorial coordinates of the two stars. The two methods will normally result in equivalent results, but the equatorial method will account for any distortion of the image if the stars being measured are not near the center of the image, which could affect the accuracy of the measure. Therefore it was decided to use the equatorial method, although in this dataset all stars were located near the center of the image.

From the Pixinsight output file, IMGRA and IMGDEC are used to calculate the astrometric measures using the following two formulas (Greaney, 2015)

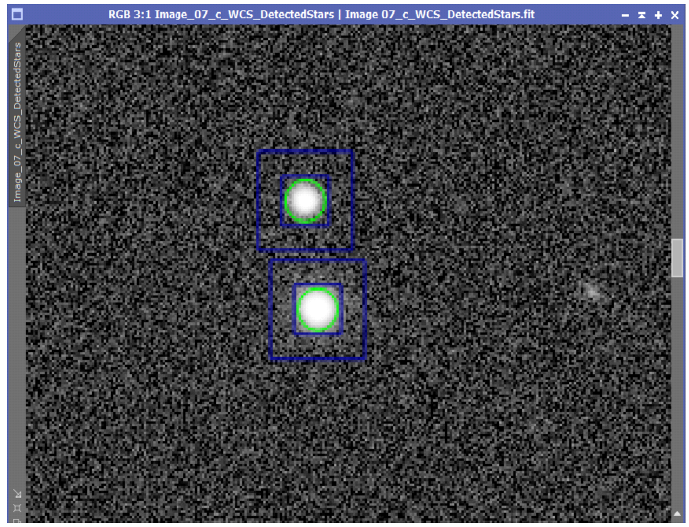

Figure 2. BVD 97. This cropped image is extracted from the detected stars images created by Pixinsight during the aperture photometry processing step.

The last equation places the position angle in the

$$\rho = \arccos[\sin(primaryDEC)\sin(secondaryDEC) + \cos(primaryDEC)\cos(secondaryDEC)\cos(secondaryRA - primaryRA)]$$

$$\theta = \arctan 2\{[\cos(primaryDEC)\cos(secondaryDEC)\sin(secondaryRA - primaryRA)], [\sin(secondaryDec) - \cos(\rho)\sin(primaryDEC)]\}$$
$$\text{if } \theta < 0.0 \text{ then } \theta = 2.0\pi + \theta$$

correct quadrant given the orientation of the camera on this system.

The Besselian date is calculated using the midpoint of the Julian date between the first and last image of the dataset:

$$BD = 1900.0 + ((jd2 - jd1) + jd1) - 2415020.31352 / 365.242198781$$

An audit trail of the entire process is saved with the raw images and provides a way to trace back the process and results for any given measurement. The audit trail includes:

- Raw images
- Calibrated images
- Calibrated image with plate solve parameters
- Detected stars images
- Output csv file from the Aperture Photometry script
- Output csv file from CLO Post Processor program

Measurements

Ten stars are measured and presented (Table 1). The column ‘n’ is the number of nights images were recorded. The column ‘m’ is the total number of measurements (i.e., number of images measured). Ideally, m should be twenty times n, but some images were rejected due to clouds or tracking errors. The column ‘σ θ’ is the standard deviation in position angle measured in degrees. The column ‘σ ρ’ is the standard error in separation measured in arc-seconds. The statistics are calculated on the entire dataset and not on an individual night. For example, for HJ 775 the mean and standard deviation are calculated from 17 measurements, and for HJ 131 from 113 measurements.

Discussion

One of the objectives of this first dataset is to evaluate the accuracy and precision of the methodology and look at changes to improve the efficiency of available telescope time.

A baseline was established by taking twenty images of each double star and repeating this on several nights. This resulted in a mean standard deviation of 0.02 arc-seconds for separation and 0.05 degrees for position angle across the entire dataset.

To check the accuracy of the measurements, the statistics could be calculated for each night across the twenty images and an average and standard deviation of the means calculated across all of the observing nights. The standard deviation of the means would then indicate a level of confidence in the mean.

Using the data from WHC 9, Table 2 shows the mean and standard deviation for the position angle and separation across all nine observing nights. The ’All images per night’ column uses all of the images from each night to calculate the statistics.

The results show excellent consistency across the observing nights with a standard deviation of the means well below the standard deviation of the samples for any given night. This indicates that one night’s data could be used to derive an accurate measure of the star.

The ’10 images per night’ columns calculate the statistics based on using the first ten images recorded that night. The data shows there would be very little change in accuracy or precision in reducing the number of images from twenty to ten.

The ‘5 images per night’ columns calculate the statistics based on using the first 5 images recorded that

Table 1. Basic Astrometric Measurements for 10 Selected Double Stars

Name	WDS	Date	θ	ρ	n	m	σ θ	σ ρ	Notes
HJ 775	08053-1549	2016.237	178.12	11.27	1	17	0.07	0.04	
HJ 131	09201-0136	2016.263	123.30	16.27	6	113	0.06	0.02	1
J 1558	09466-0504	2016.282	169.85	11.10	5	96	0.06	0.01	
ARA 411	10289-1927	2016.300	329.04	12.67	9	168	0.05	0.01	
LDS 294	09593-1956	2016.278	169.67	24.25	7	140	0.03	0.01	
BVD 97	11544-2046	2016.304	186.97	30.31	7	133	0.02	0.01	2
WHC 9	11225-1028	2016.306	179.07	10.59	9	151	0.08	0.02	3
BAL1162	12432+0000	2016.327	303.38	15.06	5	77	0.04	0.01	4
HJ 1208	12051-0907	2016.304	99.59	10.49	7	136	0.10	0.02	
HJ 209	12239-0303	2016.327	146.53	23.76	6	95	0.03	0.02	

Notes:

1. HJ 131. The last recorded values in the WDS catalogue are 123 degrees for position angle and 16.5 arc-sec for separation in the year 2007. The 2016 measures above shows a difference greater than the standard deviation of the data.
2. BVD 97. The last recorded values in the WDS are 187 degrees for position angle and 30.4 arc-sec for separation in the year 2009. The 2016 measures above show a difference greater than the standard deviation of the data.
3. WHC 9. The last recorded values in the WDS are 179 degrees for position angle and 10.7 arc-sec for separation in the year 2007. The 2016 measures above show a difference greater than the standard deviation of the data.
4. BAL 1162. The last recorded values in the WDS are 303 degrees for position angle and 14.8 arc-sec for separation in the year 2009. The 2016 measures above show a difference that is much greater than the standard deviation of the data.

Crystal Lake Observatory Double Star Measurements: Report #1

Table 2. WHC 9. Comparison of measures vs number of images.

WHC 9	All images per night			10 images per night			5 images per night		
Date	N	ρ	θ	N	ρ	θ	N	ρ	θ
2016.237	19	10.59	179.07	10	10.59	179.07	5	10.60	179.06
		0.016	0.083		0.014	0.090		0.007	0.056
2016.245	19	10.59	179.07	10	10.59	179.08	5	10.58	179.09
		0.016	0.087		0.016	0.079		0.016	0.060
2016.264	18	10.59	179.05	10	10.59	179.05	5	10.59	179.09
		0.013	0.097		0.011	0.107		0.016	0.121
2016.286	20	10.58	179.07	10	10.58	179.07	5	10.58	179.06
		0.017	0.085		0.017	0.100		0.009	0.118
2016.289	19	10.59	179.05	10	10.59	179.05	5	10.59	179.06
		0.013	0.070		0.013	0.079		0.08	0.094
2016.319	20	10.58	179.06	10	10.59	179.04	5	10.59	179.02
		0.014	0.072		0.016	0.072		0.017	0.086
2016.349	17	10.58	179.07	10	10.58	179.05	5	10.57	179.02
		0.019	0.058		0.022	0.061		0.018	0.072
2016.362	9	10.58	179.09	9	10.58	179.09	5	10.58	179.07
		0.013	0.102		0.013	0.102		0.012	0.132
2016.376	5	10.59	179.08	5	10.59	179.08	5	10.59	179.08
		0.004	0.095		0.004	0.095		0.004	0.095
μ Means		10.59	179.07		10.59	179.06		10.59	179.06
σ Means		0.005	0.013		0.005	0.017		0.009	0.026

night. As above, the data shows there would be very little change in accuracy or precision in reducing the number of images from twenty to five.

Also notice that even though the standard deviation of the means increases when using less images per night, the mean for both position angle and separation remain accurate. This would indicate good randomness of the data thus providing a high confidence in the mean values.

Conclusion

Comparison of the above results with the WDS catalog, for six stars, show similar position angle and separation, within the statistical variance of the mean. This indicates the methodology can be used for the measurement of other double stars with good confidence in the results. The remaining four stars show a difference in separation and position angle that is greater than the statistical variance of the data. This indicates a change in the astrometric data of the observed star system, requiring additional observations of these stars to confirm the movement and rate of change.

A review of the methodology shows a more efficient use of the available telescope time can be achieved by reducing the number of images recorded each night and the number of observing nights. The methodology shall therefore be updated to record 5 images per night and 3 nights used to check for any systematic errors.

Given the success of this methodology, additional stars will now be measured and reported. The stars reported in this paper will be measured again next year to provide more data for determining the proper motion of the stars and possible confirmation of whether they are a physical system. In addition, photometric measurements of the stars will be added.

Acknowledgements

Thanks to Juan Conejero, Pixinsight Development Team, and Andres Del Pozo, Pixinsight Aperture Photometry author, for their kind assistance in helping me to develop the Pixinsight data reduction process for this project.

This research has made use of the Washington Double Star Catalog maintained at the U.S. Naval Observatory.

References

Mason, B.D., 2006, "Requesting Double Star Data from the US Naval Observatory". *JDSO*, **2,** 21-35.

Stelle Doppie Double Star Database by Gianluca Sordiglioni.

Conejero, Juan, Pixinsight, http://www.pixinsight.com.

Greaney, Michael, 2015, *Observing and Measuring Visual Double Stars,* 2nd Edition, R. W. Argyle, ed., Springer, New York.

Observation Report for the Year 2012: Humacao University Observatory

R.J. Muller, J.C. Cersosimo, D. Cotto, R. Rodriguez, M.Diaz, M Rosario, Y. Nieves, E. Franco, A.Lopez, B.S.Torres, N.Vergara, Y. Del Valle, D. Ortiz, G. Espinosa, M. Reyes, O. Carromero, J. Martinez

Humacao University Observatory
Department of Physics and Electronics
The University of Puerto Rico at Humacao
Call Box 860, Humacao, Puerto Rico 00792
rjmullerporrata@gmail.com

Abstract: We report on the measurement of position angle and separation of 93 binary pairs. The data was obtained using the NURO Telescope at the Anderson Mesa location of Lowell Observatory, 20 miles east of Flagstaff, Arizona on May and September 2012. We gathered the data using the 2K x 2K CCD camera,-NASACAM-at the prime focus of the 31 inch telescope. The data was transferred and analyzed at the Humacao University Observatory by undergraduate students undertaking research projects.

Introduction

We obtained CCD images of 93 binaries with the NASA CAM CCD at the prime focus of the National Undergraduate Research Observatory (NURO) telescope. From the analysis of those images, we obtained the position angle and separation of the binaries.

The Humacao Campus of the University of Puerto Rico is a member of NURO, a consortium of primarily undergraduate institutions (www.nuro.nau.edu) with access to a 31 inch telescope, property of Lowell Observatory. It is located roughly 20 miles east of Flagstaff, Arizona at the Anderson Mesa, at an altitude of 7200 feet. We use the NURO telescope twice a year, and in 2012 we visited the telescope on May 28, 29, and 30, and also on September 4, 5, and 6. The undergraduate students that visited on those dates operated the telescope, gathered the data and brought it to the Humacao Campus Observatory of the University of Puerto Rico for analysis. The separation measurements were done by pixelizing the images, and also used software for measuring the separation of those binaries in close proximity. The position angle was simply extracted from the images. The measurement of the position angle introduces a systematic error which we call the offset and correct statistically. The Cassegrain telescope has a 2K x 2K CCD camera at its prime focus. This CCD has 15 micron pixels and a field of view of 16 arc minutes. The optical reducer in the optical path was changed preceding our observing run, and it changed our plate scale, so we had to recalculate the plate scale again for this report as we have done before. The plate scale obtained was .456 arcseconds/pixel, and is the value used for this report.

The large number of undergraduate student authors in this report is due to a generational change in the observatory students; those students that acquired the data graduated and a new group of students analyzed and organized the data for the presentation in this report.

Data

Data Tables 1 and 2 present the results for the 93 binaries; Table 1 yields 72 values for our May observing run and Table 2 yields 21 values for the September run. The September run was cut short because of clouds and rain, a very unusual set of circumstances in Flagstaff and surrounding area.

Acknowledgements

We want to acknowledge extensive use of the Washington Double Star Catalog of the U.S. Naval Observatory. We also want to thank Ed Anderson, the NURO telescope technician, for his effort during our observations. We also want to thank Puerto Rico's NASA Space Grant Consortium for its continuous support of this project.

Table 1. Measurements from May 2012 Observing Run

Name	R.A	DEC.	Magnitudes		ρ	θ	Date
GRV 849	12 02 53.16	23 45 50.8	12.03	12.35	28.95	230.63	0.408
BAL1450	12 03 11.85	00 43 48.8	11.7	12.46	23.21	210.0	0.408
STI 738	12 03 17.6	59 24 05.8	12.24	13.1	6.61	40.0	0.408
STF1594 AC	12 03 28.5	41 24 15.5	10.09	11.1	11.02	144.0	0.408
POU3120	12 04 05.70	23 11 40.6	11.09	13.1	13.55	198.0	0.408
BU 458	12 04 17.11	-21 02 21	7.87	9.97	29.85	234.13	0.408
KZA 26	12 05 07.86	43 22 46.7	13	13.6	17.59	106.46	0.408
HJ 4496	12 06 12.76	-18 53 28	10.05	10.98	10.2	26.63	0.408
STF1622	12 16 07.55	40 39 36.6	5.86	8.71	10.6	265.0	0.408
COU2707	12 30 04.89	22 22 16.5	11.77	14.1	14.29	344.46	0.408
ES 726 AC	12 30 49.06	53 5129.7	10.48	13.6	20.3	177.13	0.408
STF1650	12 31 32.99	24 37 13.1	9.54	10.47	16.99	181.37	0.408
STF1649	12 31 36.46	-11 04 20	7.97	8.43	15.89	193.79	0.408
LDS4224	12 32 13.27	31 47 19.6	13.5	15.0	10.91	313.46	0.408
HJ 211	12 32 21.12	-01 53 33.3	11.86	11.77	11.73	278.13	0.408
LDS4225	12 32 28.75	285412.4	13.3	15.3	16.22	207.63	0.408
POU3152	13 49 38.88	23 28 15.0	12.25	12.05	12.30	12.25	0.408
UC 185	13 53 44.49	12 40 48.4	8.64	13.35	20.74	145.46	0.408
HJ 2699 BC	14 03 04.57	11 54 25.3	13	13.4	14.97	301.13	0.408
HJ 542	14 12 21.20	36 46 12.6	12.9	12.5	12.07	67.6	0.408
POU3162	14 13 23.91	24 24 11.9	12.02	13.8	5.87	347.46	0.408
DAM 79	14 17 01.59	50 43 58.8	11.4	13.6	13.78	55.29	0.41
LDS4521	15 00 47.52	23 06 26.3	15.45	16.42	25.61	338.88	0.41
STF1901	15 00 57.7	31 22 38.2	8.71	10.55	19.62	186.0	0.41
HJ 1266	15 01 07.99	04 15 1 7.0	10.77	12.81	13.69	25.13	0.41
LDS4543	15 20 41.6	26 37 54.9	12.6	18.3	64.11	234.13	0.41
KZA 80	15 20 42.06	31 33 15.1	12.13	12.82	25.33	55.46	0.41
KZA 87	15 24 48.68	29 34 28.4	12	12.5	11.97	0.13	0.41
POU3188	15 25 38.91	24 01 26	12.04	14.4	11.63	21.63	0.41
KZA 90	15 27 25.45	31 01 41.8	12.5	13	20.26	297.46	0.41
HO 629	15 28 20.19	23 41 02.7	8.06	12.2	21.14	111.96	0.41
GRV 907	15 31 20.13	83 63 1.9	9.40	12.49	21.94	163.29	0.41
BRT2420	15 31 33.89	21 11 16.3	10.84	11.50	11.18	312.0	0.41
POU3193	15 35 22.37	24 08 16.8	13.2	13.7	7.48	298.79	0.41
HDS2205	15 38 16.34	-93 42 7.5	9.89	12.39	10.27	47.0	0.41

Table 1 concludes on next page.

Observation Report for the Year 2012: Humacao University Observatory

Table 1 (conclusion). Measurements from May 2012 Observing Run

Name	R.A	DEC.	Magnitudes		ρ	θ	Date
HJ 580	16 02 50.56	37 05 26.8	9.21	12.97	40.25	8.63	0.41
STF1999 AB	16 04 26.0	-11 26 58	7.52	8.05	10.74	101.46	0.41
ARA 433	16 06 35.80	-18 19 12	11.6	14.1	9.93	55.13	0.41
HJ 582	16 07 16.96	35 07 41.6	11.11	13.61	22.01	230.46	0.41
ALI 370	16 07 26.70	354827.8	12.9	13	13.09	146.63	0.41
POU3214	16 07 48.84	230529.9	11.1	13.3	12.6	83.13	0.41
STF2010 AB	16 08 04.6	170249.2	5.1	6.21	27.28	14.63	0.41
BAL 564	16 11 09.67	-20613.7	11.53	11.8	12.45	281.7	0.41
STF2032 AB	16 14 40.85	33 51 31	5.62	6.49	7.5	237.0	0.41
ES 627	16 18 35.71	51 19 51.5	9.88	10.98	12.03	291.0	0.41
BAL2429	16 54 51.18	31 84 0.8	11.77	12.8	11.13	53.63	0.41
ES 1255	17 01 00.5	46 16 26.8	8.19	11.7	7.24	43.63	0.41
WFC 186	17 06 05.4	432857.4	10.81	12.11	17.52	15.88	0.41
STF2123	17 06 57.5	06 48 03.0	9.82	9.98	18.38	219.38	0.41
STF2127	17 07 04.4	31 05 35.1	8.7	12.3	14.5	279.0	0.41
ARA1121	17 07 06.09	-20 14 44	11.8	12.4	8.2	217.38	0.41
SLE 9	17 07 06.3	20 29 21.7	10.49	12.3	20.04	173.13	0.41
BEM 26	17 08 36.72	50 22 45.2	11.06	13.34	15	196.5	0.41
FOX 211	18 00 01.77	-15 12 29	10.19	12.8	13.1	20.0	0.41
SLE 85	18 07 33.1	31 35 3.7	11.2	12.5	10.8	184	0.413
BAL1952	18 07 34.41	22 40 7.8	11.52	12.8	13.48	153.46	0.413
SLE 138	18 07 52.7	30 41 57.2	11.5	12.8	10.46	329.38	0.413
POU3350	18 07 59.95	24 06 00.8	11.8	12	10.19	68.0	0.413
BAL2474	18 08 03.42	34 31 2.1	10.0	11.0	15.89	283.63	0.413
POU3351	18 08 08.78	23 27 12.4	12.05	13.9	10.14	159.79	0.413
ARA 453	18 08 52.23	-18 26 55	10.69	12.50	8.95	57.0	0.413
SLE 111	18 08 54	27 24 56.6	10.8	12.5	14.04	312.63	0.413
ES 1417 AB	18 09 09.15	43 13 48.6	9.21	11.5	13.52	210.63	0.413
BEM 31	18 09 41.21	53 29 31.5	9.90	12.3	11.51	310.46	0.413
STF2293	18 09 53.8	48 24 05.7	8.08	10.34	13.59	83.88	0.413
BAL2483	18 14 41.54	34 20 5.5	12	12.7	12.96	198.13	0.413
ES 646	18 15 09.43	52 09 24.8	8.72	14.1	10.51	194.46	0.413
POU3380	18 17 22.66	24 56 36.2	12.4	13.3	12.75	72.79	0.413
HJ 1349	18 48 48.77	33 19 12.1	8.29	10.7	30.2	94.13	0.413
STF2459	19 07 22	25 58 23.9	9.12	10.07	14.69	231.63	0.413
AG 375	19 14 13.48	26 26 28.4	9.89	10.92	18.07	296.88	0.413
SLE 959 AB	20 11 50.1	37 26 06.8	10.69	12.5	12.55	160.29	0.413

Observation Report for the Year 2012: Humacao University Observatory

Table 2. Measurements from September 2012 Observing Run

Name	R.A	DEC	Magnitudes		ρ	θ	Date
ALI 140	18 11 25.14	35 06 45.5	10.97	11.79	38.32	250.0	0.682
BAL2474	18 08 03.42	03 43 12.1	10	11	17.32	284.27	0.682
HJ 1315	18 09 53.54	29 41 16.1	11.85	13.1	7.48	135	0.682
STF2293	18 09 53.83	48 24 05.7	8.08	10.34	14.28	74	0.682
SEI 559	18 10 27.80	33 55 55.6	11	11	12.65	175	0.682
BAL2481	18 10 37.28	32 72 3.7	11.3	11.3	11.28	106.6	0.682
POU3419	18 32 02.77	25 04 01.7	7.89	12.1	9.14	234.27	0.682
HJ 1375	19 12 29.96	28 14 26.7	11	13.6	14.56	83.93	0.684
POU3940	19 35 12.15	25 01 29.6	10.6	10.7	7.79	25.	0.684
ES 2297	19 37 28.79	33 32 31.2	9.14	9.4	9.1	181	0.684
SMA 101	19 50 48.40	44 44 42.1	12.8	13.2	9.74	48.57	0.684
SEI1012	20 13 02.39	34 50 29	11	11	16.88	55.27	0.684
CHE 235	20 14 36.19	14 52 35.1	12.3	13.6	11.62	29	0.684
POU4500	20 26 52.84	23 40 16.1	11.99	12.1	9.22	274.93	0.684
SEI1483	21 16 06.83	35 48 07.2	12.3	12.7	16.6	24.77	0.684
WSI 23 AC	21 24 42.86	36 30 30.1	11	12.2	10.74	83.92	0.684
STF2800	21 28 43.09	49 52 06.6	9.5	10.41	10.6	233.0	0.684
STI2720	22 21 30.29	58 36 48.7	12.1	12.1	17.67	160.27	0.684
ES 837AC	22 31 45.72	50 04 24.4	9.64	12.9	9.74	236.52	0.684
BRT 602	23 32 07.02	-14 31 33	10.8	11	4.87	120.27	0.684
BAL1249	23 41 02.65	00 43 06.9	10.36	12.4	12.67	330.93	0.684

Speckle Interferometry of Binary Star HIP 4849

Matthew Kehrli, Heather David, Evan Drake, Corina Gonzalez,
Joe Zuchegno, and Russell Genet

California Polytechnic State University, San Luis Obispo, California

Abstract: Binary star HIP 4849 was observed on October 18, 2013 UT, using an EMCCD camera on the 2.1-Meter telescope at Kitt Peak National Observatory. HIP 4849 had a separation, ρ, of 0.725″ and a position angle, θ, of 79.32°. This observation did not deviate significantly from the predicted orbit.

Introduction

In 1970, French astronomer Antoine Labeyrie published a paper detailing a tool for the study of double stars. Labeyrie's background in holography aided his understanding of atmospheric speckles, or as he called them, "the grainy structure observed when a laser beam is reflected from a diffusing surface" (Labeyrie 1970). He suggested exposing speckle-affected images of double stars using a high-speed camera. This technique, known as speckle interferometry, allows astronomers to circumvent resolution limitations due to the "instantaneous image broadening ... or erratic displacement of the image," otherwise known as astronomical *seeing* (Vernin 1995). Based on the premise that "speckle-affected images contain more information on smaller features than long exposure images with a blurred speckle," speckle interferometry captures many short exposure images of double stars to take full advantage of the aperture of the telescope (Labeyrie 1970).

Many new double stars were discovered by the European Space Agency's Hipparcos satellite, starting in August 1989. Hipparcos was the first space mission dedicated to "measuring positions, distances, motions, brightness, and colors of stars" (Erickson 2015). The satellite was named in honor of Greek astronomer Hipparchus and abbreviated from High Precision Parallax Collecting Satellite to Hipparcos (Watson 1997). Data collected by Hipparcos resulted in a star catalog considered to be "the most accurate database of stellar positions ever produced" (Schilling 2004).

After achieving its goal as a pioneer for astrometric research, the Hipparcos observations were completed in March 1993. Michael Perryman, the project scientist and operations manager of the mission, offers insight on Hipparcos in *The Making of the World's Greatest Star Map* (2010). He documents that Hipparcos' success was due to the work of over 2,000 individuals. When the Hipparcos mission was planned in the 1980s, computational abilities were not yet advanced enough to reduce the data. Trusting Moore's Law, the increased computational capacity by the early 1990s made data release available (Perryman 2010).

Hipparcos made observations of more than 100,000 stars, many of which were doubles. Of the 12,000 double stars observed, Hipparcos discovered 3,406 new systems (Mason et al. 1999). Shortly after the Hipparcos results were published in 1997, astronomers began follow-up observations on the newly discovered double stars. Some of these showed the beginnings of apparent orbits, and prominent double star astronomers such as Elliott Horch on the 3.5-Meter WIYN telescope at Kitt Peak National Observatory, Yuri Balega on the 6-Meter BTA-6 telescope in Zelenchuksky, Russia, and Andrei Tokovinin on the 4.1-Meter SOAR telescope in Chile worked to compile additional measurements and determine these apparent orbits.

By now, astronomers have added many observational points beyond the original data published from Hipparcos in 1997. Many of the Hipparcos discoveries have proven to be binaries, some with short orbital periods. As a result, some of these observed doubles now have calculated orbits. This current study adds another observational point to the binary HIP 4849. Out of the 12 Hipparcos discoveries that now have published orbits and were also observed during the 2013 run at Kitt Peak National Observatory, we chose HIP 4849 based

Speckle Interferometry of Binary Star HIP 4849

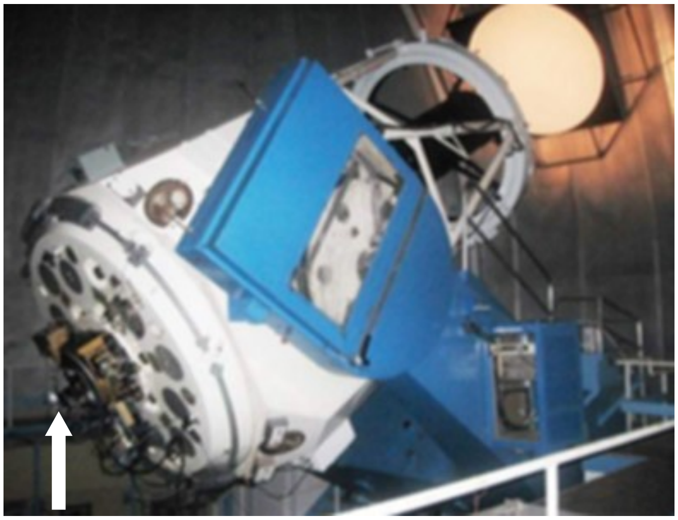

Figure 1. Kitt Peak 2.1-Meter Telescope (arrow denotes the EMCCD camera)

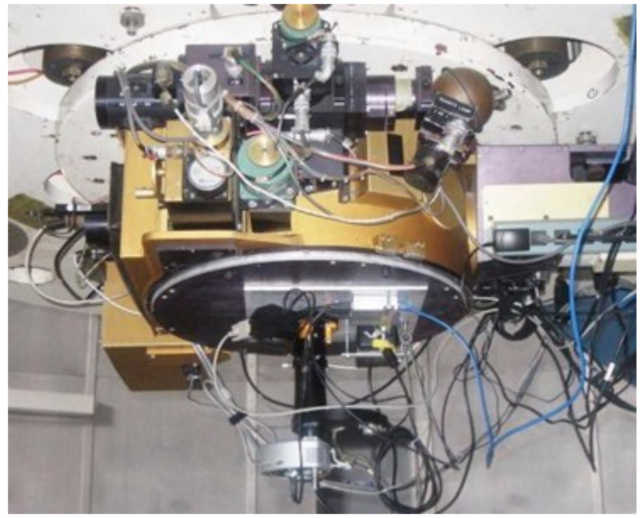

Figure 2. Camera System used at Kitt Peak

on its well-defined orbit with multiple plotted points.

The two goals of this study were to contribute a new position angle and separation to the published observations of HIP 4849, and serve as a pilot and companion project for a further study on the remaining 11 Hipparcos discoveries with known orbits observed at Kitt Peak.

Instrumentation, Observations, Calibration, and Reduction

Telescope

The binary HIP 4849, also identified as WDS 01024+0504, was observed on October 18, 2013 at 6:25:27 UT from Kitt Peak National Observatory. The observations were made on Kitt Peak's 2.1-Meter telescope, shown in Figure 1, which has a focal length of 16,200 mm (Genet et al. 2015b). The 2.1-Meter telescope is primarily used for imaging and spectroscopy (*2.1-Meter Telescope on Kitt Peak* 1998).

The instrumentation for Kitt Peak's 2.1-Meter telescope has undergone several upgrades since its creation. Originally equipped with an imaging camera and several spectrographs, it now includes modern infrared (IR) array cameras and spectrometers, the GoldCam Spectrograph, a charge-coupled device (CCD) imager, and the Phoenix infrared spectrometer (*2.1-Meter Telescope on Kitt Peak* 1998). Since Kitt Peak's 2.1-Meter telescope did not include the high-frame-rate, low-read noise camera needed for speckle interferometry observation, the observers supplied their own speckle interferometry camera (Genet 2013). The camera was attached to the acquisition guider unit and dwarfed by the 2.1-Meter telescope as shown in Figure 1.

Camera System

Inspired by the U.S. Naval Observatory's successful speckle observations of binaries using a portable image intensified charged coupled device (ICCD) speckle camera, a more portable, low-cost camera system, seen in Figure 2, was developed that featured an EMCCD camera (Genet 2013). The primary benefit of an EMCCD camera over an ICCD camera is that the "electron multiplication (EM) boosts the signal to a level where the high speed read noise is insignificant" (Genet et al. 2015a). The front-illuminated Andor Luca-R EMCCD had a quantum efficiency of about 50%, a dark noise of 0.05 electrons/pixel/second, and a read noise well under one electron RMS. The speckle camera system had a magnification of approximately 8x to provide an overall focal length of 129,600 mm and an F/ratio of 61.7 when attached to the 2.1-meter telescope (Genet et al. 2015b). The employed Andor Luca R EMCCD had "10 μ square pixels in a 658x496 pixel array" (Genet et al. 2015c).

Observations

The National Optical Astronomy Observatory's Time Allocation Committee granted eight nights of observing time to a team of university students and supporters. The team tested the equipment and conducted their observations on the nights of October 16th through 23^{rd,} 2013 at Kitt Peak National Observatory (Genet et al. 2015b).

Calibration

Observations were calibrated with data collected from multiple observations of six binaries with previously published orbits. The camera angle and plate scale were determined by comparing the data collected

Speckle Interferometry of Binary Star HIP 4849

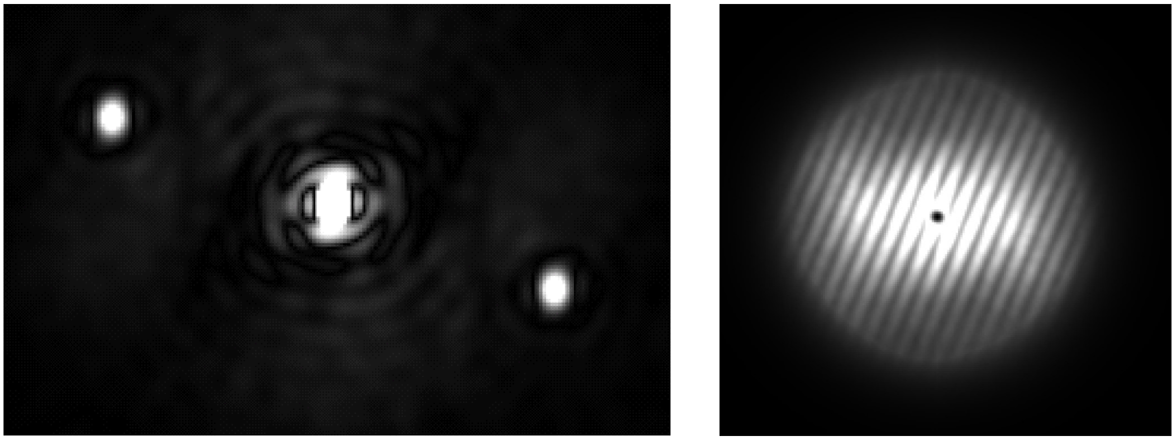

Figure 3. (Left): Autocorrelogram of the Binary HIP 4849; (Right): Power Spectral Density of the Binary HIP 4849

from the run with observed binaries with measured orbits (Wallace 2015). On the week of the observations, the camera angle was established as -11.0492° from true north and the plate scale was found to be 0.01166″ per pixel. Internal precision for the run was determined to be 0.027° and 0.00226″, while the overall accuracy was determined to be 0.4138° and 0.0147″. These values were taken from the statistical analysis of five calibration binaries made during the run (Wallace, 2015).

Reduction

HIP 4849 observations were reduced with PlateSolve 3.44, developed by David Rowe to create an autocorrelogram and power spectral density display of the double star, shown in Figure 3 (Rowe & Genet 2015). The autocorrelogram provided data on the position angle and separation between the stars. The Gaussian Lowpass was set to a 30-pixel radius while the Gaussian Highpass was set to a 3-pixel radius. The high and lowpass filters are important as they improve the signal-to-noise ratio of the images. These filters included the maximum amount of useful data while excluding all unwanted noise.

Results

The single FITS Cube was reduced six times using PlateSolve 3.44 Speckle Reduction tool. The annulus size and center of the target star were selected manually, producing the angle (θ) and separation of the binary (ρ) values as shown in Table 1. Note that the values for the standard deviation and standard error reflect only the internal precision of manually locating the reduction annulus to match the first airy null. These values do not account for any other sources of error that may result from calibration, instrumentation, et cetera.

Table 1. Reduced Data for HIP 4849 (taken from the manual data set)

Reduction	θ°	ρ"
1	79.23	0.724
2	79.44	0.724
3	79.31	0.723
4	79.36	0.725
5	79.21	0.730
6	79.38	0.723
Mean	79.32	0.725
Standard Deviation	0.09	0.003
Standard Error	± 0.04	± 0.001

Speckle Interferometry of Binary Star HIP 4849

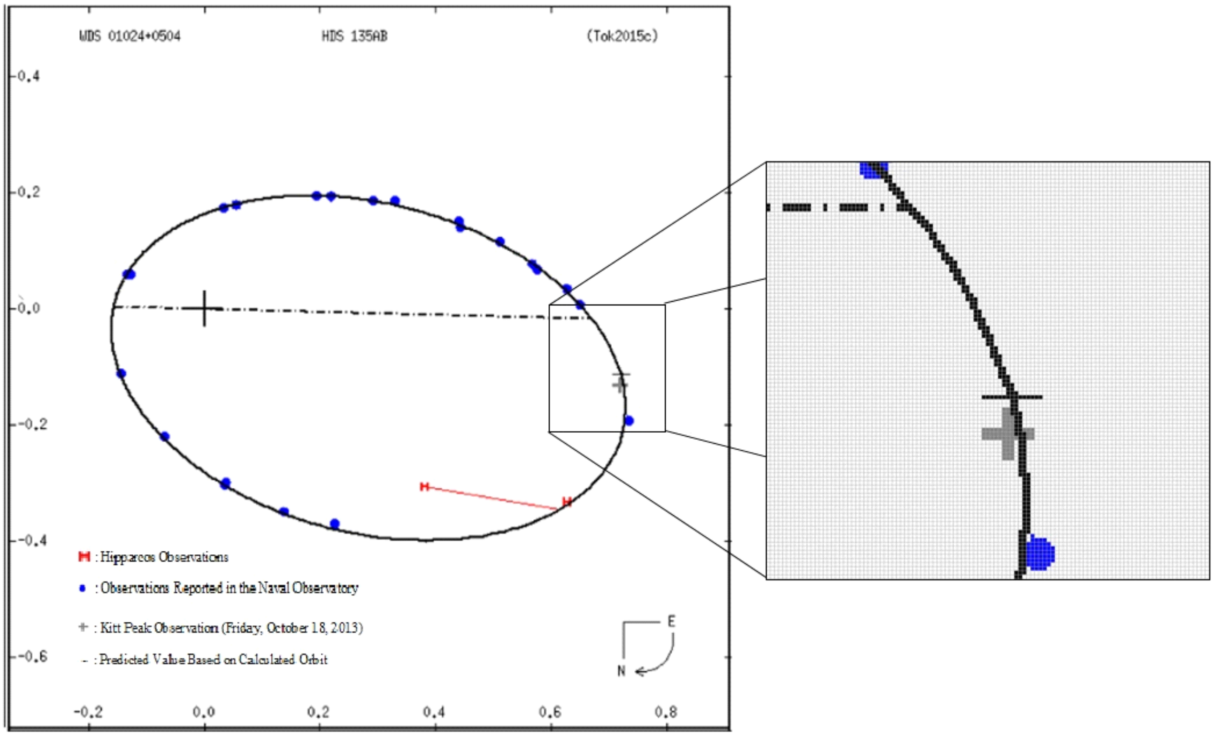

Figure 4. Orbit of Binary Star System HIP 4849. (the plus symbol denotes the added observation of HIP 4849 and the dash crossing the orbit is the predicted position provided by Jack Drummond)

Discussion

The autocorrelogram provided the position angle and separation of the secondary star relative to the primary star. HIP 4849 was compared with previous observations provided by the U.S. Naval Observatory. Using Microsoft Paint, it was determined that there were 0.2" in 97 display pixels. Therefore, the ratio of pixels per arcsecond was determined to be 485:1. This pixel ratio was calculated from the scales shown on the margins in Figure 4. Given the separation distance and angle found using PlateSolve, the distance in both the x and y direction was calculated in arcseconds. Once these values were converted to pixels, they were used to plot the binary (marked as a plus symbol in Figure 4). Our observation of HIP 4849 was plotted on the orbit showing previous observations and one subsequent observation. The location of our added observation in Figure 4 was only 0.0277" (13 pixels) away from the predicted orbit of the system.

To further evaluate the results of this study, the predicted values for the separation and position angle of the binary were determined. This was done using a binary calibration Excel spreadsheet which solves Kepler's equation for any given date. This spreadsheet, created and provided by Jack Drummond, can calculate the position of the secondary star given all published orbits (Drummond 2011). When the October 18, 2013 date was entered into the spreadsheet, it calculated a position angle for 81.0° and separation of 0.742″ for HIP 4849, marked as a dash on Figure 4. This small deviation is consistent with the other small deviations made by other observers since the binary's discovery.

Conclusion

By analyzing a 2013 observation made at Kitt Peak National Observatory of HIP 4849, this study accomplished the goal of adding a new point to the orbital ellipse of the binary. The plotted point did not deviate from patterns observed in previous research. The research served as a successful pilot project by highlighting the processes required for an expanded study on 11 additional binaries discovered by Hipparcos and observed in the Kitt Peak run.

Acknowledgments

We thank Kitt Peak National Observatory for providing the 2.1-Meter telescope used for observations, as well as the 2013 Kitt Peak observers. The speckle interferometry camera system was purchased with funds from the American Astronomical Society's Small Research Grant. We thank David Rowe for developing the PlateSolve 3.44 Speckle Reduction Tool. This research made use of the Washington Double Star Catalog maintained at the U.S. Naval Observatory. We thank Jack Drummond for providing the calibration binaries spreadsheet. In addition, we are grateful for the reviews of this paper provided by Robert Buccheim, Richard Harshaw, William Hartkopf, Thomas C. Smith, and Vera Wallen. Finally, we would like to thank William and Linda Frost for providing funding for the Frost Undergraduate Summer Research Program at California Polytechnic State University, San Luis Obispo, California.

References

Drummond, J. 2011, "Calibration Binaries", *Proceedings of the Advanced Maui Optical and Space Surveillance Technologies Conference*, S. Ryan (Ed.), Wailea, Maui, Hawaii.

Erickson, K. Hipparcos. 2015. science.nasa.gov/missions/hipparcos/

Genet, R., Rowe, D., Smith, T. C., Teiche, A., Harshaw, R., Wallace, D., Weise, E., Wiley, E., Boyce, G., Boyce, P., Brantson, D., Chaney, K., Clark, K. R., Estrada, C., Frey, T., Estrada, R., Wayne, G., Huarberg, N., Kenney, J., Jones, G., Loftin, S., McGieson, I., Patel, R., Plummer, J., Ridgely, J., Trueblood, M., Westergren, D., and Wren, P., 2015a, "Kitt Peak Speckle Interferometry of Close Visual Binary Stars", *Journal of Double Star Observations,* **11**, 234 - 244.

Genet, R., M., Smith, T. C., Clark, K. R., Wren, P., Mathis, H., Summers, D., and Hansey, B. 2015b. "Portable Interferometry Camera Checkout at Kitt Peak", *Journal of Double Star Observations,* **11**, 226 - 233.

Genet, R. M., 2013, "Portable Speckle Interferometry Camera System", *Journal of Astronomical Instrumentation* **2**, 2.

Genet, R. Zirm, H., Francisco, R., Richards, J., Rowe, D., Gray, D. 2015c, "Two New Triple Star Systems with Detectable Inner Orbital Motions", *Journal of Double Star Observations* **11**, 200 - 213.

Hartkopf, W. I., Mason, B. D., Wycoff, G. L., McAllister, H.A. 2014, April 28. *Fourth Catalog of Interferometric Measurements of Binary Stars*.

Labeyrie, A., 1970, "Attainment of Diffraction Limited Resolution in Large Telescopes by Fourier Analysing Speckle Patterns in Star Images", *Astronomy and Astrophysics,* **6**, 85 - 87.

Mason, B., Martin, C., Hartkopf, W. I., Barry, D. J., Germain, M. E., Douglass, G. G., Worle, "Speckle Interferometry of New and Problem Hipparcos Binaries", *The Astronomical Journal*, **117**, 4, 1999.

Perryman, M., 2010, *The Making of History's Greatest Star Map*. New York: Springer.

Rowe, D. and Genet, R. M., 2015, "User's Guide to PS3 Speckle Interferometry Reduction Program", *Journal of Double Star Observations* **11**, 266 - 276.

Schilling, G., 2004, "Putting the Stars in Their Places", *Science* 306, 5700. 1312, *2.1-Meter Telescope on Kitt Peak*. 1998, July 31. www.noao.edu/kpno/40th/2.1m.html

Vernin, J. and Muñoz-Tuñon, C., 1995, "Measuring Astronomical Seeing: The DA/IAC DIMM", *Publications of the Astronomical Society of the Pacific* **107**, 709. 265-272.

Wallace, D., 2015, *An Investigation of Six Poorly Described Close Visual Double Stars Using Speckle Interferometry*, Master's Thesis, Dept. of Space Science, University of North Dakota, Grand Forks.

Watson, A. 1997, "Hipparcos Charts the Heavens", *Science*, **275**, 5303. 1064-1065.

The Spring 2016 Observing Program of Brilliant Sky Observatory: Measurements of 313 Pairs

Richard Harshaw
Brilliant Sky Observatory
Cave Creek, AZ
rharshaw51@cox.net

Abstract: Until approximately a decade ago, speckle interferometry, a double star measurement technique that is capable of high accuracy (because it compensates for atmospheric distortion of star images), had been the domain of professional and graduate student astronomers using large (1 meter and larger) telescopes, high-end (and costly) cameras, and high-powered computing systems. But with the advent of relatively low-cost CCD cameras (and most recently CMOS cameras) and powerful speckle reduction software that runs on a desktop PC, amateurs can now do high quality research and contribute valuable measurements of close double stars (the ones of greatest interest, since their assumed short periods should make orbital solutions possible within a few decades or centuries of their discovery).

This paper presents the measurement of 313 pairs based on the Spring 2016 observing program at Brilliant Sky Observatory, located in Cave Creek, Arizona.

1. Introduction

Advances in high-speed low-cost CCD and CMOS cameras (Ashcraft, 2016) when properly calibrated (Harshaw, 2015) and the availability of powerful speckle interferometry data-reduction software that can run on a 64-bit desktop PC or laptop (Rowe, 2015) have opened the world of speckle interferometry of close visual pairs to amateurs. This is a field that had for decades been the domain of professional astronomers with large instruments, expensive cameras, and mainframe computers.

This report is the fourth in a series on the ongoing CCD and CMOS observing program of double stars at my observatory in Cave Creek, Arizona— Brilliant Sky Observatory. (The other three papers in this expanding series can be found in JDSO Vol 12, No. 4.)

2. Equipment Used

Brilliant Sky Observatory (or BSO - not to be confused with the WDS designation for Brisbane Observatory) houses an 11 inch Celestron SCT mounted on a Celestron CGEM-DX mount atop a Pier Tech adjustable pier. The mount is controlled by a desktop computer using TheSky 6.0.

The camera used for these measurements is a ZWO ASI290MM, a monochrome CMOS camera from ZW Optical of China (see Figure 1). The camera uses a Sony IMX290 chip that has 2.9 micron pixels in an array of 1936×1096 pixels, meaning the chip is 5.614 mm by 3.178 mm, a rather small chip, but the accuracy of the CGEM-DX makes acquisition of stars no problem. (Of course, the small pixels require less magnification

Figure 1: ZWO ASI290MM fitted with a 2x "Shorty" Barlow lens and Johnson-Cousins "R" filter.

too, a plus for acquisition and image quality.)

To get the target pixel scale of 6 pixels per arc second, a 2x Orion "Shorty" Barlow lens was removed from the Barlow and attached directly to the camera. Onto the lens was affixed a Johnson-Cousins "R" (J_cR) filter to reduce dispersion for off-zenith imaging.

After running several drift tests with this setup (Harshaw, 2016d), I used the Speckle Toolbox, a speckle reduction program by David Rowe, to determine the camera angle and pixel scale. The resulting pixel scale was almost exactly what I had targeted - 0.1426 arc seconds per pixel (or 7.013 pixels per arc second).

Images are captured using the latest version of FireCapture (2.5.07 Beta) by Torsten Edelmann. Images are saved to a 128GB USB flash drive for transport later into my home for processing after the observing session. Original files and processed files are stored permanently on a 5TB USB external HDD attached to my office desktop computer (a 64-bit Windows 7 machine), and that drive is in turn backed up to a 5 TB backup drive that is weekly updated with backup software.

3. Methodology

As reported in The Journal of Double Star Observations (JDSO) Volume 4 in the Observing Program papers, I use speckle reduction software to also analyze pairs that are too wide for proper speckle imaging.

Generally, speckle is best done when both stars can be clearly imaged at integration times of 40 milliseconds (ms) or less, and if the seeing is very bad (and it often is on Arizona's desert floor), coherence times of perhaps half that value may be necessary. Similarly, the isoplanatic patch of sky that the light of both stars must traverse must be no larger than 5 arc seconds, and in bad seeing, perhaps even less. Conversely, on nights of superb seeing, the isoplanatic patch might be pushed to 6 or even 7 arc seconds. Experiments by Clif Ashcraft (private correspondence) suggest that in good seeing, good speckle results can be obtained even if one goes a little longer than 40 ms for the integration time.

Some CCD users measure double stars using a process known as "lucky imaging." Lucky imaging is comprised of creating large files (1,000 frames or more) of a pair and then selecting the best 5% (or so) of the frames based on either a signal-to-noise rule (when the frames contain a lot of read noise) or a best-of-maximum rule when the frames are relatively noiseless. The selected frames are then aligned and "stacked" (built into a final composite image) and displayed on the computer monitor. The values for theta and rho can then be read directly off the image once the camera angle and pixel scale have been supplied to the software. Other CCD users simply take long enough exposures to register both stars and then measure them from the single image.

However, I reasoned early on that the speckle reduction software I was using was so accurate for speckle purposes that it should work equally well to measure pairs too wide for "normal" speckle imaging. My results have confirmed this thesis, and, in fact, correspondence with Brian Mason at the U. S. Naval Observatory confirmed my assumption. Mason even stated that the U. S. Naval Observatory uses speckle reduction on CCD images of wider pairs, a fact reported originally by Mason, Hartkopf, and Wycoff (2008). If you ever request a pair's measurement history (a "data request"), you may note that some U. S. Naval Observatory measurements cite a Cu or Su code. These codes indicate that speckle reduction was used on a CCD image to obtain a more accurate measurement, the C and S prefixes indicating which of two cameras were used for the measurements. Cu uses the Naval Observatory's "backup" CCD camera, while Su uses the Observatory's primary CCD camera.

When doing multiple-frame image capture, I capture images in the FITS format which is the standard for astronomical image files. When doing speckle, I capture 1,000 frames and use the Speckle Toolbox to bind them into a single FITS "cube". For speckle, I usually capture several files, depending on a number of factors, such as the seeing that night, the brightness of the pair, and other subjective factors. This approach is used on pairs that (a) are within 5 arc seconds of each other, and (b) can be imaged at 40 ms or less integration time.

My approach when doing speckle reduction of CCD images is to shoot 500 frames of the pair and select the best 10% for keeping and binding into a FITS mini-cube. This approach is used on pairs that are farther apart than 5 arc seconds and/or when the integrating times must be beyond 40 ms. (For instance, an 11th magnitude pair with rho of only 3 arc seconds is well within the isoplanatic patch required for speckle, but the integration time that the ZWO 290 must use to image both stars is beyond 40 ms. This pair would be treated as a speckle/CCD system. As another example, a pair that is, say, 12" in rho will be treated as a speckle/CCD system even if it is bright enough to record with integration times under 40 ms.)

4. Results

The results are reported in groups of stars that share specific characteristics:

1. Known orbits: pairs where an orbit has been computed. Orbits are graded from 1 to 5 and 9, with 9 being a provisional orbit (brand new, not yet tested),

and lower numbers indicating a more and more refined orbit. Normally, a Grade 1 orbit is reserved for pairs that have undergone at least one revolution since discovery and whose measured points can be accurately fitted to an ellipse (the projection of an orbit onto the plane of the sky). An orbital calculation must be accompanied, per convention, by a table of ephemerides. These tables predict the future values of theta and rho for specific epochs. The values for the night of observation can usually be interpolated from the table of ephemerides, or (for greater precision) can be computed from the orbital elements directly.

2. Linears (known or suspected): pairs that are probably optical, pairs that are passing each other like the proverbial "two ships in the night". Like orbits, linear solutions will be accompanied by ephemerides, which allow observers in the future to fit observations to the projections of where they should be for that epoch.

3. Short Arc Binaries: pairs that are showing a small section of arc in the plot of their measurements. These arcs are probably segments of a projected ellipse.

4. Proper Motion Pairs: either CPM, SPM, or DPM. See Harshaw 2016a for an explanation of how the subclasses are determined.

5. Unknown classifications: pairs that do not fit into any of the above phyla.

In Table 1, all observed values of theta (θ) and rho (ρ) are the means of the observations. Residuals are based on comparing the means of the measurements to the last measurement on record.

Table 1: 7 Known Orbit Pairs

WDS No.	Discoverer	Year Last	Last θ°	Last ρ"	Epoch	No. Obs.	Obs θ °	Resid (θ)	Obs ρ "	Resid (ρ)	Notes
11368-1221	BU 456	2014	161.9	1.18	2016.3945	5	168.358	6.458	1.267	0.087	1
12260-1457	BU 606	2014	289.3	0.54	2016.3699	5	289.327	0.027	0.646	0.106	2
13284+1543	STT 266	2013	358	2.1	2016.4548	4	357.153	-0.847	2.031	-0.069	3
13550-0804	STF1788 AB	2012	100	3.6	2016.4164	4	100.748	0.748	3.646	0.046	4
14493-1409	BU 106 AB	2010	2	1.9	2016.4027	3	4.121	2.121	1.993	0.093	5
16044-1122	STF1998 AB	2014	3	1.05	2016.4493	3	9.538	6.538	1.074	0.024	6
16044-1122	STF1998 AC	2014	48	7.02	2016.4493	4	44.734	-3.267	7.626	0.606	7

Notes to Table 1:

1. The Grade 4 orbit was computed in 2012 by J. L. Prieur *et al*. The Ephemerides for this pair show that on the night of observation, theta should be 161.5° and rho 1.162". The measurement made shows residuals of + 6.858° and + 0.105". Figure 2 is a plot of the measurements.

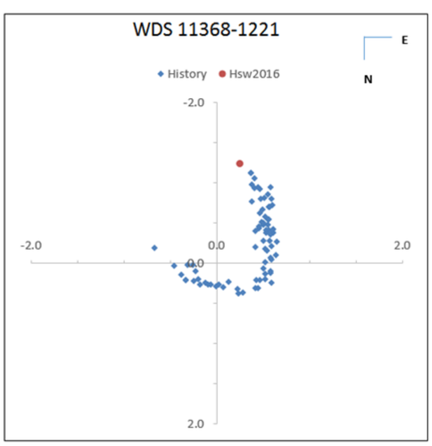

Figure 2.

2. The Grade 5 orbit was computed in 2011 by F. M. Rica Romero and H. Zirm. The ephemerides for the epoch of observation suggest 287.8° and 0.598". Residuals for the measurement obtained are + 1.527° and + 0.048". See Figure 3.

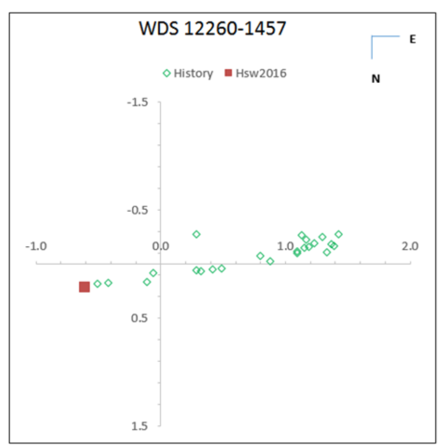

Figure 3.

The Spring 2016 Observing Program of Brilliant Sky Observatory: Measurements of 313 Pairs

3. The Grade 4 orbit was computed by Hartkopf and Mason (2011). The ephemerides suggest 357.6° and 1.999" for the date of the observation. The residuals are -0.447° and + 0.032". See Figure 4.

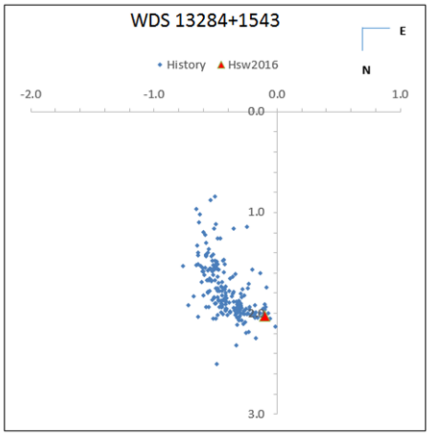

Figure 4.

4. The Grade 5 orbit was computed back in 1970 by J. Hopmann. The ephemerides extrapolate to 99.9° and 3.591" for the epoch of observation. Derived residuals are + 0.848° and + 0.055". See Figure 5.

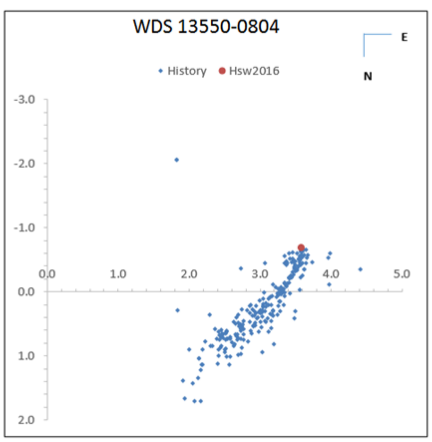

Figure 5.

5. The Grade 5 orbit was computed in 2015 by H. Zirm. The ephemerides predict values of 6.2° and 1.947". The residuals come to -2.079° and + 0.046". I consider this to be one of the weakest measurements of the Spring 2016 program. See Figure 6.

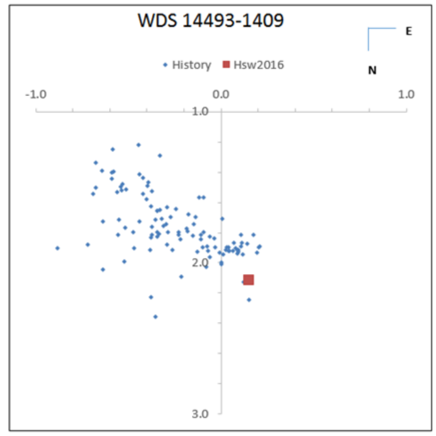

Figure 6.

6. The Grade 1 orbit was computed in 2009 by J. Docobo and J. Ling. The ephemerides predict values of 5.5° and 1.086" resulting in residuals of + 4.038° and - 0.012". This is a poor measurement and should not be taken seriously. See Figure 7.

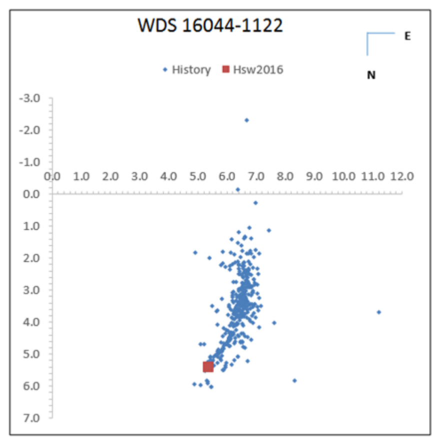

Figure 7.

7. This Grade 5 orbit was computed in 2008 by H. Zirm. The ephemerides forecast values of 43.6° and 7.538", which results in residuals of + 1.134° and + 0.088".

The Spring 2016 Observing Program of Brilliant Sky Observatory: Measurements of 313 Pairs

Table 2. 46 Linear (or suspected Linear) Pairs

WDS No.	Discoverer	Year Last	Last θ°	Last ρ"	Epoch	No. Obs.	Obs θ °	Diff (θ)	Obs ρ "	Diff (ρ)	Notes
10157-1951	ARA 666	2010	2.3	19.89	2016.3699	3	1.098	-1.202	20.674	0.784	1
10201-1356	TDS 580	2005	110.9	4.12	2016.3699	3	108.147	-2.753	5.679	1.559	2
11076-1732	ARA 225 AB	1999	176.7	8.38	2016.3918	1	173.385	-3.315	8.700	0.320	3
11128+0453	J 1011	2013	44.8	3.8	2016.4082	2	43.074	-1.726	4.094	0.294	4
11198-1247	J 1573	2010	214.2	9.2	2016.3918	1	214.102	-0.098	9.247	0.047	5
11212-1047	BRT3212	2001	261.6	4.15	2016.3918	2	261.318	-0.282	4.171	0.021	6
11358-0151	BAL 537	2011	120.9	10.64	2016.4055	1	120.638	-0.262	10.662	0.022	
11452-0248	BAL 218	2011	347.5	12.69	2016.4055	2	347.550	0.005	12.880	0.190	
12087-1050	J 2085	2014	324.7	3.68	2016.3918	1	325.386	0.686	3.540	-0.140	
12095-1151	STF1604 AC	2013	10.0	10.3	2016.3945	3	4.719	-5.281	10.544	0.244	7
12114-1647	S 634	2010	300.0	4.6	2016.4027	8	300.597	0.596	4.679	0.079	8
12151-0715	STF1619 AB	2012	266	6.9	2016.4055	4	265.506	-0.494	6.950	0.050	9
12165-0542	BRT 438	2003	220.8	4.38	2016.4055	1	223.737	2.937	4.366	-0.014	
12270-0137	BAL 541	2013	85.7	12.58	2016.4082	2	85.588	-0.113	12.714	0.134	
12274+0723	STF1644	2010	239	18.8	2016.4164	3	238.663	-0.337	18.970	0.170	10
12464-0720	J 1604	2000	327	9.14	2016.4055	3	327.051	0.0507	9.246	0.106	
12485-1746	FEN 18	2001	217.7	3.88	2016.3699	3	217.167	-0.533	4.056	0.176	
12553-0336	BRT 442	2011	201	8	2016.4055	2	201.497	0.497	8.157	0.157	
13005-0604	HJ 1224	2013	283.2	16.65	2016.4110	2	282.634	-0.566	17.353	0.703	11
13025+1533	BAR 6	2012	42.1	2.96	2016.4521	2	41.572	-0.528	3.082	0.122	
13058+0904	A 1785	2014	129.1	2.51	2016.4493	2	119.571	-9.529	2.457	-0.053	12
13081+2325	COU2708	2011	79	3.84	2016.4575	2	78.100	-0.900	4.038	0.198	13
13092+0848	A 1786	2012	96	13.84	2016.4493	2	95.545	-0.455	14.503	0.663	14
13130-0251	HJ 1228	2011	176	13.9	2016.4110	2	174.824	-1.177	14.078	0.178	
13427-0517	HJ 1239	2011	4	13.3	2016.4164	2	5.198	1.198	13.572	0.272	15
13444-0035	BAL 877	2003	269.2	4.79	2016.4164	2	268.908	-0.292	5.064	0.274	
13450-1955	HJ 2674	2008	17	17.9	2016.4164	2	18.179	1.179	17.735	-0.165	16
13483-0338	J 1608 AB	2012	248.9	6.51	2016.4164	2	248.566	-0.334	6.712	0.202	
14041+0953	HEI 778	2013	350.5	3.2	2016.4548	2	349.968	-0.532	3.357	0.157	
14098+0822	A 1098	2013	279.5	3.76	2016.4575	3	280.695	1.195	3.854	0.094	17
14195-1343	BU 116	2010	274.5	3.92	2016.4027	5	274.090	-0.410	4.184	0.264	18
14209-0458	BRT 452 AB	2003	354.7	4.72	2016.4548	2	354.571	-0.130	4.853	0.133	
14226-0746	STF1833 AB	2012	175	5.8	2016.4329	3	174.771	-0.229	5.970	0.170	19
14245-1608	FOX 183	2012	221	26.2	2016.4329	2	219.582	-1.419	26.589	0.389	
14325-1300	HU 140	2005	194.30	1.32	2016.3644	4	195.970	1.670	1.367	-0.047	
14485-1720	BU 346	2014	277.5	2.71	2016.4027	10	276.603	-0.897	2.700	-0.010	20
14490-1700	HU 477	2009	212.6	4.94	2016.4329	3	210.719	-1.881	4.725	-0.215	21
14579-1853	ARA 426	1999	318	13.96	2016.4329	2	315.631	-2.369	14.503	0.543	
15012-0406	A 14	2012	93.9	3.69	2016.4493	2	95.575	1.674	3.956	0.266	22
15148-0439	A 15 AB	2011	287.5	5.1	2016.4548	2	287.180	-0.321	5.202	0.102	
15163-0705	DOO 57	2013	211.1	5.5	2016.4548	2	210.740	-0.362	5.565	0.065	
15169-0817	STF1925 AB	2014	17.9	6.01	2016.4548	4	16.643	-1.257	6.333	0.323	23
15328-1756	HJ 1273	2000	328.4	14.55	2016.4493	2	327.835	-0.565	14.800	0.250	24
15450-1510	STF3095	2011	323.1	3.1	2016.4521	3	322.998	-0.102	3.228	0.128	25
15568-1854	BRT1495	2002	353.4	3.66	2016.4521	2	353.520	0.120	3.749	0.089	
16085-1940	ARA 703	1999	120.2	14.23	2016.4521	2	119.349	-0.851	14.565	0.335	

The Spring 2016 Observing Program of Brilliant Sky Observatory: Measurements of 313 Pairs

Notes to Table 2

1. Although this pair does not yet have a linear solution, a trend line drawn in Excel (which assigns equal weight to all measures, a process not embraced by astronomers when it comes time to analyze double star measurement data) shows a very strong fit of the points to a line, the R^2 value being 0.9715 (1.0000 indicates a perfect fit). This pair has undergone about 8" in movement in slightly over 100 years, so is probably a strong linear candidate at this time, even though it only has 7 measurements (counting this one) on record.
2. With only 5 measurements (counting this one) on the record, it may be premature to class this pair as a linear one, but the R^2 value is 0.9626 and the companion has moved along this trend line 3.757" in 25 years. The greatly different proper motions (-139 mas RA and +24 mas DEC for the primary, and -31 mas RA and-15 mas DEC for the companion) would result in a total displacement over 25 years of 2.871".
3. Only 7 measurements (counting this one) in 100 years, but showing 3.41" of displacement in 100 years, and with an R^2 value of 0.914 for the trend line. This pair may be linear, especially when one considers the different proper motions (+17 mas RA, +42 mas DEC for the primary, +7 mas RA and -40 mas DEC for the companion). The proper motions alone would account for a displacement of 8.54".
4. This pair (Figure 8) has a solution by Hartkopf (2011c). The ephemerides for the solution indicate 42.44° and 4.268" for the night of the observation, giving residuals of +0.634° and -0.174".
5. With an R^2 value of 0.9655, this pair (with similar proper motions of +45 , +36 primary, -56, +28 companion) has 9 measurements over 113 years. However, the total displacement between the first and last measurements is only 0.293". The high R2 value comes from the other measurements that show some deviation from the first and last measures. Despite the high R^2 value, it is probably premature to assign this pair to the linear solution family.
6. A high R^2 value (0.9757), but only six measures in 110 years. Despite the R^2 value being so strong, it is premature to class this as a linear solution pair.
7. Solved by Hartkopf (2011c, Figure 9), this pair has vastly different proper motions (+321, -161 for the primary, +1, -69 for the companion). The ephemerides suggest 5.6° and 10.381", resulting in residuals of -0.881° and +0.163". My measurement is in much closer keeping with the ephemerides than the last reported value (WSI 2015, a Cu measurement!)

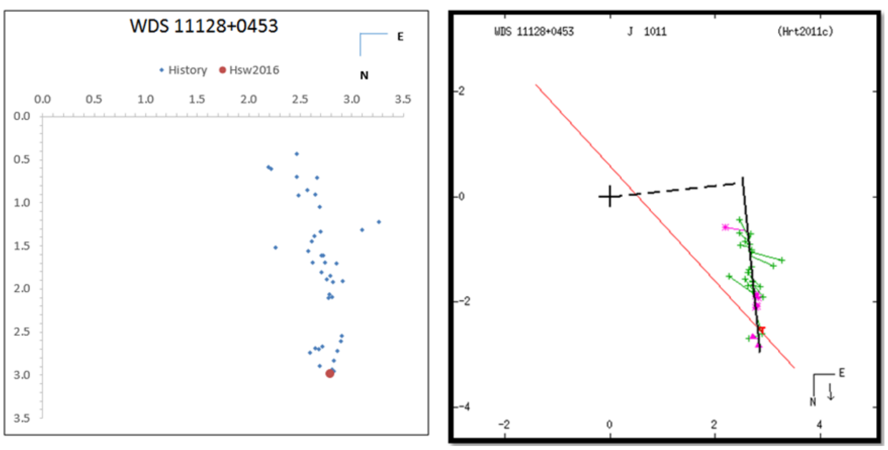

Figure 8: Historical plot of the measurements for J1011 (left) and the Rectilinear Solution

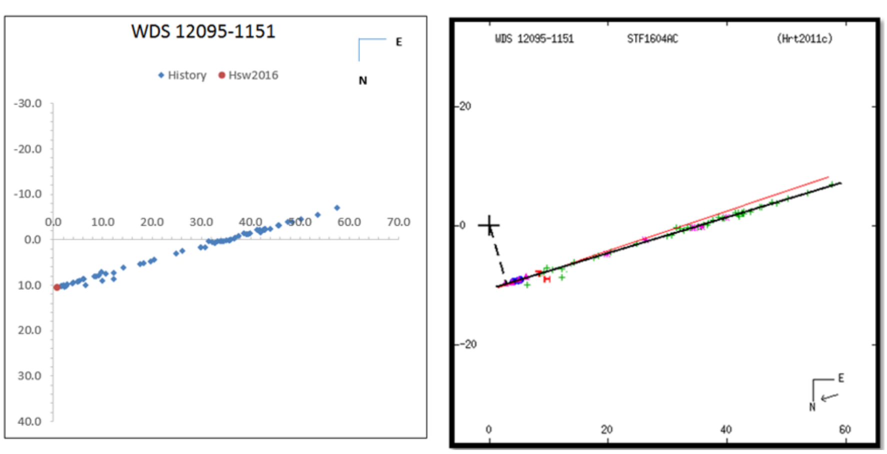

Figure 9: Historical data for STF164AC (left) and the Rectilinear Solution by Hartkopf (right).

8. Measured with speckle. A solution by Hartkopf (2011c) gives ephemerides of 299.9° and 4.673". Residuals versus the projected values show close agreement with Hartkopf's solution, being +0.697° and +0.006". This despite the similarity in proper motions (-154, -57 for the primary, -132, -43 for the companion).
9. A solution by Hartkopf (2011c) gives ephemerides of 266.0° and 6.904". Resulting residuals are -4.494° and +0.046". See Figure 10.

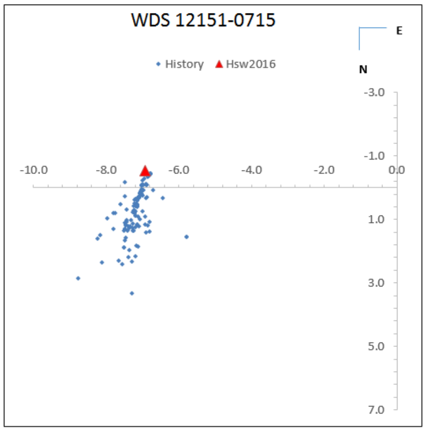

Figure 10.

10. A solution by Hartkopf (2011c) yields ephemerides of 238.6° and 18.596". My residuals are +0.063° and +0.374". In addition, there are three measures from the past that appear to have errors of some sort. These are HJ1828, HJ1830.30, and Smt1888.36.
11. Hartkopf's 2011 solution yields ephemerides of 283.1° and 17.152", giving residuals of -0.466° and +0.201".
12. The measure of Smr2014 should be discounted when attempting a solution of this pair.
13. High similar proper motion pair (-127 -14 P, -91 -15 C).
14. This pair has vastly different proper motions (-128 +17 P, +34 +3 C) and has a trend line whose R^2 value is 0.8722. The companion has moved about 12 seconds since discovery 109 years ago, and so this is most likely a true linear pair. The difference in proper motions alone could account for as much as 17.73" of movement since discovery. See Figure 11.
15. This pair has a fairly high correlation to the trend line (0.8577) and shows about 13" over the 188 years since discovery and has a large difference in proper motions (-61 -19 P, -8 -7 C). Displacement by the proper motion vectors alone would account for 10.077", so it is probably safe to class this pair as a linear case. See Figure 12.
16. Hartkopf derived a solution in 2011 which yields ephemerides of 18.2° and 17.607". The resulting residuals are -0.021° and +0.128". In addition, the measurement of EGB1880.42 looks to be in distress. The R^2 value of the trend line without it is 0.9637.

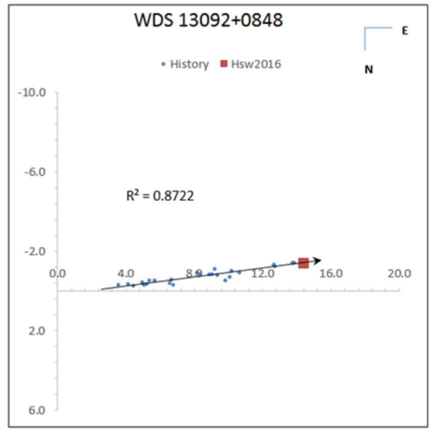

Figure 11.

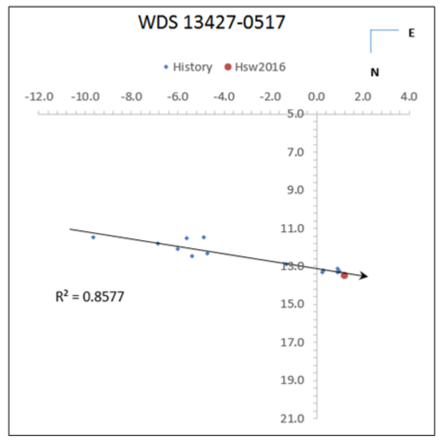

Figure 12.

17. Two measurements from the past look suspicious and should probably be assigned lower weights when a solution on this pair is someday attempted. They are Brt1919.43 and WFC1919.43. In the plot below, these data points have been removed, showing a linear pattern in better detail. See Figure 13.

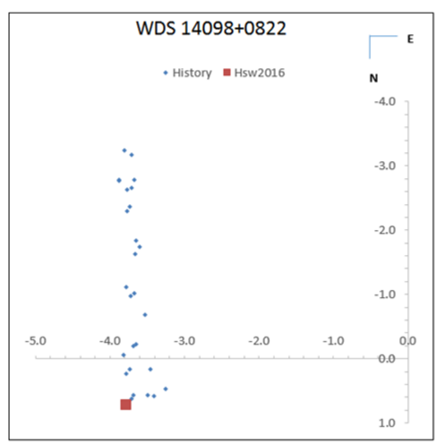

Figure 13.

18. Measured with speckle. A solution exists (Hartkopf, 2011c) and gives ephemerides for this epoch of 274.4° and 4.008". My residuals are therefore -0.310° and 0.176". These residuals are closer to the projection of Hartkopf than those based on the last measurement (WSI2010.435).

19. Measured with speckle. See Figure 14.

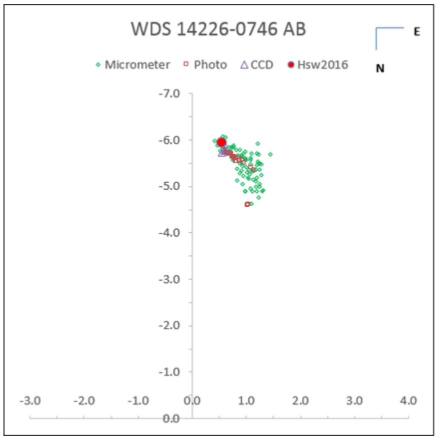

Figure 14.

20. Measured with speckle. A solution by Hartkopf (2011c) generates ephemerides of 276.3° and 2.718" for the night of the measurement. The residuals based on these data are +0.303° and -0.018", values that are a little better than those based on the last measurement (TOK2014.303). See Figure 15.

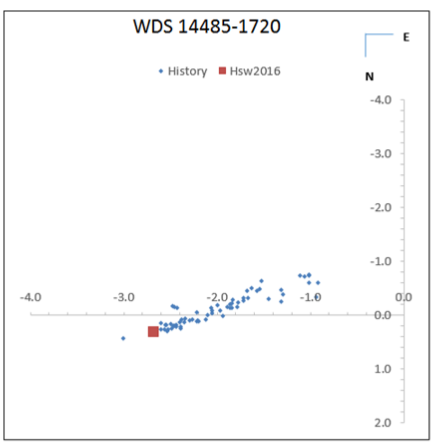

Figure 15.

21. Measured with speckle. The measure by Comellas in 1980 looks like a quadrant reversal (rho off by 180°).

22. This pair has no linear solution yet, but the R^2 value is high (0.9147) although the system has similar proper motions (-13 +3 P, -8 +5 C). The companion has moved about 4" in 117 years. See Figure 16.

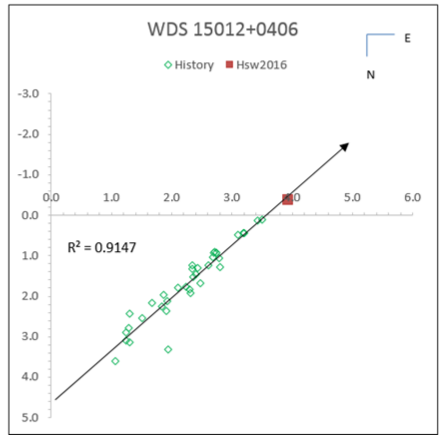

Figure 16.

23. Measured with speckle. Hartkopf's 2011c linear solution generates ephemerides of 17.7° and 6.248". This makes the residuals compared to the projection by Hartkopf -1.057° and +0.085", values that are a little better than those based on the last measurement (Schlimmer, Smr2014.504). See Figure 17.

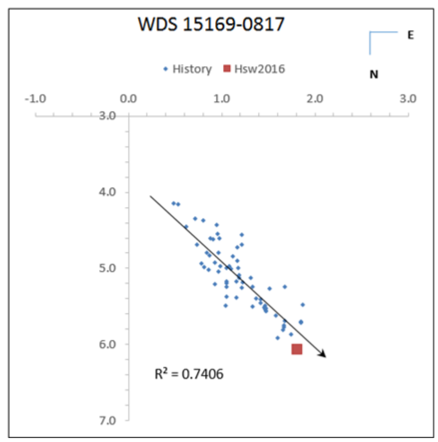

Figure 17.

24. Two measurements lie far from the bulk of the data and should probably be discounted during a solution. These are HJ1828 and WFC1916.18.

25. Measured with speckle. The Glasenapp measure of 1890.47 is well off the norm.

The Spring 2016 Observing Program of Brilliant Sky Observatory: Measurements of 313 Pairs

Table 3: 10 Short Arc Binary Pairs

WDS No.	Discoverer	Year Last	Last θ°	Last ρ"	Epoch	No. Obs.	Obs θ°	Resid (θ)	Obs ρ "	Resid (ρ)	Notes
12008-1209	HU 132	2001	84	1.7	2016.3699	5	86.607	2.607	1.722	0.022	
12413-1301	STF1669 AB	2013	314	5.2	2016.3918	4	313.170	-0.830	5.276	0.075	
13028-0631	BU 927	2004	292.7	4.26	2016.4110	2	291.083	-1.617	4.282	0.022	
13142-1634	RST3827 AB	2014	259.8	1.6	2016.4438	3	259.094	-0.706	1.662	0.062	26
13343-0837	BU 114	2013	171	1.2	2016.4438	3	172.957	1.957	1.415	0.215	27
13343-0837	HU 896	1991	20	1.2	2016.4438	3	20.126	0.126	1.167	-0.033	28
13598+1953	STF1794	2013	127	1.8	2016.4548	4	126.018	-0.982	1.972	0.172	29
14247-1140	STF1837	2006	274.00	1.10	2016.3644	6	270.088	-3.912	1.268	-0.168	30
15055-0701	BU 119 AB	2009	273	2.1	2016.4548	3	273.942	0.942	2.359	0.259	31
15399-1946	BU 122	2009	228	1.9	2016.4548	4	227.440	-0.560	1.817	-0.083	32

Notes to Table 3:

26. Measured with speckle. With such an R^2 value (0.9112) and such high common proper motion (+136 -141 P, +136 -143 C), the pair is most likely physical. See Figure 18.
27. Measured with speckle.
28. Measured with speckle.
29. Measured with speckle.
30. Measured with speckle.
31. Measured with speckle. See Figure 19.
32. Measured with speckle.

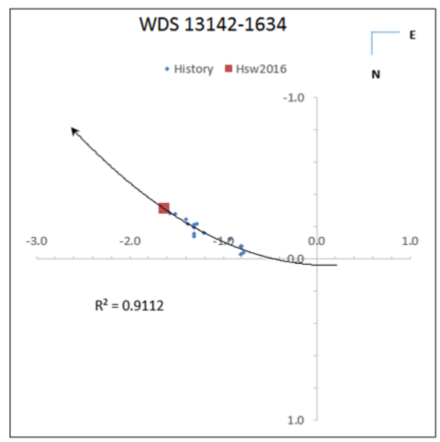

Figure 18.

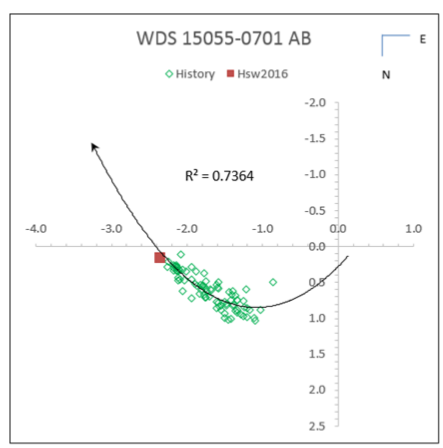

Figure 19.

The Spring 2016 Observing Program of Brilliant Sky Observatory: Measurements of 313 Pairs

Table 4: 203 Proper Motion Pairs

WDS No.	Discoverer	Year Last	Last θ°	Last ρ"	Epoch	No. Obs.	Obs θ°	Resid (θ)	Obs ρ "	Resid (ρ)	Type	Notes
09596-1457	HJ 825	2010	314.2	10.25	2016.3699	4	313.174	-1.026	10.304	0.0535	CPM	33
10006-1807	RST2664	1991	207.2	0.66	2016.3699	4	213.809	6.609	0.696	0.0362	CPM	
10066-1919	S 607 AB	2010	326.9	9.55	2016.3730	4	327.745	0.845	9.630	0.0796	CPM	
10152-1729	RST3687	2003	206.8	3.77	2016.3730	2	207.710	0.909	3.800	0.0299	DPM	
10316-1624	SKI 14	2010	82.2	7.08	2016.3699	3	80.908	-1.292	7.142	0.0621	DPM	
10325-1203	SCA 61	2010	257.2	19.28	2016.3730	1	256.815	-0.385	19.554	0.2735	CPM	
11022+0945	HJ 172	2013	94	13.4	2016.4082	3	94.129	0.129	13.589	0.1888	CPM	34
11022+0954	STF1503	2013	271	11.5	2016.4082	3	270.578	-0.422	11.578	0.0778	CPM	
11045-1940	HDS1580	2012	285	17.4	2016.3699	3	284.514	-0.486	17.529	0.1288	SPM	
11050-1510	BRT1913	2004	321.7	3.76	2016.3730	3	319.496	-2.204	3.669	-0.0914	DPM	
11061+0702	STF1507	2013	164	8.3	2016.4082	3	165.159	1.159	8.454	0.1542	SPM	
11061-0041	A 2573	2001	109.3	3.21	2016.4027	3	107.778	-1.522	3.262	0.0521	DPM	
11074-0114	BAL 865	2000	215.8	9.68	2016.4082	2	218.021	2.220	9.723	0.0434	DPM	35
11082+0634	HJ 839 AB	2013	96	12.1	2016.4082	3	95.844	-0.156	12.375	0.2745	SPM	36
11085+0118	BAL1443	2010	183	9.6	2016.4082	2	175.356	-7.644	6.424	-3.1765	SPM	37
11136-1558	ARG 24	2012	350	17.6	2016.3730	4	349.926	-0.074	17.715	0.1150	CPM	
11153-1730	HU 461	2000	76.6	1.9	2016.3699	4	76.441	-0.159	1.910	0.0099	CPM	
11154-1807	LDS 342 AB	2007	262	18.8	2016.3730	3	261.219	-0.781	18.755	-0.0445	CPM	38
11189-1146	HU 130	2005	115.4	1.1	2016.3699	4	108.621	-6.779	1.044	-0.0563	CPM	
11193+0117	BAL1445	2013	344.3	4.44	2016.4082	2	343.334	-0.966	4.622	0.1821	DPM	
11197-0654	STF1530	2013	313	7.7	2016.4055	3	313.461	0.461	7.728	0.0284	CPM	
11245-0423	STF3070	2011	277	8.8	2016.4055	3	277.171	0.171	8.877	0.0765	DPM	39
11245-0938	J 2081	2005	359.7	3.15	2016.4082	2	358.179	-1.521	2.734	-0.4156	CPM	
11262-1240	J 1575	2000	301.6	8.2	2016.3918	1	301.438	-0.162	8.370	0.1704	DPM	
11268-1626	FOX 67	2005	195.9	1.65	2016.3918	3	194.262	-1.638	1.772	0.1225	CPM	
11292-1721	H 4 112 AB	2012	331	28.2	2016.3730	4	330.198	-0.802	27.658	-0.5421	SPM	
11299-0458	HJ 2573	2011	18.6	7.94	2016.4027	4	18.607	0.006	7.969	0.0286	DPM	41
11309-0643	STF3072	2013	331	9.8	2016.4055	3	331.024	0.024	9.977	0.1766	CPM	42
11321-0332	STF1548 A,BC	2012	127	10.7	2016.4055	3	126.792	-0.208	10.899	0.1994	CPM	43
11344-1707	J 1576	1999	59	11	2016.3945	2	58.081	-0.919	11.024	0.0237	CPM	
113695-1355	HU 131	2000	155.4	3.09	2016.3945	3	152.100	-3.300	3.087	-0.0028	DPM	
11376-1656	HJ 1192	2012	358	13.6	2016.3945	3	357.961	-0.039	13.700	0.0995	CPM	
11403-0926	J 2659	2011	232.2	7.6	2016.4082	2	232.454	0.254	7.614	0.0144	DPM	
11412+0950	HJ 187	2006	11.4	9.35	2016.4082	2	8.747	-2.653	9.696	0.3461	DPM	
11426-1523	J 1579	2005	316	6.03	2016.3918	1	315.686	-0.314	6.148	0.1175	DPM	
11430-1805	ALD 49	2003	77	4.07	2016.3730	2	75.721	-1.280	3.996	-0.0739	DPM	
11480-0838	STF3074	2013	302	10.9	2016.4055	3	302.108	0.108	11.050	0.1502	CPM	
11520-0824	HJ 843 AB,C	2012	263	10.2	2016.4055	2	263.176	0.176	10.347	0.1467	DPM	
11539-1423	HLD 113	2010	269.9	3.4	2016.3945	3	269.633	-0.267	3.403	0.0026	DPM	44
11566-0437	STF1584	2013	188	13.1	2016.4055	3	188.194	0.194	13.183	0.0830	CPM	
11566-0514	STF3076	2009	55	5.9	2016.4055	3	54.163	-0.837	6.034	0.1336	SPM	

Table 4 continues on next page.

The Spring 2016 Observing Program of Brilliant Sky Observatory: Measurements of 313 Pairs

Table 4 (continued): 203 Proper Motion Pairs

WDS No.	Discoverer	Year Last	Last θ°	Last ρ"	Epoch	No. Obs.	Obs θ°	Resid (θ)	Obs ρ "	Resid (ρ)	Type	Notes
11582-1045	J 2084	2000	232.4	3.48	2016.3945	3	231.586	-0.814	3.602	0.1215	DPM	
11597-1137	BRT3213	2000	238.3	3.14	2016.3945	3	238.037	-0.263	3.279	0.1388	SPM	
12035-0227	STF1593 AB	2005	13.9	1.28	2016.4329	3	13.958	0.058	1.230	-0.0496	CPM	45
12062-1853	HJ 4496	2010	28	12.3	2016.3945	3	28.018	0.018	12.369	0.0691	CPM	
12084-1835	BU 412	2014	152.3	1.76	2016.3918	7	152.000	-0.300	1.988	0.2279	CPM	
12103-0623	TDS8253	2014	76.5	3.67	2016.4055	2	74.220	-2.281	3.546	-0.1243	DPM	
12107-0445	STF3079	2002	87	15.4	2016.4055	2	87.375	0.375	15.198	-0.2023	CPM	
12113-0753	A 142	2001	24.8	1.94	2016.4329	3	24.294	-0.506	1.893	-0.0470	CPM	46
12116-1341	STF3080	2003	200	4.7	2016.4027	3	199.730	-0.270	4.707	0.0068	DPM	
12149-0051	BAL 867	2000	357.5	6.5	2016.4055	2	357.416	-0.084	6.586	0.0858	CPM	
12153-0146	J 430	2001	274.4	3.42	2016.4055	2	273.594	-0.807	3.388	-0.0319	DPM	
12210-0131	BAL 868	2013	135.1	6.61	2016.4055	2	135.424	0.324	6.597	-0.0132	DPM	
12211-1129	STF1635	2004	173	13.3	2016.4027	2	172.573	-0.427	13.411	0.1112	CPM	
12247+0225	AG 177 AB	2013	220	7.9	2016.4164	2	219.630	-0.370	7.755	-0.1449	CPM	
12276-1826	HU 466	2000	212.3	2.84	2016.3730	3	213.344	1.044	2.778	-0.0624	DPM	
12288-1040	RST3792	2000	234.1	3.66	2016.3730	3	233.681	-0.419	3.754	0.0937	SPM	47
12303-1331	RST3795	1991	197.7	1.59	2016.3730	3	200.949	3.249	1.667	0.0775	CPM	
12306+0331	STF1648	2013	40	7.7	2016.4164	3	39.831	-0.169	8.082	0.3822	CPM	
12316-1104	STF1649	2009	196	15.3	2016.3918	4	193.515	-2.485	15.744	0.4439	SPM	
12323-0154	HJ 211	2008	278.1	11.5	2016.4082	2	278.494	0.394	11.139	-0.3608	SPM	48
12328-0104	BAL 869	2013	235.9	7.23	2016.4082	2	236.175	0.275	7.243	0.0128	DPM	
12357-1201	STF1659 AB	2011	351	27.5	2016.3699	4	350.643	-0.357	27.911	0.4107	CPM	
12387-0520	STF1665	2013	102	8.5	2016.4055	4	102.005	0.005	8.644	0.1442	CPM	
12391-0133	HJ 1220	2013	52.2	6.93	2016.4110	2	52.224	0.024	7.061	0.1312	CPM	
12420-0156	BAL 545	2004	163.4	4.35	2016.4055	2	161.673	-1.728	4.286	-0.0638	DPM	
12432+0000	BAL1162	2009	303	14.8	2016.4164	2	303.220	0.219	15.269	0.4688	CPM	
12490-1338	HU 135	2013	349.8	3.41	2016.3699	3	349.082	-0.718	3.520	0.1101	DPM	
12496+0349	STF1681	2013	18	9.1	2016.4164	3	17.432	-0.568	9.162	0.0620	CPM	
12505-1835	HU 136	1999	134.8	1.05	2016.3699	3	129.850	-4.950	1.115	0.0651	CPM	
12515-1920	J 1584	2012	273	11	2016.4027	1	273.464	0.464	11.338	0.3375	DPM	
12518-0608	STF1683	2012	198	15.3	2016.4055	2	196.880	-1.121	15.671	0.3711	SPM	
12519-1404	BRT2731	2009	75	4	2016.4027	3	72.336	-2.664	3.785	-0.2152	DPM	
12530+0638	J 1024	2013	65.2	3.54	2016.4164	2	66.109	0.909	3.598	0.0585	DPM	
12559+0812	HJ 850	2000	172.7	11.57	2016.4164	2	172.738	0.038	11.710	0.1403	CPM	49
12563-0452	STF1690	2013	149	5.9	2016.4055	4	148.532	-0.468	5.863	-0.0371	CPM	
12567+0701	STF1693	2013	332	8.7	2016.4164	3	331.972	-0.028	8.734	0.0344	CPM	
12595-1133	RST3817	1997	138.6	1.53	2016.3918	5	144.830	6.230	1.576	0.0455	CPM	
13008+0252	HLD 14 AB	2002	262.1	3.49	2016.4493	2	263.449	1.349	3.526	0.0357	DPM	
13010+0221	J 1025	2013	178.5	5.6	2016.4493	2	178.224	-0.276	5.635	0.0355	DPM	
13012+1552	STF1707	2011	40	8.2	2016.4521	2	40.516	0.515	8.257	0.0574	SPM	
13021+0717	STF1708	2012	294	11.4	2016.4164	3	294.071	0.071	11.619	0.2187	CPM	50

Table 4 continues on next page.

The Spring 2016 Observing Program of Brilliant Sky Observatory: Measurements of 313 Pairs

Table 4 (continued): 203 Proper Motion Pairs

WDS No.	Discoverer	Year Last	Last θ°	Last ρ"	Epoch	No. Obs.	Obs θ°	Resid (θ)	Obs ρ "	Resid (ρ)	Type	Notes
13025+2330	STF1709	2012	250.7	2.73	2016.4575	3	251.639	0.939	2.674	-0.0564	CPM	51
13027-0159	HJ 1225	2012	111	14.9	2016.4110	3	110.943	-0.057	15.042	0.1418	CPM	52
13031-1210	HU 137	2001	117.2	3.54	2016.3699	3	115.659	-1.541	3.679	0.1391	DPM	
13035+0928	STF1712	2011	332	9	2016.4164	3	331.987	-0.013	9.106	0.1060	CPM	
13042+1924	STF1715	2012	231	6.8	2016.4521	2	231.191	0.191	7.277	0.4772	CPM	53
13058+2614	HO 257	2010	155.2	1.99	2016.4575	2	153.547	-1.653	2.023	0.0328	CPM	54
13058-0503	A 10	2000	353.6	2.87	2016.4466	2	353.126	-0.474	2.981	0.1111	DPM	
13068+2836	AG 344	2006	156	18.7	2016.4575	2	155.769	-0.231	19.174	0.4743	CPM	
13073+0035	STF1719 AB	2012	358	7.4	2016.4493	3	357.794	-0.206	7.064	-0.3360	SPM	
13084+1529	STF1722	2011	337	2.5	2016.4521	4	336.153	-0.847	2.731	0.2314	CPM	
13085+0107	STF1721	2012	2	6.3	2016.4493	2	357.900	355.900	6.449	0.1485	CPM	55
13085-0053	J 434	2011	324.9	3.05	2016.4466	2	322.790	-2.110	3.289	0.2387	DPM	56
13095-1313	BRT2732	2001	281.3	3.83	2016.3699	3	282.345	1.045	4.144	0.3144	DPM	
13100+2840	BRT 26	2003	326.3	4.42	2016.4575	2	325.210	-1.090	4.590	0.1702	DPM	
13127-1500	BRT 579	1999	60.3	2.83	2016.4027	2	58.100	-2.201	2.796	-0.0338	DPM	
13132-0233	STF1731 AB	2011	303	9.4	2016.4110	3	302.494	-0.506	9.589	0.1887	CPM	
13133-1528	BU 221	2000	47.3	1.66	2016.4329	3	46.028	-1.272	1.669	0.0087	CPM	57
13134-1850	SHJ 161	2013	35	4	2016.4082	8	33.060	-1.940	5.437	1.4367	CPM	58
13137-0134	BAL 549	2000	289.6	19.48	2016.4110	2	290.156	0.556	19.851	0.3712	DPM	
13151+2725	B 1	2002	93.5	3.42	2016.4575	2	94.023	0.523	3.574	0.1536	CPM	
13152-1855	BU 342	2010	35	4	2016.4082	8	34.981	-0.019	4.078	0.0777	CPM	
13163+1715	STF1733	2011	129	4.7	2016.4521	3	128.389	-0.611	5.017	0.3171	DPM	59
13169+0211	AG 186	2007	307.1	3.82	2016.4493	2	305.252	-1.848	3.826	0.0058	CPM	
13196+0116	BAL1456	2002	172.3	3.37	2016.4493	2	171.773	-0.528	3.473	0.1028	DPM	
13199-1937	RST2840	2002	351.6	2.55	2016.4438	2	349.680	-1.921	2.758	0.2076	SPM	
13217+1542	FOX 177	2013	87	17.1	2016.4521	2	86.437	-0.563	17.392	0.2915	CPM	
13218+0550	STF1735	2008	110	4	2016.4493	3	109.213	-0.787	4.138	0.1377	CPM	
13218+1746	STF1737	2008	220	14.8	2016.4521	1	218.870	-1.130	15.305	0.5053	CPM	
13219-0239	BAL 224	2011	71	10.6	2016.4110	2	70.256	-0.744	10.696	0 .0963	DPM	
13223-1137	LDS 439	2000	278	15.1	2016.4110	2	277.958	-0.042	15.395	0.2953	CPM	60
13228-1311	H IV 119	2008	312	19.3	2016.4027	3	311.170	-0.830	19.521	0.2214	SPM	
13229-1854	J 1585	2013	51.7	5.9	2016.4110	2	50.060	-1.641	5.874	-0.0259	DPM	
13231-1326	BRT2734	2000	255	4.53	2016.4110	2	254.726	-0.275	4.619	0.0889	DPM	
13233-1456	STF1738	2010	278	3.6	2016.4027	3	277.808	-0.192	3.974	0.3743	SPM	61
13236+2825	BRT 27	2004	319	3.98	2016.4575	2	320.031	1.031	4.039	0.0588	DPM	
13248-1320	RST3838	1997	151.4	1.45	2016.4438	2	161.919	10.519	1.325	-0.1248	CPM	62
13252+1518	J 749	2013	286.3	2.72	2016.4548	2	286.555	0.255	2.815	0.0952	DPM	
13254-0735	STF1743	2013	78	6	2016.4110	6	77.796	-0.205	6.075	0.0751	CPM	
13263-0818	HJ 848	2012	309	11.7	2016.4110	2	308.635	-0.365	11.843	0.1431	DPM	63
13269+1422	BU 237	2013	211.6	3.08	2016.4548	2	212.842	1.242	3.193	0.1134	CPM	64
13276+0655	HJ 1232	2010	307	12.8	2016.4493	2	306.082	-0.919	12.843	0.0428	CPM	65

Table 4 continues on next page.

The Spring 2016 Observing Program of Brilliant Sky Observatory: Measurements of 313 Pairs

Table 4 (continued): 203 Proper Motion Pairs

WDS No.	Discoverer	Year Last	Last θ°	Last ρ"	Epoch	No. Obs.	Obs θ°	Resid (θ)	Obs ρ "	Resid (ρ)	Type	Notes
13291+1907	BRT2416	2002	200.5	2.89	2016.4548	2	203.052	2.552	2.898	0.0079	DPM	
13333+2301	STF1756	2004	177	14.8	2016.4575	3	176.899	-0.101	14.709	-0.0907	CPM	
13343-0837	HU 469	1999	26.5	1.24	2016.4438	3	23.370	-3.130	1.275	0.0349	CPM	
13376-0752	STF1763 AB	2010	39.1	2.66	2016.4466	4	39.051	-0.049	2.755	0.0948	CPM	66
13376-1048	STF1762 AB	2009	277	4.4	2016.4027	3	275.639	-1.361	4.702	0.3018	CPM	67
13377+0223	STF1764 AB	2011	31	15.8	2016.4493	3	30.995	-0.005	16.147	0.3467	CPM	
13384+0440	BRT2153 AB	2013	17.9	5.7	2016.4493	2	17.976	0.076	5.802	0.1018	DPM	
13403+0709	HJ 1238 AB	2013	307.3	14.33	2016.4493	2	306.940	-0.361	14.515	0.1847	CPM	68
13412+1624	COU2192	2014	273	2.4	2016.4548	2	271.499	-1.501	2.470	0.0701	DPM	
13421-0918	BRT 448	2003	3.9	4.16	2016.4110	2	5.245	1.345	4.180	0.0196	DPM	
13433+1235	TDS8944	2013	25.4	3.08	2016.4548	2	25.206	-0.194	3.099	0.0190	DPM	
13452-0319	BU 223	2000	343	18.7	2016.4164	2	343.112	0.112	18.885	0.1845	CPM	
13452-1150	STF3081	1999	66.3	2.08	2016.4329	3	65.497	-0.803	2.195	0.1153	CPM	69
13455-0301	WNC 5	2009	163	3.95	2016.4164	2	163.135	0.135	4.105	0.1550	SPM	
13461-1833	HU 473 AB	2001	65.1	2.98	2016.4027	3	63.192	-1.908	3.055	0.0754	DPM	
13464-1703	TDS8961	2003	50.7	3.6	2016.4027	3	51.594	0.894	3.719	0.1190	DPM	
13485-0124	BAL 879	2011	143.5	6.98	2016.4164	2	143.404	-0.096	7.059	0.0792	CPM	
13496+0054	BAL1460	2001	310.3	3.37	2016.4493	2	310.326	0.026	3.451	0.0810	DPM	70
13499-1523	BRT 582	2001	135.4	3.73	2016.4027	2	133.708	-1.693	3.747	0.0175	DPM	
13514-0603	HJ 1243	2000	152	8.7	2016.4164	2	150.937	-1.063	8.514	-0.1855	DPM	71
13520-1955	HJ 2687	2007	140	15.8	2016.4082	3	140.766	0.766	15.988	0.1881	SPM	
13557-0925	J 1609	2012	280.3	10.54	2016.4164	2	280.053	-0.247	10.689	0.1489	CPM	
13561-0437	STF1790	2012	62	5.7	2016.4164	3	61.568	-0.432	5.770	0.0701	CPM	
13571+1227	STF1792	2013	291.3	2.19	2016.4548	3	290.587	-0.713	2.285	0.0947	CPM	72
13572-1233	HJ 4637	2012	142	13.4	2016.4082	3	141.584	-0.416	13.622	0.2215	SPM	
13577-1717	WHC 12 AB	2008	321.4	3.15	2016.4110	3	319.650	-1.750	3.141	-0.0087	SPM	
14008-0232	BAL 229	2006	73.7	17.26	2016.4329	2	72.888	-0.813	17.573	0.3131	CPM	73
14037+0243	AG 192	2007	8	3.04	2016.4548	3	7.797	-0.203	3.195	0.1552	CPM	
14048-0633	STF1799	2008	287.5	4.44	2016.4438	3	296.427	8.927	4.367	-0.0726	CPM	
14077+0616	TDS 739	2010	230.3	2.01	2016.4575	2	231.149	0.849	2.130	0.1197	CPM	
14081-1256	STF1802	2012	276	6	2016.4027	7	275.865	-0.135	6.079	0.0786	CPM	74
14083-0012	BAL1169	2007	298.8	14.1	2016.4466	2	297.202	-1.598	13.751	-0.3489	CPM	
14089-0336	HLD 16	2012	217.2	2.91	2016.4493	3	216.724	-0.476	2.872	-0.0384	DPM	75
14097-1104	MRG 1	2002	320.1	1.21	2016.4438	2	317.282	-2.818	1.411	0.2009	CPM	
14100+0401	STF1805	2008	34	4.7	2016.4575	3	32.772	-1.228	4.914	0.2140	CPM	76
14113-0320	STF1807	2012	28	6.5	2016.4493	3	28.015	0.015	6.621	0.1208	CPM	
14114-1930	HU 899	1991	295.7	1.59	2016.4438	2	299.813	4.113	1.767	0.1765	CPM	
14121-0846	J 1611 AB	2012	337.5	6.47	2016.4521	2	337.182	-0.319	6.550	0.0799	DPM	
14134+0524	STF1813	2013	193	4.6	2016.4575	4	192.853	-0.147	4.809	0.2085	CPM	77
14152-0305	BAL 233	2006	304.1	17.21	2016.4521	2	303.788	-0.312	17.586	0.3755	CPM	

Table 4 concludes on next page.

The Spring 2016 Observing Program of Brilliant Sky Observatory: Measurements of 313 Pairs

Table 4 (conclusion): 203 Proper Motion Pairs

WDS No.	Discoverer	Year Last	Last θ°	Last ρ"	Epoch	No. Obs.	Obs θ°	Resid (θ)	Obs r "	Resid (ρ)	Type	Notes
14163+0605	STF1824	2011	280.2	5.25	2016.4575	4	279.771	-0.429	5.533	0.2827	DPM	78
14190-0713	J 2903	2003	39.3	3.69	2016.4521	2	35.587	-3.714	3.822	0.1320	DPM	79
14219-1344	HJ 4674	2010	279.2	17.46	2016.4027	2	278.988	-0.213	17.667	0.2073	DPM	
14287-1104	WFC 150	2000	167.2	6.64	2016.4329	3	166.948	-0.252	6.757	0.1171	DPM	
14295-1501	EGB 3	2011	197.7	3.74	2016.3644	3	197.642	-0.058	3.797	-0.0574	DPM	
14300-0343	BU 462 AB	2011	322.3	2.13	2016.4438	3	322.217	-0.083	2.202	0.0717	CPM	
14303-1111	TDS9221	1991	101.20	0.53	2016.3644	3	102.713	1.513	0.662	-0.1317	CPM	
14324-1524	RST3884	1943	8.40	1.67	2016.3644	1	6.502	-1.898	1.686	-0.0163	CPM	
14340-0507	A 2589	1991	203.9	0.95	2016.4438	3	202.375	-1.525	1.137	0.1872	CPM	
14343-1836	ARA 425	2001	219.20	5.49	2016.3644	2	216.372	-2.828	5.461	0.0293	DPM	
14358-0014	HJ 1256	2000	59.9	10.19	2016.4438	2	59.353	-0.547	10.356	0.1655	SPM	80
14384-1940	HJ 2734 AB	1999	215.4	13.99	2016.4329	3	214.822	-0.578	14.415	0.4249	DPM	
14497-0401	RST1807	2002	357.2	1.92	2016.4548	2	356.684	-0.516	2.038	0.1184	CPM	81
14506-0001	STF1885	2011	144.4	4.05	2016.4493	3	144.697	0.297	4.168	0.1180	DPM	82
14509-0810	BRT 551	2004	55.7	3.79	2016.4493	2	55.001	-0.700	3.861	0.0711	DPM	83
14526-1151	LDS 511	2007	108.4	16.67	2016.4329	2	107.738	-0.662	16.940	0.2704	DPM	84
14543-1810	RST2930 AB-C	2010	124.1	6.76	2016.4329	2	123.696	-0.404	6.894	0.1341	DPM	
14556-1444	HLD 21	2011	19.3	3.49	2016.4329	3	19.038	-0.262	3.619	0.1285	CPM	
14573-0551	HJ 4720	2009	212.5	12.84	2016.4493	2	211.952	-0.548	13.181	0.3415	CPM	85
14577-1318	BRT2738	2004	343.3	4.35	2016.4329	2	343.102	-0.198	4.407	0.0566	DPM	86
15045-1754	S 665	2013	90.5	24.95	2016.4329	3	90.036	-0.464	25.584	0.6336	CPM	
15069-1806	HU 1157	1999	245.9	2.65	2016.4329	3	244.525	-1.375	2.721	0.0710	DPM	
15093-0815	HLD 23 AB	2011	5	3.1	2016.4548	2	4.440	-0.561	3.307	0.2069	DPM	
15149-1841	DON 724	1991	63.1	1.98	2016.4438	1	64.149	1.049	1.862	-0.1180	CPM	
15166-0147	BAL 557	2002	305	2.64	2016.4548	2	305.288	0.287	2.700	0.0603	DPM	
15218-1822	ARA 237	2008	294.9	14.08	2016.4438	2	294.628	-0.272	14.149	0.0695	SPM	
15244-1102	RST3918	2004	74.3	4.01	2016.4493	2	74.801	0.501	4.191	0.1809	DPM	
15250-1837	HJ 1271	2008	102.1	7.79	2016.4438	2	101.400	-0.700	7.796	0.0059	DPM	87
15266-1706	HU 309	2002	46.9	1.39	2016.4438	2	45.060	-1.841	1.581	0.1908	CPM	
15275-1058	STF1939	2013	130.4	9.5	2016.4329	3	130.135	-0.265	9.713	0.2127	CPM	
15313-1259	BU 33 AB	2011	35.8	3.24	2016.4493	2	36.202	0.402	3.334	0.0940	CPM	
15399-1444	BRT2740	2008	335.1	5.32	2016.4493	2	334.780	-0.321	5.487	0.1669	DPM	
15410-1449	HWE 37	2012	269.5	5.46	2016.4548	2	268.544	-0.956	5.588	0.1281	CPM	88
15428-1601	BU 35 AB	2012	109.4	1.69	2016.4548	3	109.823	0.423	1.759	0.0694	DPM	89
15524-1714	SKI 9 AB	2013	271.8	2.46	2016.4521	3	271.351	-0.449	2.527	0.0669	DPM	90
15543-1726	J 1588 AB	2000	169	8.82	2016.4521	2	168.323	-0.677	9.019	0.1990	DPM	
15591-1956	SHJ 213	2014	317.4	17.34	2016.4521	3	317.379	-0.021	17.798	0.4576	CPM	91
16006-1739	RST2992	2008	81.3	2.29	2016.4493	2	81.282	-0.018	2.354	0.0635	DPM	
16044-1127	STF1999 AB	2013	98	11.9	2016.4521	2	97.940	-0.061	12.131	0.2308	CPM	
16054-1948	H III 7 AC	2013	20	13.6	2016.4521	2	18.838	-1.162	14.044	0.4439	DPM	

Note: *For "Type", refer to Harshaw 2016a.*

The Spring 2016 Observing Program of Brilliant Sky Observatory: Measurements of 313 Pairs

Notes to Table 4:

33. The measurement HJ1827.5 is well off the norm.
34. HJ1825 is a weak measurement.
35. Trending linear? See Figure 20.

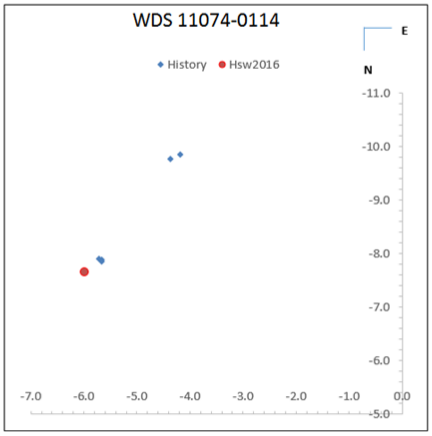

Figure 20.

36. HJ1827.5 is well off the norm. This pair is starting to show linear traits!
37. WSI2013.313 very far off from the norm.
38. Very high proper motion pair (+330 -699 P, +320 -707 C).
39. HJ1830.14 is far from the mean of the measurements.
40. HJ1830.14 is far from the mean.
41. HJ1828 is far from the mean.
42. HJ1825 should be discounted; it is quite a bit off from the measurement cluster.
43. WFD1894.80 should be discounted.
44. Measured with speckle.
45. Measured with speckle.
46. Measured with speckle.
47. Rst1938.37 and Rst1943.43, discount heavily.
48. HJ1825 should be discounted.
49. HJ1827.5 should be discounted.
50. High common proper motion pair (-125 +18 P, -127 +20 C).
51. Measured with speckle. Frm1906.26 should be discounted.
52. HJ1828 should be given less weight.
53. HJ1827 should be given light weight and HJ1831.21 should be discounted altogether.
54. Measured with speckle.
55. Nug2013 should be discounted.
56. Large difference in PM (-65 -62 P, -94 -32 C).
57. Measured with speckle.
58. MyC1777.5 should be completely discarded.
59. Measured with speckle.
60. Luy1920 should be heavily discounted.
61. Measured with speckle.
62. Does TYC1991.49 show a quadrant reversal (rho off by 180°)?
63. HJ1827.5 should be discounted.
64. High PM pair (+60 -159 P, +59 -166 C).
65. CLL1980 appears to be a quadrant reversal.
66. Measured with speckle.
67. Measured with speckle.
68. HJ1828 and Hei1983 should be given very little weight.
69. Measured with speckle.
70. First 3 measures are way off the norm (Bal1909.4, WFC1909.4, Rst1946.40).
71. Trending linear? (See Figure 21.)

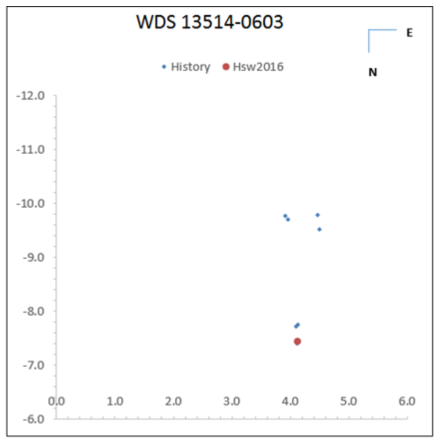

Figure 21. Measurements for WDS 13514-0603.

72. HJ1830.22 should be discounted.
73. WFD1987.30 should be discounted.
74. Measured with speckle.
75. Gbb1923.34 should be discounted heavily.
76. Measured with speckle.
77. Measured with speckle.
78. Measured with speckle.
79. High difference in PM (-91 -38 P, -16 +65 C). Over the 72 years since discovery, the PM vectors should account for 9.17" of displacement. The pair has shown nothing close to that.
80. HJ1828 should be discounted.
81. High PM pair (both stars -129 -91 mas).
82. Measured with speckle.
83. PM in opposite directions (-48 -23 P, +46 +40 C). This would result in a displacement of 9.51" in the 84 years since discovery, yet the measurements plot like a CPM pair.
84. Luy1920 should be discarded.
85. DQE1983.345 should be heavily discounted.

86. Brt1945.90 appears to be a quadrant reversal.
87. Large difference in PM (-57 +19 P, +71 -16 C). Since discovery 188 years ago, this should have resulted in a movement of 24.95", yet the measurements plot within a radius of 2".
88. Measured with speckle.
89. Speckle. High difference in PM (-116 -49 P, -68 -66 C). Trending linear? In the 145 years since discovery, the PM vectors should have produced 7.38" of motion, while the companion has moved about 1".
90. Measured with speckle.
91. Lal1798.39 should be discarded.

Table 5: 45 Pairs of Unknown Type

Pairs of unknown type are double stars that do not fit into any of the preceding categories.

WDS No.	Discoverer	Year Last	Last θ°	Last ρ"	Epoch	No. Obs.	Obs θ°	Resid (θ)	Obs ρ "	Resid (ρ)	Notes
10459-1942	HLD 110	1999	278	2.58	2016.3730	4	280.5133	2.51132	2.6456	0.0656	
10481-1458	BU 595 AB	2000	15.4	2.21	2016.3699	5	13.5758	-1.8242	2.2151	0.0051	
11022-0335	BRT 548	2004	90.7	4.34	2016.4027	3	88.9287	-1.7713	4.4715	0.1315	
11273-0852	A 138	2010	217.6	1.77	2016.4027	3	216.6363	-0.9637	1.8761	0.1061	
11344-0021	J 1015	2011	239	3.74	2016.4027	3	241.0813	2.0813	3.8027	0.0627	
11423-1513	RST3753	1999	104.7	3.01	2016.3945	3	106.2870	1.5870	3.1253	0.1153	92
11445-0805	A 140	2008	138.7	2.54	2016.4055	2	140.7540	2.0540	2.4105	-0.1295	93
11556-1815	RST2773	2005	336.2	2.32	2016.3945	3	332.2250	-3.9750	2.3131	-0.0069	
12047-1643	FOX 173	2004	332.2	5.96	2016.3699	3	331.4713	-0.7287	6.1060	0.1460	
12082-1058	RST3772	2000	348.9	1.88	2016.3945	2	350.7980	1.8980	2.2229	0.3429	
12253-0152	FOX 68	2013	168.5	3.85	2016.4082	2	165.0600	-3.4400	3.9049	0.0549	
12295-0103	J 431	2001	274.7	2.57	2016.4329	2	273.1285	-1.5715	2.7171	0.1471	
12407-0302	BAL 220	2013	41.2	7.01	2016.4110	2	41.2895	0.0895	7.0099	-0.0001	
12415-0156	BAL 544	2002	178	3.43	2016.4110	2	177.1200	-0.8800	3.3556	-0.0744	
12578-1308	STN 27	2013	69.3	2.01	2016.3918	5	69.0038	-0.2962	2.1274	0.1174	94
13029+1026	STF1710	2012	252.4	2.54	2016.4521	3	251.8980	-0.5020	2.5877	0.0477	
13045+0839	STF1716 AB	2000	149.4	2.85	2016.4493	3	149.6260	0.2260	2.9127	0.0627	95
13050+1304	J 2103	2011	200.4	3.12	2016.4521	2	199.8470	-0.5530	3.2278	0.1078	
13112-1351	RST3823	2002	307.2	2	2016.3699	3	304.1013	-3.0987	2.1193	0.1193	
13125+2050	COU 55	2010	125.7	2.27	2016.4575	2	126.8670	1.1670	2.4704	0.2004	
13162-1602	RST3832	1984	22	1.4	2016.4438	2	19.9860	-2.0140	1.5411	0.1411	
13173+2840	ES 440	2012	181.2	2.27	2016.4575	2	180.3035	-0.8965	2.6110	0.3410	96
13174+0300	J 435	2007	150	3.7	2016.4493	2	148.4470	-1.5530	3.7737	0.0737	
13175-0430	BRT2836	1983	217	2.45	2016.4466	2	214.7070	-2.2930	2.5213	0.0712	
13235-0841	BRT 550	2013	98.7	4.05	2016.4110	2	98.8485	0.1485	3.9138	-0.1362	
13251-1538	BU 460	2001	40	2.1	2016.4329	3	41.0037	1.0037	1.9788	-0.1212	97
13365+0707	BRT2604	2000	204.4	2.81	2016.4493	2	204.6345	0.2345	2.9142	0.1042	
13370+1559	HJ 3340	2013	213.1	2.21	2016.4548	2	213.4490	0.3490	2.1994	-0.0106	
13397-1315	RST3847	2008	330.8	2.01	2016.4493	4	332.2123	1.4122	2.1725	0.1625	
13403-0918	J 1607	2004	216.2	6.2	2016.4110	2	214.1170	-2.0830	6.3014	0.1014	
13403-1913	RST2859	2001	122.9	2.28	2016.4466	2	123.3640	0.4640	2.3376	0.0576	
13452-1508	SKI 7	1999	111.9	2.44	2016.4027	3	109.9827	-1.9173	2.4715	0.0315	
13531+1251	HEI 524	2013	147.3	3.05	2016.4548	2	147.0225	-0.2775	3.0846	0.0346	
13572+1151	HJ 233	2010	134	19.8	2016.4548	2	132.9625	-1.0375	20.4354	0.6353	
14007-1915	J 2661	1999	310.7	5.83	2016.4027	3	310.4720	-0.2280	5.6854	-0.1446	
14097+0459	FOX 71	2010	181.7	4.01	2016.4575	3	181.2130	-0.4870	4.0971	0.0871	
14105-0240	HLD 17 AB	2011	247	4.67	2016.4521	2	246.7315	-0.2685	4.7586	0.0886	98
14141-0615	J 2584	2011	152.7	6.92	2016.4521	2	152.3235	-0.3765	7.0052	0.0852	
14192-1634	FOX 181	1999	133.7	5.74	2016.4027	2	132.0360	-1.6640	5.5976	-0.1425	
14489-0959	RST3896	1999	344.4	2.46	2016.4493	3	344.0793	-0.3207	2.4632	0.0032	99
15144-1602	FOX 73	1991	193.8	2.3	2016.4329	2	190.3630	-3.4370	2.3064	0.0064	
15194-1003	ROE 36	2000	250.3	4.1	2016.4329	3	249.3317	-0.9683	4.3201	0.2201	
15350-1031	HLD 122	2000	339.9	2.12	2016.4493	2	337.1710	-2.7290	2.2800	0.1600	
15370-1659	HWE 35 AB	2002	331.4	6.67	2016.4493	2	331.3250	-0.0750	7.5617	0.8917	100
15546-1341	STF3099	2002	110.4	2.21	2016.4521	6	110.5523	0.1523	2.3706	0.1606	101

The Spring 2016 Observing Program of Brilliant Sky Observatory: Measurements of 313 Pairs

Notes to Table 5:

92. Measured with speckle.
93. Measured with speckle.
94. An interesting pattern may be emerging from the data, one that suggests an unseen companion. See Figure 22.

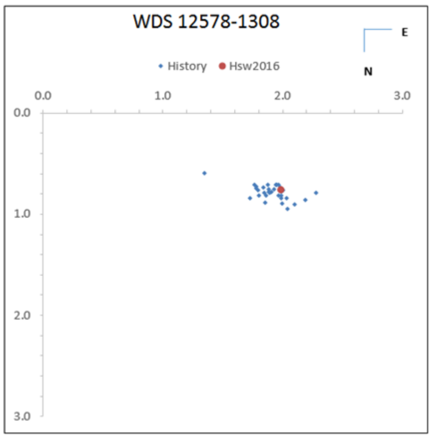

Figure 22.

95. Measured with speckle.
96. Several quadrant reversals: Es1907.30; Cou1966.34; Tor 1976.82.
97. Measured with speckle.
98. Rst1943.48, B1962.34 and Hln1970.52— all appear to be well away from the bulk of the measurements.
99. TYC1991.55 seems to be a quadrant reversal.
100. Tob1982.551 appears to be a quadrant flip of 90°.
101. Measured by speckle.

(Continued from page 106)

5. Discussion

In general, the ZWO ASI 290 MM is an excellent camera for speckle interferometry. It is fast, has low read-noise, and permits observers with modest telescopes to do speckle on relatively faint and close pairs, as well as normal imaging of wider and very faint pairs.

The cumulative residuals for theta (based on the last recorded measure) average out to +0.7805°, while those for rho average +0.1131". If we posit that half the time, the last measurement may be too high (or too low) compared to the actual value, my overall error for theta would appear to be approximately +0.3903°, while the error for rho would be approximately +0.0565". Of course, past visual observations will probably not have the accuracy capable with speckle.

In addition, several pairs in this season's report merit attention over the next several years to determine if they are indeed showing short arcs or linear behaviors. (The proper motion pairs may not show any significant motion for several decades, perhaps even millennia, and so can do with a less frequent assessment program.)

6. Conclusion

With fast, low read-noise cameras and modest apertures, the double star astronomer can do useful and highly accurate measurements, especially of those high-interest close pairs with relatively short periods, even with telescopes of modest aperture. The use of CCD and CMOS cameras, in conjunction with speckle reduction software, clearly produces better results than filar micrometers, photographs, or reticle eyepieces.

7. Acknowledgements

This research has made use of the Washington Double Star Catalog maintained at the U.S. Naval Observatory.

The author thanks Russell Genet and Vera Wallen for their reviews of the draft before publication.

8. References

Ashcraft, Clif, 2016. Speckle Interferometry with a Low Read-Noise CMOS Video Camera. *JDSO*, Vol 12 No 3, pp. 280-286.

Brian D. Mason, William I. Hartkopf, and Gary L. Wycoff, 2008. Speckle Interferometry At The U.S.

Naval Observatory. XIV. *The Astronomical Journal*, 136:2223–2226.

Genet, Russel, 2016. Speckle Interferometry of Close Visual Binaries with a ZW Optical ASI224MC CMOS Camera. *JDSO*, Vol. 12 No 3, pp. 270-279.

Harshaw, Richard, 2015. Calibrating a CCD Camera for Speckle Interferometry. *JDSO*, Vol 11 No 1s, pp. 314-322.

Harshaw, Richard, 2016a. CCD Measurements of 141 Proper Motion Stars: The Autumn 2015 Observing Program at Brilliant Sky Observatory, Part 3. *JDSO*, Vol 12 No 4, pp 394-399.

Harshaw, Richard, 2016b. CCD Measurements of 8 Double Stars with Binary Nature: The Autumn 2015 Observing Program at Brilliant Sky Observatory, Part 2. *JDSO*, Vol 12 No 4, pp 388-393.

Harshaw, Richard, 2016c. CCD Measurements of 66 Rectilinear and Probable Rectilinear Pairs: The Autumn 2015 Observing Program at Brilliant Sky Observatory, Part 1. *JDSO*, Vol 12 No 4, pp 376-387.

Harshaw, Richard, 2016d. The Speckle Toolbox: A Powerful Data Reduction Tool for CCD Astrometry, *JDSO*, in submission.

Rowe, David and Genet, Russell, 2015. User's Guide to PS3 Speckle Interferometry Reduction Program. *JDSO*, Vol. 11 No 3, pp. 266-276.

Speckle Interferometry of Eleven Hipparcos Binary Discoveries

Matthew Kehrli, Heather David, Evan Drake, Corina Gonzalez,
Joe Zuchegno, and Russell Genet

California Polytechnic State University
San Luis Obispo, California

Abstract: The 11 Hipparcos-discovered binaries studied in this paper were observed at Kitt Peak National Observatory during an eight-night run from October 16th-23rd, 2013 using an EMCCD camera attached to the 2.1-meter telescope. PlateSolve 3.44, a speckle reduction program, was utilized to reduce the observations and create autocorrelograms of the 11 binaries. Each autocorrelogram provided data on the position angle and separation between the stars. Accuracy of the results was measured by determining the mean, standard deviation, and standard error for the difference between the predicted and reduced results for both the position angle and separation. For $\Delta\theta$, this calculation resulted in a mean of 1.65°, standard deviation of 1.64°, and a mean standard error of ±0.50°. For $\Delta\rho$, it resulted in a mean of 0.0108″, standard deviation of 0.0106″, and a mean standard error of ±0.0032″.

Introduction

The Hipparcos mission was designed to determine stellar distances to facilitate stellar "internal composition, … ages, and the history of their nuclear-fuel burning" (Perryman 2010). During its time in orbit, Hipparcos observed over 100,000 stars, of which approximately 12,000 were double stars and 3,406 were newly discovered doubles (Mason et al. 1999). Hipparcos took measurements on position, parallax and proper motion. Stars with similar values for position and parallax, or double stars, underwent further observation to determine whether they were "physically associated, rather than just chance alignments" (Perryman 2010). In the Fall of 2013, a group of students and their mentors made speckle interferometry observations on some of the Hipparcos-discovered binaries at Kitt Peak National Observatory (Genet et al. 2015b).

Hipparcos double star discoveries were selected from over one thousand Kitt Peak double star observations. Binaries lacking published orbits were eliminated after consulting the Sixth Catalog of Orbits of Visual Binary Stars (Hartkopf 2016). This left 12 binaries, one of which served in a pilot project described in a previous article in this issue of the *Journal of Double Star Observations* (Kehrli et al. 2016). The current study contributes new position angles and separations for the remaining 11 Hipparcos binary discoveries observed at Kitt Peak National Observatory.

Instrumentation, Observations, Calibration, and Reduction

This paper follows a previous paper studying one Hipparcos-discovered binary, HIP 4849, observed at Kitt Peak National Observatory. An expanded summary of the instrumentation, observations, calibration, and reduction is provided in the pilot paper (Kehrli et al. 2016).

Instrumentation

The observations were made with the Kitt Peak National Observatory's 2.1-Meter Telescope from October 16-23, 2013. The telescope did not include a camera for speckle interferometry observations, so the observers supplied their own (Genet 2013). The speckle camera system employed an Andor Luca R EMCCD, which has "10 μ square pixels in a 658x496 pixel array" (Genet et al. 2015d). The portable EMCCD camera system increased "the signal to a level where the high speed read noise is insignificant," with a read noise well under one electron RMS (Genet et al. 2015a). With a magnification of 8x, the Andor Luca R EMCCD provided an overall effective focal length of

Speckle Interferometry of Eleven Hipparcos Binary Discoveries

about 129,600mm and F/ratio of 61.7 when attached to the 2.1-Meter telescope (Genet et al. 2015b).

Observations

The observers were granted eight nights of observing time at Kitt Peak National Observatory. The observing conditions were completely clear each night, except for the last half of the eighth night (Genet 2015c). The eight-night run allowed for speckle observations of over 1,000 close double stars, many of which were binaries.

Calibration

As previously mentioned, the observations were calibrated with data collected from multiple observations of six binaries with previously published orbits. A comparison of these Kitt Peak observations with the published orbits allowed the camera angle, -11.0492˚ from true north, and plate scale, 0.0116″/pixel, to be determined (Wallace 2015). Overall internal precision for the run was found to be 0.027˚ and 0.00226″, and overall accuracy was determined to be 0.4138˚ and 0.0147″. These values were obtained using statistical analysis of five calibration binaries made throughout the run (Wallace 2015).

Reduction

The PlateSolve 3.44 program, developed by David Rowe, was used to reduce observations of the 11 binaries. It also served to create autocorrelograms, such as the one seen in Figure 1, which depicts WDS 00428+1249. The autocorrelogram for each binary provided data on the position angle and separation between the stars. In order to include the maximum amount of useful data and exclude most unwanted noise, the Gaussian Lowpass was set to a 30-pixel radius and the Gaussian Highpass was set to a 3-pixel radius.

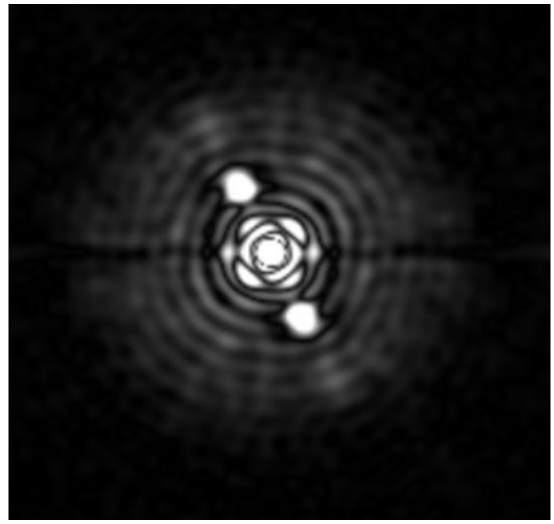

Figure 1. Autocorrelogram of WDS 00428+1249.

Results

Each observation was reduced six times using PlateSolve 3.44. The center of the target star was selected manually to find the angle, θ, and separation, ρ. These six θ and ρ values were used to derive the mean values for the binary, and were compared to the predicted values in Table 1.

Table 1. Position Angle and Separation

Figure #	Star Identifier	Date (JD)	Mean θ˚	Pred. θ˚	|Δ°|	Mean ρ"	Pred. ρ"	|Δ"|
2	WDS 00085+3456	2456585.770	52.80	52.5	0.3	0.1337	0.134	0.0003
3	WDS 03035+2304	2456583.857	4.72	5.2	0.48	0.1645	0.167	0.0025
4	WDS 18084+4407	2456587.627	204.74	207.7	2.96	0.1348	0.134	0.0008
5	WDS 01166+1831	2456584.835	234.27	234.2	0.07	0.6037	0.616	0.0123
6	WDS 02249+3039	2456583.833	264.11	263.4	0.71	0.3443	0.335	0.0093
7	WDS 00251+4803	2456586.779	272.75	274.7	1.95	0.3250	0.34	0.015
8	WDS 01129+5136	2456585.807	107.18	106.4	0.78	0.0999	0.103	0.031
9	WDS 00495+4404	2456584.788	136.12	135.6	0.52	0.1913	0.196	0.0047
10	WDS 01108+6747	2456587.757	174.08	175.4	1.32	0.1333	0.13	0.0033
11	WDS 00428+1249	2456587.781	36.39	31.6	4.79	0.2905	0.262	0.0285
12	WDS 07092+1903	2456586.987	338.18	342.4	4.22	0.1464	0.135	0.0114

Speckle Interferometry of Eleven Hipparcos Binary Discoveries

In Figures 2 to 12, the predicted values for the ρ and θ of the binaries were determined using a binary calibration Excel spreadsheet (Drummond 2011). These results, provided in Table 1, are labeled "Predicted θ" and "Predicted ρ". By finding the difference between the mean and predicted values for θ and ρ, |Δ°| and |Δ"| were determined as shown in Table 1. Drummond's spreadsheet solves Kepler's equation for any given date of every binary with a published orbit. The date for each binary was recorded in the spreadsheet.

For accuracy to be evaluated, the mean, standard deviation, and standard error were calculated for the difference between the predicted and actual values for both the position angle and separation, degrees and arcseconds. For the separation angle, this calculation resulted in a mean of 1.65°, standard deviation of 1.64°, and a standard error of ±0.50°. For ρ, it resulted in a mean of 0.0108", standard deviation of 0.0106", and a standard error of ±0.0032".

Discussion

Figures 2 to 12 plot the results alongside orbital plots provided by Brian Mason from the U.S. Naval Observatory. Microsoft Paint served as a coordinate-grid system for the orbital plots from the USNO. Since the scale varied for each plot, the arcsecond-to-pixel ratio was determined separately for each binary. The distance for both x and y coordinate positions was calculated from the angle and distance obtained with PlateSolve 3.44. After converting these values to pixel coordinates, they were used to plot the binary systems (marked as plus symbols in Figures 2 to 12). By definition, the calculated separation and position angle must fall on the path of the given orbit of the binary provided from the U.S. Naval Observatory (marked as a line intersecting the established orbit in Figures 2 to 12).

The new data points, marked on the figures below, provide substantive information that may assist in confirming, refining, or modifying the published orbits.

(Continued on page 130)

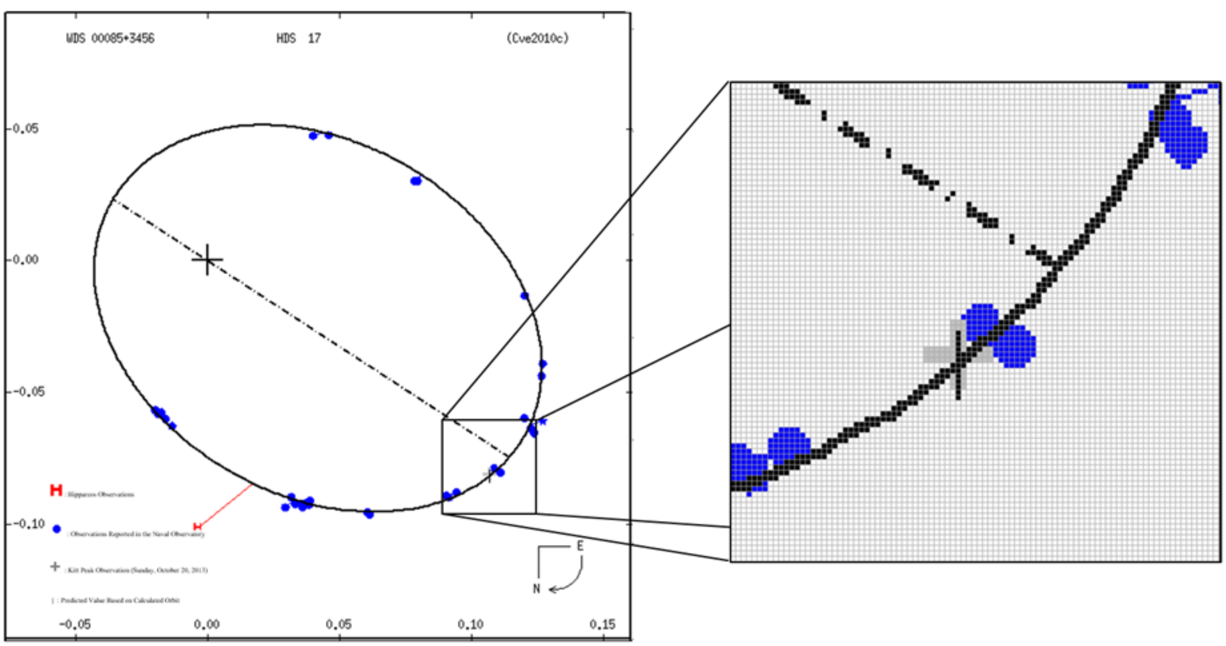

Figure 2. Orbit of Binary Star System WDS 00085+3456. Observed on Sunday, October 20, 2013

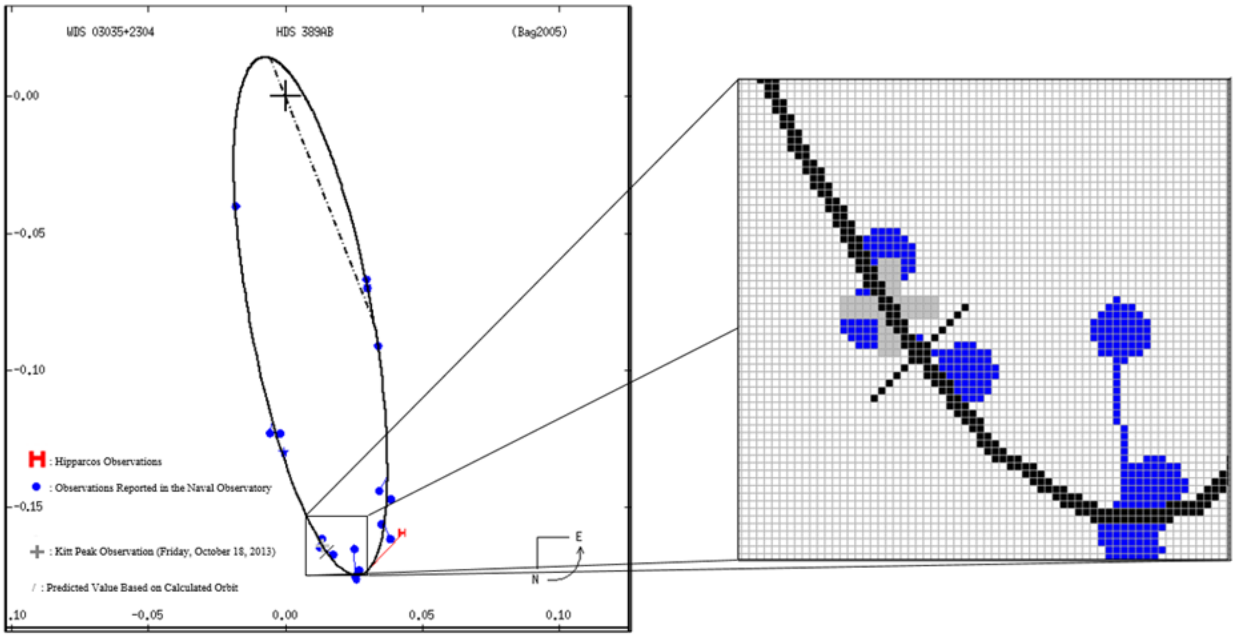

Figure 3. Orbit of Binary Star System WDS 03035+2304. Observed on Friday, October 18, 2013

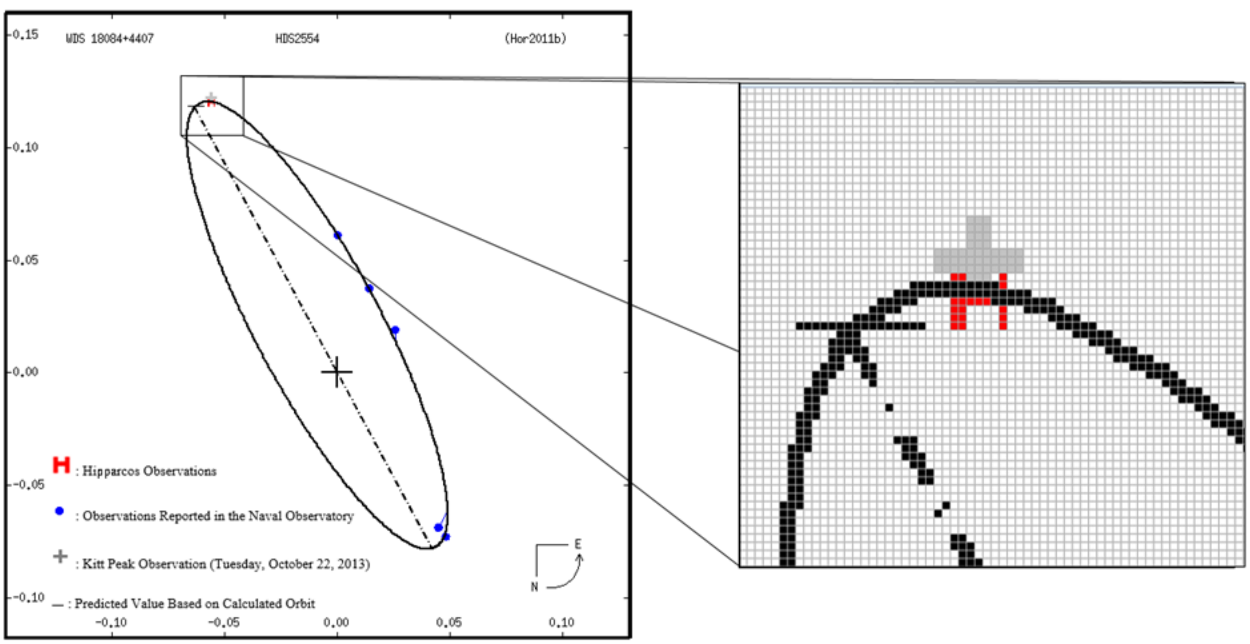

Figure 4. Orbit of Binary Star System WDS 18084+4407. Observed on Tuesday, October 22, 2013

Speckle Interferometry of Eleven Hipparcos Binary Discoveries

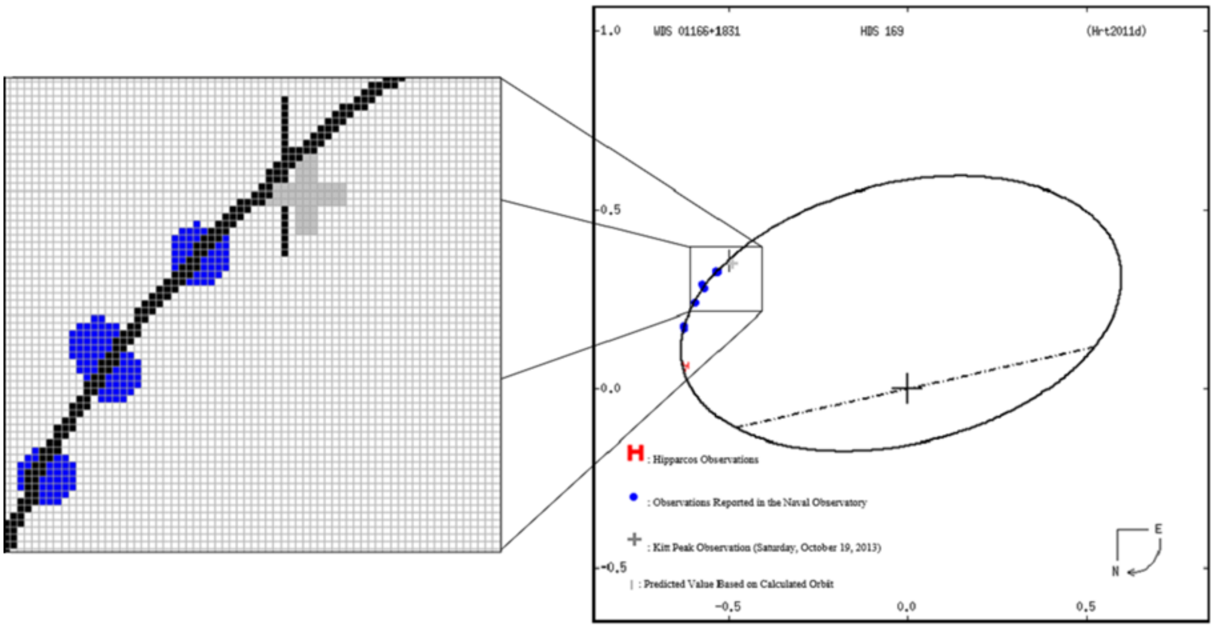

Figure 5. Orbit of Binary Star System WDS 01166+1851. Observed on Saturday, October 19, 2013

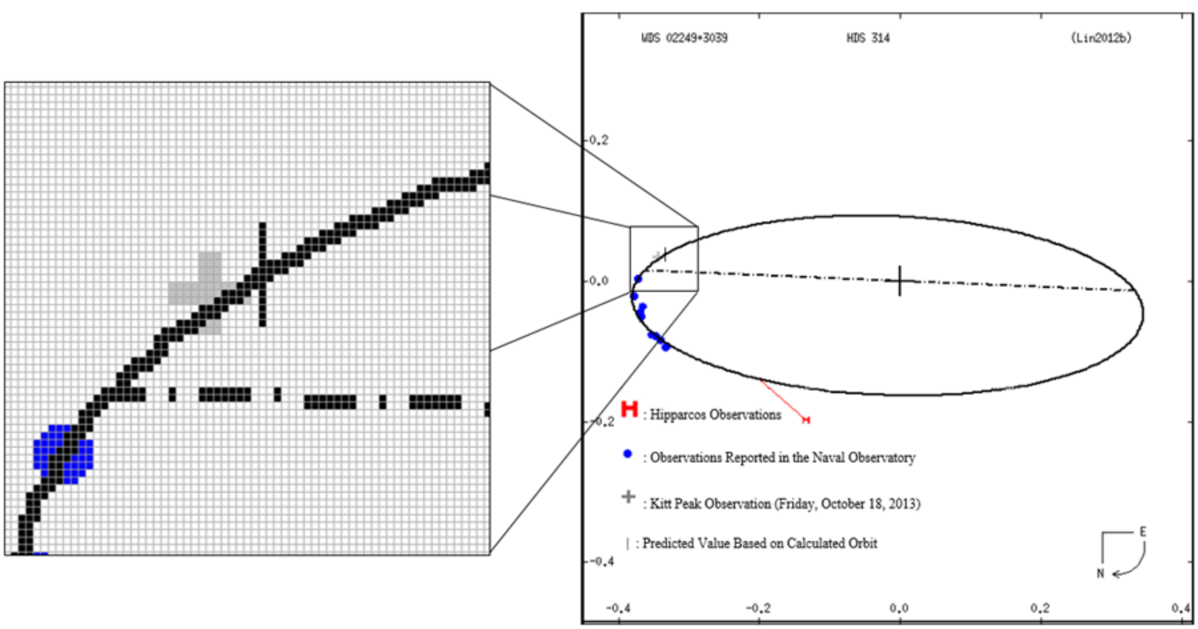

Figure 6. Orbit of Binary Star System WDS 02249+3039. Observed on Friday, October 18, 2013

Speckle Interferometry of Eleven Hipparcos Binary Discoveries

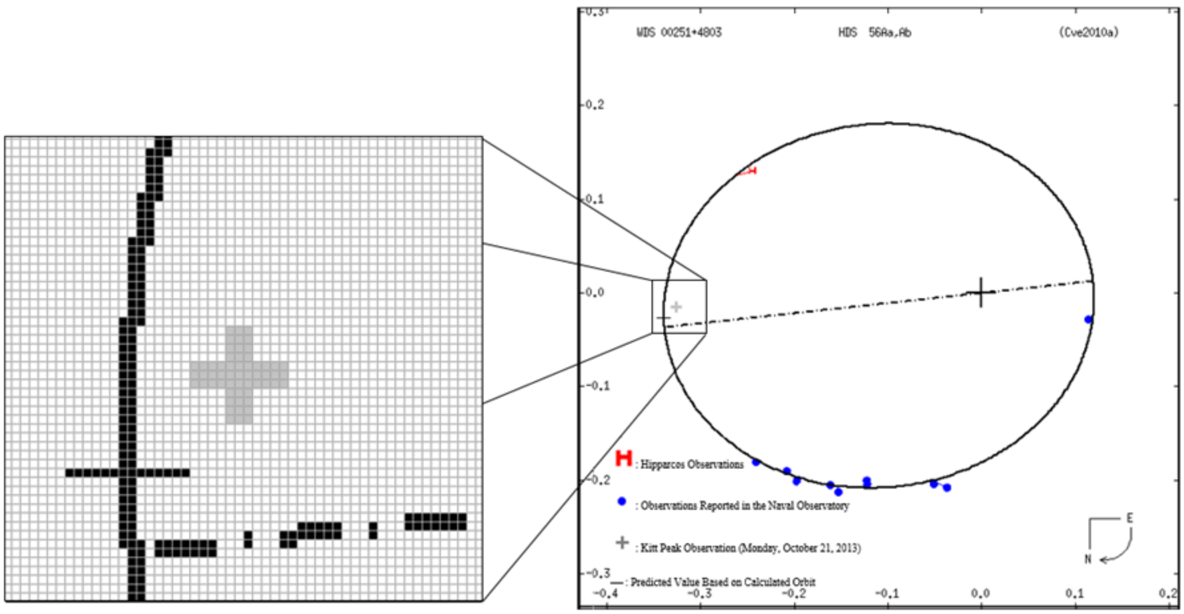

Figure 7. Orbit of Binary Star System WDS 00251+4803. Observed on Monday, October 21, 2013.

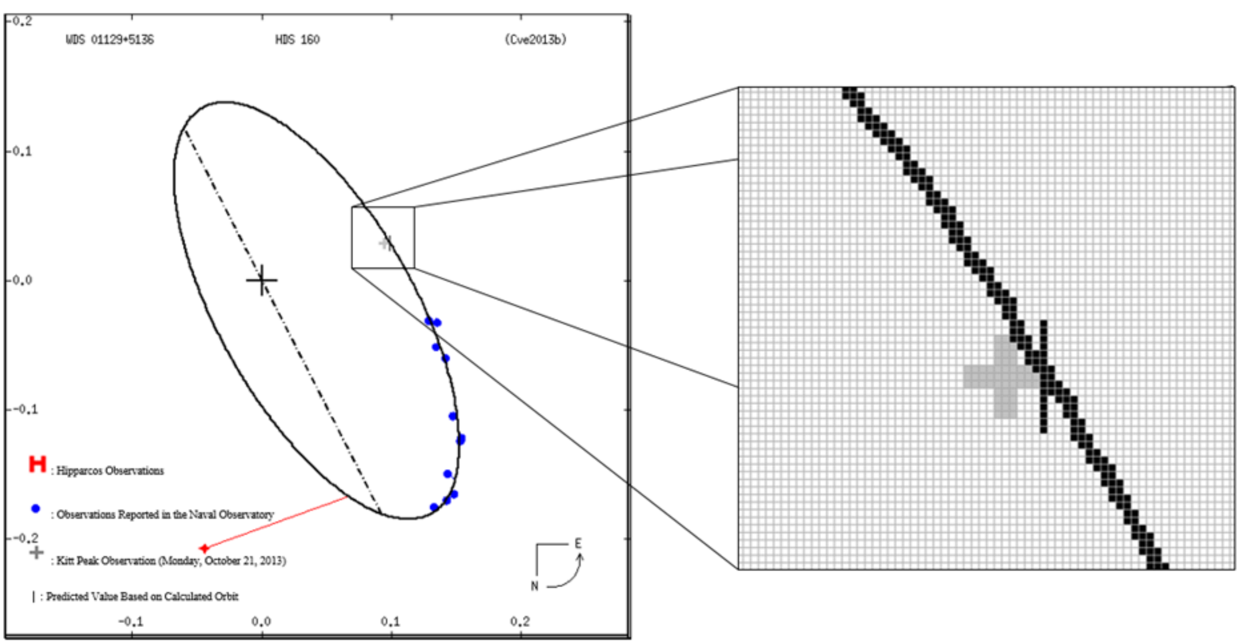

Figure 8. Orbit of Binary Star System WDS 01129+5136. Observed on Monday, October 21, 2013.

Speckle Interferometry of Eleven Hipparcos Binary Discoveries

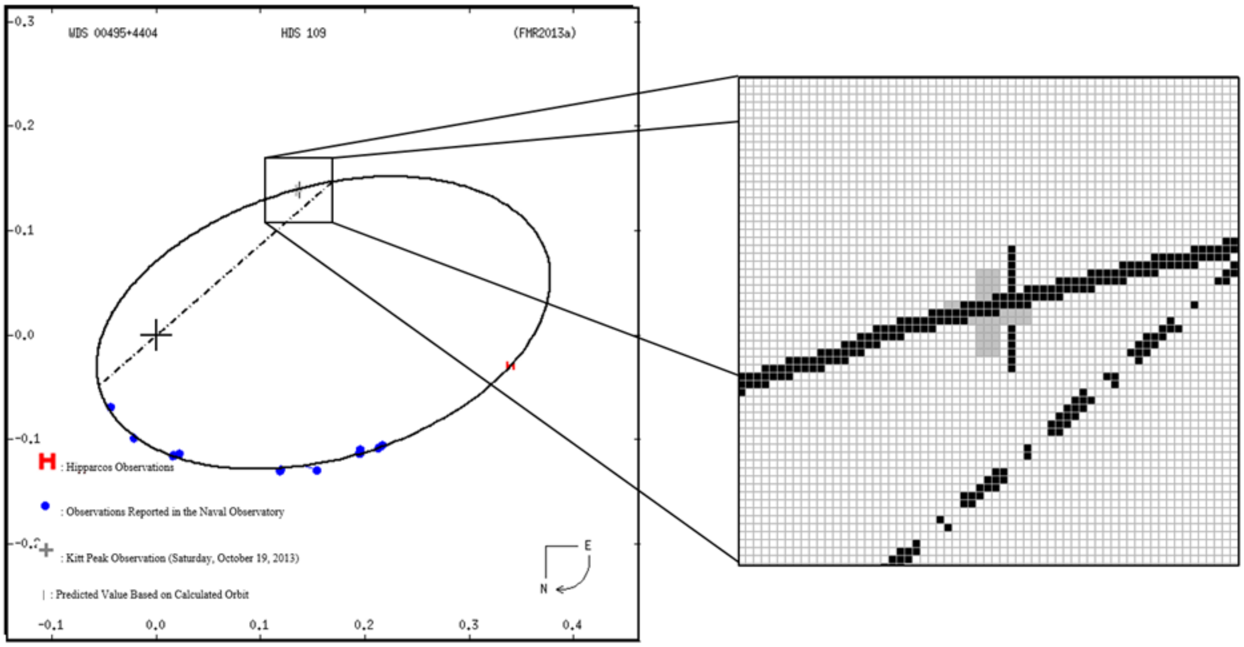

Figure 9. Orbit of Binary Star System WDS 00495+4404. Observed on Saturday, October 19, 2013.

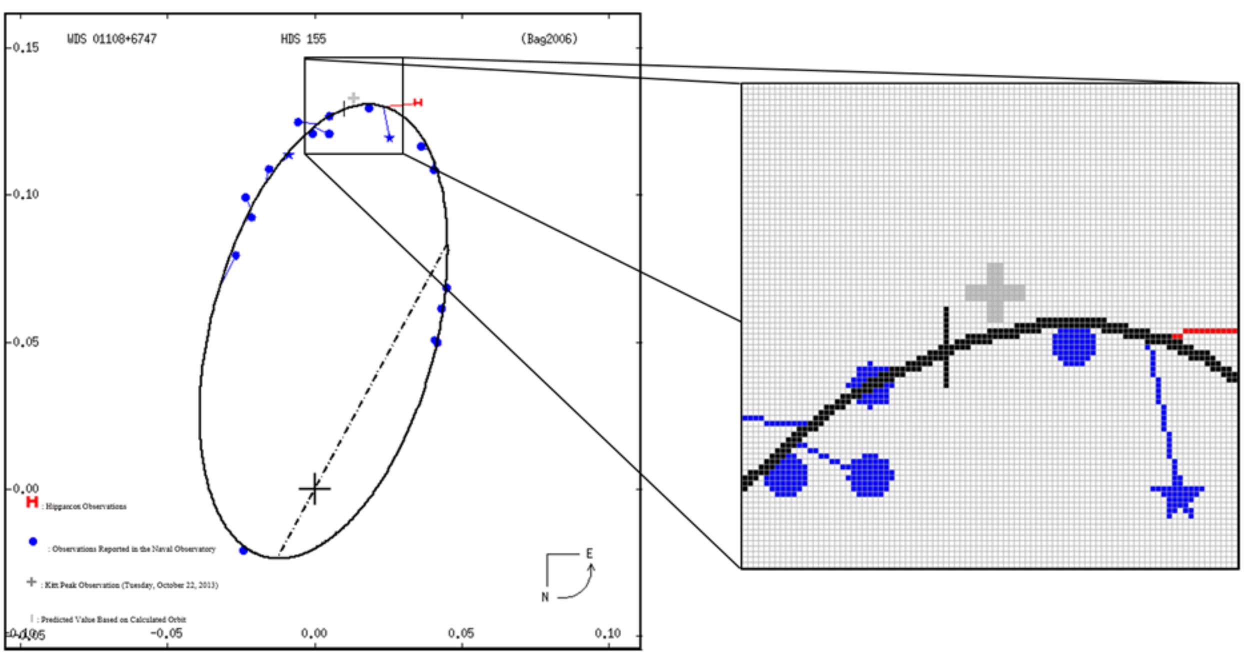

Figure 10. Orbit of Binary Star System WDS 01108+6747. Observed on Tuesday, October 22, 2013.

Speckle Interferometry of Eleven Hipparcos Binary Discoveries

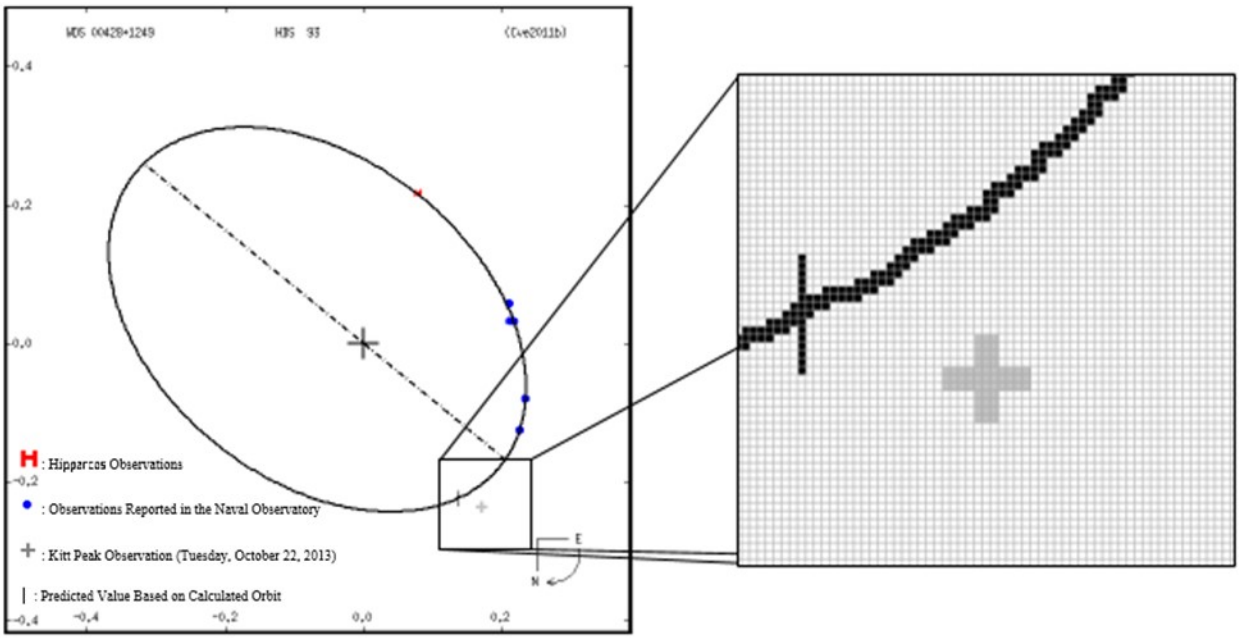

Figure 11. Orbit of Binary Star System WDS 00428+1249. Observed on Tuesday, October 22, 2013.

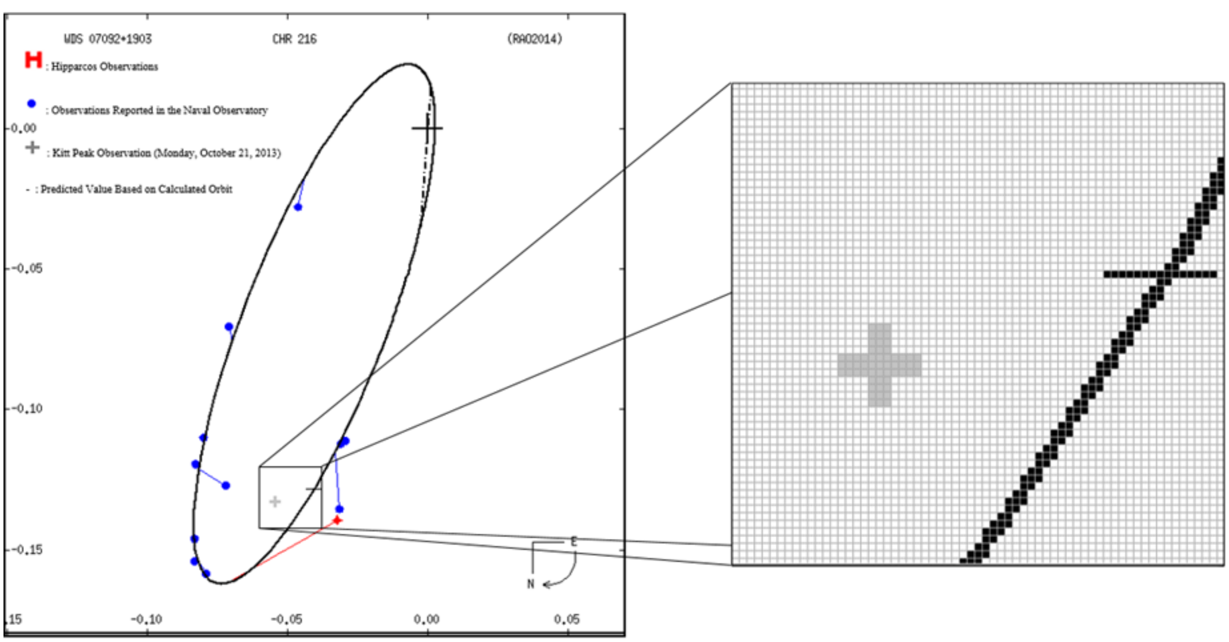

Figure 12. Orbit of Binary Star System WDS 07092+1903 . Observed on Monday, October 21, 2013.

Speckle Interferometry of Eleven Hipparcos Binary Discoveries

(Continued from page 124)

Conclusion

By analyzing 11 of the binaries observed at the Kitt Peak National Observatory, the study accomplished the goal of contributing position angles and separations to their apparent orbits. Further analysis on the data may serve to refine orbital predictions.

Acknowledgements

We are grateful to Kitt Peak National Observatory for the use of the 2.1-meter telescope, and also to the team which conducted the observations in 2013. The speckle interferometry camera was obtained through funds from the American Astronomical Society's Small Research Grants. We thank David Rowe for the use of the PlateSolve 3.44 Speckle Reduction Tool. This research made use of the Washington Double Star Catalog maintained at the U.S. Naval Observatory. We thank Jack Drummond for providing his binary calibration spreadsheet. Furthermore, we are grateful for the reviews of the paper given by Robert Buccheim, Richard Harshaw, and Vera Wallen. A special thanks to William and Linda Frost for providing funding to the Frost Undergraduate Summer Research Program at California Polytechnic State University, San Luis Obispo, California.

References

Drummond, J., 2011, "Calibration Binaries", *Proceedings of the Advanced Maui Optical and Space Surveillance Technologies Conference*, S. Ryan (Ed.), Wailea, Maui, Hawaii.

Genet, R. M., 2013, "Portable Speckle Interferometry Camera System", *Journal of Astronomical Instrumentation* **2**, 2.

Genet, R., Rowe, D., Smith, T. C., Teiche, A., Harshaw, R., Wallace, D., Weise, E., Wiley, E., Boyce, G., Boyce, P., Brantson, D., Chaney, K., Clark, K., R., Estrada, C., Frey, T., Estrada, R., Wayne, G., Huarberg, N., Kenney, J., Jones, G., Loftin, S., McGieson, I., Patel, R., Plummer, J., Ridgely, J., Trueblood, M., Westergren, D., Wren, P., 2015a, "Kitt Peak Speckle Interferometry of Close Visual Binary Stars", *Journal of Double Star Observations*, **11**, 1S.

Genet, R. M., Smith, T. C., Clark, R. K., Wren, P., Mathis, H., Summers, D., Hansey, B., 2015b, "Portable Interferometry Camera Checkout at Kitt Peak", *Journal of Double Star Observations*, **11**, 226 - 233.

Genet, R. M., 2015c, "Speckle Interferometry of Close Visual Binaries", *Journal of Double Star Observation* 11, 183 - 199.

Genet, R. Zirm, H., Francisco, R., Richards, J., Rowe, D., Gray, D., 2015d, "Two New Triple Star Systems with Detectable Inner Orbital Motions", *Journal of Double Star Observations*, **11**, 200 - 213.

Hartkopf, W., Mason, B., 2016, April 25, "Sixth Catalog of Interferometric Measurements of Binary Stars".

Kehrli, M., David, H., Drake, E., Gonzalez, C., Zuchegno, J., Genet, R. M., 2016, "Speckle Interferometry of Binary Star HIP 4898", *Journal of Double Star Observations*, **13**, 100-104 (this issue).

Perryman, M., 2010, *The Making of History's Greatest Star Map*, New York, Springer.

Wycoff, G. L., Brummelaar, T. T., Franz, O. G., 1999, "Speckle Interferometry of New and Problem Hipparcos Binaries", *The Astronomical Journal*, **117**, 4.

Wallace, D., 2015, *An Investigation of Six Poorly Described Close Visual Double Stars Using Speckle Interferometry*, Master's Thesis, Dept of Space Science, University of North Dakota, Grand Forks.

Journal of Double Star Observations

January 1, 2017
Volume 13, Number 1

The Journal of Double Star Observations is an electronic journal published quarterly. Copies can be freely downloaded from http://www.jdso.org.

Questions, comments, or submissions may be directed to rclark@southalabama.edu or to rmollise@bellsouth.net

The *Journal of Double Star Observations* (*JDSO*) publishes articles on any and all aspects of astronomy involving double and binary stars. The *JDSO* is especially interested in observations made by amateur astronomers. Submitted articles announcing measurements, discoveries, or conclusions about double or binary stars may undergo a peer review. This means that a paper submitted by an amateur astronomer will be reviewed by other amateur astronomers doing similar work.

Submitted manuscripts must be original, unpublished material and written in English. They should contain an abstract and a short description or biography (2 or 3 sentences) of the author(s). For more information about format of submitted articles, please see our web site at http://www.jdso.org

Submissions should be made electronically via e-mail to rclark@southalabama.edu or to rmolise@bellsouth.net. Articles should be attached to the email in Microsoft Word, Word Perfect, Open Office, or text format. All images should be in jpg or fits format.

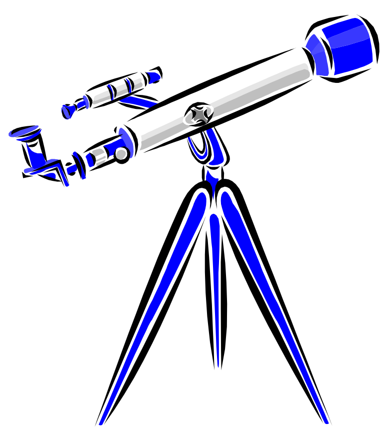

We're on the web!

http://www.jdso.org